Smart Seat Design

An integrated approach for product development in automotive industry

Filipe Miguel Ferreira Nascimento

Janeiro 2014

A dissertation submitted to the Faculty of Engineering of the University of Porto for the degree of Doctor of Philosophy in Leaders for Technical Industries of the MIT-Portugal Program

Supervisor: Professor Francisco Manuel Andrade Pires

Co-supervisor: Professor Pedro Miguel dos Santos Vilaça da Silva

Life is like a box of chocolates
you never know what you're gonna get

Abstract

The reduction of the environmental impact is one of the major concerns in the automotive industry, as well as other industries. A growing concern for the reduction of CO_2 emissions and the increase of fuel efficiency has been observed. The alignment of these concerns, on one hand, and the improvement of the comfort and safety of the vehicle occupants, on the other hand, together with the compliance to other regulations increases the need for the adoption of new solutions that can attend all these goals.

The adoption of lighter solutions seems to be one of the possible routes to take since the weight reduction will be able to improve the fuel efficiency. However the introduction of new materials will require the adoption of new technologies in the manufacturing process or of technologies to replace existing ineffective processes. The implementation of these processes in an existing environment is a complex process. Therefore, a cautious approach was carried out requiring an assessment of the processes on the properties of the adopted materials.

To perform this study an evaluation of the Friction Stir Welding (FSW) process was executed. This process was the object of interest of several industries, especially aeronautic industry. The effect of this process on the material properties of aluminium and magnesium alloys was addressed and the effect of the process parameters was studied using mechanical and corrosion testing. The applicability of this process in aluminium and magnesium alloys for the seat was confirmed. However, its applicability in dissimilar welds between magnesium and aluminium alloys was cast aside because the mechanical and corrosion properties were not promising.

A new solid state spot joining was also the focus of this research. This process has several characteristics to replace the resistance spot welding (RSW) process, which is highly used in automotive industry, in aluminium alloys. This process is cheaper and faster than other existing solid state processes. The applicability of this process in steels and aluminium alloys was confirmed. The optimization steps led to a better understanding of the process parameters' effect on the aluminium alloys concluding that lower rotation speeds and medium plunge speeds are preferable for higher strength welds. The applicability on the steels needs more study since RSW is very efficient and fast for the steels.

Finally, it was possible to conclude that the introduction of these alloys in the automotive industry needs to be made in a step-by-step approach. The aluminium alloys are the most suitable alloys to be adopted in a short-term given their ability to answer to the market needs

for lighter solutions. However, due to the improvement of both the composites materials and high strength steels a grey area of the materials that should be adopted is originated, making it up to the industry trends or the original equipment manufacturer (OEM) preferences to define the material to be used.

Resumo

Embora não seja exclusiva da indústria automóvel, a redução do impacto ambiental tem sido uma das maiores preocupações deste setor, que tem demonstrado uma preocupação crescente com a redução das emissões de CO_2 e aumento da eficiência do combustível. O alinhamento destas preocupações com a melhoria do conforto e segurança dos condutores, bem como a necessidade de cumprir com os regulamentos existentes, aumentou a necessidade de adoção de novas soluções que consigam responder a estas exigências.

A adoção de soluções leves tem-se apresentado como um dos possíveis caminhos a seguir, estando associado à redução de peso a melhoria da eficiência do combustível. No entanto, a introdução de novos materiais para redução de peso estará associada também a introdução de novas tecnologias no processo produtivo ou, por um lado, ou de processos para substituir processos existentes que se tornem obsoletos com os novos materiais, por outro. A implementação destes processos num ambiente industrial ativo é um processo complexo requerendo uma análise dos processos nas propriedades dos materiais adotados.

Para realizar este estudo, foi realizada uma análise do processo de soldadura por fricção linear (SFL). Este processo tem sido alvo de estudo por várias indústrias, com especial incidência a indústria aeronáutica. O efeito deste processo nas propriedades das ligas de alumínio e magnésio foi estudado através do efeito dos parâmetros do processo nas propriedades mecânicas e de corrosão. Observou-se que se tratava de um processo eficaz na sua aplicação às ligas de alumínio e magnésio; no entanto a aplicabilidade na soldadura dissimilar entre a liga de magnésio e da liga de alumínio não foi promissora e sugere-se, por isso, abandonar este caminho.

Adicionalmente, foi também estudada a utilização de um processo de soldadura por pontos no estado sólido. Este processo apresenta muitos pontos fortes para substituir a existente soldadura por pontos, utilizada extensivamente na indústria automóvel, na sua aplicação a ligas de alumínio. Este processo demonstra ser mais barato e rápido que outros processos de soldadura por pontos no estado sólido. Foi confirmada a aplicabilidade deste processo em aços e ligas de alumínio. O estudo de otimização permitiu perceber melhor a ligação do efeito dos parâmetros do processo nas ligas de alumínio, concluindo que a utilização de baixas velocidades de rotação e de velocidades de mergulho médias são necessárias para soldaduras com uma maior resistência ao corte. A aplicação deste processo em aços requer um estudo mais aprofundado, visto que o atual processo de soldadura por pontos é bastante eficiente e rápido para este material.

Por fim, foi possível concluir que a introdução destas ligas em ambiente industrial requer uma estratégia passo-a-passo. As ligas de alumínio são as mais indicadas para serem adotadas a curto prazo de forma a responder a necessidades de mercado por solução leves. No entanto, futuramente e em função da melhoria contínua de materiais compósitos e dos aços de alta resistência cria-se uma área difusa sobre que materiais a adotar. Esta decisão será eventualmente definida pelas tendências de mercado ou gerida pelos produtores de equipamento original.

Acknowledgements

The development of this research has led to interact with several people and I would like to acknowledge their support on the conclusion of this thesis.

Firstly, I would like to thank my supervisor, Professor Francisco Manuel Andrade Pires, from the Faculty of Engineering of the University of Porto for accepting me in this project and for the continuous support in my research work. I really appreciated his accessibility and openness to make this research experience both stimulating and motivating.

I would also like to acknowledge my co-supervisor, Professor Pedro Miguel dos Santos Vilaça da Silva, who suggested me to take the challenge of doing a PhD in the MIT-Portugal program. I really endear the relationship that we have established over the years and the support and availability to use the research equipment in IST.

My stay at MIT has been possible thanks to Professor Jeremy Gregory from MIT that showed interest in my research which enabled interesting conversations about the possible introduction of the process in industrial context. The development of the cost model that allowed us to view the economic impact of these processes and materials, along with the evaluation of their introduction in automotive industry, was very stimulating.

For his availability and interest in my work, I would like to thank Professor João Salvador Fernandes for allowing me the use of his lab, where the corrosion testing in the welded samples was carried out. His openness and availability allowed me to better understand the influence of the FSW process in the different materials.

I would also like to extend a special acknowledgement to Eduarda Silva and Ricardo Sá. Our relationship started as group colleagues in the first year and our interaction and energy has led us to develop very interesting projects that enabled the contact with several companies that showed interest in our results. I think our relationship has bloomed since then and I think that your proactivity has also influenced me lot. I am looking forward for the next steps together or apart and I think either waywe will be successful.

The PhD is not an easy road and I think my relationship with other people in order to loosen up and try to get a different view point for the problem that I or they were facing enabled several friendships. I would like to give special thanks to Jorge and Anton for being able to cheer me up and stand me when I was being annoying. I also endear our relationship and hope to have a "*Francesinha*" with them when they return to Portugal. These thanks are also extended to Carla Monteiro, Deborah Perrota, Samuel Moniz, Tiago Faro, Sérgio Tavares, João Gandra,

Alexandre Marcelo, Filipe Chaves, Miguel Ferreira, Bruno Nunes and Gonçalo Monteiro for good and bad times shared together, from the fun times and the work times and, especially, for the ideas exchange that helped in some steps of the PhD.

For her problem solving skills with bureaucratic load and rules imposed by the different institutions I would like to give special thanks to Carla Monteiro who has been my aid kit in several problems that occurred with bureaucracy during this period.

I would also like to thank Miguel Figueiredo, Rui Silva and José Almeida, from FEUP, as well as Pedro Teixeira from IST for their important contribution in the development of this research work.

Special thanks are in order to the MIT Portugal program and all the Faculty for the functioning of the program. I also like to gratefully acknowledge the funding source that made my PhD research possible, *Fundação para a Ciência e Tecnologia* of the Portuguese government, through the scholarship SFRH/BD/33729/2009 obtained through the 3º Quadro Comunitário de Apoio, and the POCTI and FEDER programmes. Part of my project was developed under the *"Smart Interiors"* project.

Lastly, I would like to thank my parents and my brothers who have always believed and supported me with their continuous availability for helping when needed. My final appreciation goes to my wife, Irene, the person that supported me the most this last years through the good and sometimes very bad times. She has continuously believed in me even when I lost faith in myself. There are no words to describe the support she has given. Thank you for your support and patience.

Contents

List of Figures

List of Tables

List of Acronyms

%Weld – Weld efficiency

ABS – Anti-lock Braking Systems

ANOVA – Analysis of Variance

BM – Base Material

CFRP – Carbon Fiber Reinforced Polymer

CR – Corrosion Rate

FCC – Face Centered Cubic

FSW – Friction Stir Welding

GFRP – Glass Fiber Reinforced Polymer

GEB – Global Efficiency to Bending

GETS – Global Efficiency to Tensile Strength

HARD – Hardness Drop Ratio

HAZ – Heat Affected Zone

HCP – Hexagonal Close Packed

JIT – Just in Time

OEM – Original Equipment Manufacturer

RSW – Resistance Spot Welding

SFL – Soldadura por Fricção Linear

TMAZ – Termo-mechanically Affected Zone

ZRA - Zero Resistance Amperometry

Symbol list

α – Pitch Angle

ρ – density (g/cm^3)

Ω - Tool Rotation Speed

σ_y – Yield Stress

σ_{UTS} – Ultimate Tensile Stress

A – Elongation at Break in the tensile test

C_x – Efficiency coefficient for x parameter

CR – corrosion rate, (g/s) , (mm/year)

F_B – Maximum load in the bending test

d – Displacement to the maximum load in the bending test

D_s – Shoulder Diameter

D_P – Pin Diameter

D_T – Dwell Time

E – Young Modulus

E_{cor} – Open circuit corrosion potential (V)

EW – the equivalent weight of the corroding species (dimensionless)

F – Applied Force

i_{cor} – Corrosion density ($\mu A/cm^2$)

K – constant $3{,}27x10^{-3}$ ($mm.g/(\mu A.cm.year)$)

L_P – Pin Length

M –Molecular weight

N – Number of electrons involved in the chemical reaction,

P_s – Plunge Speed

Q – Charge passed (Coulombs)

U_B – Energy consumed until the beginning of the fracture in the bending test

U_T – Toughness

V – Advancing Speed

W – Weight of the electroactive species

1 Introduction

Nowadays, the automotive industry seems to be reaching a paradigm where new solutions need to be developed to answer to both governmental and environmental regulations. The automotive vehicle has been considered one of the most ineffective transportation vehicles since most of the energy produced by the motor vehicle is dissipated by heat. Therefore, solutions must be found to answer to this impeding need that is not restricted to the automotive industry.

1.1 Motivation

The reduction of fuel consumption and subsequent reduction of CO_2 emissions is one of the concerns that need to be answered by the automotive industry. Companies have the option to develop lighter solutions that can effectively reduce the weight of the vehicle hence reducing the fuel consumption. However the use of new materials will imply either the introduction of new production processes or the replacement of current production processes that are not as efficient as the existing vehicle. This research aims to provide a new process design strategy for the adoption of new technologies in the automotive industry. To be able to perform this improvement, different methods were used to aid in the determination of the best process parameters for the different processes; besides a thorough study of the properties of the processed materials was performed.

1.2 Thesis Synopsis

The developed research along this project has covered different aspects about the manufacturing of a lightweight seat in automotive industry as well as the study of different properties that should be considered in the development of this work.

This dissertation was divided in seven chapters, including introduction and conclusions. The first chapter introduces the research that was made during the scope of this thesis, as well as the motivation that led to the development of this work.

The automotive industry environment is explained on the second chapter which focuses on the industry interaction with their suppliers, not disregarding the upcoming trends of this market. The importance of the seat is explained and information regarding the research that is being developed focusing on car seat is presented. The research question and the strategy adopted for the development of the seat are also presented.

Chapter three focuses on the choice of materials and process selection approaching the problem using benchmarking and seat simulation tools to characterize the existing seat. From this stage on, it the industry production strategy was considered in order to define the route to follow through this research. At this point, the processes and materials to be studied were selected.

Chapter four focuses on the parameter study using the Friction Stir Welding (FSW) process and its effects on the properties of the welded samples. The Taguchi method has been applied for some materials, while others required a more trial and error approach.

Chapter five presents the results from the corrosion studies performed on the welded samples using the best parameters defined in the prior stage. A more in-depth study was made trying to understand the causes for the higher corrosion rates in some samples while trying, at the same time, to create measures to reduce this effect.

Chapter six presents a method by which a new solid state spot joining technique can replace the existing one in its applications. Several studies were performed to understand not only the effect of the process parameters on the material properties but also their toll on the welding machine. The applicability in stainless steels and copper alloys was also performed.

Chapter seven presents the decision of which seat should be produced taking into account different strategies such as the evaluation using simulation tools and the properties of the seat. Externalities and the business strategy have also been considered for this decision. The cost model and results from simulation and modeling steps are also presented in this chapter.

The conclusions and future work are presented in chapter eight. Besides, some recommendations are made regarding the introduction of novel technology in a demanding work environment as the automotive industry.

2 Automotive Industry

Automotive industry is a complex system in which different companies produce different products that will be used in the proceeding company and, subsequently, in the Original Equipment Manufacturer (OEM) also known as automaker. This industry is, therefore, composed by a set of different companies established across distinct areas of the automotive industry (Figure 2.1). On the manufacturing side there are the automakers, the tier suppliers (that have different levels) and the raw materials suppliers. On the marketing side there are the automakers, the dealers and customers.

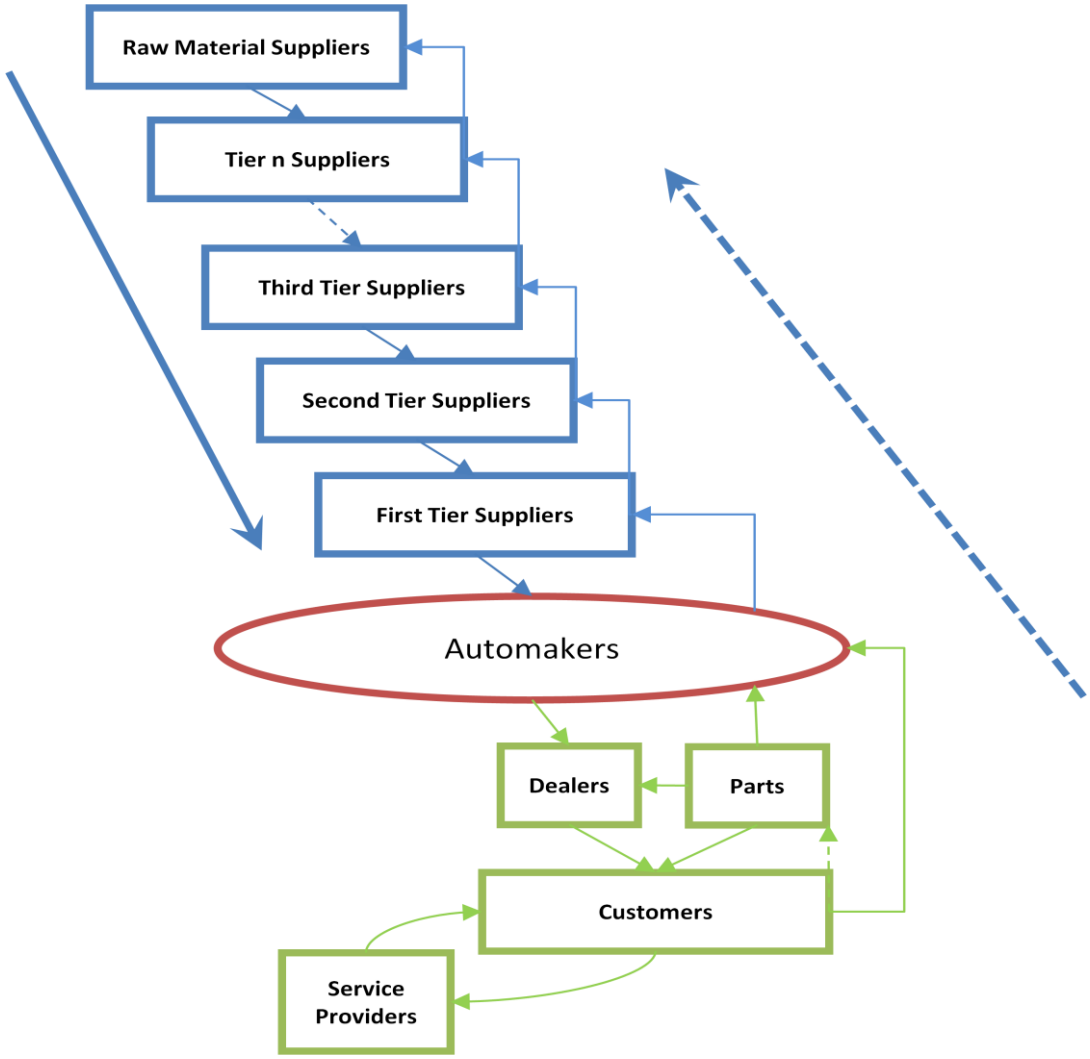

Figure 2.1 – Automotive industry supply chain.

On the manufacturing side, the automaker and its suppliers must have a trust relationship, assuring that during the development and production of a car model the supplier provides all required products. On a later stage, with new car models, the automakers will try to keep doing business with the suppliers in which they trust more. Also, one of the demands of car

companies is that the companies that supply them must be geographically close, in order to be able to reduce delivery times and enable them to work in just in time (JIT). Depending on the level and closeness of the Tier 1 company it can also enable the coordination of manufacturing between supplier and automaker, thus allowing the product to be sent from the Tier and delivered in time for the start of production in the automakers' plant [1].

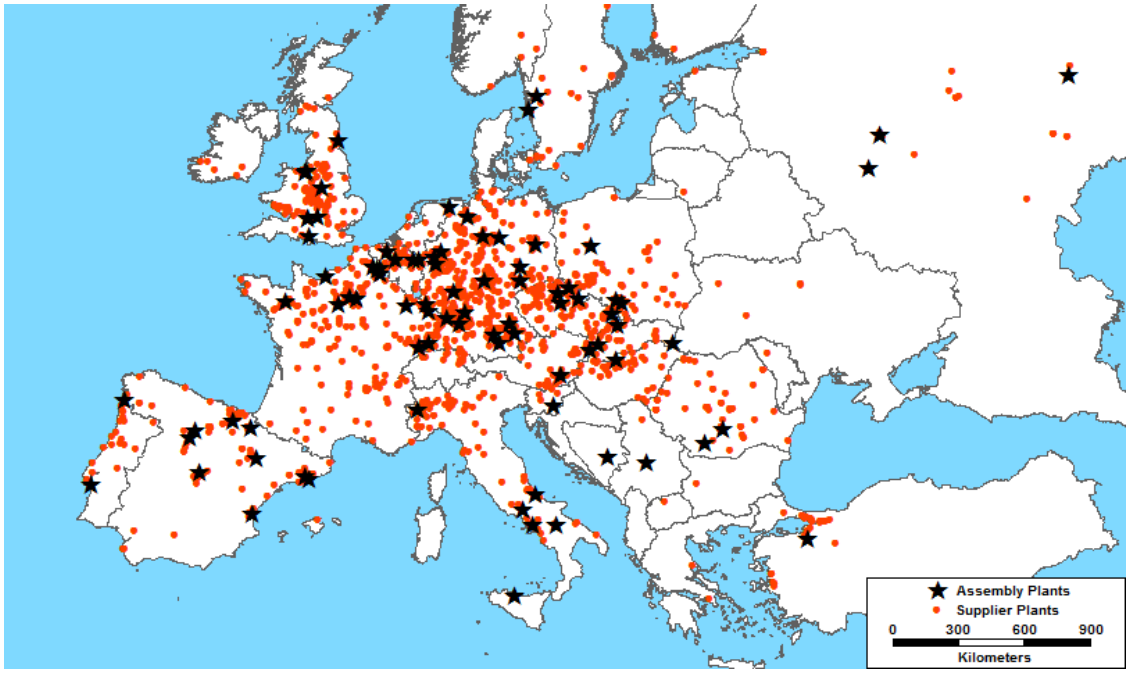

Figure 2.2 – Map showing the distribution of the suppliers in Europe for different assembly plants [2]**.**

Automotive OEMs tend to have their suppliers close to their factories, usually in a predetermined radius, like 200km, enabling a faster communication between them, which translates into a more efficient distribution of the parts needed by the automaker (Figure 2.2).

To accomplish this, the automaker will establish relationships with regional suppliers that, due to this closeness, will enable the companies to be more responsive to changes in the production thus allowing an easier delivery of the different parts for the company. This relationship is usually very well established with the Tier 1 companies that are closer to the main automaker operational area, while other downstream companies' closeness can be outside this preferred interaction distance because they will not answer directly to the automaker but to the upper Tier company. Since the automotive industry works in a JIT method, efforts will be made to have their suppliers as close as possible. Another reason for the use of local suppliers is related with the time needed to make and deliver. If the company is close this time is shortened and these companies can have a more flexible production adjusting to the automaker needs. However, if the company is far away more time is required to send the parts. In fact, this time can go up to three weeks before the OEM needs a

particular part; therefore these companies will have much more difficulties to comply with the automakers demands for different stages of production. Another important reason is that the cost of transportation ends up being very high and there might be some stoppage time at customs entry depending from where the supplier is sending its items [1], [3].

As previously mentioned, it is important to acknowledge that suppliers and automakers within the automotive industry have a trust relationship. It is also important to understand that the automakers will usually try to establish relationships with local suppliers, in an effort to reduce costs and enable more flexibility in their production line.

On the marketing side, the automakers have several dealers in different countries that will try to acquire clients using different advertising strategies. There are also the services companies that will provide services to the customers as the automaker liaison providing parts or services in the automobile lifetime.

The automotive industry also works in two systems: a pull system in the manufacturing side and a push system in the marketing one. The automaker controls both these systems and is able to also control the production of the company aligned with the marketing demands.

2.1 Industry trends and objectives

One of automotive industry main goals is to reduce costs and increase revenues. However, they need to comply with government and safety rules in order to be able to deliver a car to the general public. Several trends have been identified (Figure 2.3) for the future and the challenges have been identified for the foregoing years [4]. Specifically, it has been identified that for the next few years the development pace in technology development and complexity in the automotive industry will increase; hence companies need to be more active in order to develop the equipments. However, companies will have to make choices regarding which technologies they will introduce in detriment of others. This trend is already appearing with the companies focusing on powertrain technologies (hybrid-electric, all-electric or fuel cell). Suppliers are going to play a key position in this by developing expertise in these novel technologies and helping to fill the gap that the automaker has in this area. Nonetheless, this is also an opportunity for new suppliers that are experienced in these new fields to find themselves in a strategic point to enter automotive industry and aid in the development of parts that would take the R&D departments a longer time to reach positive results due to their lack of experience in the area.

Becoming decentralized will be one of the biggest challenges for the OEMs because it means that they will begin to lose control over the technological development. Besides, it also means

that a new operating paradigm in automotive industry will start to flow and the suppliers will become responsible for the technological innovation, developing their knowledge in important areas, while OEMs will have the role of an integrator in which they receive the different body parts and join them together without any glitches. This predicted change will involve an even greater level of trust relationships between the automaker and their suppliers in which the technological development of the different parts will no longer be in their domain. Thus the goals and operating principles of both suppliers and automakers must become aligned to allow a more thoughtful and strategic approach.

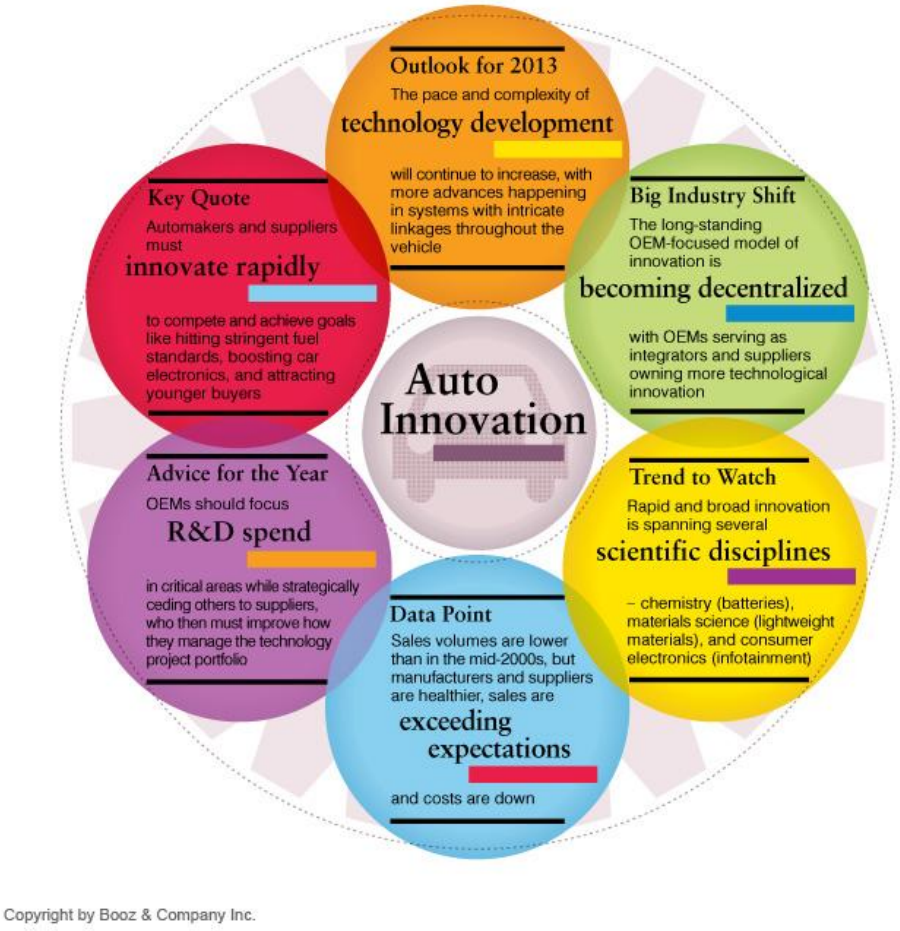

Figure 2.3 – Trends in automotive industry [4]**.**

In order to adjust to this new reality, automakers will have to strengthen their existing innovation capabilities and develop new ones. To achieve this automakers [4]:

- will have to select the most essential technologies they have and remain proprietary,
- must become experts in network management to manage a broad, far-reaching and active innovation network,
- need to strengthen the system and the vehicle interaction expertise.

The first implies that the automakers will have to plan carefully how they will spend their R&D budget in the most critical area, precisely where it will have most impact, introducing make-versus-buy discipline in the technology innovation. To be successful the automakers need to have a clear insight on their own capabilities but also of their suppliers' capabilities.

With the dispersion of technology, automakers will need to create an active and extended innovation network, while reducing costs through competitive sourcing incentives and partnering with advanced sourcing entities.

For ensure that automakers still have power in this innovation changing environment companies will need to increase their control over the car system, besides strengthening their expertise in the cross-system and vehicle integration areas. This will be essential for automakers to maintain control over the process and achieve high-level quality and reliability targets across an increasing innovation spreading environment.

On the other hand, automotive suppliers will take upon more responsibility in the innovation portfolio of the company and several responsibilities and decisions from the innovation point of view. Decisions regarding which technology development must be taken into consideration and also the development road map of that selected technology. These companies must ask themselves whether or not a technology offers a competitive advantage over others. Will the development of such a technology make the final product more attractive for clients? Is there any way for such a technology to become less attractive on a long-term perspective? Being aware of the possible evolutions and trends of the market will help the supplier companies to position themselves as experts in their area and this might give them leverage in the contracting of the different companies [4].

There are several future trends that must be taken into consideration for the development of the new automotive models. These new developments must fulfill both the different regulations established by government entities and the emerging needs that are identified by the car users.

The Kyoto Protocol has established goals for different companies to reduce their CO_2 emissions, not only during the manufacturing process, but also during the vehicles lifetime. This has made companies to increase their efforts in order to improve the performance of the vehicle. There are several ways to accomplish this [4]:

- improve the motor vehicles' performance;
- changing the vehicles' power source, which can be electric, hybrid and fuel cells, and improve their performance;

- reducing the overall weight by changing the materials used in the vehicle.

The motor vehicle performance has been described as one of the most inefficient energy transformers. Vehicles today use most the energy produced to run the vehicle and feed the electrical system of the car. However, most of the energy produced motor vehicle is dissipated in the form of heat. In fact, some studies have shown that 90% of the energy produced is dissipated in the form of heat. The increase of the efficiency of the motors would enable to reduce the fuel consumption.

The replacement of the vehicle power is also aligned with the CO_2 emissions reduction goal; however, there is still some research left so that these cars can give the same level of comfort as fuel powered cars. Needless to say, batteries powered cars have limitations on the performance because some of them have a very small distance of performance between charges. One of the goals in this research area is to improve the batteries to make them last longer and if possible charge them faster.

The weight reduction is another research area that is aligned with this main goal. The reduction of the car weight would mean that the motor would have to spend less energy to make the car advance. However, simply replacing the materials of the car is not as easy as it seems and several variables must be taken into consideration. These variables are the material properties, how the different materials will react between themselves, how the car design will change with this development and whether or not it is possible to join different materials in the same car structure.

Another trend that is also evolving is focused on the human-vehicle interaction that includes the following trends [4]:

- development of newer systems for human-interaction,
- development of newer and more secure safety systems,
- focus on comfort issues inside the vehicle.

Several researches are under development trying to attract a newer generation that can include the development of newer open architecture and flexible systems compatible with popular electronic devices such as smartphones and tablet computers [4].

The second point focuses on the safety inside a car whenever a car crashes and impacts. This is one of the most studied areas in the automotive field and, in fact, several safety systems inside the car can be mentioned, such as the safety belts and airbags. Safety systems are classified in three classes: passive, active and warning. Passive safety systems are systems that exist in the

car to protect the driver during the car crash. These systems are the seatbelt, the airbags or the car structure. Active systems are those that will activate to prevent a possible crash. These systems can be anti-lock braking systems (ABS), electronic stability control and pre-crash systems. The third class is related to the after crash stage in which some systems will automatically communicate with authorities to warn about the accident that occurred or communicate with the occupants, assessing the damage and take actions to help them. Apart from these classes some research has been developed in low-speed impacts that can affect the driver leaving long-term injuries without any visible injury in the car occupants. Research has focused on the development of systems and injury analysis methods to understand and decrease the number and severity of injuries sustained in a car crash.

Comfort is one of the most difficult parameters to assess given its subjective and constantly changing parameter dependent on how the occupants will perceive it when driving their cars. Developments have spread in different areas and there is a clear focus in the evaluation of comfort parameters that can be used in the future to simulate the comfort and detect the best comfort parameters to include in an automotive vehicle. Other areas have focused in the occupant reactions to car systems under different conditions. An automotive vehicle needs to feel comfortable even in long trips because the car occupants will not want to have a car that causes them discomfort and pain during drive. It is possible to sustain that pleasant looks and comfortable seats and systems are seen as main trends in the development of comfort in automotive industry.

Our goal with this work is to select and develop a car system in alignment with industry trends and yet profitable by the industry standards.

2.2 Importance of the seat

The seat is the feature that is closer to the car occupants during the vehicle use. Although it requires little or no maintenance is the feature that in a first instance offers protection during car accidents and provides comfort to the car occupants its utilization. Another important factor is the joining of this feature to the rest of the vehicle. The connection of the seat to the rest of the vehicle needs to be safe but also needs to be adjustable so that a different person can use the same vehicle. This chapter describes the safety and comfort concerns allied with automotive seating. These concerns are important and must be taken into account when developing the different seats. Each one of these properties affect different seat properties in different manners and some sub-systems might be included in the seat in order to improve the

car user experience, like seat heating systems, active head restraints and several airbag systems adjusted for different impact.

2.2.1 Materials and Processes used in the Car Seat Manufacturing

2.2.1.1 Steels

Steel is the most common material used in the automotive industry and it has several properties that makes it very attractive. It is a high strenght alloy with high formability and has a low price. Also the process to work with steels is already established and mass production has been achieved which makes the final product cheap. One of the main problems with steels, however, is that it has a high density (7,8 g/cm^3). This high density gives room for improvement by using new concepts and lighter material. Even so this material is commonly used for automotive applications because the technologies for other materials are not fully developed. Steel car seats can have three types of seatback configurations (Figure 2.4):

- Tubular seatback – uses round tubular steels tubes to form the back.
- Stamped seatback – uses a non-tubular structure at reclining mechanism
- Hybrid seatback – that has a significant ammount of both tubular and stamped components.

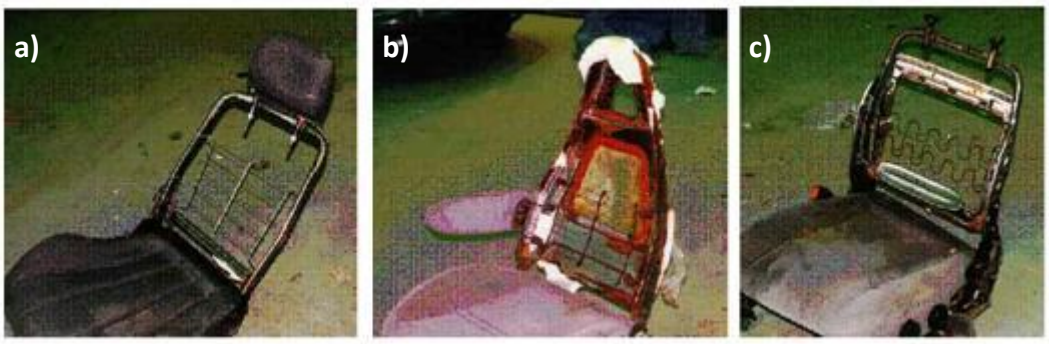

Figure 2.4 – Seats with different seatbacks: a) tubular, b) stamped and c) hybrid.

The sheet metal stamping is the process used today to give the different parts existant in the seat their desired shape. Different stamping processes can be used in order to obtain the required shape of the different parts, such as blanking, drawing, piercing, notching, hemming, trimming. These processes can be used individually in order to obtain a part or in sequence. The following sequence is usually applied in automotive industry:

- Blanking is usually the first step and prepares the flat sheet into the approximate form of the part.
- Drawing, it is the operation that gives the first approximate depth related form to the part.

- Piercing, Notching and Hemming are subsequent operations that are usually related with the product design.
- Trimming the extra material is removed from the periphery of the part provided for blankholding during the draw operation. In order to obtain a good draw it is necessary to make a good decision on the trim line.

Resistance welding and fusion welding are the joining techniques used in the automotive industry. Resistance spot welding [5] is usually used to join the stamped metal sheets together. In this process, contacting metal surfaces are joined by the heat obtained from resistance to electric current flow. Work-pieces are held together under pressure exerted by electrodes. The process uses two shaped copper alloy electrodes to concentrate welding current into a small "spot" and to simultaneously clamp the sheets together. Forcing a large current through the spot will melt the metal and form the weld. One of the advantageous features of spot welding is that a substantial amount of energy can be delivered to the spot in a very short time (approximately ten milliseconds).

The amount of heat (energy) delivered to the spot is determined by the resistance between the electrodes and by the amplitude and duration of the current. The amount of energy is chosen to match the sheet's material properties, its thickness, and type of electrodes. Applying too little energy won't melt the metal and will make a poor weld. Applying too much energy will melt too much metal, eject molten material, causing a hole rather than a weld. Another advantageous feature of spot welding, is that the energy delivered to the spot can be controlled to produce reliable welds.

Usually spot welding is a very time demanding process and for a high production rate it is required that process becomes faster and this need has probably lead to the development of the multiple-spot welders (Figure 2.5). These multiple spot welders increase the number of electrodes and the distance between electrodes can be easily defined.

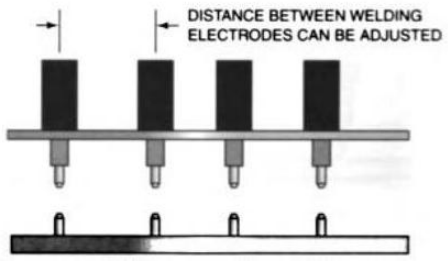

Figure 2.5 – Multiple-spot welder [5]**.**

Metal Inert Gas/Metal Active Gas (MIG/MAG) welding is another joining technique that is applied to car seats to join tubular structures among others. MIG/MAG welding is a semi-automatic or automatic arc welding process in which a continuous and consumable wire

electrode and a shielding gas are fed through a welding gun. A constant voltage, direct current power source is most commonly used, but constant current systems, as well as alternating current, can be used. This welding process is usually used for large amounts of pieces that need to be welded and the weld is usually of good quality.

2.2.1.2 Aluminium and its alloys

Due to the advantage of its low special weight, high strength and corrosion resistance aluminium alloy sheet is becoming one of the main materials to take the place of steel components in an effort to reduce the vehicle weight. In fact, the use of lighter materials can influence the fuel economy, since a weight reduction of 100 kg represents a fuel saving of about 0.5 l per 100 km for a vehicle [6], [7]. The aluminium alloys mostly used in the automotive industry are from the 5xxx and 6xxx series due to their higher strength values and because these aluminium alloys present a better strength-weight ratio than the steels [8], [9].

Aluminium is three times lighter than the steel with a density of 2,7 g/cm^3 , also presenting an elasticity modulus that is one-third of the steel elasticity modulus. In orderto apply the aluminium to seat, different shapes were selected in order to improve the stiffness of the seat to decrease the potential of failure during its lifetime.

The processes used for aluminium are very similar to the ones used in steels, but the joining process are very difficult to handle. Aluminium has a very high heat coefficient and this makes the aluminium alloys to present poor weldability features. Therefore, the joining processes used for steels can not be used in the same fashion for the aluminium alloys. Resistance spot welding is the welding process that shows more capability of being used with aluminium and has shown good results. The usual processes used for aluminium are mechanical joining processes and these processes usually involve a preparation of the parts to be joined together, that can be drilled together and afterwards the parts can be screwed together.

The use of aluminium sheet plates follows the process shown in Figure 2.6. It can be seen that the aluminium alloys have a similar process to steels. Tailored blanks are usually used to save weight by distributing the weight for the parts that need it the most. This means that the material will present different thicknesses, being thicker where it is more solicited to loads. The use of tailored blanks in aluminiums offers the possibility of creating new designs, but compared to steel it is needed to have more caution handling aluminium due to its low formability. This means the stamping process requires extra-caution in order to obtain the continuous weld-line and and thickness differences [10].

The phosphating and painting are made to protect the materials from exterior agents, preventing it from corroding and/or having their properties compromised. In Figure 2.6 it can be seen that one the future tendencies is the introduction of the Pickling and Zr/Ti Conversion. The introduction of these two operations as pre-treatment of the material has demonstrated to improve the material's performance and reduce the production cost.

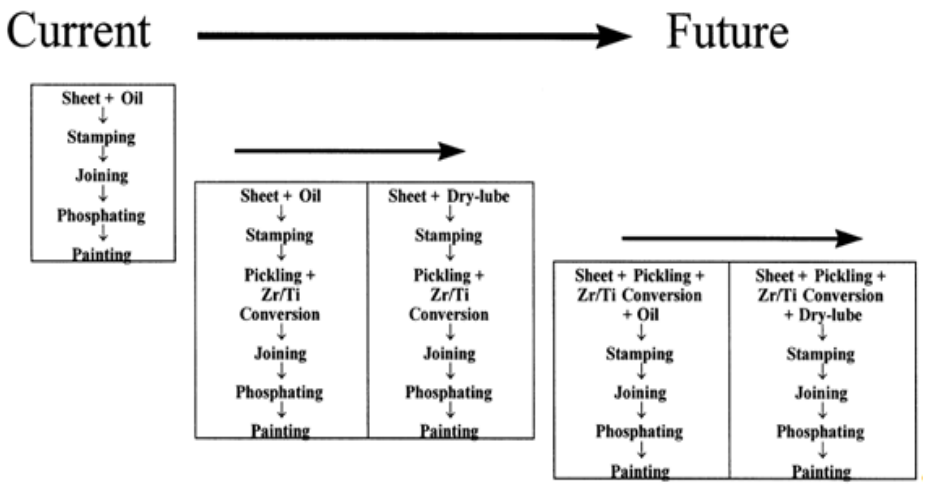

Figure 2.6 – Aluminium process in automotive industry and future trends [6]**.**

To conclude, aluminium was successfully implementated across the automotive industry and, in 1997, there are references of a new A-class seat being made in aluminium composed by a tubular seatback, a panel for the seat cushion frame and the rails where made of extruded aluminium parts [11].

2.2.1.3 Magnesium and its alloys

Magnesium is one of the lightest of all the engineering metals, having a density of 1.74 g/cm^3 . It is 35% lighter than aluminium (2.7 g/cm3) and over four times lighter than steel (7.86 g/cm3). Magnesium is also recyclable and major increases in automobile usage would eventually require a production capacity expansion [12]. The use of magnesium in the automotive industry might be crucial. Although aluminium alloys and steels have already been prepared to reduce the car weight, magnesium has a great potential to reduce this weight even more. However, there are several disadvantages related to the magnesium alloys. The disadvantages of Mg alloys rely on its high reactivity in the molten state, inferior fatigue and creep resistance, when compared to aluminium, and lower galvanic corrosion resistance. The problems about using magnesium alloys stems from their low melting points 650°C and their reactivity (inadequate corrosion resistance). During fabrication and usage, the main problem for Mg alloys is the fire hazard/risk, especially in machining and grinding processes, due to their relatively low melting point. Magnesium tends to corrode faster than other materials, so

coatings are needed to be planned during the design phase. Magnesium has a high electrode potential which makes it susceptible to show galvanic corrosion requiring protection when there is contact with other metals. A good design and appropriate protection concepts can reduce/eliminate these concerns [7]. One important fact even with all the restraints of the magnesium alloys, these alloys still present a good creep resistance property enabling its applicability in automotive industry.

Another problem related with magnesium alloys is the price of the magnesium. It has one of the highest prices in the market and it has a very unstable behavior in spite of improvements over the last few years.

In order to protect the magnesium from corroding away, a Teflon resin coating is layed over the metal parts; this way the magnesium will not be in direct contact with other materials, effectively protecting the magnesium from corrosion problems.

Usually, the magnesium parts are made in pressure die casting and thixomolding processes. Magnesium has an advantage over steels and aluminium having an excellent castability; therefore complex shapes can be obtained during casting. In 1997, the Manufacturing Science and Technology Group of the Commonwelth Scientific and Industrial Research Organization replaced a 13 part steel seatback for a one part magnesium seatback [13].

Pressure die casting is a process that is characterized by forcing molten metal under high pressure into a mold cavity. The mold cavity is created using two hardened tool steel dies that have been machined into shape and work similarly to molds during the process. Most magnesium parts have been produced using this process, but recently a new process has been adapted to be used.

For magnesium alloys, thixomolding uses a machine similar to injection molding. In a single step process, room temperature magnesium alloy chips are fed into the back end of a heated barrel through a volumetric feeder. The barrel is maintained under an argon atmosphere to prevent oxidation of the magnesium chips. A screw feeder located inside the barrel feeds the magnesium chips forward as they are heated into the semi-solid temperature range. The screw rotation provides the required shearing force to generate the globular structure needed for semi-solid casting. Once enough slurry has been accumulated, the screw moves forward to inject the slurry into a steel die [14], [15]. Since the magnesium has such good castability it is possible to obtain very complex seat designs in just one step using these processes.

Figure 2.7 – Magnesium seat [7]**.**

Several examples of magnesium seats exist. Some of them are presented in Figure 2.7 and it can be observed that even though the seat is not stamped, the metal sheet like shape was obtained using the discussed processes.

Several seats developed until the end of the nineties used the pressure die casting, but only after the thixomolding process hadbeen adopted. The advantages of using thixomolding over die casting are at least the following:

- Less melt loss, less contamination and less scrap
- Lower energy consumption
- Longer die life and a more flexible mold design
- No risk of fire, no dross (foundry free environment)

The magnesium parts produced by thixomolding have better properties than the parts made by die casting. The use of magnesium has enabled not only a reduction of parts but has also decreased the expenses with the joining process [11], [13].

2.2.1.4 Foams

Polyurethane foams are the most commonly used in the car seat cushion and are the responsible for the comfort of the car occupants during trips. In order to make car journeys more comfortable, the seat must present several features in order to comply with the time spent in the car.

Polyurethane foams are extensively used because of their superior cushioning, ease of handling and physical properties [16]. The polyurethane foam has been widely used and most of its properties are well know; however some concerns exist because the seat has an organic nature that might ignite when exposed to a source of heat energy [16]. This is a very proeminent concern, but the process has been studied and it is very unlikely that the combustion of the polyurethane seat cushion might actually happen.

Seat design is based on previous experiences and the composition of the polyurethane used will have a significant effect over the foam properties. Several studies have been made to try to understand and simulate the behavior of the seat cushions [17]. Some advances in foam technology have enabled to produce the required foam density and moulded shapes while also achieving the desired comfort. The seat is designed to carry high abuse loads, and it normally lasts the life of the vehicle with little or no maintenance [18]. The polyurethane also carries another function related with the attenuation of the vibration produced during a trip. The first method usedapplied a manipulation of the suspensions' stiffness, i.e. stiff suspension provided a good handling but bad driving quality, while a soft suspension improves the ride quality but neglets the car handling. In order to improve the drive quality, the seat springs' stiffness are usually manipulated; nowadays, however, the foam properties can be adjusted for this goal and decrease the transmissibility of vibration to the car occupants. The development of a full foam seat has enabled to fully use the foam properties in order to decrease the transmissability of the cars' vibration hence increasing the perceived comfort during the trip [19]. As a consequence, the use of foams have a clear impact on the person comfort and the development has lead to deeper understanding of the seat properties and its effects on the car occupants.

2.2.1.5 Remarks

It is established that different materials are used in the manufacturing of car seats. In fact, apart from these material polymer-matrix, composites can also be used in the structure of the car seat. However, most of these materials are only used to small to medium level productions because it is not profitable to use them in automotive industry environment. Replacing the regular materials used in the seats by lighter materials can have a great effect on the fuel efficiency of the car. The replacement of these materials must be done taking into account the goals of the company, its production level and seat design.

2.2.2 Safety concerns

When building a car seat there are several aspects that must be taken into account in order to answer to every driver´s need since they start driving. Safety systems need to be responsive in order to protect the car occupants in case of sudden accidents.

The safety of a car driver is very dependent of the seat, since during a car impact the body of a person is under several stresses which might injure different parts of the drivers' body.

In fact, as it is well known, during a car crash, a person can develop several injuries in different body parts that can ultimately cause death or long-term disabilities, depending on the severity of the injury. There are several injuries that may occur as a result of a car accident, such as the following:

- Neck Injury;
- Head Injury;
- Chest Injury;
- Femur Injury;
- Pelvic Injury.

These injuries have different levels of severity that are correlated with the abbreviated injury scale (AIS) for different levels of severity. This scale was developed in 1971 to aid vehicle crash investigators and revised in 1990 to be more relevant to medical audit and research. The AIS coding has a 6 point severity scale that is described in the Table 2.1.

Table 2.1 – Six point severity scale used in the AIS [20]**.**

Scale	Severity
1	Minor
2	Moderate
3	Serious
4	Severe
5	Critical
6	Maximum (considered Untreatable)

This scale is usually specified with the designation of AIS x, where *x* depends on the injuries' severity as described in Table 2.1.

In the following pages, which injury can be caused as the result of a car impact will be discussed as well as possible expected outcomes, the related criteria and the mechanisms that influence these injuries. The models that have been used to study the outcome of the impacts and their relevance on the specific injury and the relevance with each injury criteria will also be presented. The number of fatalities and car accidents has reduced during the last years. It can be seen in Figure 2.8 and Figure 2.9 that the evolution of severely injured and the numbers of deaths in Portugal have decreased substantially over the years.

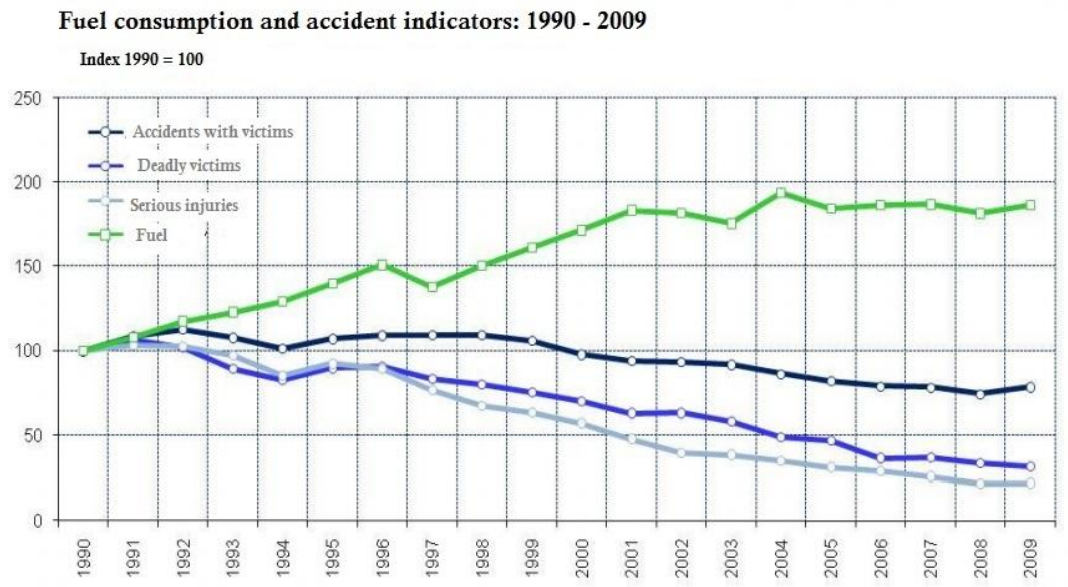

Figure 2.8 – Evolution of the fatal and severe injuries in a car accident (adapted from[21]**).**

One explanation for this phenomenon is the increase of the passive safety inside a car that has enabled the driver to have protection during different impacts, making it possible to withstand more severe car accidents. Another reason that can be clearly seen in Figure 2.9 is the implementation of program and actions to increase the drivers´ awareness. Another outcome of this program are the rules imposed by law to the driver, forcing a higher effort in security during driving, Among such laws is the imposition of the Blood Alcohol Concentration (BAC) >1,2g/l as a criminal offense, mandatory periodic inspections and the use of seatbelts for children may be quoted.

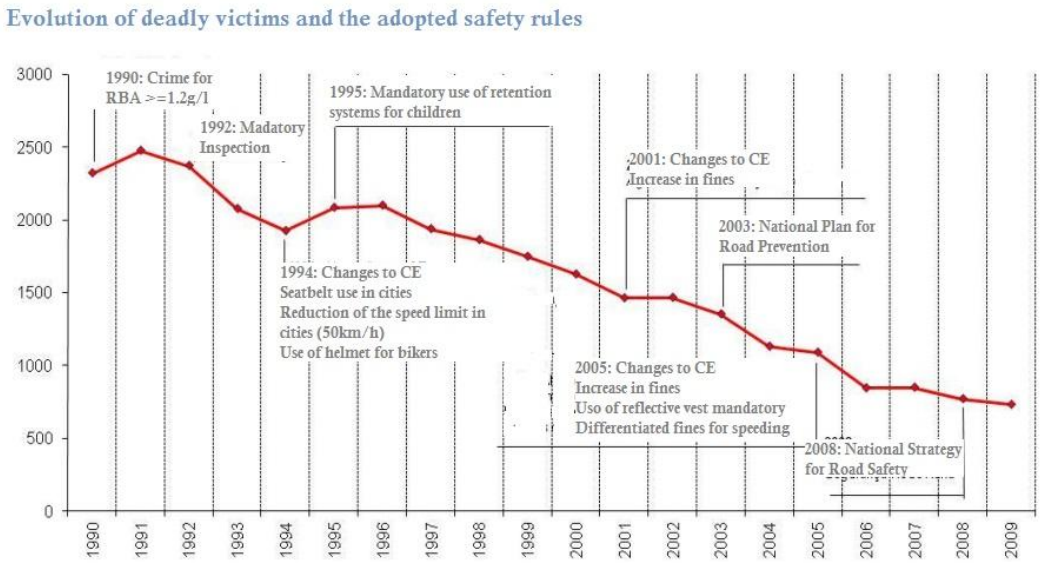

Figure 2.9 – Evolution of the fatal victims in a car accident during 1990 until 2009 in Portugal (adapted from [21]**).**

It can be clearly seen that the tendency of the accidents is to decrease along time, although this data does not include minor accidents that might have minor or non-existent injuries. Even so, it is possible to conclude that in Portugal the tendency is to have a reduction in the fatal and severe injuries during a car crash. This implies a reduction of the more severe injuries, mainly due to better efficiency of passive safety, increase in the awareness of the drivers and the applicability of laws for car crashes.

Kullgren et al [22] state that in the last few years one injury has increased, not following the trend shown by the other injuries. These happen even in slow speed impacts, usually from back impacts that do not cause the other type of injuries, but may originate neck injuries with high severity. So, in order to learn more about it, the different mechanisms involved in these injuries must be studied. It is also important to understand how their activation occur during the different impacts (frontal, back and side impacts).

2.2.2.1 Neck injury

The Whiplash Associated Disorder (WAD) is usually associated with car impacts and it represents a large range of neck injuries caused by a sudden distortion of that part of the body. After an impact, in an initial phase, the head will usually undergo a translational motion relative to the torso, inducing neck protraction (in frontal impacts), or neck retraction (in rear impacts); the neck is exposed to several mechanical loads when it reaches the limit of the protraction/retraction and will undergo another mechanism, flexion for frontal impacts and extension for rear impacts. These mechanisms are represented in Figure 2.10.

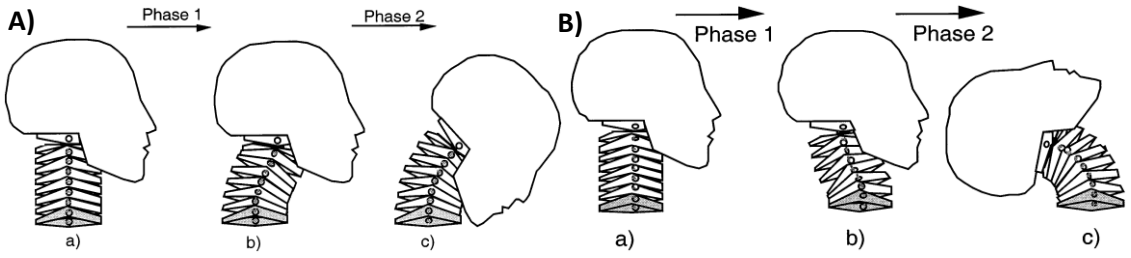

Figure 2.10 – Schematic representing the different mechanisms of the head-neck during a car impact. A) Frontal impact: a) Before Impact (No motion), b) Protraction motion and c) Flexion Motion; B) Rear Impact: a) Before Impact (No motion), b) Retraction motion and c) Extension Motion [23]**.**

Even knowing these mechanisms, several criteria for neck injuries have been implemented in which they try to foresee the severity of the injury that may appear during a car impact. However, there are still many challenges to be faced along the investigation of neck injuries; one of them is that still not all mechanisms involved in neck injuries are well understood. Another point is that the dummies used in car crash tests do not fully represent the

mechanisms that might lead to neck injuries in a crash, although it is also true that there are recent and significant developments and some of these dummies, like the BioRID [24], have presented good results that are very close to what factually happens to the neck. Yet another challenge is related to the modeling of the human neck during a car impact. Nowadays, most simulations do not use the human body but dummies that have better behavior and are easier to compute in a simulation.

The mechanisms that are employed in the neck, during a side impact, are not established and most investigation in this area is trying to understand such mechanisms and to develop a dummy that can recreate with a reliable fidelity the human response during such event.

Even so some of the studies that have been done on human and corpses by the means of sled tests and results have been the basis for the development of dummies for side impacts [25]. MacIntosh *et al.* [25] have analyzed the experimental data from Heidelberg University on side impacts in order to identify some mechanisms regarding neck injuries. After analyzing the results, the author proposes that an ideal side impact dummy neck would have rotation in three planes which would influence the orientation of the head and probably lead to injuries in the anterior head. His study has also lead to the conclusion that resultant force and moment data are valuable for setting the injury assessment reference values for side impact dummies and injury criteria.

2.2.2.2 Head injuries

Head injuries are still the most common injury that can cause death in a car accident. Several test procedures have been introduced in order to assess the car crash safety performance in terms of risk of head/brain injuries. These procedures involve tests using crash dummies or subsystem tests using head impactors (mechanical replacements of the human head). All of these procedures rely on the Head Injury Criterion (HIC).

This criterion relates the translational acceleration of head mass centre to the skull fracture risk [26]. This criterion has the advantage of being simple and the acceleration of the mass centre on the dummy can be accurately determined using three accelerometers usually presenting good repeatability results.

Wittek [26] also states that the introduction of the airbag has led to the development of a new criterion that accurately predicts the severity of brain injuries without skull fracture, also mentioning that the models developed for this aim have not been successfully implemented in the car design.

Huber *et al.* [27] evaluated how the head injuries evolved during the years after the introduction of new airbag systems. It was identified that the head injuries have increased along time; besides, both the minor and medium head injuries have also increased with the introduction of the second generation airbag systems. This study clearly shows that although the systems designed for a car has clearly reduced the number of fatalities inside the vehicle. These developed systems seem to have increased the head and facial injuries. Therefore a window of opportunity can be reached at this point.

Deck and Willinger [28] tried to develop a new finite element model in order to assess injuries in motor sport, motorcyclists, footballers and pedestrians. A statistical regression analysis was performed on the head loading parameters from sixty eight accidents so that they could determine which parameters would provide the most accurate metrics for the injuries sustained. It was concluded that this model brought several improvements on the injury prediction based on finite element (FE) models which is related to skull fracture and that this model has presented a greater correlation with the injuries than the HIC. Another improvement is that with this model the sub-dural hematomas (SDH) can be better predicted than with the usual HIC.

2.2.2.3 Femur, pelvic and chest injuries

Besides these 2 injuries, there are 3 more injuries that have been looked in with concern for both physical and psychological effects, which are the femur, pelvic and chest injuries.

Although the focus of this research proposal is going to be centered in neck injuries these other should not be disregarded since there is always the possibility that some solutions proposed will affect as well them. Therefore, in order to make a proper assessment of the solutions proposed in future stages, understanding the mechanisms behind these injuries is an important step in the development of the car seat. One important injury that should be taken into account in the development of this seat is the femur injuries. This kind of injury is usually related with the submarining effect and consequently pressure made on the legs that. Being this an injury directly related with the seat, some improvements can be made in order to decrease or nullify the probability of its occurrence. Having this in mind, a study was conducted by Tencer et al. [29] to identify the drivers for femur injuries. For this purpose, several accidents that resulted in femur injury were selected. It was concluded that most accidents should have a probability of injury inferior to 10%. However, in all accidents there was some kind of injury; this can be explained by two factors: the first one is that the driver is out of his/her regular driving position in order to try to avoid the accident and this position

causes a hit in the stiffer regions of the dashboard. Another factor is that the driver, due to the stress induced increases the applied force on the femur trying to stop the car. The increase in force will make it possible to surpass the threshold or femur injury. The author also suggests that these results might show an opportunity for changing the design of the bolster area that comes in contact with the knee.

Another injury that might be decreased by the developed safety system is the pelvic injury. This injury might occur due to the same events involved in the femur injury, although the mechanisms are different and not very well known. Some studies are being made in this field in order to develop a precise to properly prediction aboute these types of injuries. Salzar *et al.* [30] started to develop a criteria that could answer to this need and study this effect in different positions. In the study made, they came to the conclusion that a good indicator for the predictive criterion would be based on the axial force which should be smaller than the peak axial force because the force necessary to initiate a fracture is smaller. It was also found that this injury is position dependent in which the extended driver position has the best tolerances when compared to flexed positions.

Chest injury is another injury that can occur during a car crash; this one is currently associated with the impact of the seatbelt and airbag. Several studies have been conducted, but one in particular [31] shows that the oblique impacts present greater deflections on the chest when compared to strictly side impact. This was concluded to be due to an added shear component on side impacts which would increase demand on the soft tissues and the hoop tension.

2.2.2.4 Solutions for injury prevention

Many systems have been developed that act when sudden vehicle stops in order to decrease the severity and number of injuries that can be sustained during a car accident. These safety systems are focusing on the protection of the automotive user and several and different methods have been developed to this goal. This section intends to show some of these solutions and explain its importance in the eventuality of a car accident. One of these solutions is the active head restraint that reacts on impact to reduce the blow to the brain that a person might sustain during a car crash.

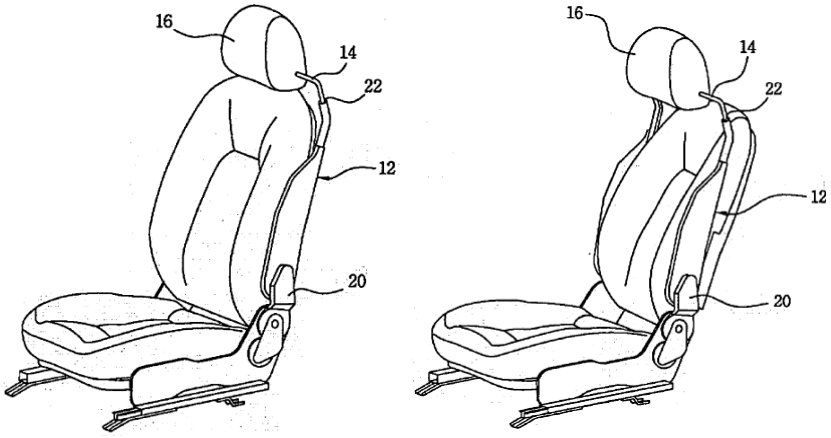

Figure 2.11 – Example of the development of an active head restraint to avoid neck injuries: a) Normal aspect; b) System activation on impact. [32]**.**

Figure 2.11 shows the development of the active head restraint to reduce the severity and number of injuries that can be sustained in a car accident. This system is projected to reduce the injuries from whiplash by reducing the course and speed of the head movement during a car crash. This action will reduce the damage made on the soft tissue of the neck, hence reducing the severity of the injury sustained during a car crash. Other systems have been developed to protect car occupants from external accidents. Figure 2.12 shows different safety systems and how they react to protect the car occupants from different car impacts. The first system (Figure 2.12 a) and b)) presents a system that activates during side impact car crashes and dislocates the car occupant from the impact area. In this system, some sensors are mounted on the vehicle to predict an impact. When identified an emergent impact, the seat is moved up vertically and towards the centerline of the vehicle thus creating space between the car occupant and the vehicle´s sidewall. Afterwards, an inflatable system is activated reducing the injuries that can be sustained by the car occupants.

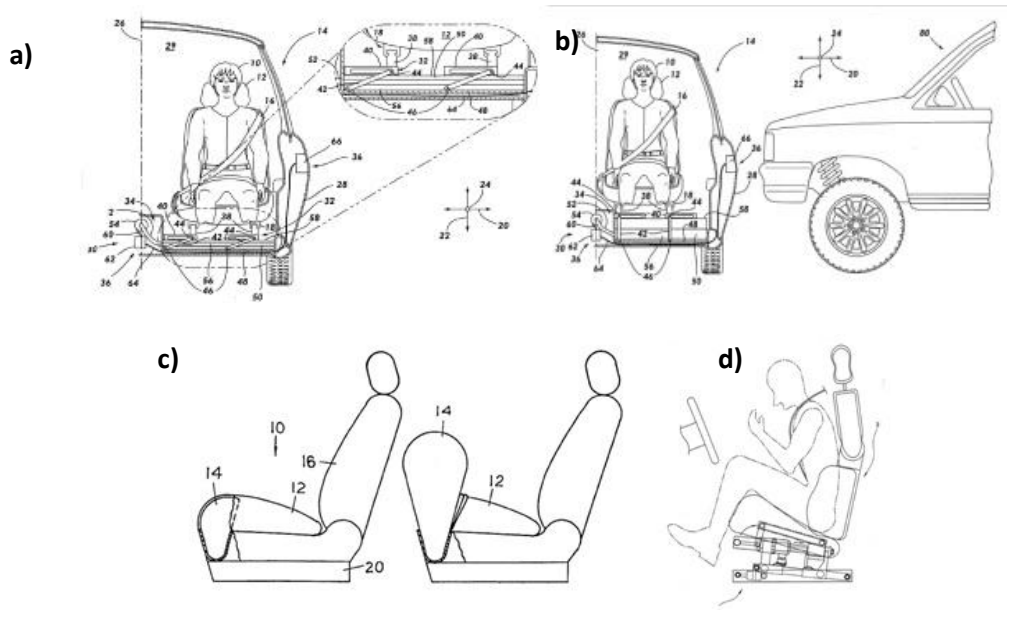

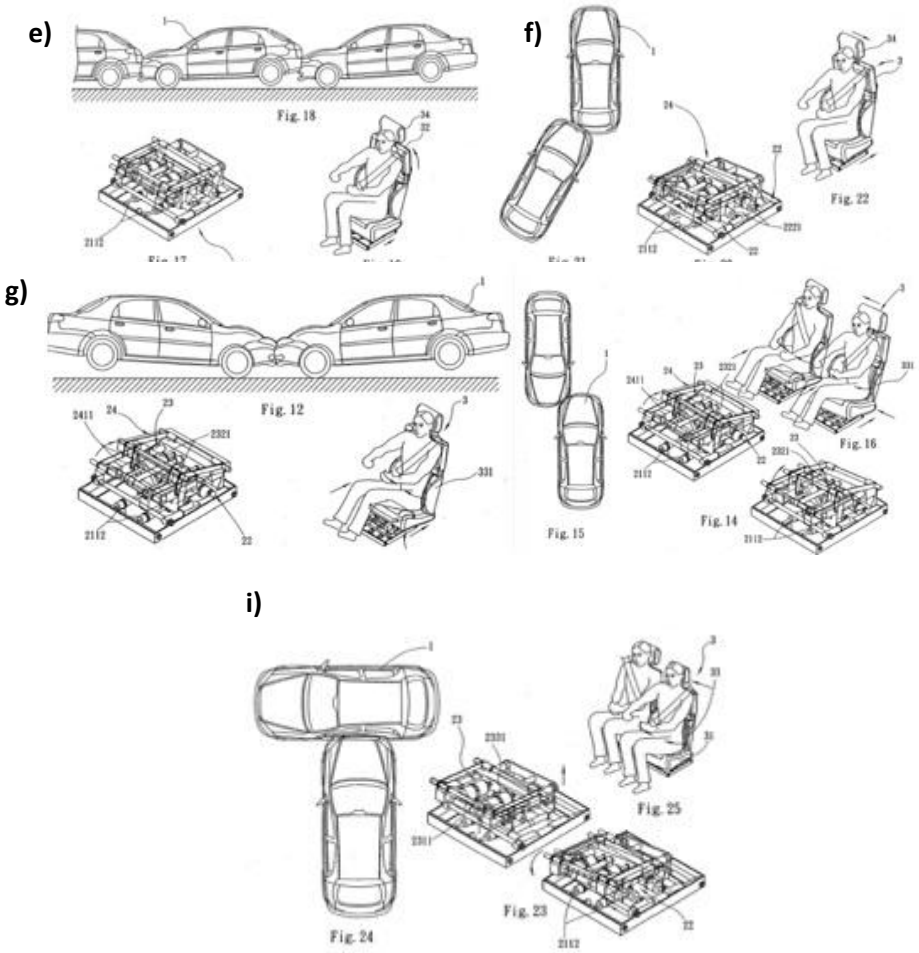

Figure 2.12 – Different safety systems: a) and b) Safety systems for side impacts [33]**, c) Airbag system mounted on seat** [34]**, d-i) seat adjusted for different impacts on the vehicle** [35]**.**

Another system is presented in Figure 2.12 c) were a deploying air system is mounted in the seat bottom and shoots upwards with the deployment of an inflating airbag during a severe car accident. The inflated airbag forms an enlarged effective surface area with the occupant's lower body , forcing the car occupant to a folded restraining position. The upward motion of the inflatable airbag creates a backward motion on the car occupant that opposes the forward motion of the crash. This backward motion restrains the car occupant's body from the initial inertial movement therefore protecting him from severe and likely fatal injuries.

Another seat system (Figure 2.12 d) – i)) presents a seat system composed by several cylinders, a displacement tipping device and a seat assembly. When the car body is subjected to a collision force in any direction, the displacement tipping device produces a relative reaction to eliminate or reduce the hitting force and also drives the seat assembly to quickly move toward the central portion of the car body protecting and preventing the driver's body from being hit directly. The different actions of the seat are presented in Figure 2.12 e) – j) and it can concluded that the seat acts differently for different car occupants, depending on impact to

better protect and reduce the severity of the injuries that can be sustained by the vehicle occupants.

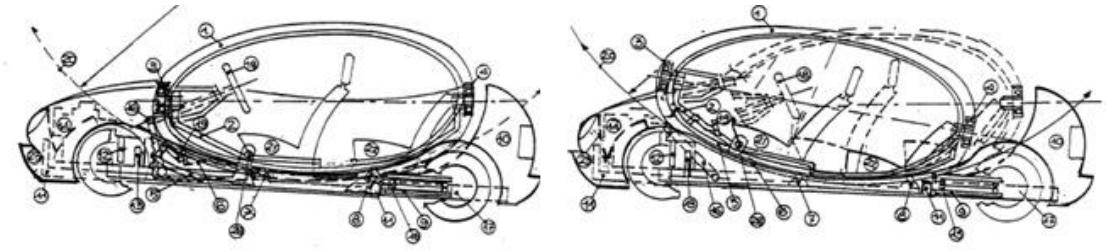

Figure 2.13 – Fluctuating compartment for injury prevention [36]**.**

Figure 2.13 presents another approach that focuses on changing the design of the vehicles to make it safer for the car occupants. In this system, the chamber where the car occupants usually stay is replaced by a fluctuating chamber that eliminates the forces consequent from car collisions. The inventors [36] state that this invention is particularly suitable for minimizing the driver and passengers' trauma during violent impact due to car accidents.

2.2.3 Comfort assessment and development

Comfort is a subjective perception that needs to be accounted for very carefully in the development of the seat, since a car occupant can spend a lot of time driving and needs to feel comfortable in order to spend all of his time focused on driving.

Kolich [37] identified that a discipline or methodology focused on the seat development comfort does not exist and that the most usual tendency is for the development teams to deal with this issue in a reactive way rather than a proactive manner.

Comfort parameters are very hard to determine, because they are keenly dependent on the persons' physiology and therefore comfort is not felt in the same manner among the all different potential drivers. This means that a seat comfortable for the 50 percentile male might not be as comfortable for the 95 percentile male or 50 percentile female.

Kolich [37] identified that the usual process used for the seat comfort development process follows the path identified in Figure 2.14.

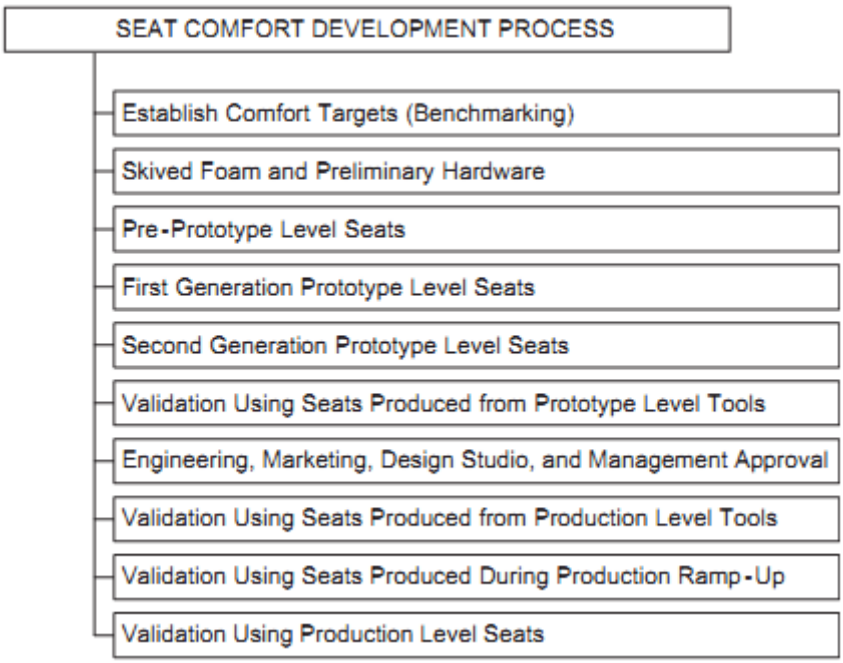

Figure 2.14 – Flow chart for typical seat comfort development process [37]**.**

Kolich recognized that the current seat comfort development process (Figure 2.14) is very inefficient and expensive. One of the reasons is that the evaluation of the seats during a ride is usually performed through a ride and drive evaluation. The time established for an appropriate ride and drive testing is usually limited by cost and by the number of evaluations that the team deems to be enough to provide a robust assessment about the seat evaluation process. This can also be related with the problem that when you have a large program you can have one hundred configurations of a seat and, therefore, it is very difficult to evaluate every seat through a single ride and drive evaluation. The usual process is to identify a good level of comfort for a high vehicle volume seats configuration and then try to check if the comfort is not negatively affected In other combinations.

Another issue arises from the fact that the seat interacts with the vehicle system. This system also has several development cycles and it is usually not finalized until the production stage. The allocation of the different parts of the vehicle like the powertrain, vehicle suspension and package characteristics also affect the seat comfort ratings.

With this assessment, Kolich reached the conclusion that the current process is extremely time consuming not to mention expensive, due to tooling iterations and very prone to measurement errors. As a result from this conclusion, Kolich also identified the main areas that require a methodological framework in the comfort seat development. These steps have been the object of several researches but they need further development in order to reach a consensus that can be applied to the automobile seat comfort.

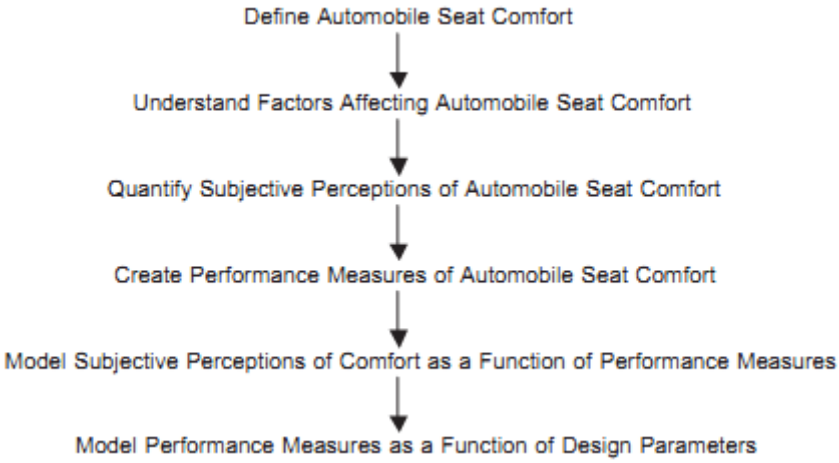

Figure 2.15 – Research required to establish a theoretical and methodological framework for the science of automobile [37]**.**

2.2.3.1 Definition of seat comfort

Kolich defined that the one of the causes related with the inability to formulate positions can be argued through experimentation and is caused by the lack of consensus regarding the definition of comfort [37]. In fact, it has been identified that there are many schools of thought regarding the definition of comfort, from the "absence of discomfort" defended by Branton (1969) and Hertzberg (1972), to a position that defends that comfort and discomfort are separate dimensions with the possibility of comfort increasing when discomfort decreases, a position defended by Shen and Vertiz in 1997.

It seems that in order to be able to define comfort, one of the major issues that should be quickly defined is in what school of thought will be chosen as the basis of our analysis to develop a seat.

2.2.3.2 Identification of factors affecting comfort

Comfort is a subjective and environmental dependent variable and, therefore, it is very difficult to develop a solution that satisfies everyone. Because of this, Kolich [37] identified several factors that can affect the perception of comfort that a person can have when sitting on a seat. A summary of these perceptions is summarized in Figure 2.16:

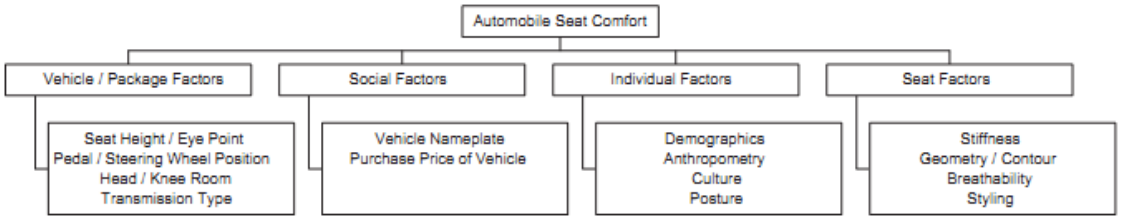

Figure 2.16 – Factors affecting subjective perceptions of automobile seat comfort [37]**.**

Four main areas that can affect the perception of automobile seat comfort were identified: vehicle/package, social, individual and seat factors. All these factors affect the perception of comfort and the results are dependent on the anthropometry and social background of the different persons.

The vehicle/package factors are related with the environment surrounding, the seat and the effects that it has on the perception of comfort for each person. The vehicle system affects the eye point of the driver and the space that the car users have for their body like legs, knees and arms. The important point is that if car users feel restrained inside the car they will perceive the car seat as being uncomfortable even if they had classified the seat as comfortable in other testing areas.

The social factor is a very subjective factor that can influence the perception of comfort of a car seat without any direct influence over the seat properties. These factors are related with the value that each person gives to the evaluated object and the environment where this object is inserted. Taking this factor into account, similar seats can be evaluated differently only because of the car's nameplate. This means that the same seat made for a high-class brand and for a medium-class brand might receive different ratings based only on the brand. This effect on the comfort perception seems to be dependent on the social status. The purchase price is related with the nameplate and therefore affects the perception of comfort in the same manner as the nameplate affects this perception.

The individual factors are related to individual preferences of the drivers. Although these factors may be easy to assess, it is not simple to transform these factors into global characteristics of the seat. This is due to the fact that several persons with the same characteristics can have a completely different perception of comfort since their usual sitting positions can be very different and therefore feel comfort in different manners. The seating posture is a field that still needs more study. The introduction of this data on the product development of the seat can help to optimize the seat design and help in the development of more comfortable seat solutions.

Kolich [37] also identified that culture or demographics can affect the perception of comfort. For example, Western Europeans prefer firmer seats than North Americans. This means that the way a person is educated influences the way they perceive comfort and, therefore, this variable should be accounted when developing a product directed to different markets.

The seat development is affected by several factors. The users' anthropometry is one of the study areas that need more research because in order to be able to obtain results about the factors that affects the perception of comfort by different persons. Developments in this area should focus on the development of better dummies and a better understanding of the different variables related to the human body. The decisions that take into account comfort and the anthropometric characteristics of different persons are usually very subjective and the final decision ends up being made based on feeling and not on the different data collected. Hanson *et al.* [38] made a study regarding the reach comfort and were able to conclude that the perception of comfort changes with anthropometry of the driver. In their case study, they were able to observe that the tallest persons were more comfortable inside the car than the smaller persons.

More data about the effects of the perception of users regarding comfort needs to be collected and relationships must be made in order to improve the decision-making process of seat comfort in seat design. Several studies have been made about the ideal position and how people usual seat during driving.

2.2.3.3 Quantifying factors affecting automobile seat comfort

There are several factors that affect the seat design; however, since the perception of these factors is usually subjective data, dependent on the perception of the users, one can conclude that questionnaire data is very important to the development of comfort in seats. However Kolich [37] identified that little emphasis is given to the seat comfort questionnaire design, which is very surprising attending to:

1. the high dependency that seat comfort development has on these questionnaires, and;
2. the several problems related with the collection of subjective data, which has been well known for a while.

A questionnaire needs to be valid and reliable such that the information collected can be effectively used in the development of the seat comfort. To achieve this, the questionnaire measures should be reduced to two components: the true score and measurement errors. A reliable questionnaire should have a very small measurement error; however, it is very difficult

to observe the actual score of a specific questionnaire item. The actual score of an item can be obtained through correlation techniques relating the data and giving the extent which an item relates to the true score.

The important indicators are: the test-retest reliability, internal consistency, criterion-related validity, construct –related validity and face validity [39], [40]. It has been stated by several authors that the reliability and validity of a questionnaire can be assured by considering the following principles:

a) The wording of the questionnaire items;
b) The number of rating scale categories;
c) The verbal tags associated with the categories;
d) The interest and motivation of the respondent, as a function of the questionnaire length.

Kolich [37] states that the quantification method must be well thought otherwise the obtained results cannot be used as a basis for the car seat development. If the quantitative aspects are not taken into account and well thought-out, the results can be biased or even invalid. If comfort researchers produce a rigorous questionnaire accounting for all aspects that were here described, current comfort design process can improve and possibly define meaningful variables for prediction purposes.

The same author [41] stated that the automobile specifications cannot be established without considering the comfort expectations of the target population. With this in mind, the author performed a study to correlate the ergonomic criteria with the anthropometric characteristics. For this intent the author evaluated 5 different seats with known contour and geometry and related with anthropometric criteria. Some discrepancies between the published anthropometric accommodation criteria were observed and the occupant preferences found in this study. The main conclusion of this study is that comfort cannot be standardized because it depends on unique characteristics dependent on each driver and therefore more focus should be given to the target population when evaluating developing the seats.

Since the need to develop a reliable questionnaire with valid conclusions on the seat comfort was identified, with this in mind Smith *et al.* [42] developed a questionnaire, the Automotive Seating Discomfort Questionnaire (ASQD), that contains significant questions and wording, readability, face validity, VAS repeatability, and reliable and internally consistent sub-scales. This questionnaire is sensitive to the subjective perception of seating discomfort over time. The author considered a 20 minute testing in which the subjects were influenced by internal

and external factors chosen to ensure the realism of the trial. This questionnaire was prepared focusing on the discomfort over time and they obtained reliable information about the components of the seat that most influence the discomfort when different people are driving. In an analysis to prove the validity of the ASQD, the author compared the results with other questionnaires and concluded that the ASQD is able to provide more detailed and comprehensive results than other questionnaires. In addition, it can measure the seating discomfort in a reliable and detailed way. This questionnaire can also provide information on how different areas of the seat contribute to the discomfort. This questionnaire can be adjusted for different research purposes regarding comfort.

In a similar study, Kyunga *et al.* [43] studied the influence in the comfort and discomfort perception during a ride. The tests performed lasted 20 minutes and 6 different seat conditions were tested. These authors used 2 scales to evaluate comfort and discomfort (Figure 2.17) and also took in consideration where in the body the subject feels discomfort and comfort. In order to reduce confusion about the obtained information, the authors systematized how the information was obtained in order to reduce the errors related to it.

The results of this questionnaire show that if we focus on the overall comfort it is difficult to have a complete perception if the subject feels comfort or discomfort. If the assessment of comfort/discomfort is differentiated in different body parts it becomes easier to identify which parts of the seat need improvement to increase the comfort. Also, comfort ratings were more suitable to differentiate between seats. Based on these results, the author suggests that in similar approaches discomfort ratings should be used to evaluate the basic properties of the seat focusing on preventing pain while comfort ratings should be used to promote pleasure approaches and is related with more subtle qualities of the seat.

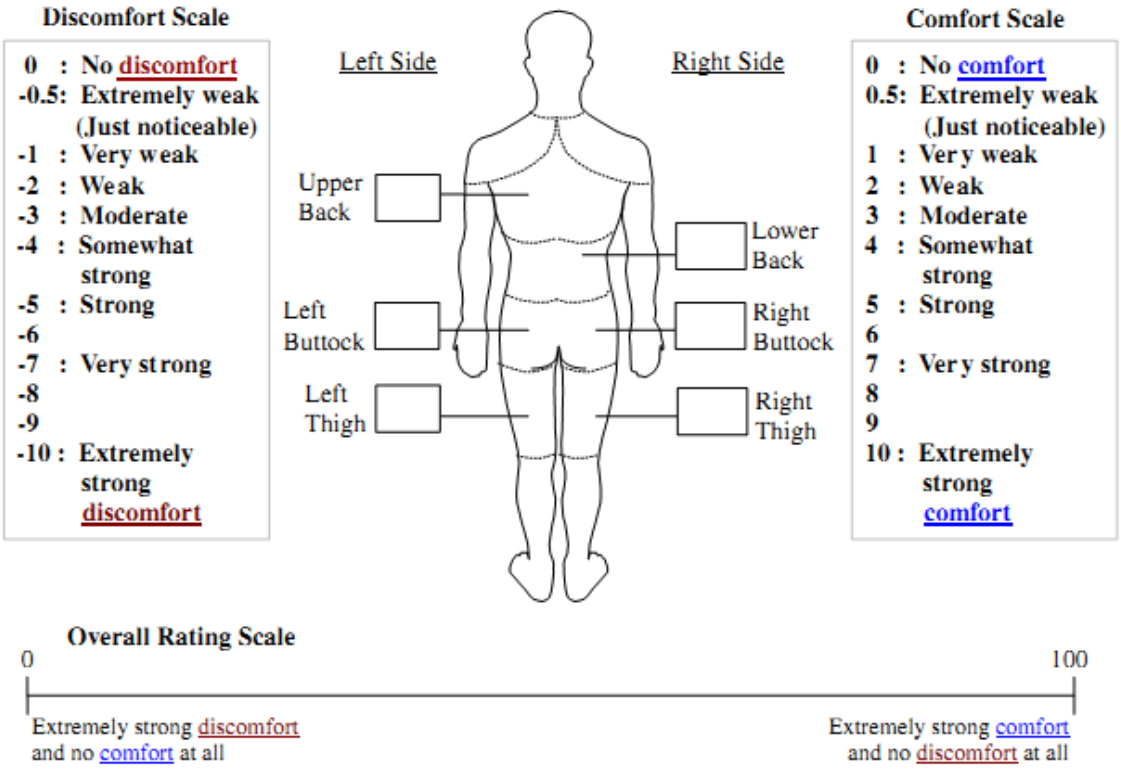

Figure 2.17 – Areas used for comfort evaluation [43].

Kamp [44] made a study to assess the comfort felt by the subjects regarding the seat. Instead of using the usual methods of numerical assessment this author used emocards (Figure 2.18) that represented different emotions. These could give an evaluation of the seat and which features are related to different seats.

The study made took into account different seat contours and found that people relate different feelings and features to the seat depending on their class. With this, the author tried to find which features of the seat are associated to the different classes of seat. The main features of a sporty seat are the width, contour, steepness of wings and hardness, while for a luxurious seat the main features that people relate to it are width, steepness of wings and hardness. The importance of this study comes from the fact that a novel way to study the subjective perception of the subjects is used, by making drivers choose feelings that they relate with a specific property; knowing what people value in a specific seat can focus the development in those areas in order to augment their influence on the subject.

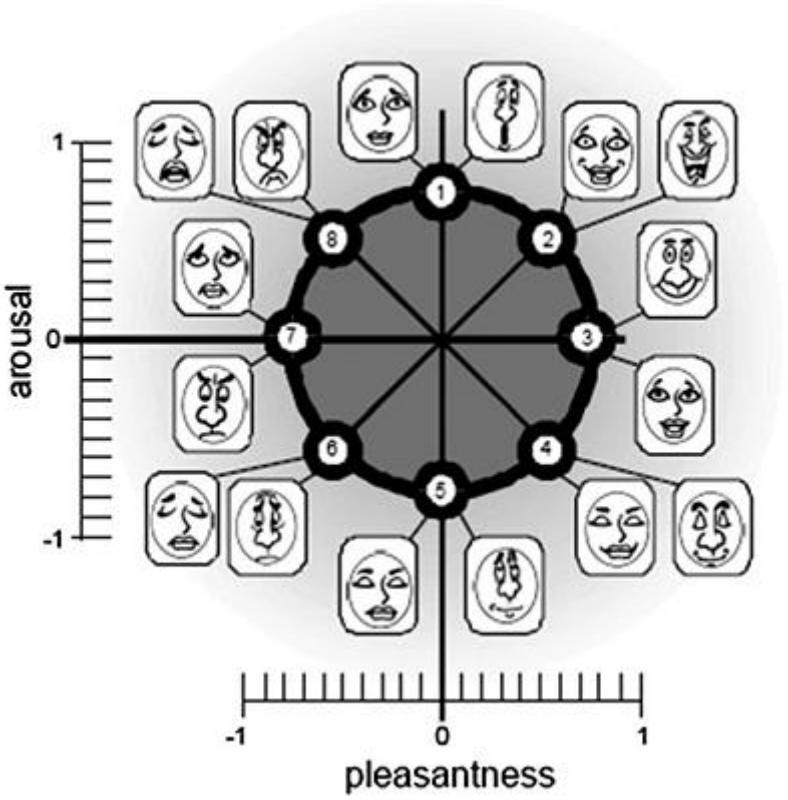

Figure 2.18 – The 16 emocards placed in a Russell's circumplex of emotions [44]**.**

During seat rating exercises it is necessary to establish the time to evaluate the seats and have a high confidence in the results obtained. Fernandez and Poonawala [45] made an experiment to determine what is the ideal time that these experiments should take in order to have a high validity and reliability. They started making experiments that lasted 8 hours and determined that the optimal time to evaluate a seat is around 3 hours. This is because the results that are obtained at the end of the third hour are not significantly different from the ones obtained at the end of the 8 hours. This evaluation was made for office seats; however, a similar exercise should be performed for car seats to determine the best times considering different conditions. These conditions can be static seat testing, short driving and long driving testing. For these different conditions it is important to make a careful analysis and determine the best times for each. This would make the testing reliable and prevent the use of excessive time in each experiment.

2.2.3.4 Creation of performance measures for automobile seat comfort

There are several factors that can be influenced in order to improve comfort:

- the seat properties,
- thermal comfort,
- muscle fatigue,

- vibration transmissibility.

The coupling of these factors would be enough to compare different seats and assess their differences. However, the seat comfort industry needs objective and measurable laboratory standards that are linked to the subjective perception of comfort.

The pressure distribution might be dependent on the person anthropometry. For example, a large person can feel comfortable in almost all seats because the weight is well distributed on the seat. The same person can feel comfortable even in hard seats. A slimmer person will have a higher pressure peak and might feel uncomfortable even on well-padded seats. Therefore, research in this area should be focused in specific groups to obtain more accurate results regarding their anthropometry.

Hostens *et al.* [46] studied the pressure distribution on 4 different seats and was able to conclude that there is a linear relationship between the body mass index and the mean pressure. The author took precautions to eliminate pressure distribution differences by other factors and was also able to increase the reproducibility of the results. The main precaution was to force people to have their feet hanging free, which decreased the variability of the pressure distribution since weight stops being supported by the feet and legs. Although this method seems to be very suitable to find the pressure distribution in the seat, because the subjects have their feet hanging, it does not give the result of the real life situation. Even so, the results and experimental methods are interesting to read and probably to apply in a full seat testing. One possible way to develop this assignment could be to relate the proposed methodology to real life situations. The author concludes that the cushioning should have modularity characteristics that could enhance the comfort by adjusting the countering of the seat.

Another factor that affects the seating comfort is the seat depth. The seat depth is related with the cushioning which is, in its turn, related with how much the seat deforms when a person sits. It has been observed that these values depend on the target population and several sources have identified different depth intervals (Table 2.2) that are dependent on the target population.

Goonetilleke and Feizhou [47] developed a methodology to study the effects of changing the seat depth on people's perception of comfort. From the study it was observed that with an increase in the seat depth the driver would feel more uncomfortable after an extended period of time in that position. One reason that is pointed out is that a big seat depth deprives the driver from the full benefit of the backrest. The authors found out that for a student

population of south China the most suitable seat depth would be from 31-33 cm. Attending to the different seat depth in literature and regulations (Table 2.2) it can be said that in order to have an effective depth size it is necessary to know the person anthropometry in order to make an effective choice.

Table 2.2 – Seat depth recommendations.

Source	Criterion	Recommended seat depth (cm)
ANSI/HFS 100-1988	Standard industry practice	38–43
BS 5940 Part 1 (1980)/BS 3044 (1990)	Smallest person in design range (38–43 cm with fixed back)	40.5[a]
BellCore (1985)		40.6–43.2
CEN[b]		38–47
DIN[b]		38–42
Swedish standard[b]		38–43
Bennett (1928)	Less than 6–8 in. between popliteal part and the front edge of seat	more than 20–25[a]
Diffrient et al. (1974)		33–41
Kroemer et al. (1994)	Do not press into sensitive tissues near knee	38–42
Ayoub et al. (1987)	10 cm clearance between popliteal part and the front edge of seat	30.5[a]
Grandjean (1986)		38–42
Courtney and Wong (1985)		40
Pheasant (1991)	Not exceed 5th %ile BPL	<40.5[a]
Shao and Zhou (1990)	Three-quarters of the thigh length	30.4[a]
Lee et al. (1998)	5th% ile BPL-2 cm (for leisure clothing)	38.5[a]
Keegan and Radke (1964)		40.64 (16 in.)
Floyd and Roberts (1959)	Distance between popliteal area and seat edge of 6–8 in. (15.2–20.3 cm) for large adults; 3 or 4 in. for small children	

[a] Based on 5th %ile BPL of 40.5 cm as given in Pheasant (1994).
[b] Adapted from Chaffin and Andersson (1991).

Kyunga and Nussbauma [48] evaluated the drivers seating comfort and discomfort during short-term driving and tried to establish a relationship between pressures and subjective responses. The authors made different tests where the subjects had a driving experience of 20 minutes to test the seat and assess the seat. The authors identified several pressure variables that were suitable to assess sitting comfort and discomfort. Based on the results, the authors recommended having a lower pressure ratio at the buttocks and a higher pressure ration on the upper and lower back. It was also concluded that comfort ratings were more suitable to evaluate comfort based on the human-seat pressure distribution.

Thermal comfort is a one of the factors that greatly affects the passengers when they are driving an automobile. Raising the temperature and humidity will provoke discomfort on the person driving. One of the issues is related to the person perspiration that increases with the augment of temperature and humidity. In this situation, the skin needs to breathe so water vapor needs to be able to pass through the seat. Therefore, the selected seat cover material needs to have a big water vapor diffusion coefficient. With the increase of the permeability of the seat cover it is possible to decrease the temperature that a person perceives from the seat.

Cegiz and Babalik [49] studied the thermal comfort on road trials environment. Three different seats were tested and, in order to guarantee that the performance was similar, covers that had the same perception of thermal comfort between them were used. It is suggested that traffic conditions affect the driver´s perception of comfort and that this influence is also dependent on his experience. In the search for comfort, the authors found that there was a small difference between the perceptions of comfort in the different seats but this difference was considered negligible. Another interesting result was that during driving the driver felt warmer around the waist. This result suggests that in-road conditions should be accounted when designing the seat.

Sven-Erik *et al.* [50] developed a series of evaluation mechanisms using sensors in order to evaluate the different seats based on mechanical, thermal and humidity tests. The moisture test method has shown the importance of the surface material to obtain a comfortable seating. This test measured the resistance to moisture transportation through different covers and established that the lower the resistance the more comfortable the seat is. The sensors were able to provide information about the pressure distribution, heat flux, air permeability and moisture transport. These analyses can provide a good idea of the comfort in these seat systems.

The muscle fatigue is one of the issues that most disturb the drivers when they are driving during several hours. So muscle fatigue ends up being one of the variables that can influence comfort the most in long drives. Usually, to quantify the fatigue, an EMG is used to measure the electrical activity of contracting muscles.

Vibration transmissibility is related to the fact that the seat is a component inside a bigger system (the vehicle). With the help of accelerometers, it is possible to quantify the vibration passed from the seat to the car occupant. The vibration that the car occupant receives will eventually be perceived as discomfort, so in order to diminish it, efforts must be done to decrease the vibration that passes to the car occupant.

In a study to validate metrics to better assess the vibration transmissibility, van der Westhuizen and van Niekerk [51] made a study to validate if seat effective amplitude transmissibility (SEAT) could be used as a reliable metric for the evaluation of the vibration transmissibility inside a vehicle. The main premise of this study is that the vibration of the vehicle is passed on to the seat that influences the comfort of a person. So an optimum seat would be the one that can minimize unwanted responses of the occupant related to the

vibration environment. The SEAT (Eq. 1) is the ration of the vibration seat and floor and accounts for the human sensitivity.

$$\text{SEAT}\% = \frac{\text{Vibration on the seat}}{\text{Vibration on the floor}} \times 100 \qquad \textbf{Eq. 2.1}$$

A test was performed with 6 different subjects to analyze the validity of the SEAT as a vibration metric. It was found that some subjects were not so sensitive to different levels of vibration. Overall, the SEAT was able to have a good correlation between the measured values and the results obtained from the tests. This metric seems to be a good one to measure the vibration transmissibility.

Ng *et al.* [52] evaluated an intelligent seat design. This seat system is a micro-processor based seat that automatically adjusts itself to the person making small sensitive based adjustments. An evaluation of the system based on subjective and objective parameters was performed and it was concluded that this seat system improved comfort qualities. The subjects felt that the self-adjusting system made the seat more comfortable and customized itself better to the drivers' needs. Despite having a very good feedback from the subjects, there were some complaints about some properties of the seat, like the seat cushion could be firmer, the seat depth could be bigger, and have a higher support for the thigh and shoulder. The tests show a decrease in pressure distribution across the buttocks and thighs and an increase in the pressure on the lumbar region. This increase in pressure in the lumbar part relieves most pressure from the upper back. This intelligent system can also easily adjust itself to people of different weights and sizes which can be a good principle in the dissemination of this technology. This seat is an intelligent system that can adjust itself to increase the comfort for a given person and the different tests done seem to be enough to validate this seat for usage. However, there is the concern that it has not been seen how such an intelligent system handles itself when submitted to sudden changes in pressure usually related with car crashed and impacts. Despite these, the basic safety measures must be taken into account sudden stops like car crashes occur. This system will make adjustments in the seat in this situation which might result in a bigger damage to the car occupant than what can be foreseen.

2.2.3.5 Modeling subjective perceptions of comfort as a function of performance measures

One of the main questions in seat comfort development is how can the information acquired from subjective perceptions of comfort (obtained from questionnaires) be linked with performance measures (obtained through different methodologies).

There are several modeling techniques for this end, statistical techniques are one of the alternatives which can have solutions with enough information, while neural networks seem to be a viable alternative that can give predictions about the trends with enough data collected. These prediction models [37] can provide insight on:

1. how well subjective perceptions of comfort can be explained by knowing the value of a set of predictor variables,
2. which subset from many measures is most effective for estimating subjective perceptions of comfort (i.e. weighting the performance measures).

With validated models, the seat system design teams would be able to focus on the most important performance parameters. The main goal of the predictive models is for them to help design teams earlier in the process and help them understand how they can improve comfort earlier in the process.

Hansona *et al.* [38] used the fuzzy logics approach to model relations between human perception, human characteristics and workplace structure. The authors built a comfort model that considers the drivers' posture and anthropometry in the perceived comfort when handling the inside of a car. This study focused on understanding how different people perceived comfort when trying to reach different things inside the car; it was possible to establish a relationship between the comfort and the comfort perception. The driver's anthropometry and control positions are used as inputs which can be assumed as the body postures of the driver. The developed model by these authors was able to provide more information about the reach comfort which can later be introduced to seat development engineers. Fazlollahtabar [53] developed a multicriteria decision making technique where he couples techniques like AHP (Analytical hierarchical process), Entropy Method and Technique for Order of Preference by Similarity to Ideal Solution (TOPSIS) to help quantify the qualitative results into seat comfort parameters. This study was confirmed with a target population and the author suggests that this technique could be used by the car manufacturers to identify the best options for the existing seat and particular target population. This decision making technique has the advantage of joining different techniques that can transform qualitative inputs and transform them into numerical values taking into account the importance of the criteria used.

Kolich *et al.* [40] compared neural networks to the typical statistical model and evaluated them to see which of the methods could better predict the perception of comfort by drivers. Neural networks have been deemed superior to the regression model because the results had less errors related to them. This is due to their ability to deal with interaction effects. Neural

networks consider a large number of inputs and can determine how a specific set of inputs will affect a more focused subset of a target population. Because the perception of comfort evolves along time, the use of neural networks can enable more accurate predictions of how the seat should be developed in order to reply to the increasing demand of more comfort inside a vehicle. Kolich [54] in a similar work reached the same conclusion in which he used the neural networks to predict the pressure distribution; one advantage of the neural networks is that it can relate the subjective interpretation of comfort to the pressure distribution results making the seat evaluation simpler and meaningful. With this method design teams can us reduce the time spent on the seat development and replace the jury evaluation that ends up being dependent on the decision-maker opinion. When neural networks have a large enough database, they can predict future evolution in the comfort trend. This would be a great advantage taking into account the identified change of comfort perception along time.

Lee *et al.* [55] focused their efforts in developing the Structured Equation Model (SEM) that allows to assess ride comfort in high speed train. They used different characteristics, including fatigue and medical symptoms, to evaluate seating comfort during a train ride. For this study they interviewed 450 people and were able to obtain reliable results. Besides it was also possible to identify that riding comfort is mainly affected by seat, fatigue and interior variables. The decomposition of the different factors together with the answers obtained allowed them to clearly identify the main components that affect the most the comfort inside the train. The seat width, seat shape and seat pitch were the variables that if changed could improve the comfort in a very significant way. However, this study has limitations because it focused on train rides; nonetheless the ride comfort model can be applied to other transportation applications.

Some authors are trying to join different predictive models together in order to increase the robustness of the predictions. One of such works is the one developed by Chen *et al.* [56]: these authors joined the fuzzy logic with neural networks to improve the predictions and interpretations that are provided by these systems. The main reason to introduce this combined model is that thermal comfort is a very vague term not easy to grasp so the authors thought that by combining these two models it would be possible to make non-linear regressions over the existing results, therefore improving the model learning from the collected data. The authors considered the temperature and humidity as the main variables of the system and it was shown that the results of the temperature were highly dependent on this area. The authors state that in order to make this model more effective more information must be included not only considering thermal comfort, but also other kinds of comfort. This

would make the model more effective and much more suitable to be applied during the seat development stage.

2.2.3.6 Modeling performance measures as function of design parameters

The modeling of the performance measures provides a great deal of information but they do not offer information about the changes needed to obtain the desired result. The previous modeling does not give results to obtain the desired properties in a seat and therefore cannot help the design team to obtain the aimed result.

Other modeling techniques that deal with different properties of materials and human-seat interaction can help in this. These modeling techniques include:

- Finite element modeling;
- Multibody modeling.

These models try to characterize the human body through different models that are connected in different points (nodes). Researchers are focusing on the development of human body models to model the human behavior under different loads, paying special attention to the pressure distribution and vibration transmissibility.

Multibody modeling models a human body using rigid bodies connected by massless elements such as dampers or springs. Several joints that constrain the degrees of freedom connect the elements in chain. External forces will cause motion on the interconnected elements. This type of modeling allows the definition of flexible bodies instead of rigid ones.

Two types of modelling techniques can be considered for seat models involving multi-body and finite element analyses each with their own advantages and disadvantages. Finite element models can accurately predict deformations but at high computational costs, while multi-body models can only globally describe the effects of deformations but with high computational efficiency. The multi-body technique enables the definition of rigid and flexible bodies.

Verver *et al.* [57] studied the use of multibody modelling to simulate the transmissibility of vertical vibrations seat-to-human. Some experimental studies were done which supported the results obtained. With this model together with the utilization of the human model the authors were able to predict the (dis)-comfort caused by vertical vibration with a variation of the cushion and suspension properties. If this tool is introduced earlier in the project it could aid in the development of better seat designs focused on the comfort of the drivers. The author also states that the use of multibody enables a high reliability in the human-seat interaction and it is an efficient method in terms of computational time. This method is

attractive to replace simulations that take long CPU times and that do not require information about deformations.

Grujicic *et al.* [58] developed a model in finite element to assess the comfort that can be perceived by a car occupant. For this purpose the authors developed a human and car model and studied the human/seat interaction to assess comfort. The developed model calculates contact pressures, contact shear stresses and in-body stresses; these values can be correlated with the car occupant comfort perception. Although the developed model provides results that can be used to assess the perception of comfort, the author states that they had some difficulties simulating soft tissue material and, in order to have more reliable results, further development should be done in this area. Another issue that arises is that no study to obtain subjective perceptions of different people was developed and this type of study could improve with this subjective assessment.

2.3 Research questions

This analysis has shown that there are several aspects that must be taken into consideration when developing a new car seat. The materials and processes that are being used by the car manufacturers are important, but the safety and comfort of the car occupant must also be a high priority to make the seat more attractive and help in the seat design.

The automotive industry has been following the trends imposed by Kyoto regulations that focus in a reduction of the CO_2 emissions. In order to accomplish this it has been observed that there are two possible ways:

- The increase of efficiency of the motor vehicles,
- Decrease in the overall weight of the motor vehicle.

This research is focused on the seat and therefore the actions made will focus on the latter approach, weight reduction. This research intends to answer the following research question:

"What is the best strategy to reduce weight in a seat in automotive industry?"

There are several options to reduce the weight of a seat; it can be either by changing materials or by changing the design of the seat. A combination of the seat design optimized for the material seems to be the best option. Changing the materials does not seem to be a straightforward process, since different materials from the existing ones will have special requirements that might not be answered with the existing equipment. The choice of the material and design should consider the processes needed to successfully build this seat at a lower cost.

"Which processes should be included to produce these seats?"

It has been confirmed that different materials and design will require a more thorough investigation to determine if the chosen processes can be used to effectively change the materials as it is expected. To do this the existing processes to fabricate the existing seats must be studied and the changes that must be performed to enable the manufacturing of the new seat require evaluation. A more experimental approach must also be performed regarding the processes that will be implemented in order to understand the viability of such processes and the best parameters to accomplish the desired goals.

"How to decide which product should go to manufacturing stage?"

Seat development may have several iterations that can lead it to be a very expensive process. Different methods can be used to predict the behavior of the seat under different stimulus. It is necessary to replicate the different tests to guarantee that a seat is safe and that it complies with regulations standards. The selection of the simulation and prediction tools must be made to guarantee that the seat can have at least the same performance of the existing seats. Apart from this analysis other concerns must be taken into account in the development stage. Externalities like the variation of the products or the location of the suppliers, which have a great influence in the business, should also be taken into account.

To be able to reach a conclusion to these research questions a research strategy divided in three main areas was developed (Figure 2.19):

- Information Gathering;
- Technology Assessment;
- Decision Making.

The Information Gathering Stage is identified by the Figure 2.19 as the yellow area of the research stage. In this stage the goal is to identify the material and existing processes that can be used in the manufacturing of this seat. The chosen processes can be an already existing processor processes that are in a later stage of development. The benchmarking brought ideas regarding the design of the existing seats. The client interaction with the seat can provide important indicators regarding the seat design and some requirements that will be reflected the decision making stage.

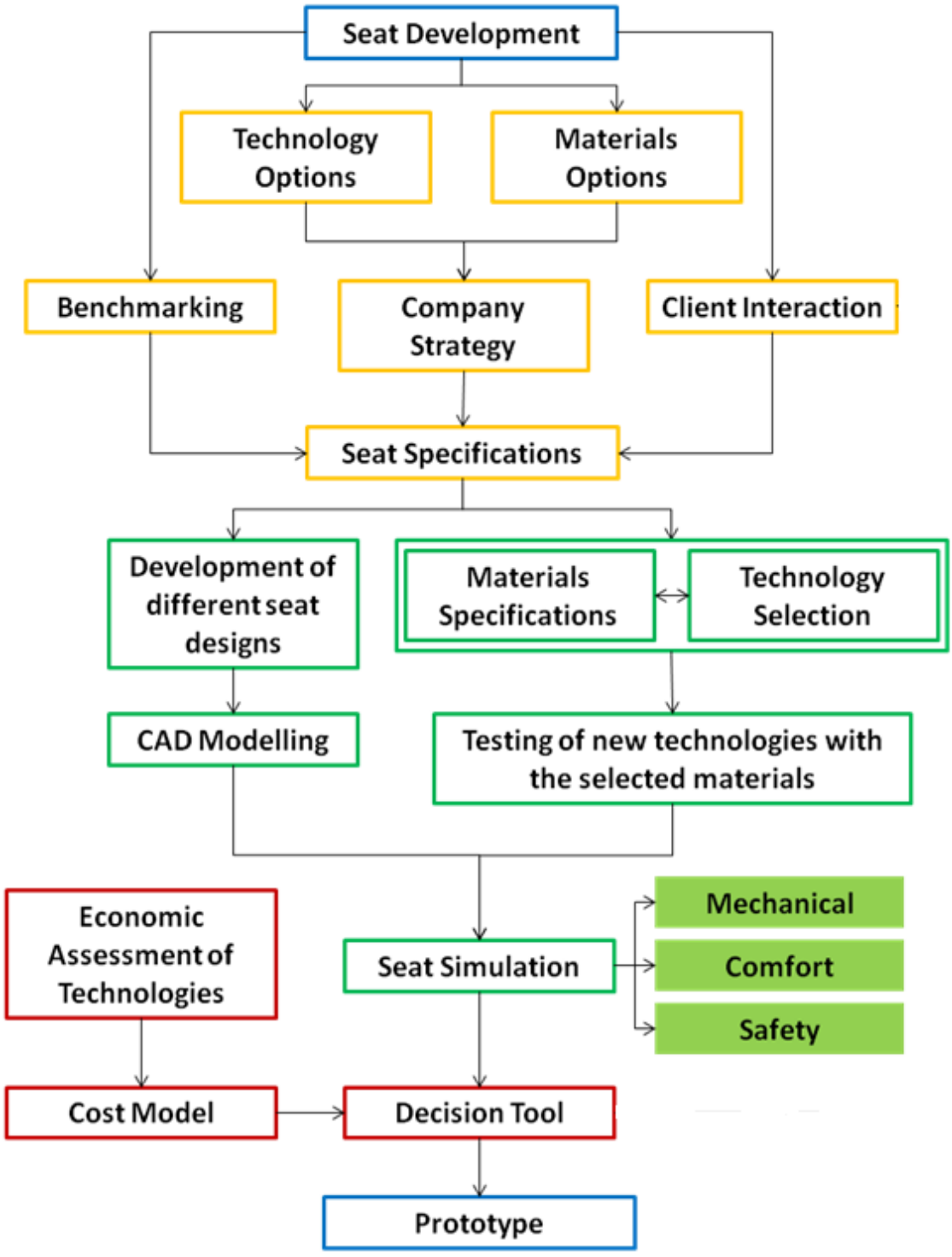

Figure 2.19 – Research strategy for seat development.

The technology assessment stage is depicted in green in Figure 2.19. In this stage an assessment of the materials and processes that can be used in the development of lighter seats is performed. The new seats will be developed using CAD modeling and simulations tools to evaluate the seats under different loads. This assessment needs to comply with the existing automotive and other standards depending on the selected technology.

The decision tool stage is depicted in red (Figure 2.19). In this stage the seats are evaluated according to the automotive standards but also the economic advantages that this seat will bring to the company. These seats must also guarantee that they are safe and comfortable for the car occupants as the existing produced seats.

The main goal of this research work is to find a framework that can help the automotive companies to introduce new technology. This research works wants to help addressing some important issues that can be found in the new technology introduction. Another goal is to reduce the time needed for this stage. Therefore, the purpose of the present research is to follow the aforementioned strategy to accomplish these goals.

3 Improving the seat

This section is focused on the selection of processes and materials that can be used to improve the weight of the seats while maintaining their performance. To come to a decision different selection stages were used to make this selection. The different selection stages are the following: material selection, finite element evaluation, benchmarking, process selection and alignment with industry trends.

3.1 Materials selection

The first step in this selection process was to analyze a large number of materials in order to identify the best materials that could be used to reduce the weight of the materials. To make this selection the CES Edupack 2011® program was used, allowing to relate different material properties and enabling to view how each stands before another. This program can provide a listing of the materials most suitable for the required function. In this stage, the aim was to find the materials that can provide lighter solutions and that can be introduced very easily in the normal day operations of a company.

Table 3.1– Constraints and objectives for material choice.

Function	Bending beam
Constraints	High stiffness High yield strength Not flammable
Free Variable	Thickness
Objective	Reduce weight

In Table 3.1 the objectives and constraints of this selection process are depicted. These constraints take into consideration the conditions to which the seat can be subjected to during its lifetime. In Figure 3.1 and Figure 3.2 the two steps in this selection process using CES Edupack® are presented. The aim is to minimize the weight of the seats while keeping the same performance. In this process the materials located in the upper left area present the best relationship between stiffness and yield strength over weight.

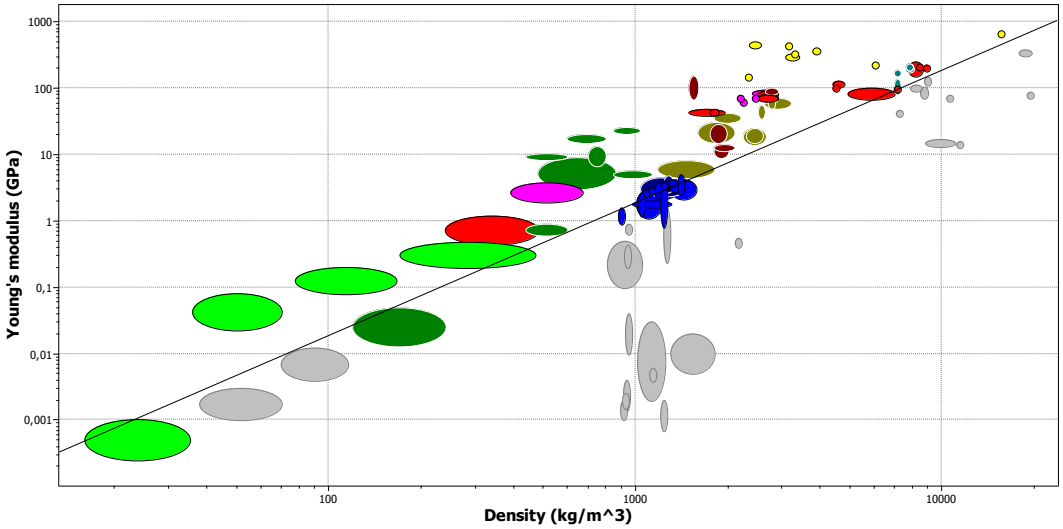

Figure 3.1 – First material selection step using CES Edupack® 2011.

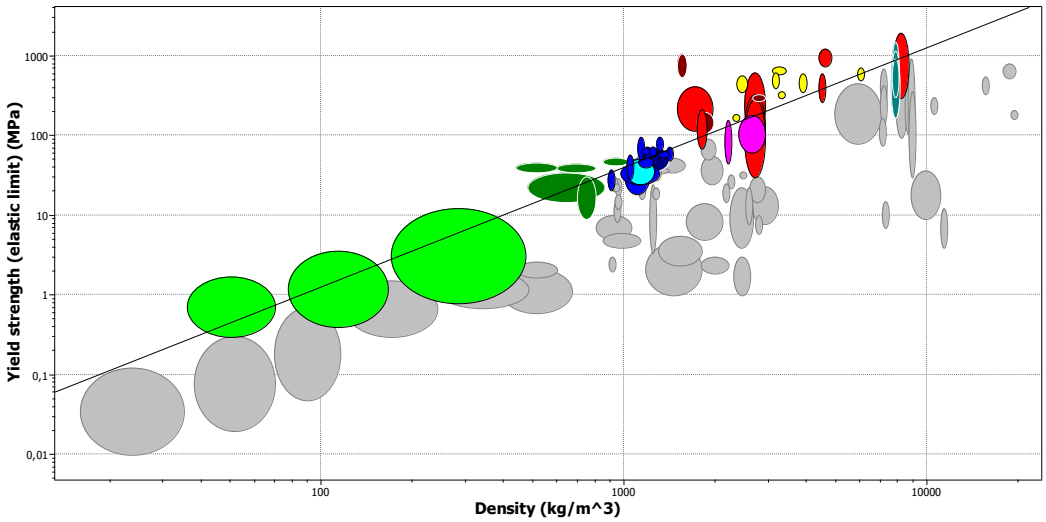

Figure 3.2 – Second material selection step using CES Edupack® 2011.

A third step was included in this process in order to rule out flammable materials and materials with low fracture thoughness. The materials that comply with all these boundaries in the three selection steps will provide the range of materials that are most adequate for the coming application. In Table 3.2, the results from all the previous selection steps are presented.

It can be concluded that metallic and composite materials survived these selection process. The metallic materials can be divided in steels and aluminium and magnesium alloys. The composite materials have two materials: the GFRP and CFRP. The next selection step is the introduction of finite element simulation in order to assess how the different materials can influence the different properties of the seat that are taken into account in this selection process. This next stage assesses how the different materials need to improve to have the

same performance as the steel seat. It also presents a combination of the differences and the influence on their properties.

Table 3.2– Materials that survived all selection steps.

Composite Materials	Non-ferrous Metals	Ferrous Metals
Carbon fiber reinforced polymers (CFRP)	Age-hardening wrought Al-alloys	Cast iron, ductile
Glass fiber reinforced polymers (GFRP)	Cast Al-alloys	High carbon steel
	Cast magnesium alloys	Medium carbon steel
	Non-age hardening wrought Al-alloys	Low alloy steel
	Wrought magnesium alloys	Stainless steel

3.2 Finite element selection process

3.2.1 Development of comparison model

In this stage, it was evaluated how the materials that have passed all stages will influence the performance of the seat. For this purpose, a seat that is already in use [59] has been selected for this sensitivity study allowing an evaluation of these materials in the chosen application. In Figure 3.3, a picture of the actual seat and the model developed by Finite Element Method (FEM)are presented This is a hybrid structure that uses both tubular and stamped parts with 2mm in thickness. This seat has a weight around the 13.84kg.

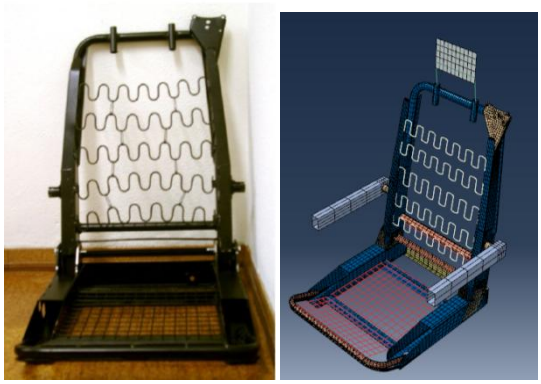

Figure 3.3 – Images of the chosen seat (on the left) and the FEM model (on the right) [59]**.**

In order to make a proper evaluation of this seat, the steel seat was simulated to evaluate its performance in different tests that are usually performed according to the automotive industry standards [60]. There are four tests that are usually applied in order to evaluate how the integrity of the seat performs. In one of these (Figure 3.4) the integrity of the headrest in which is applied a force of 890N is tested besides the dislocation of the headrest that should be at most 102mm.

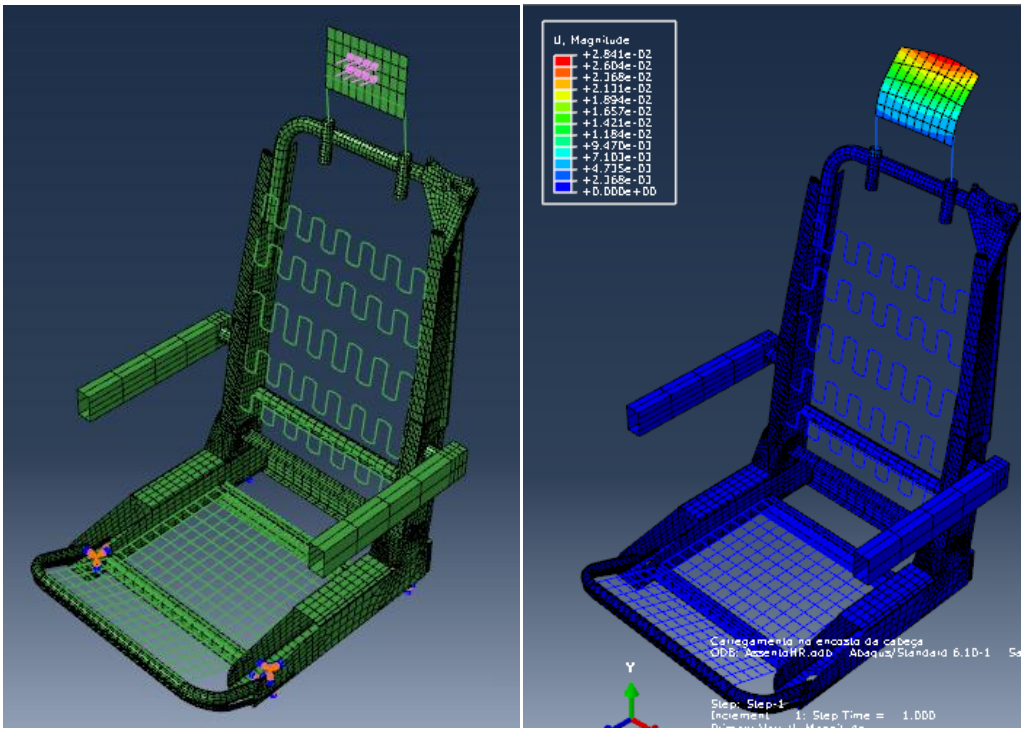

Figure 3.4 – Test to headrest integrity: model with applied forces (left) and displacements (right).

In this test it was observed that this seat meets the specifications established by the automotive regulations. It was also observed in this simulation that the seat does not surpass the 30mm displacement therefore fulfilling the requirements set by the standards.

In the second test [60] a moment of 374N.m is applied on the seat in the seatback upper cross member. The main purpose of this experiment is to observe whether or not the material surpasses their tensile strength in any area of the structure. Figure 3.5 shows the model and results of this test.

It was observed that the maximum stress on the seat is around 159MPa. Taking into account that this seat is made of steel it is possible to conclude it will not have any problems regarding this force because the tensile strength in these alloys is around 310MPa. It was also observed that this seat design made in steel can withstand this test; however there are two more tests that can provide further information about the seat integrity.

Another test according to the standards was applied. Here a force of 20 times the weight of the seat is applied in a longitudinal direction on the gravity center of the seatback. Like the previous one, this test is meant to observe the integrity of the seat and the influence on the seat properties. Figure 3.6 presents the model and results regarding this stage.

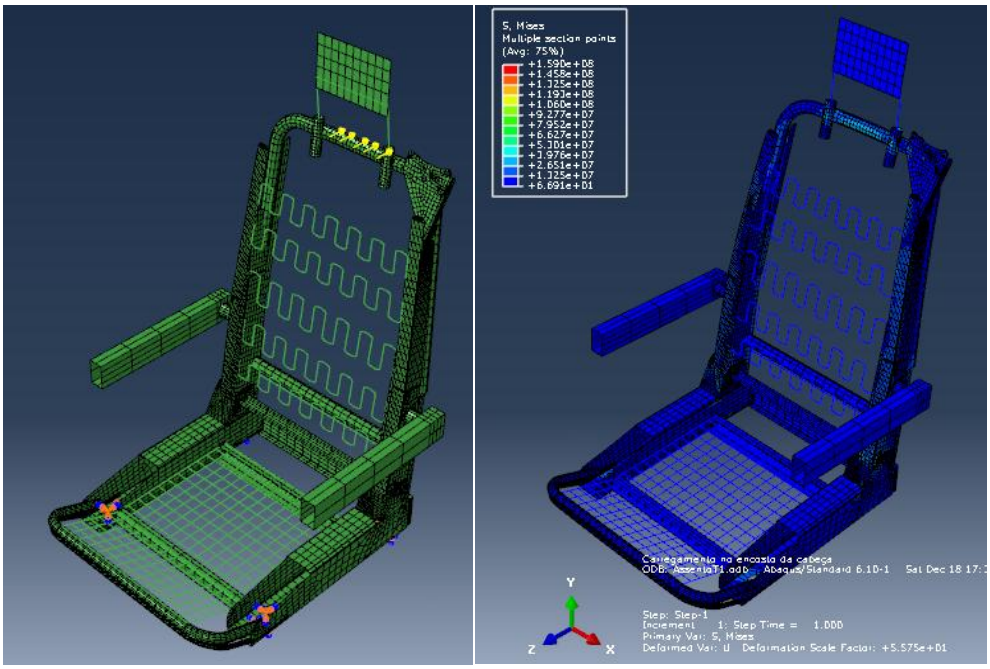

Figure 3.5 – Test to integrity of seatback: model with applied forces (left) and stresses.

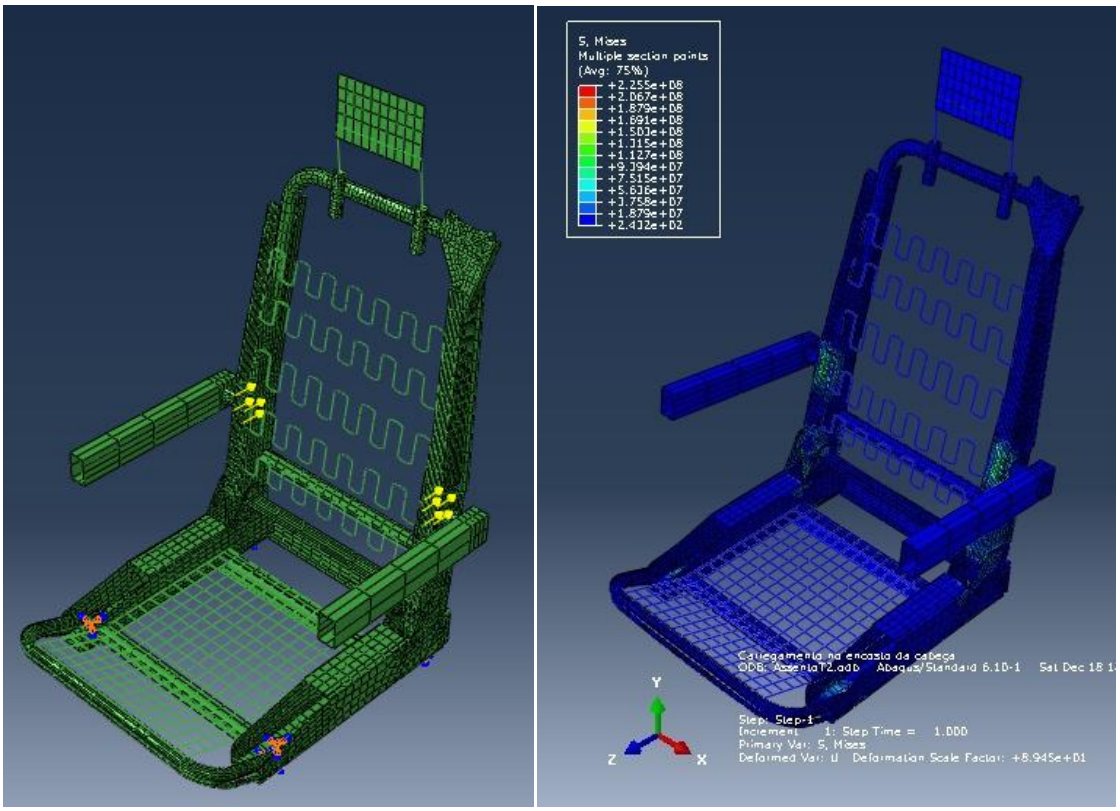

Figure 3.6 – Simulation test to seat integrity: Model with applied forces (left) and stresses (right).

It can be observed that the maximum stress on this simulation is 225MPa which is still inside the materials tensile strength. It was observed that the seat can endure both these tests and that the thickness of the steel is enough to withstand these loads.

In the last test the seat was submitted to a force 20 times the seat weight on the gravity center of the seatback and it was applied a force of 22,2 kN on the seat belt anchorage. As a simplification this later force was directly applied to the seatbelt structure present on the upper right of the seat on Figure 3.3. A seat endures this test if its maximum displacement does not surpass 178mm.

A simulation was performed on this seat in order to establish a basis for comparison for the second step of the material selection. The maximum displacement of this steel seat is 33.93mm located on the seatbelt structure as shown in Figure 3.7.

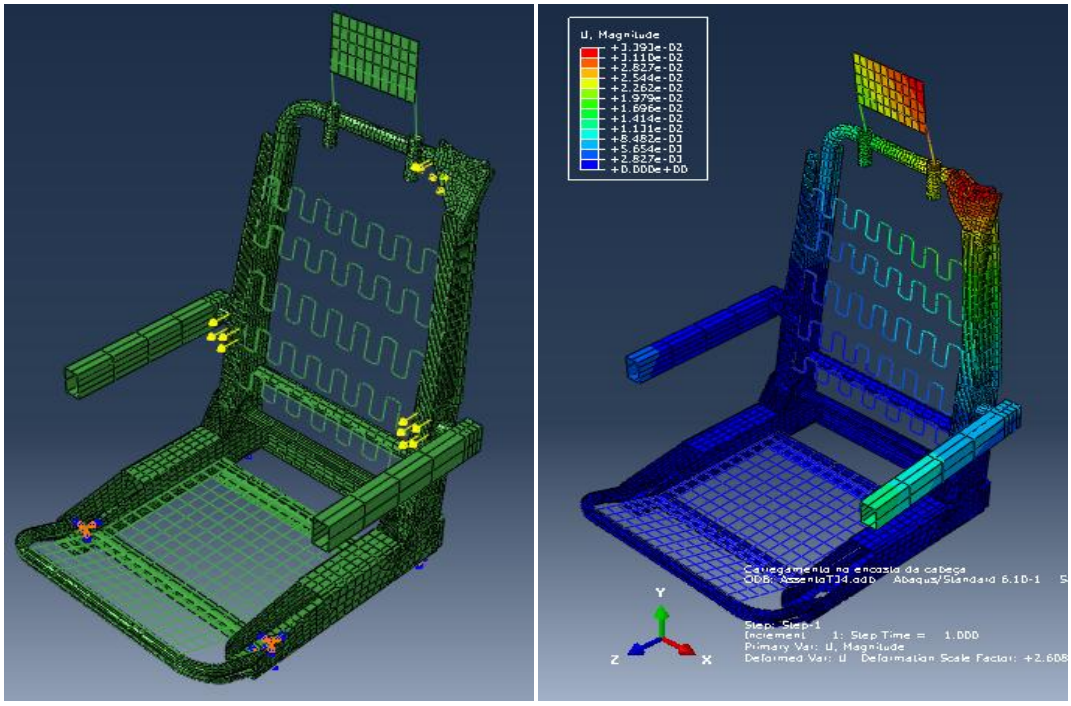

Figure 3.7 – Simulations on steel seats – Model with applied force (left), displacement (right).

The general spectrum of stresses showed that stresses on the seat are below the yield stress of the steels that were chosen for the development of this seat. There some punctual high stresses in the simulated seat that are related with some punctual high stresses that can be dismissed due to computational errors.

These results have been confirmed with simulation and practical results from other authors [59], [61] and it has been confirmed that this seat complies with the requirements of the industry. This model was adapted from other works and it will work as the basis for comparison for the cases that will be developed here.

3.2.2 Sensitivity study of other alternatives

The next step was the evaluation of different materials. The collected information shows that GFRP has similar properties as the magnesium alloys and therefore a simplification was made and considered to have the same behavior has these alloys during these early simulations. This next analysis focuses in the replacement of the materials. This evaluation was the most demanding test w because if the seat is able to comply with these requirements it is able to subsist through the other applied tests. The changes in the seats will be made until the performance is similar to the performance obtained with the steel seat.

A sensitivity study was performed to evaluate the weight improvement of these seats taking into account the materials that withstood the previous selection step. In Table 3.3 the different results for displacement are presented and it was established that the minimum thickness should be the one that has a similar displacement as the steel seat. In this study, the thicknesses of the plates used would increase until the value of the seat displacement was similar to the steel seat near the 34mm; however it should be noticed that all material have a safety gap until the 178mm.

Table 3.3– Displacement results of simulation using different materials.

Displacement (mm)				
Thickness (mm)	**Steel**	**CFRP**	**Aluminium**	**Magnesium**
1		80.55		
1,5		50.18		
2	33.93	36.21	94.82	151.4
3		28.21	60.31	96.3
4			44.,36	70.96
5			34.94	55.92
6				46.17
7				39.34

From the results of stresses and displacement simulations it was observed that the aluminium alloy would have a similar performance with 5mm thickness; although this value is a high one, the aluminium could be adopted with 3mm because the displacement is still inside the accepted interval. The thickness for magnesium/GFRP and CFRP seat ought to be 7 and 2 mm, respectively. The steel seat should have the same thickness in order to keep the same performance. From these results, it was estimated that the CFRP has the best weight saving with 76%, followed by magnesium alloys and aluminium alloys with 11.5% weight saving (Table 3.4).

Table 3.4 – Weight savings from the different materials.

Weight Savings			
Steel (2mm)	**Aluminium (5mm)**	**Magnesium (7mm)**	**CFRP (2mm)**
Reference (0%)	11,5%	20,0%	76 %

After this analysis, it was concluded that combinations of different materials could help to improve even further the weight in this seat. In this case, one of the materials would be used in the area that is more susceptible to suffer the loads during the normal use of the seat, while the other materials would be located in areas to improve weight in sectors less susceptible of suffering recurring loads.

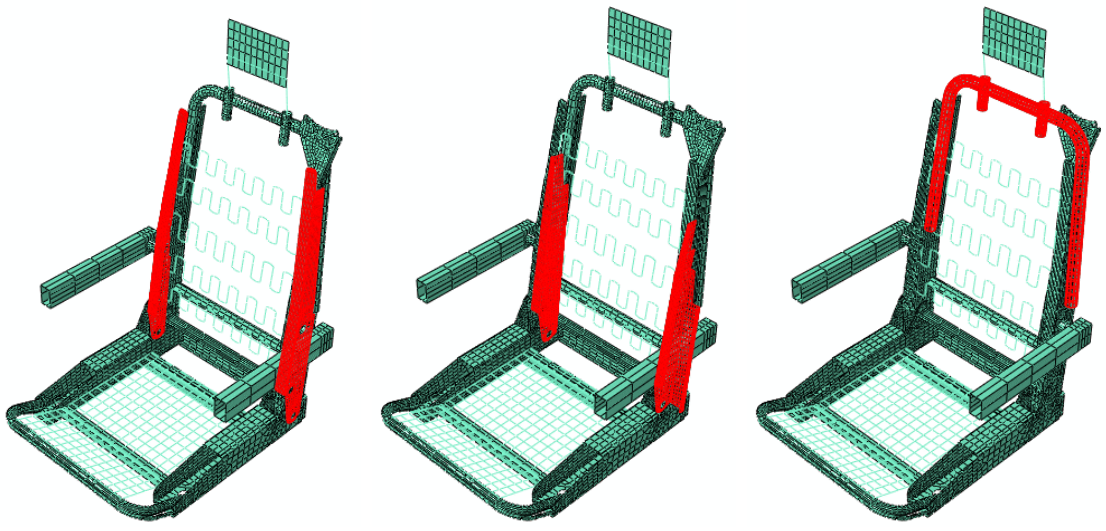

Figure 3.8 – Parts changed in the course of the case study.

The seat was analysed and the parts that sustain most of the force applies in this testing were identified. Figure 3.8 presents the parts that changed during these simulations. The left and middle present the left and right support pillar while the right picture presents the support

tube. It was observed that these three structures are the ones that required to be changed in order to improve the weight saving in each seat. From the previous observation, it was concluded that the CFRP material can have a substantial improvement on the seat weight translating into a critical difference over the other solutions. For this step, only combinations of metallic alloys were considered.

Three material combinations were tested:

- Magnesium and aluminium alloys;
- Magnesium and steel;
- Aluminium and steel;

For these material combinations no changes were made in the material thickness except for the parts presented in Figure 3.8.

It was observed that for the first seat combination the seat would be made of magnesium with 2 mm in most of the structure. However, the magnesium support tube would need to have a thickness of 4mm. The right and left pillar would be made out of aluminium and these pillars would have a thickness of 5mm. It was observed that under the test conditions the seat would have a displacement of 40.4mm.

For the second scenario, a similar analysis was performed but in this case the material of the right and left pillars were replaced by steel with 2.5mm in thickness. It was observed that displacement of the seat increased in this situation to 41.6mm. This combination of material has severe corrosion problems in which the magnesium will start to corrode in favour of the steel. To use this combination several cautions must be addressed to guarantee that there is no contact between these two alloys.

Table 3.5 – Simulation results regarding displacements and weight savings of the seat.

Materials	Mg/Al	Mg/St	Al/St
Displacement (mm)	40.4	41.6	32.4
Weight Savings	46.2%	45.7%	35.9%

The third case study kept the right and left pillars, the same as the case before, and changes were made in the rest of the structure replacing the magnesium alloy for aluminium. This combination has the best displacement in the seats; however there are some constraints regarding weight. The displacement in this case has been 32.4mm.

Table 3.5 shows that the performance of the seat combining steels and aluminium parts is the closest to the seat; nonetheless its weight saving is smaller when compared with the other two solutions. From this case study, it is possible to conclude that the aluminium/magnesium seat had the best weight saving and has a good performance in the displacement of the seat. This study allows us to confirm that the combination of different alloys can have several advantages; such has higher weight saving with same performance. It seems to be very interesting to develop a study using dissimilar combinations of material to observe how the seat would perform under those conditions. This seat was not optimized for the other lightweight materials and it is possible that the weight might be higher in this evaluation. The next steps will focus on the possible processes that can be adapted for the manufacturing of a seat with different materials and the existing designs.

3.3 Benchmarking

The benchmarking analysis was done to observe different designs of the seats and also to observe which production techniques are used in the development of each seat. This analysis can provide some feedback that will be used in the process selection step.

There are three different types of seats structures, depending on the seatback, being tubular, stamped or hybrid. The seat structure used in this sensitivity study had a hybrid seatback structure (tubular and stamped parts). The next step was to study seats with only tubular seatback and with only stamped seat in order to assess the main differences between them and with the hybrid seat.

Figure 3.9 – Seat structures with tubular seatback (left) and stamped seatback (right).

In Figure 3.9, the examples of the seats that were used in this study are presented. The assessment focused on the reinforcements that are used in the structure, the joints used and

some mechanical and physical differences. The material in all these was steel so the relationships between different seat designs could be established. The main conclusion of this part of the work is that the tubular tube has a greater thickness (1,5mm) than the stamped seat (1mm). In this type of seat, the seatback does not have any reinforcement in the seat back. The joints were made by MIG while in some stamped parts resistance spot welding was used. In the stamped parts, it was verified that the upper part of the seatback was reinforced with transversal beams that give more stability to the structure and guarantee that the performance of this seat is according to regulations. In this analysis it was also observed that the tubular seat was the lightest one by 2kg.

It has been observed that there are different designs of the seat and that the tubular design seems to be the most efficient in weight saving. The seats use different manufacturing processes such as drawing, stamping, bending. In the joining stage, mechanical joining can be used but also welding processes such as MIG and resistance spot welding.

3.4 Process selection

In this step, it was made an assessment of several techniques that can be used in order to define which technologies can be selected to aid in the introduction of these materials in a production line.

The material selection process showed that steels are an option in this process; however in order to improve the performance fn the seat it is required to use high strength steels which allows the use of thinner steel sheets, despite but loosing performance regarding the displacement. Since these are more costly it would increase the overall price of the seat if it was to keep the same performance without changing the material thickness. Some redesigning of the seat would be needed to introduce these new steels.

Regarding the composite materials, it was observed that the CFRP has a better performance than the GFRP and therefore these next steps it will be focused in the CFRP although the processes are similar between them. The CFRP seat presents the best performance from all seat simulations. However the production of a CFRP seat follows a very different direction than metallic seats because it has the cure time to give the shape to the different parts but due to this has a smaller production rate. Therefore, it is not very interesting to make a complete shift to these materials in all trends because some areas in automotive industry can have production rates of 200,000 cars annually while the production of these parts might be located from 20,000 to 50,000 parts annually. For this reason, the use of these materials should be focused on smaller level productions.

The magnesium seat also has several advantages but needs some shifts in the process. It was observed that it isdifficult to machine the magnesium at will due to its lower bending properties. Therefore there is some restriction in the stamping processes. However due to its high castability characteristics it is easy to obtain the different parts in their final shape. Once again the increase cost to buy the machines to obtain these shapes would imply a very high investment. The introduction of magnesium should be done step by step so there would be a lower disturbance in its introduction on the production line. However, problems linked to galvanic corrosion should be taken into account when selecting this material.

The aluminium presents itself as the best prospective material to be adopted in short term because most of these processes are already established in the companies, only requiring some adjustments of the tolerances to be able to form the material to the desired shape. One of the main issues might be the joining of aluminium alloys because the usual techniques have several problems when dealing with small thickness aluminium sheets. These problems go from high deformation of the aluminium sheets after welding, restrict material so that there are any failures during the joining process. Friction Stir Welding (FSW) presents itself as a technique that can answer to these problems and therefore a study was performed to evaluate the possibility of introduction of this technique in the production of automotive and other transportation applications.

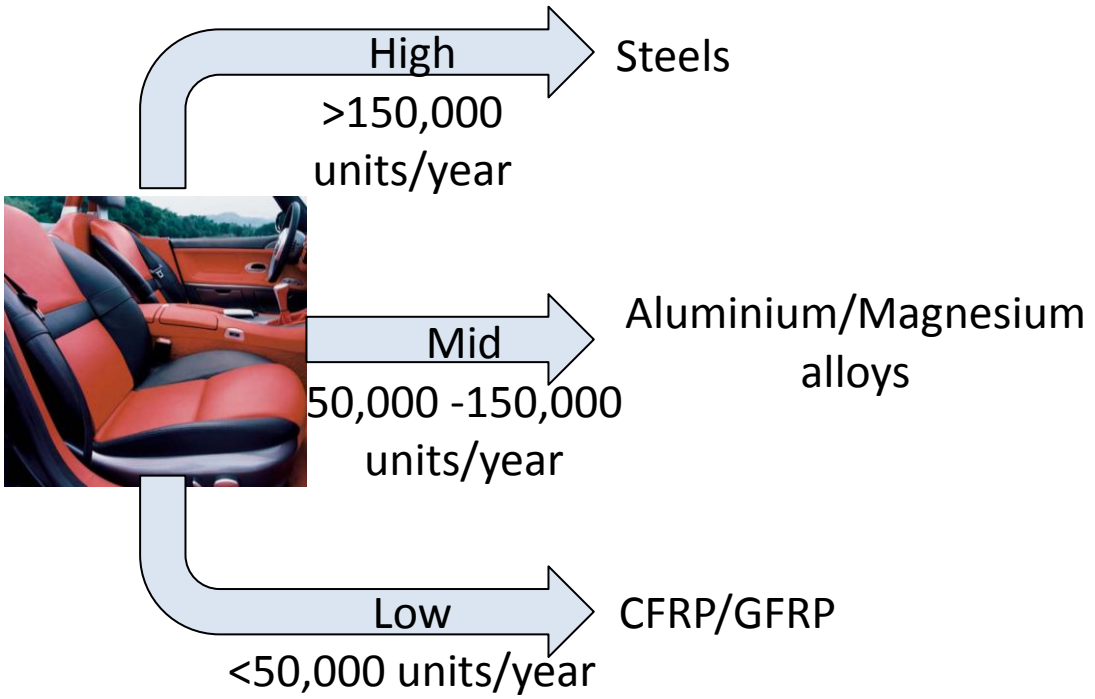

Figure 3.10 – Material alternatives according to production level.

Figure 3.10 presents the material alternatives according to production level. These values have been calculated taking into account different process production rates. The composite materials require a curing time that usually will increase the production time and makes it very difficult to compete with high volume production such as steel. Aluminium requires slower times in the stamping so the material does not fracture during stamping. Magnesium alloys require a change in production and a cooling stage which also increase the time of fabrication of these alloys. In order to choose which material the products volume rate must be taken into consideration, not disregarding the easiness of integrating such a material in the company's usual production. This means that for high volumes it will be easier to integrate high strength steels because most production processes are similar with the existing ones and the companies that produce these products are not flexible enough to change process. From another perspective, flexible companies with small production volumes will probably be able to integrate better composite material in their production lines.

It was decided that our case study would focus on the mid volume production where it aluminium or magnesium alloys can be chosen to produce the seat. It was observed that most production processes for magnesium are similar to steels' options; however improvements must be made in the joining area where the welding processes must be altered. Magnesium presents itself as a distinct process from the existing ones which will promote changes to both production processes changing to die-casting processes and joining processes where Friction Stir Welding (FSW) is also a good option for this material. Since both of these materials present different options in both material and process design the next steps will focus on a more experimental approach where the influence of FSW is studied to evaluate the use of these materials and processes in a car seat production line.

4 Friction Stir Welding

4.1 Introduction

Friction Stir Welding (FSW) is a solid state joining process developed by Thomas Wayne of The Welding Institute (TWI) in 1991 [62]. In this process, a non-consumable rotating tool is introduced in the joint of the plates to be joined. The friction between the tool and the plate is the main cause of the heat produced in the process. The joining of the materials will be made through the combination of the advancing speed and applied force that will join the material together with the passage of the tool (Figure 4.1).

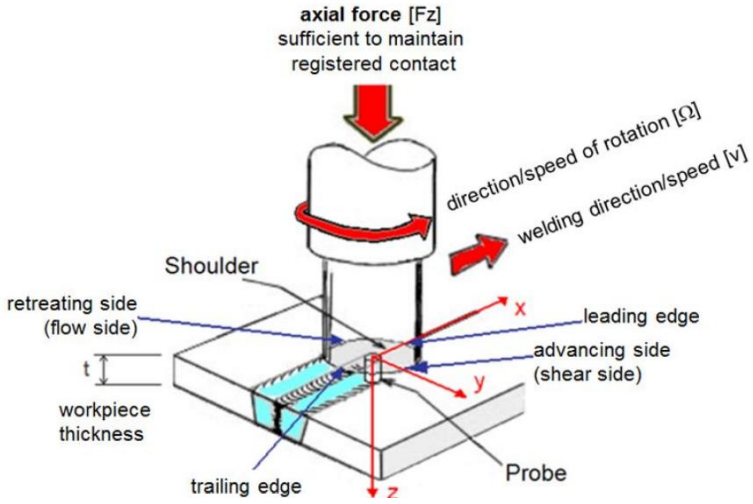

Figure 4.1 – Schematic of the FSW process [63]**.**

The FSW is composed by two different parts: the pin and shoulder. The composition of these tools is the main factor for a successful weld using this process. The pin will enter the joint and promote the flow of material around it. This flow of material together with the advancing speed will promote the joining of the two plates. The heated material flowing around the pin is constrained by the plates on the side, the backplate at the bottom and the shoulder on the top. The applied force together with the shoulder will contain the material under the shoulder and will be able to contain the processed material under the shoulder.

4.1.1 Metallurgical Characteristics of Welded Samples

Four distinct zones are visible in FSW welded samples. These different zones have different metallurgical properties that are imbued through the mechanical and thermal strains promoted by the FSW tool.

The nugget (Figure 4.2) region has a very small and homogeneous grain size due to the dynamic recrystallization. The high temperature and mechanical strains promoted by the movement of the pin are the main factors that induce the mechanical recrystallization.

The thermomechanically affected zone (TMAZ) (Figure 4.2) –is usually located right next to the nugget, and usually has an elongated grain size typical of deformation processes. This zone is also affected by mechanical strain and high temperature, however the mechanical strain was not high enough to promote dynamic.

The heat affect zone (HAZ) (Figure 4.2) is located right next to the TMAZ and is only affected by the temperature induced by the process. Usually there is a coalescence of the grain size that induces a decrease in the hardness of the material in this zone.

Base material - the zone that was not affected by this process located after the HAZ.

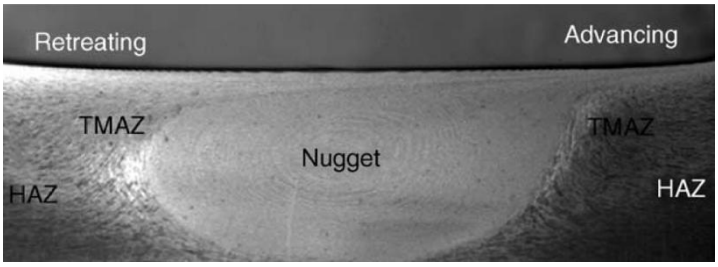

Figure 4.2 – Micrograph showing the different zones of a FSWed AA7075 aluminium [64]**.**

The local thermo-mechanical cycles promotes severe plastic deformation that will change the microstructural properties of the materials [65]; besides, the superficial oxide layer is destroyed promoting the joining of the materials. It has been established that this process usually takes place at 2/3 of the melting point [64]; therefore deformation from heat input is mitigated. Su e*t al.* [65] studied the dynamic recrystallization phenomena on the AA7050 aluminium alloys and identified that the *"Dynamic recrystallization in the DXZ can be considered a continuous dynamic recrystallization (CDR) on the basis of dynamic recovery. Subgrain growth associated with absorption of dislocations into the boundaries is the CDR mechanism. Repeated absorption of dislocations into subgrain boundaries is the dominant mechanism for increasing the misorientation between adjacent subgrains during the CDR."* It was also identified by these authors that the strengthening precipitates in TMAZ are dissolved in the matrix and re-precipitate in the grain boundaries depending on the heat released.

The application of this process in aluminium alloys also has a great effect in the microstructure of the materials. Some authors have focused their attention on the evolution of the microstructure in the different zones of the FSWed alloys. Chen *et al.* [66] observed the precipitate evolution in the different zones of the FSWed AA2219 aluminium alloys. It was

observed that the metastable precipitates solutionized back into the Al solid solution in the stir zone, while these same precipitates coarsened in the HAZ. It was also registered that both behaviors were observed in the stir zone with solutionization of the precipitates near nugget and coarsening of these same precipitates further away from the nugget. The coarsening and solutionization of the precipitates is dependent of the temperature released of the process. Another work [67] has reached the same conclusions and compared the different zones with the hardness profile. It was concluded that the HAZ area with coarser precipitates displays the lower hardness which is related with the local overageing of these alloys.

4.1.2 Process Parameters

The different parameters of the process will define the mechanical properties that can be imbued in the joined alloys. These parameters are described below:

- Rotational speed – it starts before the penetration of the tool on the plate. The rotation of the tool will end after the end of the weld.
- Advancing speed – this parameter is related to the welding speed. It has been established that a relationship between the rotational speed and advancing speed, i.e. Ω/v. It is considered a cold weld for values under 4 and a hot weld for values over 4. The cold welds usually have a smaller heat affected zone and the larger TMAZ while the hot welds have a larger HAZ and a smaller TMAZ.
- Applied force – this is a very sensitive parameter in this welding process being a very important parameter to obtain a sound weld. Too high applied forces will lead a higher penetration of the tool on the material while low applied forces will not be enough to contain the material under the shoulder resulting in poor to non-existent welds.
- Tilt angle – this is the angle made by the tool to the welding plates. The increase of this angle can reduce the amount of produced flash. The increase in angle over 0^{o} restricts the welding to be only along one axis.
- Dwell time – this is the time the tool stands still when reaching the welding position before advancing. During this time the tool rotation heats the material to promote better welding conditions.

Other than the process parameters, the geometric tool parameters are also very important to promote a sound weld. The FSW tool is composed by the pin and base. The pin can have different geometries depending on the welding conditions and materials to be joined, like:

- The material used in the tool is dependent on the material to be joined, the chosen material must resist the friction mechanisms imposed to it during the process and

should also have mechanical properties to resist the strains and stresses promoted in this process. Usually steel alloys (typically tool steel) are used in the joining of light alloys such as aluminium, copper or magnesium while in the joining of steel, ceramic material or hard metals can be considered.

- The pin length and diameter is usually dependent on the thickness of the plates to be joined. The pin must be long enough to join the plates without any trouble and its diameter must be large enough to resist to the stresses of the process without failure. However, if the diameter is too large it will promote a large flow in the welded sample causing too many residual stresses on the sample.
- The pin design will influence the flow of material. A conical pin will have a better flow of material than a cylindrical pin. The introduction of threads in the pin potentiates the flow of material around the pin. A better flow can reduce the defects produced by this process. In this case it will be the volume defects that can be reduced by this action. Other pin designs have been developed with the goal of increasing the material flow and increase the processed area.

The shoulder has different geometries and necessary characteristics to successfully weld two plates together.

- The shoulder diameter is necessary to contain the material under the shoulder. The diameter is related with the containment of the processed material in the processed area. This characteristic is also related to the heat input in the joined area. The relationship between the shoulders over pin diameters is important to promote a sound welded of the different materials. One author [64]has observed that the use of a factor of 2 is important to promote a good weld without causing a big change in the material properties.
- The shoulder design can influence the process parameters. The use of scrolled concave and flat shoulders a usually used to contain the material under the shoulder also helping with the entry of material for processing. The scrolled shoulder is able to join the materials together with a tilt angle of 0^{o} while the flat or concave shoulders need to have a tilt angle to be able join the materials together.

4.1.3 Applicability of FSW

FSW is a solid state process that brings several advantages in the joining of aluminium alloys. The fusion processes usually face several problems with this process and will have difficulties related to the higher melting point of the oxide layer. When dealing with low thickness plates

this becomes a severe problem due to the higher deformation in the metal plates from the heat input. Balasubramanian [68] has studied the influence of the FSW process in different aluminium alloys concluding that the definition of the optimal parameters is dependent on the mechanical properties of the aluminium alloys. It was observed that different parameters had to be used to promote defect-free welds in the different aluminium alloys.

4.1.3.1 Non-heat treatable aluminium alloys

Several authors have studied the influence of the FSW process on the mechanical and metallurgical properties of the aluminium alloys. Hirata *et al.* [69] studied the influence of the FSW parameters on the grain size and formability of the AA5083 aluminium alloy. These authors concluded that there is an increase of the formability with the decrease of the grain size. The lower heat flow is responsible for the lower grain size and consequently, lower ductility. Casalino *et al*. [70] studied the influence of the shoulder geometry and coating on the mechanical properties on the AA5754 aluminium alloy. It was observed that conic tool and large shoulder with carbide coating produced almost defect-free welds for all tested parameters. It was also observed that the flat shoulder was sensitive to process parameters. These authors also confirmed that the shoulder size influenced the microstructural zones and hardness profiles. The larger shoulder had the lowest hardness which can be explained by the higher heat released with this tool.

Tao *et al.* [71] studied the influence of the process parameters in the mechanical and fracture properties of the Al-Mg-Sc alloys. It was concluded that the tensile behavior was very similar to the base material for the different parameters with the ultimate tensile strength around 96-98% of the base material. The fracture showed different behaviors between the samples; the lower rotational speed presented lack of penetration showing the “kissing bond” defect while at higher rotational speeds no such problems were presented.

Peel *et al.* [72] studied the effect of the friction stir welding parameters on the mechanical properties of a AA5083 aluminium alloy. It was observed that the hardness and tensile properties of the nugget region were smaller than the base material. It was also observed that the residual stresses increased with the increase of the advancing speed concluding that this increase is due to decrease in time for stress relaxation.

Chen *et al.* [73] investigated the influence of the typical defects of FSW in a AA5456 aluminium alloy. The *“Lazy S”*, *“Kissing bond”* and voids defects are addressed in this research. It was concluded that the *“Lazy S”* is a joint line remnant induced from the chaotic mixing of the oxide layer and can reduce the ductility of the joint. The *“Kissing Bond”* which is the defect

resultant from the lack of weld penetration is difficult to detect and negatively affects the tensile behavior. The voids or channels inside the welded area can be reduced with the aid of the tool tilt angle. These results show the general concern regarding the FSW defects; however with the right tool parameters these defects can be mitigated and eliminated.

4.1.3.2 Heat treatable aluminium alloys

In heat treatable alloys, there is usually a decrease in the mechanical properties after being FSWed. This is mainly related to the fact that the zone processed by this process will lose the heat treatment in the processed zone and its surrounding zones which will result in a decrease of the mechanical properties. Liu *et al.* [74] confirmed this effect having a decrease in the ultimate tensile strength to 82% of the base material in the AA2017 welded alloys. It was confirmed that defect free welds usually fracture in the interface between the nugget and TMAZ. Chen *et al.* [75] confirmed this observation while assessing the mechanical properties in a AA2219 aluminium alloy in both T6 and O condition. It was confirmed that the tensile strength decreased in the T6 condition while no significant changes were observed in the O condition.

Other authors focused their research in observing the effects of the mechanical properties in different alloys. Cavaliere *et al.* [76] observed the effect of FSW in the mechanical and mechanical properties of AA6056 aluminium alloy. It was studied the effect of different rotational and advancing speeds on the properties of the welded samples. It was observed that the best ductility was obtained for the lower advancing and rotational speeds. The highest tensile strength was obtained for the higher advancing and rotational speeds. The results also show that the welding different parameters have a great influence on the fatigue behavior of the aluminium alloys. Gaafer *et al.* [77] also studied the influence of the rotational and advancing speeds on a AA7020 aluminium alloy. It was confirmed that increasing the welding speed for a fixed rotational speed would improve the tensile strength. It was also confirmed that for a fixed advancing speed the grain size would be higher with the increase of the advancing speed; this is related to the heat released in the process which increases with the elevation of the rotational speed. Lee *et al.* [78] studied the applicability of this method in a cast aluminium alloy. It was observed that the microstructure of these alloys was completely deformed in the nugget region presenting a homogeneous distribution of Si particles. It was confirmed that these alloys had a similar behavior to the base material. In addition, tensile tests were performed focusing only the nugget region where it was observed a 20% increase of the tensile strength. Wei *et al.* [79] studied the influence of different FSW parameters in the mechanical properties of aluminium-lithium alloy. The parameters were previously optimized

and it was related with the heat input and the mechanical properties in the different welded samples. It was observed that the hardness and bending behavior have different relationships with the hardness reducing with the increase of the heat input, while the bending increases. It was also observed that the bending behavior did not have many changes with the different tested parameters. The pin profile also has a great influence in the imbedded properties of the materials. Elangovan and Balasubramanian [80] confirmed that the use of square profiles usually have better tensile properties than other profiles. It was also confirmed in that this pin did not develop any defects in the different tested parameters unlike other tested profiles.

The use of multiple passes can be used to eliminate defects from previous passes. However the overlapping tend to reduce the mechanical properties of the welded sample [81]. Brown *et al.* [81] observed the effects of multi-pass in a AA7050 aluminium alloy. It was observed that HAZ hardness and tensile strength decreased with the increasing number of passes. This is related to the increase of the HAZ and the increase of the overlapping passes that negatively affect the mechanical properties as previously stated. It was confirmed that the residual stresses decrease with the increase of overlapping steps which is a result from the increased heat of the region promoting the stress relaxation of the samples. In a similar study [82], it was observed that the multi-pass improved the hardness and tensile properties with the increasing number of passes which is not according to other works [81]. This author [82] also confirms the application of the multipass technique can be used to eliminates defects that were introduced in the previous steps.

4.1.3.3 Applications

FSW has been applied in several industrial cases to evaluate its applicability and feasibility for the defined goals in the different industries.

One of such cases is the employment of this process in industrial applications where there is a need to maintain the microstructure of the materials to be joined. This process presents several advantages due to its lower released heat. Salem *et al.* [83] studied the FSW parameters in superplastic AA2095 aluminium alloys. It was concluded this material was able to retain the superplasticity behavior of the samples for all tested conditions. It was also observed that the higher welding rates results in higher elongation to fracture. The retention of superplasticity was also observed by Sato *et al*. [84] who concluded that the low heat input and plastic strain were able to retain the small grain size in the equal channel angular pressed aluminium alloy. The authors [84] also confirmed that the welded alloys had higher strength and toughness properties related to the microstructures developed during FSW. A roll bonded

AA1100 aluminium alloys [85] was welded with friction stir welding. The roll bonded aluminium has been studied because in the joining processes there is usually an increase of heat which can lead to a decrease in the mechanical properties of these alloys and compromise its use. The FSW was confirmed to be able to reduce the softening of the properties of these alloys which is crucial to keep the homogeneity of these plates. The applicability of the FSW process in the roll bonding alloys was confirmed by Topic *et al* [86] in their investigation of influence in the mechanic properties in AA1100 and AA6016 aluminium alloys. It was confirmed that this process can be applied and that the ultrafine grained structure of these material had some softening in the nugget region; however the hardness did not suffer any influence. The applicability of the process in these alloys is therefore justified.

An AA6016 aluminium alloy was welded by FSW using two different tools to observe the behavior of this aluminium in a deep drawing application. It was confirmed that both set of parameters induced good deep drawing behavior on the aluminium samples. However, strong wrinkling was displayed in the samples welded with the conical shoulder. It was confirmed that the samples welded by the above mentioned tool had a bigger loss in ductility than the scrolled shoulder. Silva *et al.* [87] applied the single point incremental forming of tailored blanks produced by FSW. It was concluded that if there is a good quality control of the welding joints this process is capable of producing complex shapes without any defects.

The improvement of properties is related to grain size refinement and homogenization due to the large processing strains in the nugget [88]. Cavaliere *et al.* [89] studied the evolution of the microstructure and mechanical properties of an AA6082 alloy with the different process parameters. It was observed that the grain size decreased with an increasing transverse speed. These results are aligned with the FSW principles because with the increasing transverse speed, the weld will be in a colder state and therefore the grain size will be smaller.

Several authors [80], [90], [91] have studied the effects of FSW parameters in different aluminium alloys to understand the best parameters to have the best joining efficiency of a weld. It was observed that the joining of different aluminiums is possible and that the properties are usually between the properties of the base materials [92], [93]. Most studies have been focused on understanding how the parameters influence the properties of the welded samples. This creates a need for a structured approach that can help in understanding the interaction between the welded samples properties and process parameters. Taguchi method is a method to achieve this and it has been applied to other friction stir processed aluminium alloys [94], [95] however no definite relationship has been established in the studied alloys.

Different authors have carried out several works focusing on the use of the FSW process in the production of metal matrix composites. However, it has been found severe wear in the FSW tool as a result of the abrasion of the particles in the FSW tool [96]. Devanathan and Suresh Babu [97] studied the effect of a TiAlN coating the tool in the production of metal matrix composites. It was observed that the coating is effective enough to eliminate the wear in the FSW tool. The effects of friction stir welding in existing metal matrix composites [98] have also been studied, confirming that the particles are homogeneously distributed in the nugget region. It has also been observed that conductivity profiles allow for a better observation of the different areas showing an increase in conductivity in the nugget region. A similar study [99], also concludes that the particles are homogeneously distributed inside the nugget region. These studies have shown that FSW process is a very good candidate for the production and treatment of metal matrix composites and widens its applications spectrum in a larger variety of industries.

4.1.3.4 Taguchi method

Several authors have developed different strategies to understand the phenomena involved in FSW and understand how the FSW influences the mechanical properties of the welded materials [76], [77], [79], [80], [89], [91]. These authors have shown the evolution in mechanical properties of the welded materials by changing the process parameters for this goal. However, these studies require several tests in order to cover all the parameters and observe the relationship between the process parameters and material properties. Taguchi method was developed using statistical methods developed by Genichi Taguchi in order to improve the quality of manufactured goods and has been recently applied to engineering, biotechnology, marketing and advertising. The contribution of each tested parameter is quantified and it is possible to understand how the changes are felt during testing. This allows us to identify the best parameters inside the tested results. The design of experiments allows the reduction of the number of tests needed to evaluate the different parameters which has been one of the major contributions of this statistical model. It has been confirmed that to study the influence of three parameters at three different levels it would require 27 tests while using the aforementioned method there is a reduction to only 9 tests.

Lakshminarayanan and Balasubramanian [95] used this method to optimize the tensile strength of a friction stir welded RDE-40 aluminium alloy. The authors confirmed that the rotational speed, advancing speed and applied force played an important role in the decision of the tensile strength. It was also found that the rotational speed gives the biggest of contributions for improved properties followed by advancing speed and axial force. This

technique can also be used to determine the parameters of dissimilar alloys. Koilraj *et al.* [100] applied this method for the joining of AA2019 to AA5083, studying 4 parameters at 4 different levels. It was found that the ratio between shoulder and probe was the most important parameter in this analysis contributing with 60% for the overall contribution. It was also observed that the fracture usually occurred on the side of the AA5083 alloys in the HAZ. Other authors [101] used this method to evaluate its applicability in a lap joint between an aluminium alloy and brass. A L9 matrix was used to study the effects of the rotational speed, tilt angle and advancing speed. It was confirmed that the rotational speed played an important role in this context contributing with 40%. A small discrepancy was found between the calculated value through Taguchi and the experimental results.

Other works have focused on the combination of other methods with Taguchi in order to improve the efficiency for a given goal. Vidal *et al*. [94] used the Taguchi method for the determination of the best parameters for tensile, bending and hardness properties. It was found that the best parameters for these different material properties were different so an algorithm was developed to combine these results and provide the best parameters for fatigue testing. The main goal was for the aluminium alloy to have the closest properties to the parent material and therefore improve its fatigue behavior. The results of this study showed the applicability of this method which was confirmed by subsequent tests. Other authors [102] also combined 2 different methods: the cellular and Taguchi methods. The cellular method was used to simulate the microstructural properties which were later confirmed by experimental testing. A good correlation between the simulation results and the results from the optimal parameters of Taguchi method was observed, thus validating the simulations results of the cellular automation method. These studies have confirmed the applicability of the FSW process in the joining of the aluminium alloys. Besides, the results obtained from Taguchi method have showed a good correlation with the experimental results. In this work, the influence of FSW in aluminium and magnesium alloys is going to be studied. An analysis will be performed comparing the applicability of the Taguchi method as opposed to the usually used method. The use of the Taguchi method will also be performed to better understand the influence of the process parameters.

4.1.3.5 FSW applied to magnesium alloys

Nowadays one of the main goals shared by several industries is the reduction of the carbon emissions. In the automotive industry this can be obtained through the reduction of the fuel consumption during a car drive or by the development of more efficient engines where the energy losses from heat are decreased [103].

Nowadays, weight reduction is a common goal of several industries that are trying to comply with recent environmental regulations and improve the efficiency of their products. It is well known that in the automotive industry the reduction of weight can reduce costs in transportation, but also improve fuel economy and reduce the CO_2 emissions. The use of magnesium brings several benefits towards these goals due to its low density (1700kg/m^3) and good mechanical properties. These alloys are very promising and can efficiently decrease the weight of many engineering components. However, there are some limitations to the use of magnesium in the industrial context. Magnesium alloys are not easily formed due to their hexagonal close packed (hcp) microstructure, which limits the ductility of magnesium and its alloys at room temperature. However, magnesium has a good castability and formability at high temperatures which enables the production of complex and thin walled shapes with casting processes without much effort. Some of these works have focused in the shaping and forming of magnesium alloys using sheet metal forming at high temperature. Doege and Droder [104] reported that the AZ31 alloy has excellent deep drawing properties at temperatures between 200-250^{o}C. Chung *et al*. [105] were able to form an AZ61 magnesium alloy using a superplastic gas pressure forming with at a temperature of 400^{o}C and in an applied gas pressure range of 0.46 – 1.2 MPa. Huang *et al.* [106] studied the forming limit of an AZ31 magnesium alloy at different temperatures. It was observed that the formability of the magnesium alloy increased with the increase in temperature. Yuan *et al.* [107] verified that although it is easier to form and shape AZ31 magnesium, the increased temperature can induce microvoids in magnesium that will ultimately affect and reduce the mechanical properties. These number of microvoids increase with the temperature having a large number of microvoids at 400^{o}C, while a small number microvoids was found at 200^{o}C. Joining complex shapes produced by forming thin magnesium plates is a requisite for the industrial use of this material. Therefore, several studies have been conducted to assess traditional welding techniques in the joining of these complex shapes. Some works show the use of laser and TIG to weld the AZ31 and AZ91 magnesium alloys; however pores appear in the welded area from the reaction of the magnesium due to the introduction of H_2 in the molten magnesium. Liu e*t al* [108] reported that the use of a hybrid laser and tungsten inert gas has been used to weld magnesium; however, the formation of macropores aligned with the weld path that was formed with the introduction of air in the molten was observed. It was also concluded that a possible solution would be the use of lateral gas shielding in the process that unlike coaxial gas shielding does not disturb the welding process and promotes a perfect bead without macropores. Shen *et al.* [109] observed the formation of macropores in double-sided gas tungsten arc welding (GTAW) in which there was an abnormal pore growth appearing on the

first welded side when welding the second side of the AZ91 magnesium alloy plate. In order to reduce this problem, lower temperatures were used in double sided welds recurring filler material during the use of GTAW, on AZ91 magnesium alloy. While having lower mechanical properties, magnesium alloys also have a poorer corrosion resistance when compared to aluminium alloys. These alloys are also known for being temperature sensitive. Wu and Zhang [110] made a review of the state-of-the-art of magnesium and different corrosion processes and it was concluded that that magnesium has a low open circuit potential and negative differential effect; furthermore, the protection mechanisms usually applied to AL and Fe cannot be applied directly which means there is still furtherresearch needed in this area. Zhang *et al.* [111] observed that mechanical and corrosion properties can be enhanced by refining the β-$Mg_{17}Al_{12}$ in the AZ31 magnesium material structure. Walton *et al.* [112] established that the common corrosion mechanisms in the AZ31 magnesium alloy are general corrosion, pitting corrosion and intergranular corrosion; however it was not possible to identify ways to protect thee alloys from this type of corrosion. Samaniego *et al.* [113] remarked that even though the AZ61 alloy has a better corrosion behavior than the AZ31, in the early stages of exposure to saline environments, fter long exposure times the AZ61 alloy will corrode more than the AZ31. This is the result of a poor corrosive film and accelerated microgalvanic corrosion. This means that the development of protective films will be more suitable to the AZ61 alloys.

Friction Stir Welding (FSW) can be a good solution to weld magnesium alloys. This process is a solid state process based on friction mechanisms that promote the joining of the materials. Such technique has been proven to efficiently weld magnesium alloys without leaving any defects inside. FSW is a solid state process that was developed by the TWI institute in 1991. Studies have shown that this process enables the production of sounds weld without any pores or defects in the joint area. Wang et *al.* [114] were able to successfully join AZ31 magnesium alloys and the joints presented a tensile strength very close to the base material around 93%.However, no indication was given about the ductility of the welded sample. Padmanaban and Balasubramanian [115] observed that threaded pin profiles and high carbon steel tools displayed the best mechanical conditions due to the absence number of defects in the nugget. Yu *et al.* [116] successfully joined the AZ31 alloys. It was found that the welded samples had lower tensile strength and ductilities than the base material while tensile testing of the nugget region showed a behavior similar to the base material. In addition, Zeng *et al*. [117] showed that magnesium welded samples have a good tensile strength when compared to the base material in spite of the strain being usually much smaller in the welded samples. Chowdhury *et al*. [118] studied the effect of pin tool thread orientation and weld pitch in the welding of

magnesium alloys and verified that a left-handed tool thread was a good parameter to obtain good mechanical properties. It was also verified that the increasing weld pitch improves the mechanical properties of the welded samples. However, no upper limit hawas verified during this experiment. Like aluminium, Friction Stir Welded magnesium alloys usually have 4 distinct regions: the nugget, the termomechanically affected zone (TMAZ), the heat affected zone (HAZ) and the base material (BM), the zone that is not affected by the process. Afrin *et al.* [119] verified that the mechanical properties from tensile testing do not vary with the change of the test parameters and that the results are usually very stable. It was concluded that the hardness of the nugget can differ from the base material but this depends on the heat treatment of the base material and production process. Hung *et al.* [120] confirmed that the properties in the nugget are very similar to the properties of the base material. Gharacheh *et al.* [121] observed that with the increase of the rotational speed over the advancing speed a larger nugget with a higher heat input is originated and an easier material flows. This author concludes that one reason for the deterioration of the mechanical properties in transverse tensile testing is due to the formation of an oxide layer between the nugget and transition zone. Dhanapal *et al.* [122] studies on the corrosion properties of Friction Stir Welded magnesium alloys showed that the corrosion rate has a tendency to be higher in acidic medium when compared to alkaline and neutral media. Srinivasan *et al.* [123] observed that the corrosion behavior of welded samples and base material are similar in the AZ61 magnesium alloy even though the surface treatement is very effective to decrease the corrosion rate of both alloys. It was also verified that welded samples have a higher potential of stress corrosion cracking in the nugget of the welded sample. Zeng *et al.* [124] verified that in the AM50 magnesium alloy the corrosion rate varies along the different areas of the welded sample, being higher in the base material and lower in the welded area. Most corrosion studies have focused in other alloys than the alloy presented for this study that is usually pointed out as a suitable solution for automotive industry. Also, most of the works have focused in the identification of the best parameters to achieve the best mechanical properties. Many structured approaches have been presented, however they involve several steps and many trial and error attempts. Taguchi method has never been applied for this situation and there is still no clear definition of the limitations of applying the FSW in magnesium. The corrosion effects in FSW of magnesium are still underdeveloped and more research is needed to identify the causes of this effect.

4.1.3.6 FSW applied to dissimilar joints

Several works focused in which combinations of materials are the most suitable to accomplish it, namely Steel to Al alloys [125]–[127], Steel to Mg alloys [128], [129], Al alloys to Mg alloys [130]–[138], Al alloys to Ti alloys [139]–[141], Mg alloys to Ti alloys [142], [143], among other combinations. The use of light alloys such as aluminium and magnesium alloys have shown to have promising results with the weight reduction of the different components. Each material has their own limitations considering the physical properties which end up hindering their proposed effect. Both alloys are known for their low density and good mechanical properties. Magnesium has a density of 1750kg/m^3 while aluminium has a density of 2700g/cm^3. This makes magnesium more suitable for low weight applications; however the mechanical and formability at room temperature are not as good as aluminiums'. Aluminium is known for having a good mechanical behavior and properties being easy to form and machine. The combination of these two materials is promising because the right combination of material can take advantage of the low weight of the magnesium alloys and mechanical resistance of the aluminium alloys.

Friction Stir Welding (FSW) is a promising technique that has been able to join aluminium, magnesium, and different combinations between these two materials. Some concerns must be taken into account when welding dissimilar material, even those from the same material family. One of these concerns relies on the limitations of the materials that require precise parameters to have similar flows and have a better joint. Dissimilar welds can be made between different materials as presented before, or between different alloys inside the same material class. This can be in order to join a more brittle material with a more ductile or use a more corrosion resistant alloy with a material with higher mechanical properties but susceptible to corrosion. The weld between different alloys of the same material class is easier as it is easier to establish conditions that enable a similar flow between the two materials. When joining Al alloys to Mg alloys it must be taken into account that their properties differ. In fact, even at higher temperatures some precautions must be taken during the welding process otherwise some flaws will be found in the joint [130], [131]. These defects can go from a high amount of flash, inability of the material to close the weld and difficulty to properly join the materials. These problems can be solved by adjusting the weld parameters [91], [130], [144]–[146] or by offsetting the tool from the centerline of the materials to be joined [131], [142], [147]. It has been observed that in the nugget of dissimilar weld of Al alloys to Mg alloys the hardness is usually higher than the base materials [131]–[133] and this is related to the formation of intermetallic structures in the nugget [131], [137] mainly the formation of Al_3Mg_2

and $Al_{12}Mg_{17}$ intermetallic elements. It has also been confirmed that these fracture of the welded samples is related associated to these secondary elements. It has also been observed [130], [131], [133] that these elements greatly deter the ductility and yield strength of the welded samples.

In the dissimilar alloys of different aluminium alloys it has been concluded [144] that the joint has a high level of residual stresses and that the residual stress increases with the rotational speeds which affects negatively affects the properties of the dissimilar joints. One author [145] has confirmed that the final yield strength is dependent on the remaining solid solution which may compensate the loss of strengthening effect of larger precipitates in a lower volume fraction. This author also confirms that while the similar welds of heat-treatable alloys have a W profile, the profile of dissimilar weld of two heat-treatable alloys is composed by 2 W-halfs. In addition, it has been confirmed that the mechanical properties can improve with an offset of the pin; this also occurs [147] with the fatigue properties of a dissimilar weld between AA2024 and AA7075 alloys. It was observed that the fatigue properties improved when the pin was moved up to 1mm to the AA2024 side. A study in properties of ageing effects [148] has shown that the properties do not vary much between aged and non-aged samples. Other studies have shown [93], [149] that the fracture of the materials can be related to several mechanisms like the increase in the residual stresses in the nugget area or existent irregularities. In the weld of different alloys of magnesium [146] it has been observed that the position of the different alloys and the advancing speed are very important in definition of their mechanical properties. Corrosion studies [138], [150] have clearly shown that dissimilar joints between different materials and different alloys of the same materials have completely different behaviors. Galvanic corrosion is promoted between different materials which makes these joints much more corrosion susceptible. In contrast, the joining of alloys inside the same material class is not so susceptible to be affected by such corrosion mechanisms and is more resistant to corrosion. In this work the mechanical and corrosion behavior between two aluminium alloys and one magnesium alloy is going to be studied. The alloys chosen for this work are AA6082-T6, AA5754-H111 and AZ31 B and the study of the mechanical properties of the dissimilar welds in these alloys is yet to be thoroughly studied. Another focus are the corrosion mechanisms and properties of these joints that are yet to be defined and need more attention in order to look for ways to improve this behavior.

4.2 Experimental Procedure

The present work intends to evaluate the applicability of FSW in aluminium and magnesium alloys for automotive industry. Three aluminium alloys and one magnesium alloy were used. Table 4.1 shows the chemical composition of these alloys.

Table 4.1 – Chemical composition of used alloys [151]**.**

Elem. (%)	%Al	%Mg	%Si	%Zn	%Cr	%Cu	%Fe	%Mn	%Ti	%(Cr+Mn)	%Ca	Other
AA6082	Bal.	0.6-1.2	0.7-1.3	≤0.2	≤0.25	≤0.1	≤0.5	0.4-1	≤0.1	-	-	≤0.15
AA5754	Bal.	2.6-3.6	≤0.4	≤0.2	≤0.3	≤0.1	≤0.4	≤0.5	≤0.15	0.1-0.6	-	≤0.15
AZ31	2.5-3.5	Bal.	≤0.1	0.6-1.4	-	≤0.05	≤0.005	≥0.2	-	-	≤0.4	≤0.005

The base materials were tensile, bending and hardness tested accordingly to different standards [152]–[154]. In the hardness testing, a 3x3 matrix was made using a load of 500g. The average of these 9 indentations was used to compare the welded materials to the base material. Both base material and welded samples were tested to tensile strength and this test was made at a speed of 5mm/min and the tested samples had a T-shape made according to the tensile testing [152]. The bending testing was performed at a speed of 6mm/min and the samples were made according to the standard [153].

The alloys were friction stir welded with a tool with a scrolled shoulder and a threaded conic pin (Figure 4.3). The shoulder had a diameter (D_s) of 15mm and the pin was conical with a diameter (D_P) of 4mm near the shoulder and 3 mm in the tip. This process used a plunge speed (P_s) of 0.1mm/s, a pitch angle (α) of 0^o and a dwell time (D_T) of 6 seconds. The other parameters like advancing speed (V), tool rotation speed (Ω), applied force (F) and pin length (L_P) were varied to define the best conditions for each material condition.

Figure 4.3 – Tool used the tests.

These tests have been conducted in a LEGIO^{TM} FSW 3U welding equipment from ESAB (Figure 4.4). This equipment allows us to do the welds in a force or position controlled welds which

allow for different applications in welding. This welding equipment also allows four degrees of movement, x-, y- and z-axis and rotation around the z-axis.

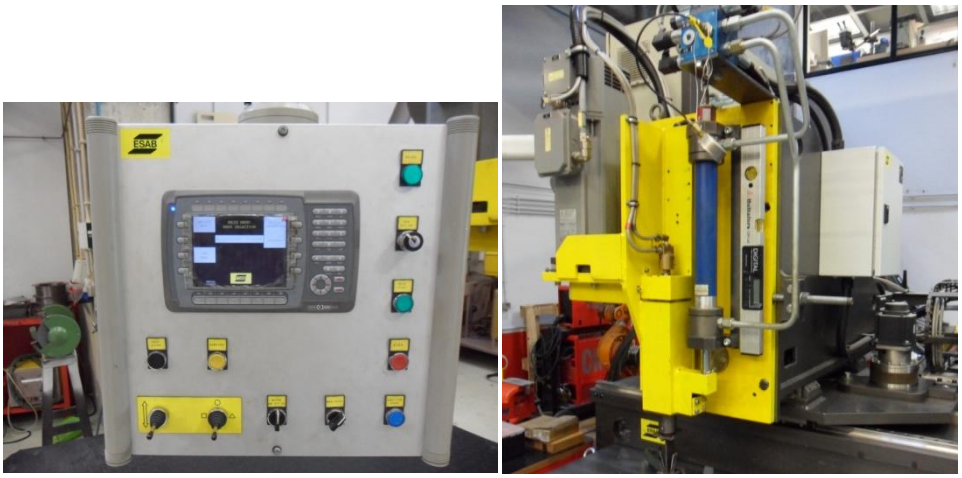

Figure 4.4 – LEGIO™ FSW 3U welding equipment from ESAB, control panel (left) and welding machine (right).

FSW was applied to the described base materials and their combinations. This has divided the performed welds into 2 categories similar and dissimilar welds. In the similar welds only one material was used in the joining process and the goal was to evaluate the performance of the joint. In dissimilar welds, the different materials were joined in three combinations: AA5754-AA6082, AA6082-AZ31 and AA5754-AZ31. The goal here was to evaluate the viability of these dissimilar welds and compare the results with the similar welds and base materials.

Samples of both base material and welded samples were taken and used to characterize the different welds through metallurgical characterized using the following reagents [155]:

- *Keller's reagent*: 2 mL HF (48%), 3 mL HCl (conc), 5 mL HNO_3 (conc), 190 mL H_2O;
- *Poulton modified reagent*: 50 mL Poulton's reagent, 25 mL HNO_3 (conc), 40 mL of solution of 3 g chromic acid per 10 mL of H_2O;
- *Acetic-picral:* 5 mL acetic acid, 6 g picric acid, 10 mL H_2O, 100 mL ethanol (95%);
- *Acetic-picral 2:* 10 mL acetic acid, 4.2 g picric acid, 10 mL H_2O, 70 mL ethanol (95%).

The first two reagents were used to identify the microstructures of aluminium alloys while the other two were used for magnesium alloys. Welded samples were also tested to tensile and bending forces. The best results were then submitted to corrosion testing to identify any corrosion mechanisms induced by this process.

The welded samples efficiencies were measured to tensile strength with the help of performance coefficients based on these tensile testing. The tensile tests were performed in Instron model 4507 equipment with a loading cell of 200kN. Tensile tests were also performed in an Instron model 5566 equipment with a loading cell of 10kN. The Global Efficiency to

tensile strength (GETS) assesses the tensile strength efficiency of the welded joint (i) against the BM properties. This coefficient was developed by Vilaça [156]and takes into account the different coefficients that are taken from tensile testing. The GETS formula is given by:

$$GETS = C_E \frac{E_i}{E_{BM}} + C_{\sigma_y} \frac{\sigma_{y_i}}{\sigma_{y_{BM}}} + C_{\sigma_{UTS}} \frac{\sigma_{UTS_i}}{\sigma_{UTS_{BM}}} + C_A \frac{A_i}{A_{BM}} + C_{U_T} \frac{U_{T_i}}{U_{T_{BM}}} \qquad \text{Eq. 4.1}$$

Where E is the Young Modulus, σ_y is the yield stress, σ_{UTS} is the ultimate tensile stress, A is the elongation and U_T is the toughness. In Table 4.2 the coefficients are used to relate the different properties of tensile strength. The values of the coefficients are given taking into account the final application, therefore these values can change in order to better comply with the final application.

Table 4.2 – Coefficients for GETS efficiency calculation.

CE	$C\sigma_y$	$C\sigma_{UTS}$	CA	CU_T
0.1	0.3	0.3	0.15	0.15

With the results from the welding tests, the efficiency to bending was measured with the assistance of performance coefficients based on these tests. The bending tests were performed in the LEGIO™ FSW 3U equipment. The Global Efficiency to Bending (GEB) [94] assesses the bending efficiency of the welded joint (i) against the BM properties. In an analogy to GETS, GEB takes into account the different coefficients that are taken from bending testing. The GEB formula is given by:

$$GEB = C_{F_B} \frac{F_{Bi}}{F_{BM}} + C_d \frac{d_i}{d_{BM}} + C_{U_B} \frac{U_{B_i}}{U_{B_{BM}}} \qquad \text{Eq. 4.2}$$

Where F is the maximum load, d is the displacement to the maximum load and U_B is the energy consumed until the beginning of the fracture. In Table 4.3 the coefficients used to relate the different properties of tensile strength are presented:

Table 4.3 – Coefficients for GEB efficiency calculation.

F_B	d	UB
0.25	0.25	0.50

Hardness profiles were made in the mid-section of each sample and 21 were taken indentations in order to guarantee that the points covered all the area affected by the process. Afterwards, the hardness profile was compared to the base material hardness through a performance coefficient. The Hardness Ratio Drop (HARD) [94] was calculated by relating the

minimum hardness found in joined materials compared with the average hardness. The HARD is given by:

$$HARD = \frac{H_{min}}{H_{Bm}} \quad \text{Eq. 4.3}$$

Where H_{min} is the minimum hardness in the welded sample and H_{BM} is the base material average hardness. The global weld efficiency (%Weld) is a weighted average from the previous parameters; and much like GETS and GEB is a coefficient of efficiency dependent of the application and is given by:

$$\%Weld = C_{GETS}GETS + C_{GEB}GEB + C_{HARD}HARD \quad \text{Eq.4.4}$$

The coefficients are given in Table 4.4:

Table 4.4 – Coefficients of the weld efficiency calculation.

C_{GETS}	C_{GEB}	C_{HARD}
0.4	0.5	0.1

After this analysis, the parameters to use to prepare for corrosion testing were made and their performance was evaluated. The corrosion testing was made according to the ASTM B117:95 standard [157]. The samples were put in a saline environment (5% NaCl) in an environment control chamber (Figure 4.5) and their corrosion behavior was tested for 350h. The samples were tested both in the front and back of the welded samples.

Figure 4.5 – Equipment for saline testing.

Electrochemical tests were performed to evaluate the corrosion rate between the dissimilar materials. These tests were performed to understand the interaction between the joined pairs of materials and understand the behavior observed in the saline testing. Two tests were performed for this evaluation:

- Polarization curves;
- Zero resistance amperometry (ZRA).

For both these tests the samples were inserted in a salt solution with 3% NaCl were. The use of this solution was to facilitate the transfer of the electrons which helps in the data acquiring.

In the polarization curves testing, each individual material would be introduced in the solution; after stabilizing the potential would vary (increasing or decreasing depending on the goal) and it would be observed how the current would vary with this change in the potential. In the experimental setup, the sample is considered as the working electrode, and there is also the auxiliary electrode to close the circuit and reference electrode from which it is obtained the information in this test.

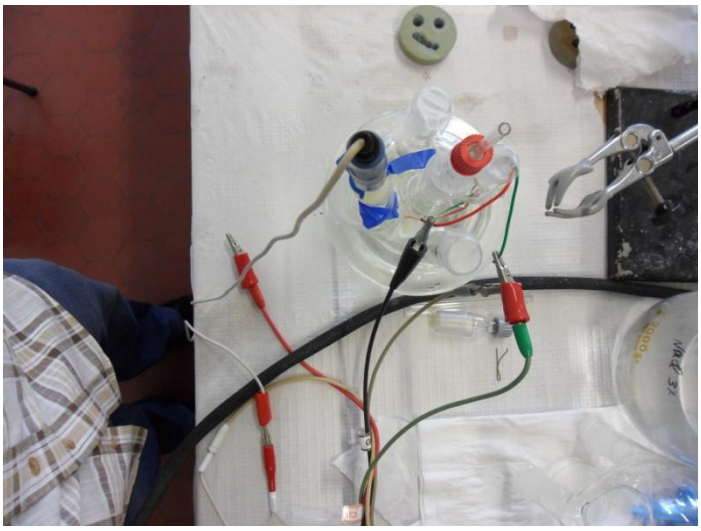

Figure 4.6 – Experimental Setup of the electrochemical test ZRA.

In the ZRA (Figure 4.6), a material pair was introduced in the solution and the samples were immersed for 24 hours in order to observe the interaction between the 2 materials without any outside interference. In this experiment, one of the materials was considered to be the working electrode while the other is the auxiliary electrode. The reference electrode was also included in this test and is located really close to the surface of both materials. During this test no contacts between the samples are allowed. Figure 4.6 shows the experimental setup for both electrochemical experiments.

4.3 Materials Analysis

The viability of introducing aluminium and magnesium alloys in car seat systems is going to be studied. The chosen aluminium and magnesium alloys have been identified to be viable solutions for replacing steels in automotive industry and have been applied in different parts of the motor vehicle.

Table 4.5 – Properties of the base materials.

	Tensile Values					Bending Values			Hardness
	E (GPa)	σ_y (MPa)	σ_{UTS} (MPa)	A (%)	U_T (J/m^3)	F_B (N)	d (mm)	U_B (J)	HV05
AA6082	74	299	342	12	52855	2930	15	36790	125
AA5754	75	129	242	20	44388	1806	15	22370	72
AZ31	45	145	252	17	41959	2094	5.5	9075	74

Table 4.5 presents the tensile, bending and hardness properties for the different materials. It can be observed from this characterization that the AZ31 and AA5754 share many similarities in the tensile and hardness properties while the AA6082 has higher properties compared with these two alloys. It should be remarked that even though the properties are very different the material matrix of the AA6082 is similar to the AA5754, since both of these have a face centered cubic (CFC) arrangement, while the magnesium alloy has a hexagonal close packed (HCP) arrangement.

Figure 4.7 shows the microstructure of the magnesium alloy which presents a small and homogeneous grain size. The etchant acetic-picral 2 was used to reveal the microstructure of the AZ31 alloy. It can also be observed that despite the smaller grain size the grain size is not homogeneous showing a large distribution of grain size.

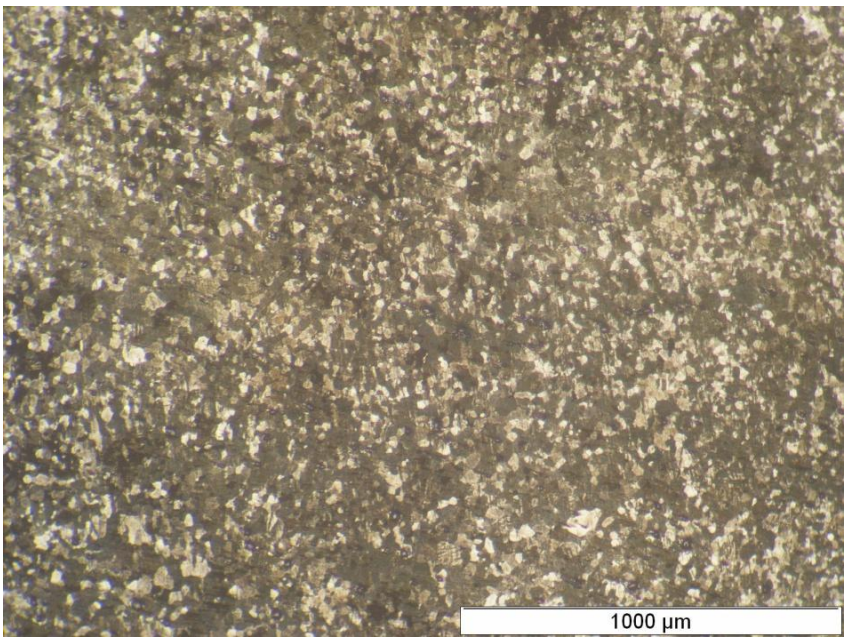

Figure 4.7 – Microstructure of the AZ31 alloy.

4.4 FSW applied to aluminium alloys

4.4.1 Aluminium AA6082-T6

A study has been performed to identify the FSW parameters that are most suitable to obtain efficient welded samples and that provide a performance closer to the base material properties. Several methods can be applied and tests focused on the weld integrity have to be introduced to evaluate the defect from this process.

Table 4.6 – FSW parameters for AA6082-T6 alloy.

Designação	F (kg)	Ω (rpm)	v (mm/min)	l_{pin} (mm)
6.1	650	800	100	1.92
6.2	650	800	200	1.92
6.3	750	800	200	1.92
6.4	750	800	400	1.92
6.5	650	800	100	2
6.6	650	800	200	2
6.7	750	800	200	2
6.8	800	800	200	2
6.9	850	800	400	2

One of the most problematic issues in FSW welded samples is the *"root defect".* The root defect refers to a lack of penetration in the nugget area that joins the two plates together. In order to have a sound weld, it is required that this defect is completely eliminated. One way to confirm this is to observe if the welded sample presents the same behavior to bending as the BM. It was observed that the BM of the AA6082-T6 alloy can be bent to 180^{o}. In this testing, the samples will be bent and the ones that are able to reach the 180^{o} will be considered valid and evaluated for the different considered tests. Table 4.6 presents the FSW parameters that have been performed, different applied forces, advancing speed and pin lengths that were studied. All tests were performed at a constant rotational speed of 800 rpm with a dwell time and plunge speed of 6s and 0.1mm/s, respectively.

These were the tests that led to sound welds with a good finish. The next step was to perform bending tests to guarantee that the material had the same performance as the BM. The tests were stopped when the material reached the crack initiation; if until 180^{0} no crack had been initiated the sample would be considered valid. Figure 4.8 shows the results for the different coefficients in the bending results from the FSWed AA6082 samples.

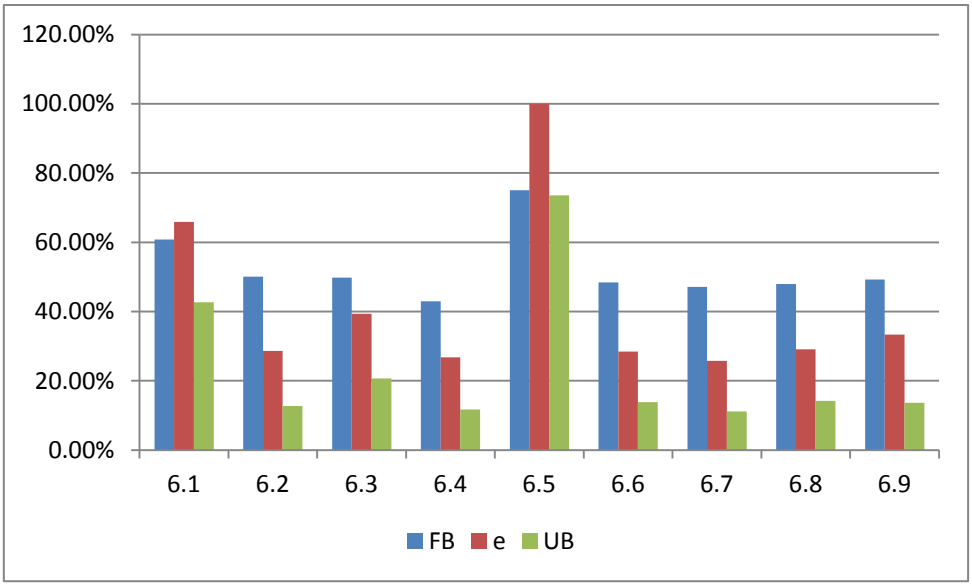

Figure 4.8 – Efficiency of the different parameters considered in the GEB calculation.

It was observed that the lowest advancing speeds gave the best results regarding the GEB efficiencies in these trials. It was also observed that the trial 6.5 is the only trial that was able to comply with the pre-established passing conditions. This was the only sample that reached the 180^{o} and endured this test. After this analysis, the welded sample was submitted to hardness and tensile testing.

Figure 4.9 presents the hardness testing of the AA6082-T6 samples. It can be observed that this sample has the typical behavior of the heat treatable aluminium alloys.

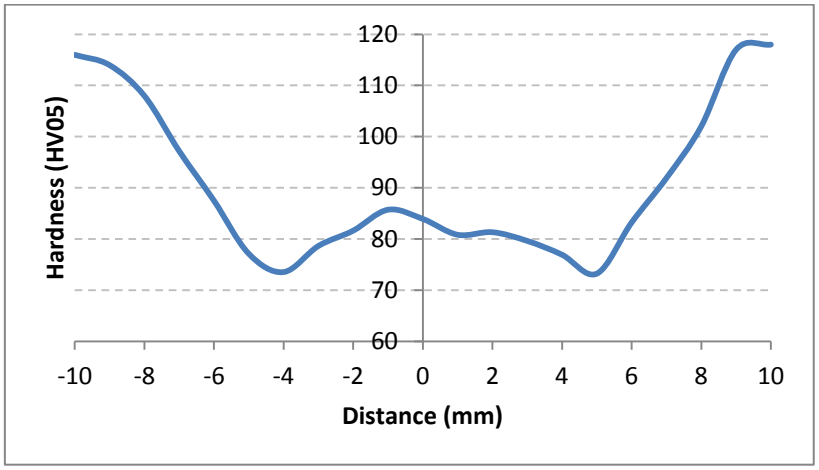

Figure 4.9 – Hardness profile of the AA6082-T6 alloy.

The average hardness of the nugget area is around the 83HV05. This hardness then decreases to the lowest point in the heat affected zone. This is a decrease of the hardness in this alloy that reaches its minimum hardness around the -4/5 mm where heat affects very aggressively the material. After that area the hardness increases until the average hardness of the base material.

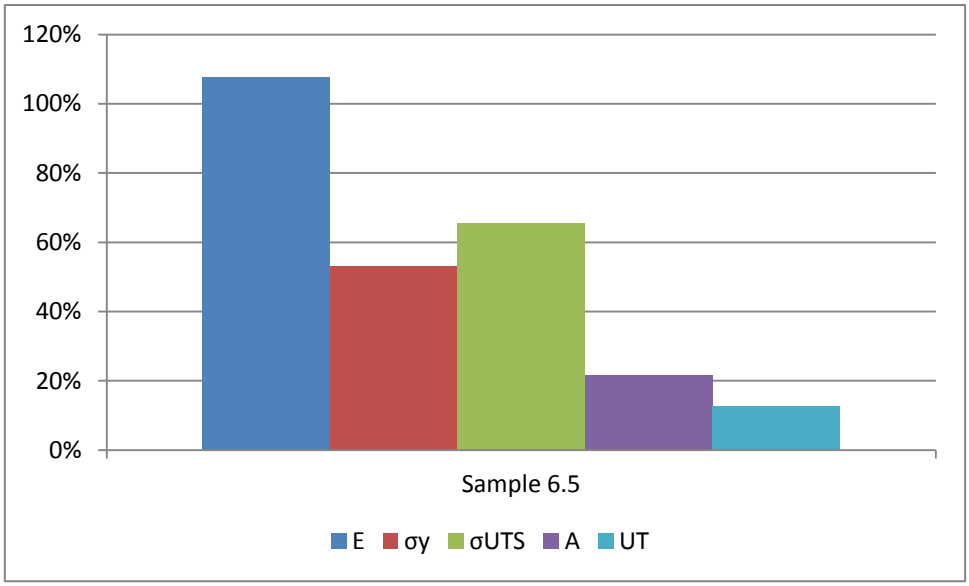

Figure 4.10 - Efficiency of the different parameters considered for the GETS calculation of AA6082-T6 alloy.

It was observed in the tensile testing that the AA6082-T6 alloy is very affected by this process losing most of its ductility along it. . It can be observed that in damage this parameter has greatly affected the toughness of the welded sample. The tensile and ultimate strength have also been affected by this process decreasing to nearly half of the value of the BM. It was possible to understand that the GETS has a value of nearly 51%. The GEB and HARD factors had the values of 80% and 59%, respectively. It was observed that this process, despite indicating a good mechanical performance to bending, does not guarantee a good performance in other tests due to the heat involved in the process. Another problem is that it is difficult to view how the different process parameters affect the welded samples properties. In the aluminium AA5754-H111 it will be used a known process to identify how the different parameters affect the properties of the welded samples.

4.4.2 Aluminium AA5754-H111

4.4.2.1 Taguchi method and mechanical results

Another method was applied in aluminium alloys to identify the most suitable parameters for joining them together. In the case of the aluminium AA5754-H111, Taguchi method hwas successfully applied. This is a statistical method that allows the reduction in the number of trials needed to obtain the best parameters for a particular goal. Usually for 3 different parameters at 3 different levels it would be necessary to perform 27 trials to understand the results. However, using Taguchi method it only takes 9 trials as this method uses interactions between parameters. In fact, this method allows understanding how the different parameters influence the properties of the welded materials. To study the influence of the process

parameters in the AA5754-H111 alloy 3 parameters were studied at 3 different levels. The parameters are advancing speed, applied force and pin length. These 3 parameters were studied for 3 different levels.

Table 4.7 – FSW parameters for AA5754-H111.

FSW Parameter	Symbol	Level 1	Level 2	Level 3
Variable Parameters				
Advancing Speed (mm/min)	A	100	200	400
Applied force (kg)	B	500	550	600
Pin Length	C	1.92	2	2.09
Fixed Parameters				
Rotational speed (rpm)		800		
Dwell time(s)		6		
Plunge speed (mm/s)		0.1		
Pitch angle		0		

The advancing speed was studied at 100, 200 and 400mm/min, while the applied force was studied at 500, 550 and 600 kg. The pin length was studied for 1.92, 2 and 2.09 mm. These trials were performed using a rotational speed of 800rpm, plunge speed of 0.1mm/s, a pitch angle of 0^{o} and a dwell time of 6s. These parameters were kept constant during these trials and the tool worked on a clockwise rotation. These values are depicted in Table 4.7. A matrix of the trials developed for this process was developed. It uses a L_9 matrix in which 3 parameters at 3 different levels are considered. Each parameter has 2 degrees of freedom having a total of 6 freedom degrees in this study. The developed work uses the same strategy as it was used by Vidal *et al.* [94] concerning the applicability of the Taguchi method.

Table 4.8 – Ortogonal vectors matrix L_9 (3^4).

	Parameters			
Trial	**A**	**B**	**C**	**D**
1	1	1	1	1
2	1	2	2	2
3	1	3	3	3
4	2	1	2	3
5	2	2	3	1
6	2	3	1	2
7	3	1	3	2
8	3	2	1	3
9	3	3	2	1

For this study, only 3 parameters were studied. Therefore, the 4^{th} column of this matrix will be eliminated allowing the study the selected variables. Table 4.9 presents the different trials that have been performed to identify the best parameters to improve the behavior to tensile and bending loads and also identify the parameters that give the best results taking into account

both loads. This method will also be used to identify the trends of the parameters and their influence on the welded sample properties.

Table 4.9 – Test parameters according to Taguchi L_9 matrix.

Trial	V (mm/min)	F (Kg)	Pin Length (mm)
1	100	500	1.92
2	100	550	2
3	100	600	2.09
4	200	500	2
5	200	550	2.09
6	200	600	1.92
7	400	500	2.09
8	400	550	1.92
9	400	600	2

All tests in the Taguchi method were considered valid and this enables us to proceed with this optimization method. Also, a kissing bond was identified in the faster and colder welds although no other major defect was found in these samples. The samples were metallurgically characterized and it was observed that there was a flow of material that became clearer with lower speed. Table 4.10 shows the effect mentioned before: the nugget seems to be more visible for lower advancing speeds and the decrease in this effect can also be observed. As it can be observed, this effect takes place on the advancing side of the samples and it can be related with the changes in speed of the material and possibly the material is more affected by the flow of the material on this side.

Table 4.10 – Images showing the pronounced effect in the nugget.

Advancing Speed (mm/min)	Macrographs
100	
200	
400	

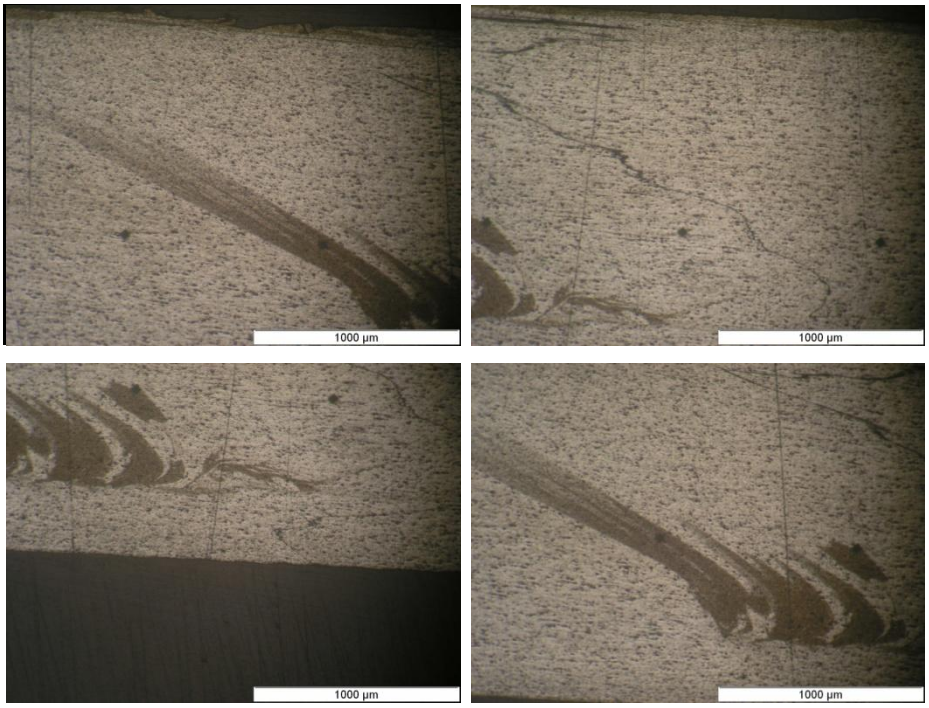

Figure 4.11 – Microstructure of the AA5754-H111 welded sample.

Figure 4.11 presents the images of a welded sample with an advancing speed of 400mm/min in different sections. It can be observed that the boundary is on the advancing side of the nugget. It can also be observed a line that might be related with the boundary between the plates to be joined. This boundary was deformed by the pin and its outline can be related to the oxide layer that remained even after cleaning.

The hardness testing showed that the welded samples with the same advancing speed had similar profiles between themselves. In Figure 4.12, the profiles between the samples are presenting, showing that the welded samples have small differences between themselves. There is an increase in the hardness in the nugget of each sample with the increase of the welding speed but besides that there are not many differences between the different selected parameters. One can also observe that outside the nugget region the average hardness is most of the times close to the average hardness taking into account their standard deviation. The average hardness in the heat affected zone (HAZ) and BM is similar between the three samples.

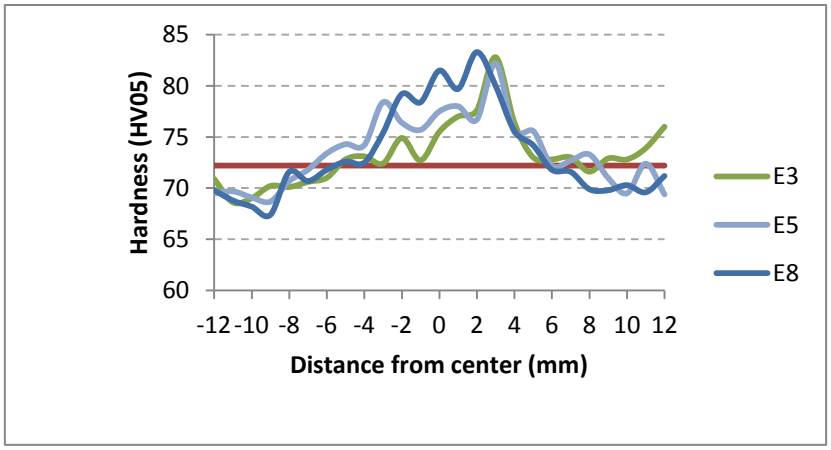

Figure 4.12 – Hardness profiles of the E3, E5 and E8 trials.

It can be observed that the highest hardness is located at the advancing side of the nugget. This increase in hardness can be related with the effect shown in nugget in the metallurgical analysis (Figure 4.11). The hard efficiencies are given in Table 4.11 and show how the heat affected these alloys during the FSW process. It can be observed that the values of the hardness profiles are very similar between them and that these changes in hardness are complemented in the equipment error measurement.

Table 4.11 – HARD efficiencies for welded samples.

E1	E2	E3	E4	E5	E6	E7	E8	E9
88.49%	97.77%	95.00%	94.17%	95.14%	89.88%	93.75%	93.34%	87.94%

The calculation of the GETS efficiency (Figure 4.13 and

Table 4.12) shows that the lowest advancing speeds have the best behavior regarding the efficiency. It also shows an improved efficiency for the bigger pin length.

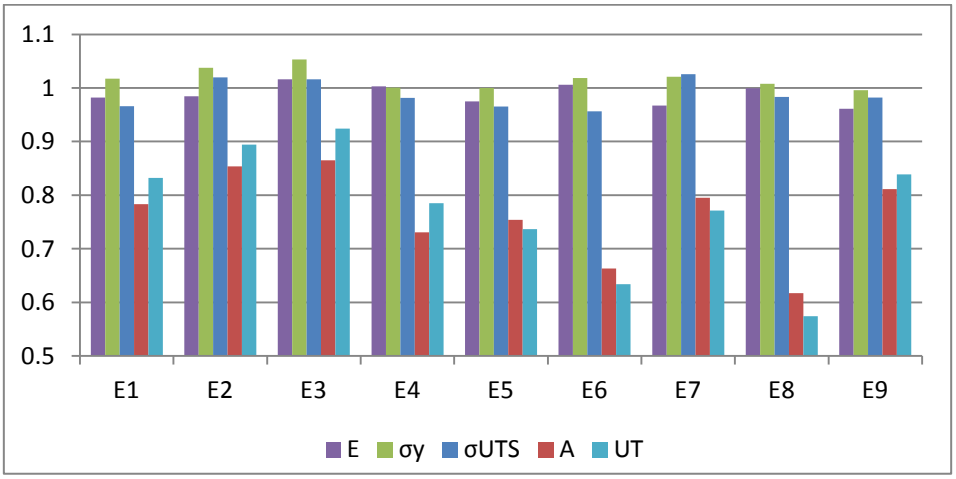

Figure 4.13 – Efficiency of the different parameters considered for the GETS calculation.

Table 4.12 – GETS efficiencies for the AA5754-H111.

E1	E2	E3	E4	E5	E6	E7	E8	E9
92.69%	97.05%	97.62%	92.81%	91.06%	88.20%	96.03%	88.35%	94.56%

It can be clearly observed that the pin length has a great influence in the efficiency of the weld being emphasized the low efficiency visible in the trials with the lowest pin length. This lower efficiency is particularly visible for the higher advancing speed in which the lower pin length clearly affects the performance of the welded samples. It is also possible to observe that the samples with the lower advancing speeds have the highest efficiencies when compared to the other advancing speeds. This can be related to the higher stresses that the material might have due to the higher deformation that exists in the TMAZ area.

The results from GEB (Figure 4.14 and Table 4.13) show that most trials have a performance better than the base material although E1 trial is below. Despite these results it was observed that in the faster welds with lower pin length it a fissure was visible in the bottom of the weld compliant with the “kissing bond” defect.

It can be observed that welded samples efficiency improve with the increasing advancing speed. This can be related to the increase in advancing speed that intensifies the hardness of the material. Since this test is focused on the nugget area, the results are affected by the properties of the nugget and therefore the faster welds have a higher hardness which will translate in a higher resistance during this test.

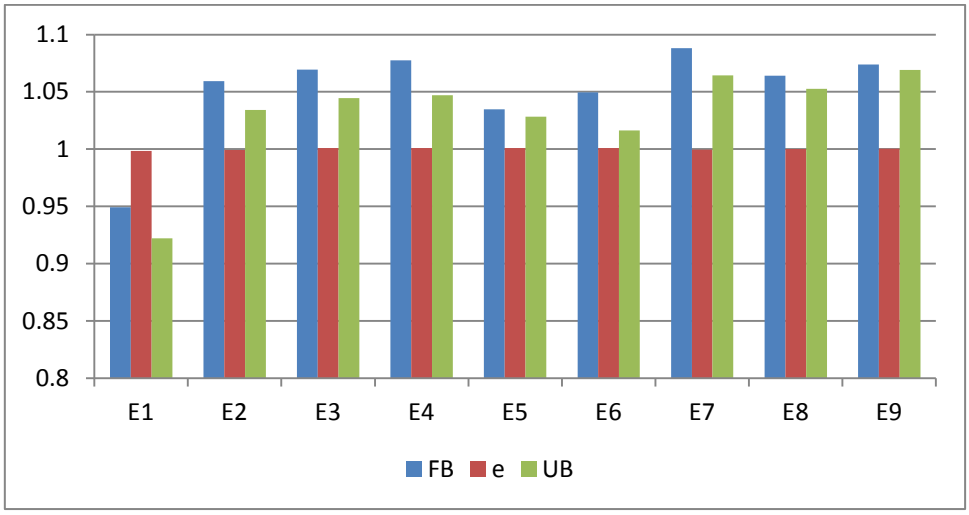

Figure 4.14 – Efficiency of the different parameters considered for the GEB calculation.

Table 4.13 – GEB efficiencies for welded samples.

E1	E2	E3	E4	E5	E6	E7	E8	E9

94.79%	103.16%	103.98%	104.31%	102.31%	102.08%	105.40%	104.23%	105.31%

4.4.2.2 Identification of optimal parameters

The 3 levels for each parameter are equally represented in the 9 trials made. The planning for these is orthogonal which makes it possible to separate the effect of each in each level. Because of this, the average response of the parameter X in the level Y is given by the results obtained in the different trials with the parameter X at the level Y. For example, the average value of GETS for the level 1 applied force (F1) is calculated by averaging the trials with F1 force (trials 1, 4 and 7). Figure 4.15 shows the average results for the GETS, GEB and HARD, it can be observed the influence for each parameter at the each level.

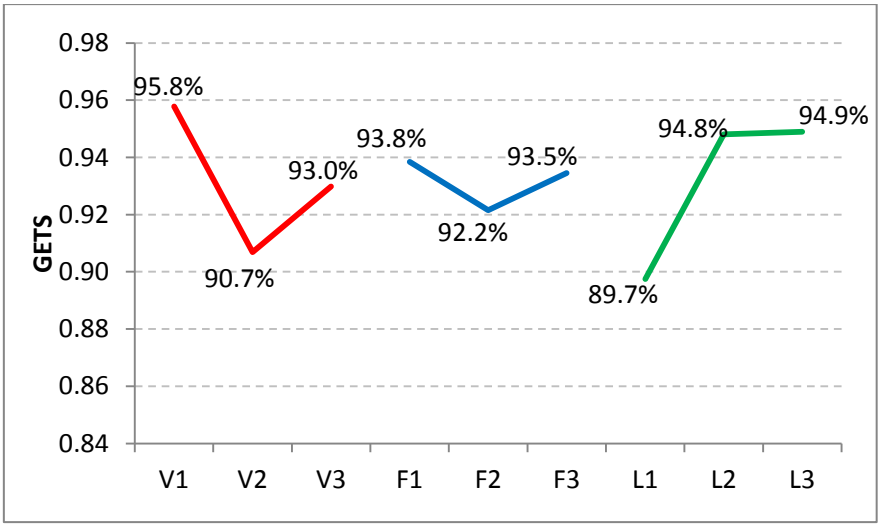

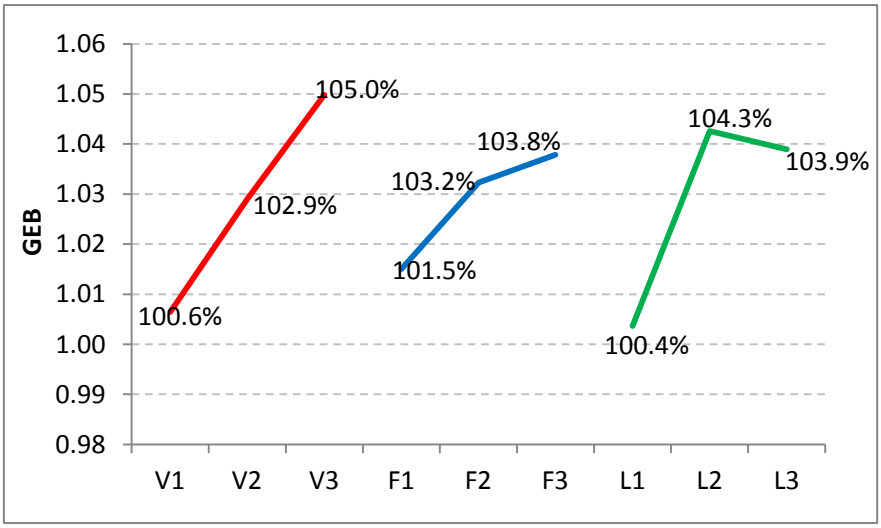

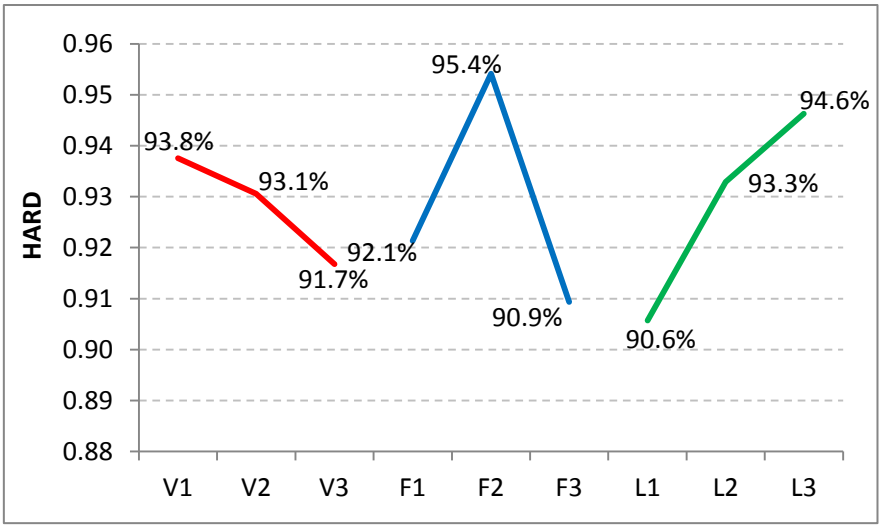

Figure 4.15 – Effect of the process parameters on the GETS, GEB and HARD.

In the GETS analysis, it was observed that the lower advancing speeds in the welded samples provide a better behavior in these materials. This observation can be related with the material, a non-heat treatable alloy, and therefore the increased heat of the lower advancing speeds does not influence the welded sample properties so much. For the higher advancing speeds, the distortion promoted by the process made the samples more susceptible to tensile loads. The applied forces do not seem to influence the behavior of the samples that much; however there seems to be a slight tendency for the welded samples to have a better behavior for lower applied forces. The pin length is the most crucial parameter in this analysis. In fact, the lowest pin length seems to have the lowest performance from all studies. With the higher advancing, there is a higher flow of material which makes the tool rise higher when in a force controlled process. This makes the lowest pin length very susceptible to process conditions especially to the increased welding speed. From the analysis of Figure 4.15 it can be observed that the best performances for the GETs were reached at the first level of advancing speed (A1), first level of applied force (B1) and third level of pin length (C3).

The GEB results have brought some very interesting results. It can be observed that with the increasing speed the GEB augments and the GEB efficiency is usually better than the BM. This is an important result that is dependent not only of the process conditions but also of the testing conditions. The bending test, unlike the tensile one, was focused on the welded area; therefore if there is an improvement or damage to the welded area due to the testing conditions this process will provide a more accurate perspective of the welded area. The applied force has the same behavior as the advancing speed and it seems that in the tested forces the highest applied force is the one that gives better results. The pin length influence for the GEB is similar to the pin length influence assessed on GETS efficiency. The lowest pin

length has been observed to have the worst efficiencies. It has also been observed that the higher pin lengths have similar behaviors between both of them and that the 2mm is only a bit better. The pin length continues to be very important for this parameter; however for the tested conditions as long as it can be guaranteed that the sample is processed in its full thickness a good performance can be guaranteed on bending loads. Using the logic as in GETS, it can be observed that the best performance for GEB was reached at the third level of advancing speed (A3), third level of applied force (B3) and second level of pin length (C2).

The HARD results show a trend with the increasing speed and pin length where there is a drop on the HARD efficiency. However, some of these results do not seem to be aligned with the FSW process characteristics and aluminium. The increase of the advancing speed should have a positive effect in the HARD because less heat is produced by the process and therefore the material should have an improvement in its HARD efficiency. The influence of the pin length does not make sense because the pin length should not influence the material in this manner. With the increasing pin length there should exist no difference at most the efficiency should decrease with the increasing length due to higher released heat. The applied force has given some important results to the material and it seems level 2 force has a better effect over the material. These results are greatly influenced by the BM hardness and it seems most results are within the calculated standard deviation of the base material. The best performance for HARD was reached at first level of the advancing speed (A1), the second level of applied force (B2) and third level of pin length (C3). A deeper analysis will be performed to better understand these results. This will enable us to understand if these hardness results should be disregarded in the following steps of the selection of the optimal parameters and if it makes sense to consider the optimal results.

4.4.2.3 Analysis of Variance (ANOVA)

ANOVA is a normalized statistical technique to calculate the contribution percentage of each parameter in the chosen performance factors. This technique was used to identify the most significant parameters and quantify their effect in the GETS, GEB and HARD factors.

The ANOVA technique uses the total sum of squares deviations (SS_T) and is calculated through the equation:

$$SS_T = \sum_{k=0}^{n} (Y_i - \overline{Y})^2 \qquad \text{Eq. 4.5}$$

Where n is the number of trials (n=9), Y_i is the experimental result for the Trial i and $\bar{Y}$ is given by:

$$\overline{\mathrm{Y}} = \frac{1}{n}\sum_{i=1}^{n} \mathrm{Y_i} \quad \text{Eq. 4.6}$$

The total sum of square deviations is composed by the sum of square deviations for each process parameter (SS_P) and by the sum of square deviation due to error (SS_e). SS_P can be calculated using the following equation.

$$\mathrm{SS_P} = \sum_{j=1}^{r} \frac{(\mathrm{SY_j})^2}{\mathrm{r}} - \frac{1}{\mathrm{n}}\left[\sum_{\mathrm{i}=1}^{\mathrm{n}} \mathrm{Y_i}\right]^2 \quad \text{Eq.4.7}$$

In which P represents one process parameter, j is the level of the parameter P, r is the number of trials at each level for the parameter P and SY_i is the sum of the experimental results involving the parameter P at the level j. The sum of the square deviations due to error is given by:

$$SS_e = SS_T + SS_A + SS_B + SS_C \quad \text{Eq. 4.8}$$

The total number of degree of freedom (D_T) is given by n-1. The number of degrees of freedom for each parameter (D_P) is given by r-1 and the variance for each parameter (ρ_P) is calculated using the following formula:

$$\rho_P = {}^{SS_P}/_{SS_T} \quad \text{Eq. 4.9}$$

Table 4.14 to 4.16 present the values of the variance analysis for the GETS, GEB and HARD factors, respectively. The contribution percentages of each process parameter are shown in Figure 4.16 to Figure 4.18.

Table 4.14 – Variance analysis results for the GETS factor.

Parameter	DOF	SS	V	F	Ro
Advancing Speed	2	0.003910324	0.001955162	23.17616	0.400465
Applied Force	2	0.000470347	0.000235174	2.787709	0.048169
Pin Length	2	0.005215074	0.002607537	30.90931	0.534087
Error	2	0.000168722	8.43609E-05	-	0.017279
Total	8	0.009764467	-	-	1

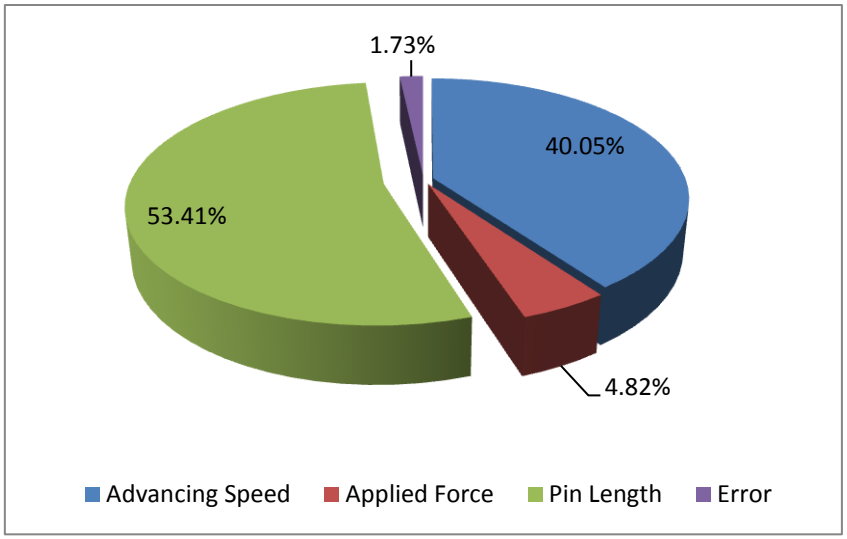

Figure 4.16 – Parameter contribution for GETS factor.

Table 4.15 – Variance analysis results for the GEB factor.

Parameter	DOF	SS	V	F	Ro
Advancing Speed	2	0.00282301	0.001411505	16.73174	0.336931
Applied Force	2	0.000853771	0.000426885	5.060227	0.101899
Pin Length	2	0.002775982	0.001387991	16.45301	0.331318
Error	2	0.00192584	0.00096292	-	0.229852
Total	8	0.008378603	-	-	1

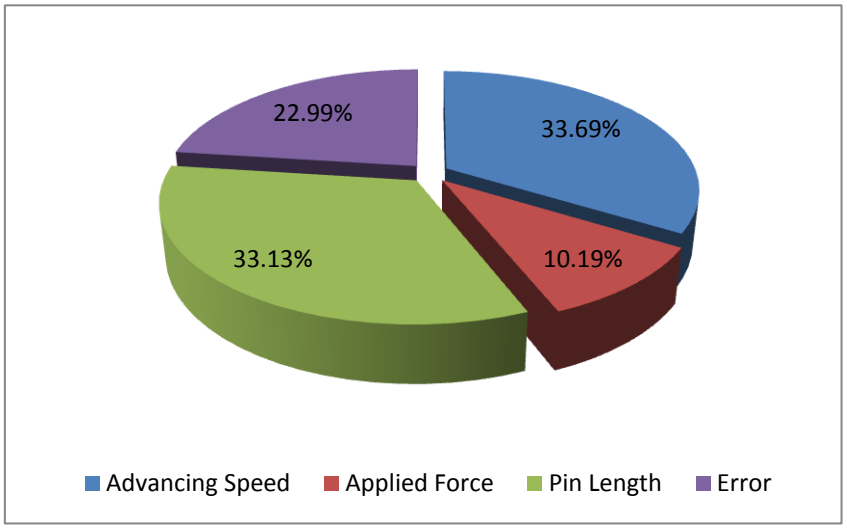

Figure 4.17 - Parameter contribution for GEB factor.

Table 4.16 - Variance analysis results for the HARD factor.

Parameter	DOF	SS	V	F	Ro
Advancing Speed	2	0.000671212	0.000335606	3.97822	0.075561
Applied Force	2	0.003223098	0.001611549	19.10303	0.362838
Pin Length	2	0.002571063	0.001285532	15.23848	0.289436
Error	2	0.002417643	0.001208822	-	0.272165
Total	8	0.008883017	-	-	1

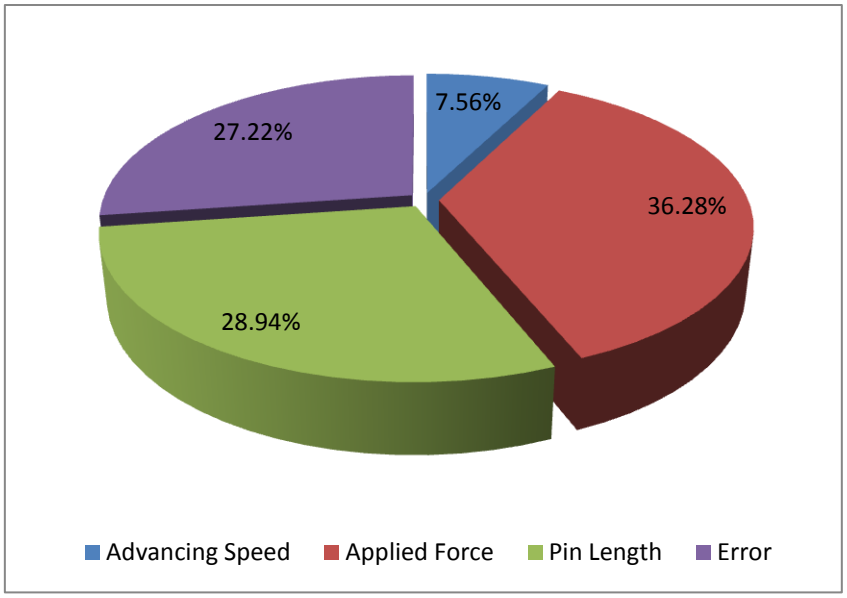

Figure 4.18 - Parameter contribution for HARD factor.

In both GETS and GEB analysis (Figure 4.16, Figure 4.17 and Table 4.14 and Table 4.15), it can be observed that the pin length is a determinant contributor that needs to have good performances in this sector. This fact relates to typical defects of the FSW, the root defect. It has been observed that this defect is very important in the FSW because it can have a big negative effect in the welded samples. Having even a small root defect can greatly decrease the resistance to tensile and bending tests. The second major contributor for both the properties is the advancing speed where this effect seems to affect the samples in different manners. The GETS factor seems to be better for lower speed while the GEB seems to improve for higher speed rates. This different relationship is associated with the fact that these alloys are not affected by the heat released in the process. Therefore, this implies that GETS will present less distortion for lower speeds, while GEB, in the higher speeds, will increase the hardness of the nugget where the bending test is performed.

The HARD factor is usually performed to understand how the heat decreased the properties of the material in the heat affected zone. However, these alloys are non-heat treatable and this effect is reduced. In fact, in these alloys, it would only be visible under really high temperatures. This explains the reason why the advancing speed has such a low influence in the materials. The applied force can influence this factor by restraining the material harder under the shoulder. However there are some concerns regarding this result. The pin length also does not seem to be an important parameter that can greatly influence the material and the variation in the pin length should be disregarded. The standard deviation regarding the average hardness of the base material might be enough to contain these values. One important detail about factor is the high error related to this parameter that can make some of

the results be disregarded because of it. The next steps will take into consideration this variation in the hardness.

4.4.2.4 Prediction of optimal performance

After determining the optimal condition for each factor (Figure 4.15) the performance for the established parametric combination, Y_{opt} is going to be predicted. The quality characteristic sustains that the higher the value the better it will be considered for this study. The optimal parametric condition for maximizing the GETS factor is $A_1B_1C_3$. The optimal performance of this factor can be established by the following relationship:

$$Y_{Opt} = \frac{T_R}{N_R} + \left(\bar{A}_1 - \frac{T_R}{N_R}\right) + \left(\bar{B}_1 - \frac{T_R}{N_R}\right) + \left(\bar{C}_3 - \frac{T_R}{N_R}\right) \quad \text{Eq. 4.10}$$

Where T_R is the results total, N_R the total number of results and $\bar{A}_1$, $\bar{B}_1$ and $\bar{C}_3$ are the average values for the A, B and C at the levels 1, 1 and 3 respectively.

Using the same procedure for GETS, the optimal performance of the GEB was predicted using the formula below. $A_3B_3C_2$ was the parametric combination found.

$$Y_{Opt} = \frac{T_R}{N_R} + \left(\bar{A}_3 - \frac{T_R}{N_R}\right) + \left(\bar{B}_3 - \frac{T_R}{N_R}\right) + \left(\bar{C}_2 - \frac{T_R}{N_R}\right) \quad \text{Eq. 4.11}$$

For the HARD factor the optimal parametric combination was $A_1B_2C_3$ and the optimal performance was calculated using the following formula:

$$Y_{Opt} = \frac{T_R}{N_R} + \left(\bar{A}_1 - \frac{T_R}{N_R}\right) + \left(\bar{B}_2 - \frac{T_R}{N_R}\right) + \left(\bar{C}_3 - \frac{T_R}{N_R}\right) \quad \text{Eq. 4.12}$$

The results for the optimal performance results for the GETS, GEB and HARD factor are presented in Table 4.17.

Table 4.17 – Optimal performance results.

	GETS	**GEB**	**HARD**
Y_{Opt}	98.2%	107.3%	98.1%

4.4.2.5 Algebraic manipulation Algorithm

From the Taguchi method it three distinct optimal parametric combinations that maximize each one of the performance parameters were obtained.

Table 4.18 – Optimal values from Taguchi Method.

	GETS		GEB		HARD	
Advancing Speed (mm/min)	**A1**	100	**A3**	400	**A1**	100
Force (Kg)	**B1**	500	**B3**	600	**B2**	550
Pin Length (mm)	**C3**	2.09	**C2**	2	**C3**	2.09
Optimal Performance (%)	98.2		107.3		98.1	

One of the goals of this thesis is to find process parameters that can enable weld characteristics able to provide balanced properties to the welded sample. An algorithm that encloses in a measured way the different Taguchi results was applied, obtaining a more robust parametric combination that globally improves the properties of the samples. For this goal, the contribution percentages for each parameter (Table 4.19), obtained from the analysis of variance, were considered:

Table 4.19 – Contribution percentages (%).

	Advancing Speed		Applied Force		Pin Length	
GETS	ρA_{GETS}	40.05	ρB_{GETS}	4.82	ρC_{GETS}	53.41
GEB	ρA_{GEB}	33.69	ρB_{GEB}	10.19	ρC_{GEB}	33.13
HARD	ρA_{Hard}	7.56	ρB_{HARD}	36.28	ρC_{HARD}	28.94
Total	ρA_T	81.30	ρB_T	51.29	ρC_T	115.48

The matrix $[P_C]$ is given by:

$$[P_C] = \begin{bmatrix} \frac{\rho A_{GETS}}{\rho A_T} & \frac{\rho B_{GETS}}{\rho B_T} & \frac{\rho C_{GETS}}{\rho C_T} \\ \frac{\rho A_{GEB}}{\rho A_T} & \frac{\rho B_{GEB}}{\rho B_T} & \frac{\rho C_{GEB}}{\rho C_T} \\ \frac{\rho A_{HARD}}{\rho A_T} & \frac{\rho B_{HARD}}{\rho B_T} & \frac{\rho C_{HARD}}{\rho C_T} \end{bmatrix} \quad \text{Eq. 4.13}$$

After the variables have been defined, the following developed algebraic formulation will be used:

$$\begin{bmatrix} Advancing\ Speed & x & x \\ x & Applied\ Force & x \\ x & x & Pin\ Length \end{bmatrix} = [V_0].[F] \quad \text{Eq. 4.14}$$

The matriz $[V_0]$ given by:

$$[V_0] = \begin{bmatrix} A_1 & A_3 & A_1 \\ B_1 & B_3 & B_2 \\ C_3 & C_2 & C_3 \end{bmatrix} \quad \text{Eq. 4.15}$$

where each column is the optimal parametric combination found for the GETS, GEB and HARD, respectively. These parameters are presented in Table 4.19. Matrix [F] is given by:

$$[F] = [Weights][P_C] \quad \text{Eq. 4.16}$$

where

$$[Weights] = \begin{bmatrix} Weight_{GETS} & 0 & 0 \\ 0 & Weight_{GEB} & 0 \\ 0 & 0 & Weight_{HARD} \end{bmatrix} \quad \text{Eq. 4.17}$$

is the matrix that defines the level of importance given to each performance parameter. In a first stage it was considered that all performance parameters are important in the quality of the welds. The algorithm was applied in its simplified form:

$$\begin{bmatrix} Adv.Speed & x & x \\ x & Applied\ Force & x \\ x & x & Pin\ Length \end{bmatrix} = \begin{bmatrix} A_1 & A_3 & A_1 \\ B_1 & B_3 & B_2 \\ C_3 & C_2 & C_3 \end{bmatrix} \begin{bmatrix} \frac{\rho_{A_{GETS}}}{\rho_{A_T}} & \frac{\rho_{B_{GETS}}}{\rho_{B_T}} & \frac{\rho_{C_{GETS}}}{\rho_{C_T}} \\ \frac{\rho_{A_{GEB}}}{\rho_{A_T}} & \frac{\rho_{B_{GEB}}}{\rho_{B_T}} & \frac{\rho_{C_{GEB}}}{\rho_{C_T}} \\ \frac{\rho_{A_{HARD}}}{\rho_{A_T}} & \frac{\rho_{B_{HARD}}}{\rho_{B_T}} & \frac{\rho_{C_{HARD}}}{\rho_{C_T}} \end{bmatrix} \quad \text{Eq. 4.18}$$

The matrix [Weights] was considered has the identity matrix. Replacing these values by the values presented in Table 4.18 and Table 4.19 which will give the following parameters:

$$\begin{bmatrix} Adv.Speed & x & x \\ x & Applied\ Force & x \\ x & x & Pin\ Length \end{bmatrix} = \begin{bmatrix} 100 & 400 & 100 \\ 500 & 600 & 550 \\ 2.09 & 2 & 2.09 \end{bmatrix} \begin{bmatrix} 0.49 & 0.09 & 0.46 \\ 0.41 & 0.20 & 0.29 \\ 0.09 & 0.71 & 0.25 \end{bmatrix} \quad \text{Eq. 4.19}$$

The final parametric combination is the following:

Advancing Speed = 225 mm/min;

Applied Force = 555 kg;

Pin Length = 2.06 mm.

Taking into account the particularities of the process that did not seem to have any influence in the HARD factor, the matrix was adjusted to eliminate these results. The contribution percentages will take this new look:

Table 4.20 – New contribution percentages table.

	Advancing Speed		Applied Force		Pin Length	
GETS	ρA_{GETS}	40.05	ρB_{GETS}	4.82	ρC_{GETS}	53.41
GEB	ρA_{GEB}	33.69	ρB_{GEB}	10.19	ρC_{GEB}	33.13
Total	ρA_T	73.74	ρB_T	15.01	ρC_T	86.54

This means that the algorithm will change to the following formula:

$$\begin{bmatrix} Adv.Speed & x & x \\ x & Applied\ Force & x \\ x & x & Pin\ Length \end{bmatrix} = \begin{bmatrix} A_1 & A_3 \\ B_1 & B_3 \\ C_3 & C_2 \end{bmatrix} \begin{bmatrix} \frac{\rho_{A_{GETS}}}{\rho_{A_T}} & \frac{\rho_{B_{GETS}}}{\rho_{B_T}} & \frac{\rho_{C_{GETS}}}{\rho_{C_T}} \\ \frac{\rho_{A_{GEB}}}{\rho_{A_T}} & \frac{\rho_{B_{GEB}}}{\rho_{B_T}} & \frac{\rho_{C_{GEB}}}{\rho_{C_T}} \end{bmatrix} \quad \text{Eq. 4.20}$$

In this formula, the contributions of the HARD factor have been removed and this analysis will focus on the linear behaviour of these parameters. This formula will have the following development:

$$\begin{bmatrix} Adv.Speed & x & x \\ x & Applied\ Force & x \\ x & x & Pin\ Length \end{bmatrix} = \begin{bmatrix} 100 & 400 \\ 500 & 600 \\ 2.09 & 2 \end{bmatrix} \begin{bmatrix} 0.54 & 0.32 & 0.62 \\ 0.46 & 0.68 & 0.38 \end{bmatrix} \quad \text{Eq. 4.21}$$

These adjustments lead to some changes in the parameters; however these changes are not very different from the one obtained before. The new parametric combination is the following:

Advancing Speed = 237 mm/min;

Applied Force = 567 kg;

Pin Length = 2.06 mm.

4.5 FSW applied to magnesium AZ31

4.5.1 Taguchi method

Sheets of AZ31 with 2mm thickness were friction stir welded using a tool with a scrolled shoulder and a threaded conic pin. The shoulder had a diameter of 15mm and a variable pin depth. Different process variables were investigated in order to identify the best variables for magnesium alloys. Table 4.21 resumes the variable parameters that were tested in this work.

On the other hand, other parameters were kept constant in our studies, namely the tool rotation speed of 1500rpm, the plunge speed of 0.1mm/s and a the dwell time of 6s. The

tested parameters hawere selected for being the parameters that most influence the properties of the welded samples.

Table 4.21 – Test parameters with Taguchi N9 matrix.

Trial	V (mm/min)	F (Kg)	Pin Depth (mm)
E1	100	400	2,10
E2	100	450	2,18
E3	100	500	2,26
E4	200	400	2,18
E5	200	450	2,26
E6	200	500	2,10
E7	400	400	2,26
E8	400	450	2,10
E9	400	500	2,18

4.5.2 Weld characterization

From the results obtained, a lot of flash was formed during the process for slower transverse speeds with the highest applied force there was (Figure 4.19 a). This result was not satisfactory because it implies the loss of material in the welded area and further rework would be needed to eliminate the extra material.

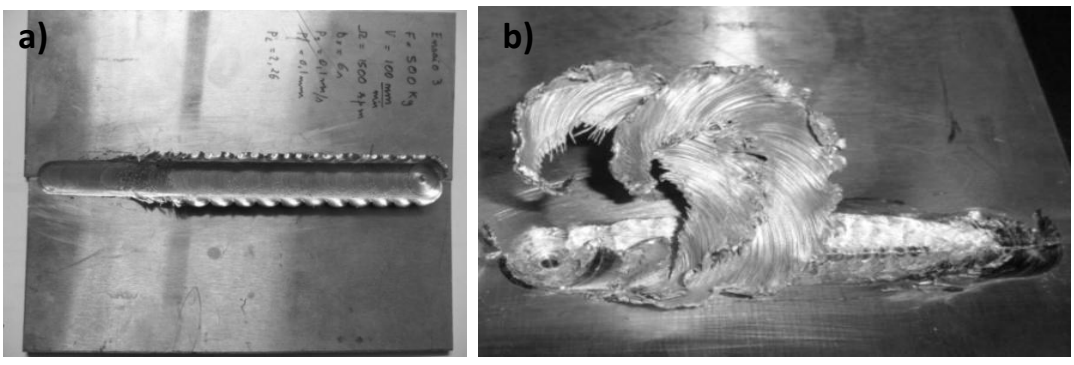

Figure 4.19 – Defects of FSWed magnesium alloys: a) continuous flash and b) material detachment.

It was also possible to conclude that for low applied forces and high transverse speeds there was a detachment of the material under the shoulder (Figure 4.19 b). The detachment of material is clearly visible and it can be related to the flow of material under the shoulder and

since the applied force is small and not able to retain the processed material. This detachment of flash is also related with the high rotational speeds, which heats the material and allows the material to flow in this manner

These results show that magnesium alloys have a smaller working interval when compared to aluminium alloys. Magnesium alloys are known for being temperature sensitive and therefore they are more sensitive to differences in the process parameters. Figure 4.20 shows a summary of these results where three distinct areas can be observed. In the upper left corner, which corresponds to very high applied forces, the samples create a continuous flash. The bottom right corner is the area related with material detachment. The section in-between these two previous areas shows the parameters that can provide the best welding conditions for joining magnesium while minimizing flash.

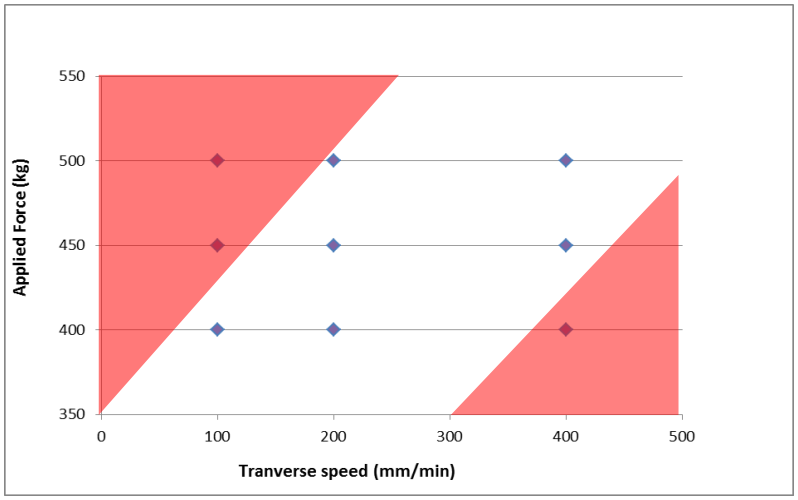

Figure 4.20 – Optimal parameters for magnesium joining with FSW: Top left corner – Continuous flash, Bottom right corner – material detachment and middle section – good processing parameters.

The results from this first analysis limit the application of the Taguchi method because in order to properly analyze all the conditions, all test parameters should be valid and tested. The next steps will focus on the evaluation of the samples using performance coefficients that take into account their end use.

4.5.3 Metallurgical characterization

The samples were metallurgical characterized and the different areas were identified. In Figure 4.21 a), the distinctive area of the nugget can be observed.

In Figure 4.21 b) it is possible to observe that the dynamic recrystallization promoted a decrease in the grain size when compared to the base material (Figure 4.21 c). In addition, it is hard to distinguish the TMAZ area; however there is a significant area where the limit of the

nugget is clearly depicted. All the samples had this effect and the reduction in grain was visible in their nugget area when compared to the base materials.

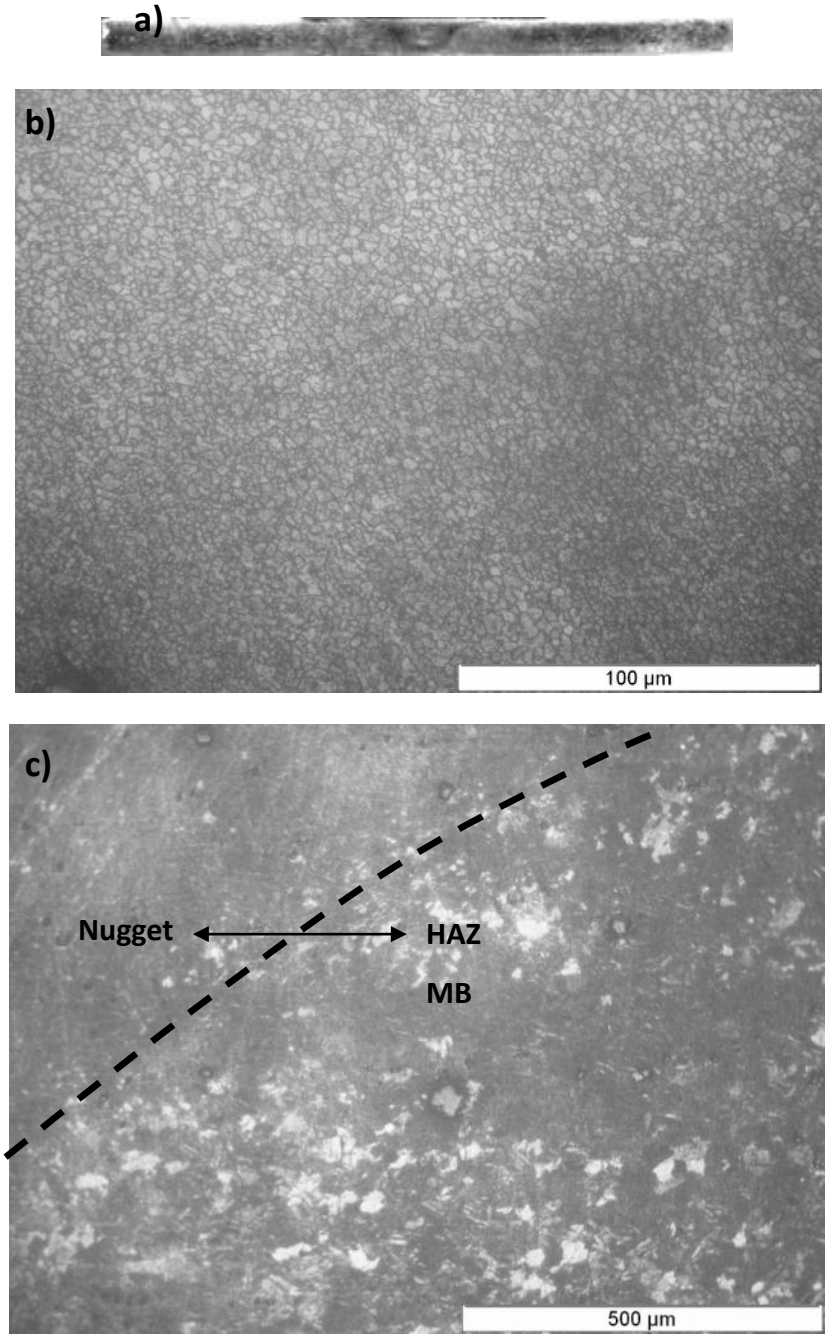

Figure 4.21 – a) Macrography of the welded sample; b) micrography of the nugget area and c) boundary of the nugget.

4.5.4 Hardness profiles

Hardness profiles were made across the mid-section of the samples. The hardness of the base material showed that this material has a hardness of 73±5 HV05. The hardness of the nugget region presents a constant hardness slightly higher than the base material (BM). Figure 4.22

presents the hardness profiles of all samples without any visible defects and the gray dashed line represents the average hardness value of the base material.

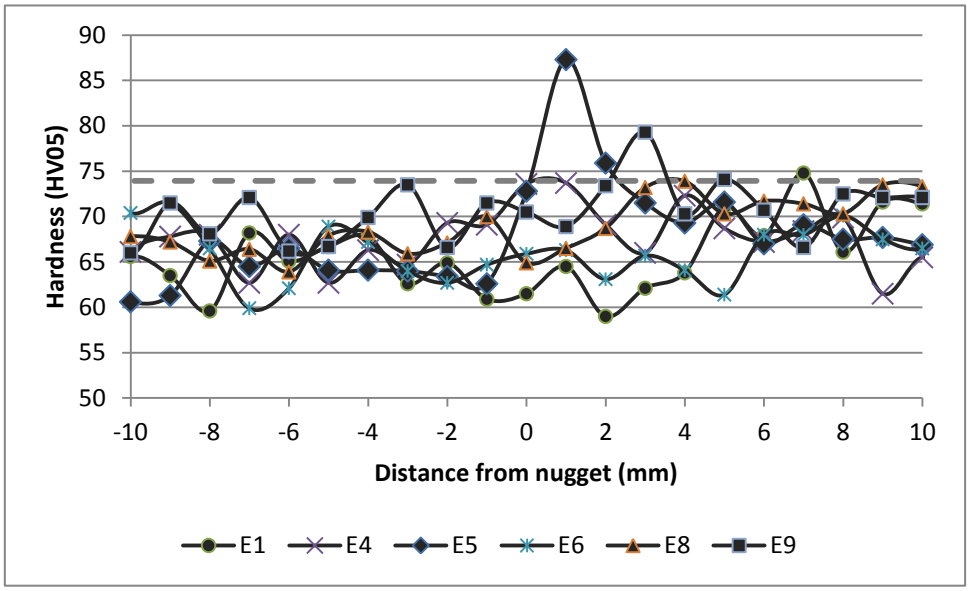

Figure 4.22 – Hardness profiles.

In order to analyze how the heat of the process influences the properties of the material, the Hardness Drop Ratio (HARD) efficiencies were calculated to compare the lowest value from the hardness profile it with the base material.

Table 4.22 – HARD efficiencies.

E1	E4	E5	E6	E8	E9
75.76%	79.95%	81.98%	81.03%	86.44%	89.28%

It can be observed that the HARD efficiencies are influenced by the advancing speed of the process since it increases with the advancing speed. This behavior is observed in all samples and it is confirmed that there is a trend for the hardness of the nugget to increase with the advancing speed. This behavior seems predictable because with the increase of the advancing speed the weld becomes colder and thus the grain size in the nugget area will be smaller. Nevertheless, there are some exceptions, like the E5 and E9, which have the highest hardness in the nugget. However, this is just one value that falls out of the trend but is near the limits of the standard deviation of the base material average hardness. Overall, it can be observed that the average hardness decreases in all welded samples although this effect is more visible on the retreating side of the samples, where the average values are lower than on the advancing side. This decrease in hardness is related with the high sensitivity of magnesium alloys to temperature.

4.5.5 Global Efficiency to tensile strength (GETS)

The tensile testing showed that the welded joints (see Figure 4.23) have a much smaller ductility and toughness than the base material. These results are aligned with other works developed in friction stir welding of magnesium alloys mentioned before [117], [118]. Figure 4.23 presents each efficiency parameter of the GETS normalized taking into account the base material property.

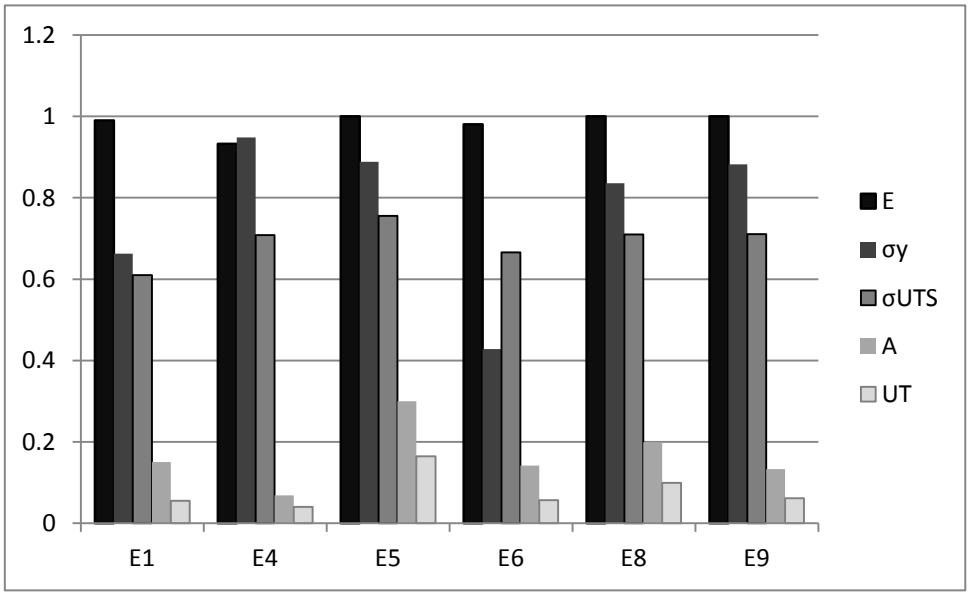

Figure 4.23– Efficiency of the trials made for the different tensile parameters.

This effect seems to be more pronounced in the magnesium alloys because of the different properties of the areas in the welded zone that increase the stress in the material and make it more prone to fracture.

Table 4.23 – GETS efficiencies.

E1	E4	E5	E6	E8	E9
51.15%	60.64%	66.30%	45.60%	60.82%	60.67%

The GETS efficiencies for the different trials are shown in Table 4.23. These efficiencies were calculated taking into account the coefficients presented in Table 4.2. The value of this efficiency is particularly important if the aim is to apply this material in a structural application for automotive industry; this tensile stresses are the most important mechanical properties followed by the elongation and toughness. The Young Modulus is also important; however it is the parameter that is less relevant for the application.

It is clearly seen that the welded joints E1 and E6, which were obtained with the smallest pin depth, had the lowest efficiency of all the welded joints. This behavior is not observed in the E8 welded joint, which presents one of the higher GETS efficiency in these tests. The lower pin length is therefore decisive in the use of this process to weld different materials. Both E6 and E8 samples had a kissing bond defect where the material fractured. The E1 the fracture is on the HAZ and the main reason for this low GETS efficiency is the stresses that developed between the different zones.

It is observed that welded joint E5 presents the highest efficiency of all these tests. This test sample seems to be the most suitable since it can resist to more deformation than most alloys .Taking into account the final application based on these results, it is possible to sustain that the E5 is the best applicable solution for this project. This trial had the longest pin and the second highest force applied because it is a hotter weld; this was enough to allow a better flow of the material in the welding process and make a sound weld along the full thickness of the magnesium sheet.

4.5.6 Global Efficiency to Bending (GEB)

The bending results show that the lower ductility of the welded samples is also observed in the bending testing. Figure 4.24 presents the efficiency of each parameter for the different trials made. The values presented in Figure 4.24 are the normalized values of the GEB formula for each parameter. The normalization was made taking into account the base material values.

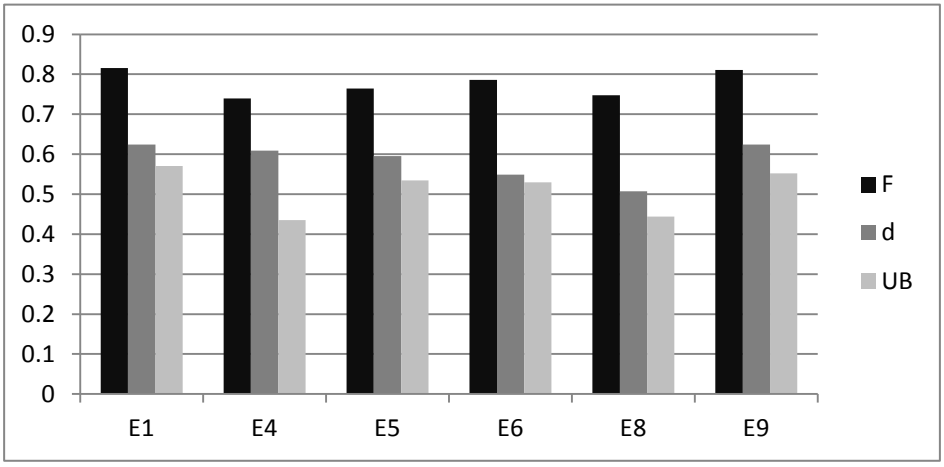

Figure 4.24 – Efficiency of the different trials for the different bending parameters.

In Figure 4.24 it is possible to observe that the different parameters are more or less stable between the different trials made.

Table 4.24 – GEB Efficiencies.

E1	E4	E5	E6	E8	E9
64.51%	55.45%	60.73%	59.86%	53.56%	63.49%

From the GEB efficiencies listed in Table 4.24 it can be observed that trial E8 presents the worst efficiency of bending tests. It can also be observed that welded joint E1 improved and has the best bending efficiency in these tests. It seems that the higher temperature has enabled the improvement of the bending efficiency of these alloys which allowed for E1 to present a higher value when compared to the other samples. The E1 trial has the hottest weld parameters and therefore it is easier to weld in its full thickness than in the E8 trial which had coldest weld parameters. This result however conflicts with the tensile testing. This can be explained by a higher residual stress in the joint of the hottest weld that is related with the magnesium temperature sensitivity and lowest hardness verified in the HARD (Table 4.22).

The results from trials E4, E5 and E6 are inconclusive and not logic because of the lower performance of the trial E4 over E6 even though the prior has a bigger pin length. This can be explained by the applied force, since it was seen before that small changes in the applied force can greatly influence the properties of the joints. The higher applied force to the welded joint E6 is enough to improve the behavior of the samples to bending. The E5 has the best performance because it has the highest pin length and second highest force and it was enough to have a better performance when compared to E4 and E6 trial.

It is also possible to conclude that in E8 and E9 trials the difference in the results are related to the pin length and applied force which lead to a difference of 10% between these 2 joints. Because the parameters used for both these joints make them the coldest welds and thus the more vulnerable to changes in the process parameters. These results show that the pin length is the parameter that mostly influences the bending properties of the magnesium. It can also be noticed that hot welds are very important for this effect since the best result is related with it. The hotter weld allows an improvement of the material flow; however it should be taken into account that there is an increase in the residual stress and if the part is submitted to other forces the hotter weld parameters are not the best for that case.

4.5.7 Weld efficiency

The weld efficiency is the weighted average from the previous parameters and similar to the GETS and GEB, further explained, the weld efficiency is a coefficient of efficiency dependent of the application, which is given by equation 4.4.

The coefficients for %Weld are also dependent on the application; for this case it is expected the part built to be submitted to several bending forces although the tensile forces are also present. The weld efficiencies values are given in Table 4.25:

Table 4.25 – Weld efficiencies for the different trials.

E1	E4	E5	E6	E8	E9
60.29%	59.98%	65.09%	56.27%	59.75%	64.94%

The results show that the most efficient is welded joint E5; however, the trial E9 should not be disregarded since it obtained the second position in the weld efficiency calculation. As mentioned before, the E5 has the best parameters in the GETS from all welded samples. Because the difference in the efficiency between trial E9 and E5 is small, both of them can be considered to have similar results. In addition, since the difference between them in bending is very small it is going to be considered that the E5 has the most suitable set of conditions and corrosion testing will be performed with samples using the E5 trial parameters.

4.5.8 Remarks

A first approach for the definition of optimum friction stir welding procedure in magnesium alloys was proposed and it can be concluded that a thick continuous flash appears for high applied forces and small advancing speeds of related with the high amount of generated heat and high force that pushes the material. On the other side, there is the detachment of material related with a high transverse speed and small applied forces that heats the material but is unable to contain the material under the shoulder. Therefore, this study proved that a small change in the parameters can effectively affect the performance of a joint. These changes can vary from having a sound weld to a completely useless weld and no joint being formed.

The results of this study also made evident that there are some restrictions surrounding the welding of magnesium alloys. The strain values of the welded samples are significantly affected and this can be related with the residual stresses that might exist between the processed area and the other zones. This result has been confirmed by previous works with tensile testing but these results are also confirmed by bending tests.

4.6 FSW applied to dissimilar alloys

4.6.1 Experimental procedure

Sheets with 2mm in thickness were used to make the dissimilar welds between two aluminium alloys AA6082-T6 e AA5754-H111 and a magnesium alloy AZ31. These alloys were friction stir

welded with a tool with a scrolled shoulder and a threaded conic pin. The shoulder has a diameter of 15mm and the pin was 2mm in length. This process used a plunge speed of 0.1mm/s and a dwell time of 6 seconds.

Table 4.26 presents the parameters that differ from the different trials and enabled a successful joint of the dissimilar materials combination. In this table, it can be observed the changes of applied force (F), tool rotation speed (Ω), advancing speed (v) and weld pitch (α) between the different material combinations.

Table 4.26 – Welding parameters of dissimilar joints.

Designation	Material (AS)/Material (RS)	Force (Kg)	Ω (rpm)	v (mm/min)	α (°)
A5R6 100	AA5754/AA6082	550	800	100	0
A5R6 200	AA5754/AA6082	550	800	200	0
A5RMg	AA5754/AZ31	650	1500	50	2
A6RMg 1	AA6082/AZ31	600	1200	50	1
A6RMg 2	AA6082/AZ31	650	1500	50	2

4.6.2 Weld Characterization

While performing the joining of the dissimilar materials, the positioning of the different materials proved to be very important, especially in the joining of the aluminium alloys to the magnesium ones. In these joints, the magnesium alloy was positioned in the retreating side while the aluminium alloys were on the advancing side [Table 4.26]. In a similar fashion in the dissimilar weld of the aluminium alloys the AA6082 was positioned in the retreating side while the AA5754 was on the advancing side.

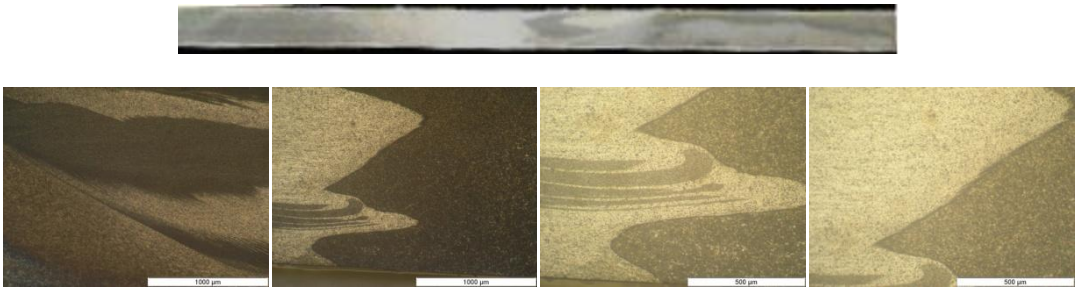

Figure 4.25– Optical microscopy of dissimilar AA5754/AA6082: a) Macrograph; b) transition nugget-HAZ, c) Nugget, d) Detail in Nugget and e) Nugget Boundary between AA5754 and AA6082.

The parameters presented for the welding of these materials are the ones that were able to provide a sound weld between the dissimilar materials. The welds of aluminium alloys and magnesium alloys were observed and it was not possible to properly join them using lower rotational. In the dissimilar welds of aluminium it was viewed that for this arrangement it was difficult to have a sound weld for rotational speed over 200mm/min. It was also difficult to stabilize the welding process outside these parameters and guarantee a sound weld.

The different joints were welded together and etched using the etchants mentioned before. It can be observed that the joint of the 2 dissimilar aluminiums (Figure 4.25) was able to join together the different materials and that there is a distinctive region between the 2 of them that it is a very soundly weld.

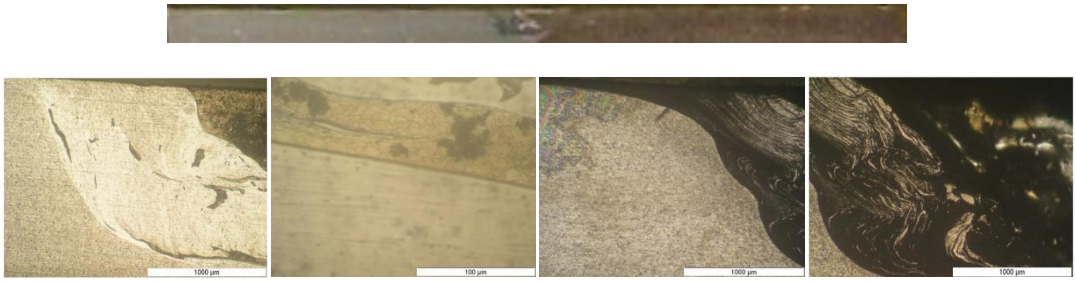

Figure 4.26 – Optical microscopy of dissimilar AA5754/AZ31: a) Macrograph; b) nugget, c) transition Nugget-HAZ Al side d) Transition Nugget-HAZ Al side and e) Nugget.

In Figure 4.26, the sample was etched using two reagents; Figure 4.26 b) and c) were etched using the acetic picral 2 suitable for magnesium alloys, while for Figure 4.26 d) and e) the etchant used was the Poulton modified reagent which is suitable for the aluminium alloys. The use of these 2 reagents allows to distinguish the different products inside the nugget based on the aluminium and magnesium alloys. The different tints in the nugget allow us to understand that there are different compounds inside the nugget that are related with the mixture of these 2 alloys.

Figure 4.27 – Optical microscopy of dissimilar AA6082/AZ31: a) Macrograph; b) nugget, c) transition Nugget-HAZ aluminium side d) magnesium side and e) detail of Nugget.

In the joints of the aluminum to magnesium alloy (Figure 4.26 e Figure 4.27) it was observed that the nugget presents some particles of magnesium in aluminium side and vice versa, although this effect is more visible in the joint AA6082/AZ31. In terms of shape, the nugget of

the AA5754/AZ31 is more similar to the AA6082/AA5754 nugget. The AA6082 is more fluid at higher temperatures than the AA5754; because of this reason the deformation mechanisms have allowed that the magnesium penetrated much further inside the AA6082 than in the AA5754.

4.6.3 Hardness profiles

Hardness profiles were made in the middle section of the different samples and it was observed that the hardness behavior between the samples of different materials and the same material are significantly different (Figure 4.28 and Figure 4.29). It can be detected that the hardness profile of the weld between AA6082 and AA5754 (Figure 4.28) manifests a very similar behavior to similar welds on each half of the welded sample. In this case, the nugget seems to be a transition between both materials without having any unforeseen effects. In the weld of aluminium to magnesium (Figure 4.29) it is clearly visible the peak in hardness found in the nugget. This peak in hardness has been related with the development of intermetallic compounds in the nugget of this joint.

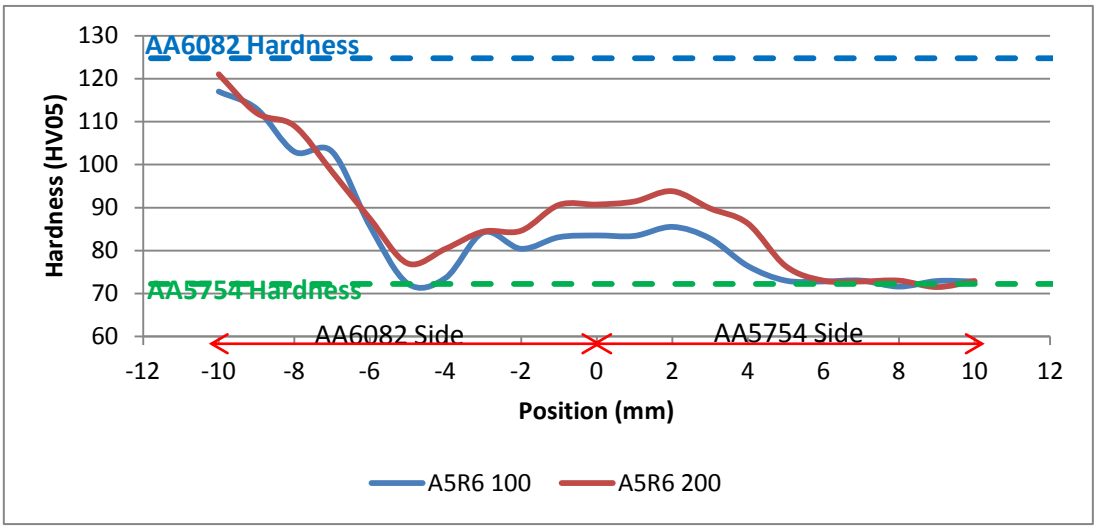

Figure 4.28 – Hardness profiles of dissimilar welds of AA6082 with AA5754.

The profile of the joints between AA6082 with AA5754 (Figure 4.28) shows us that each half has the typical behavior of the corresponding alloy. It can be observed a plateau related with the increase of hardness in the area processed by the pin. In the retreating side, the behavior is similar to FSWed heat treatable aluminium alloys where the hardness drops up to a minimum value (around the 5 mm) and then increases to the base material hardness. On the opposite side, the hardness decreases straight away to the base material average. The higher hardness observed in the area processed by the pin is related with the dynamic recrystallization effect and subsequent grain refinement in this area.

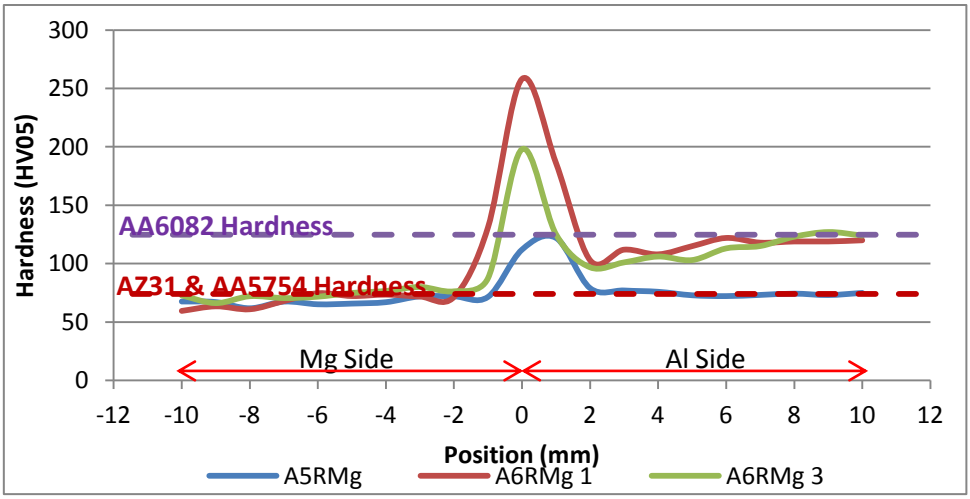

Figure 4.29 – Hardness profile of dissimilar of aluminium alloys with magnesium alloys.

The hardness profile of the magnesium-aluminium joints (Figure 4.29) clearly shows a peak in hardness allocated in the nugget region. This increase in hardness is related to the formation of intermetallic phases of the material that are more brittle and can damage the properties of the joined materials. The HARD was calculated taking in to account the hardness of each side and the corresponding material. In Table 4.27, the results of the hardness are presented for each tested sample.

Table 4.27 – Lowest hardness and HARD efficiencies of the welded samples.

		A5R6 100	A5R6 200	A5RMg	A6RMg 1	A6RMg 2
Lowest Hardness	AS	71.6	71.5	72.3	103	96.8
	RS	72.3	77	61.9	59.6	66.1
HARD	AS	99.15%	99.02%	100.12%	82.55%	77.58%
	RS	57.94%	61.71%	83.74%	80.63%	89.42%

The AA6082-AA5754 joints show that even though the lowest HARD efficiency belongs to the AA6082. This means that the process does not affect the AA5754 alloy as much as the AA6082 alloy even considering the decrease in hardness. It is very likely that the material will first break on the AA5754 side. The same effect mentioned before is also observed for the AA6082-AZ31 joints. In this case, the magnesium alloy is more susceptible to break first than the aluminium alloy. For the magnesium-aluminium joints it is possible to observe that the magnesium alloy is also mildly affected by the process and that there is a small reduction in hardness. The combination of the HARD efficiency and hardness value allows us to properly analyze the results of these tests and also to be more effective in the identification of the

material that is more likely to fail. In this case, the magnesium seems to be the material that has the worst performance while for the AA5754-AA6082 joints this characteristic falls to the AA5754 alloy.

When dealing with dissimilar alloys, it is very important to take into consideration the different areas where the test is being performed. This step is very important because the properties of the materials can be very distinct, making the efficiency measured unsuitable to analyze them. In this case, the efficiencies must be chosen taking into account the material that is most probable to fail. Yet, from this analysis, it is still not possible to identify which material is more prone to break; it is so either because the hardness is very close together or the joining mechanisms are not fully known. These results must be linked with the results from tensile testing in order to make the proper choice of which parameter to use.

4.6.4 Global Efficiency to tensile strength (GETS)

The efficiency coefficients for the tensile testing were made by comparing the A5R6 100 and A5R6 200 with the AA5754 alloy properties, while the remaining samples were compared with the AZ31 magnesium alloy properties. The choice of parameters was made by selecting the material with the averaged lowest properties because it acts as the limiting material. The tensile testing shows that the dissimilar welded joints (Figure 4.30) have smaller elongations to break despite which material combination is performed. It can also be observed (Figure 4.30) that even though the elongation to break and toughness are hindered, when compared to the other parameters, the results are still better than the one presented by dissimilar welding of magnesium to aluminium alloys. One explanation for this result can be related with the increase of residual stresses by the process that decreases the ductility of the alloy.

The weld of magnesium to aluminium alloys proved that this joint is very brittle, breaking before entering in the plasticity stage. This shows that there is a connection between the two materials; however there are several problems with this connection related to the different materials properties and matrices that difficult the proper joining of these two materials together. The connection made seems to be a mechanical connection where the material are joined due to the strains and stresses of the process; however there is a missing a cohesion joint between the two materials. Adding to this, the increase of residual stresses between the two materials, makes this joint even more likely to easily fracture.

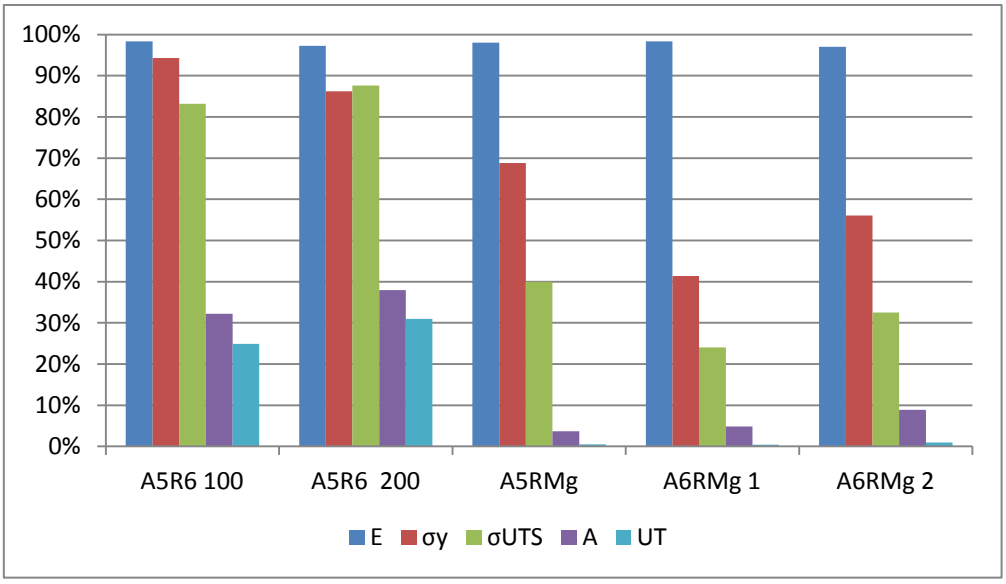

Figure 4.30 – Efficiencies for the different tensile parameters.

Table 4.28 – Failure location of the tensile tested samples.

Sample	Figure	Failure location
A5R6 100		HAZ Retreating Side
A5R6 200		HAZ Retreating Side
A5RMg		Nugget Joint between different materials
A6RMg 1		Nugget Joint between different materials
A6RMg 2		Nugget Joint between different materials

In Table 4.28, the fracture locations of each sample set can be observed. It was detected that in the different combinations of AA5754 and AA6082 the sample fractured on the retreating side on the AA6082 sample. The AA6082 had a lower ductility than the AA5754 and the interaction with this process reduced its ductility leading to the reduction of the material properties. The joints of aluminium alloys to magnesium alloys fractured in the nugget of the material. This confirms that the connection between these two materials was not has strong.

Table 4.29 – GETS efficiency of welded samples.

	A5R6 100	A5R6 200	A5RMg	A6RMg 1	A6RMg 2
AS	71.63%	72.20%	42.42%	18.36%	23.49%
RS	50.36%	53.31%	43.05%	30.24%	37.74%

In Table 4.29, the GETS efficiency was given for both materials to perceive better the effects on the efficiency parameters. GETS efficiency of the welded samples clearly show that the efficiency for both combinations AA5754/AA6082 joints is similar although there is slightly better performance on the A5R6 200, due to its faster welding speed and hence lower temperature released during the process; despite this fact the efficiency difference does not seem to be high enough to make a clear choice for which process to follow. The efficiency of the aluminium alloys to magnesium is much smaller than it was expected. It can also be observed that the combination of the AZ31 with the AA5754 presents a better efficiency than with AA6082. It can be confirmed that since the AA5754 has mechanical properties very similar to AZ31 it is easier for them to interact and form a sounder weld. This result directs that future efforts should focus on using materials with similar properties to the magnesium alloy as to produce sounder joints.

4.6.5 Global Efficiency to Bending (GEB)

The calculation of the GEB efficiency was also made to understand the limitations of these alloys to bending loads and understand the difference to the tensile results. Regarding these, and complying with the results already obtained from the tensile testing, it is possible to say that the joints between different aluminiums have a much better efficiency when compared to the joints between aluminium and magnesium. Figure 4.31 presents the GEB efficiencies for the different joints; the properties of AA5754 were used to established the efficiency of the joints of AA5754 to AA6082 while the properties of the magnesium alloys was used to establish the efficiencies of the other joints.

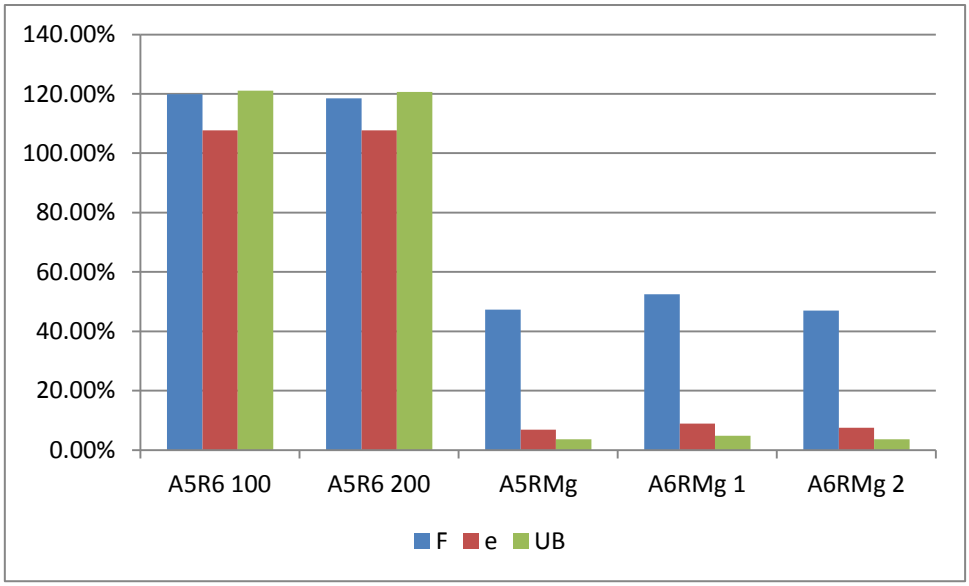

Figure 4.31 – Efficiencies of the different bending parameters.

For the dissimilar weld between different aluminiums, it can be observed that that their properties are much better than the bending properties of the AA5754 alloy. This means that there is an improvement of the properties by introducing the higher aluminium alloys. This improvement is also related with the increase in hardness in the nugget area that can be related with an enhancement of the mechanical properties.

The bending behavior of the aluminium-magnesium joints is very brittle, which is in compliance with the tensile behavior of these samples; however it is also visible that the bending properties are worse when compared with the tensile properties. These results are similar independently of how the specimens are being tested, showing low efficiency of these tests are dependent on the type of joining itself.

Table 4.30 – GEB efficiency of the different samples.

	A5R6 100	A5R6 200	A5RMg	A6RMg 1	A6RMg 2
AS	117.41%	116.89%	15.06%	10.71%	9.49%
RS	80.05%	79.74%	15.32%	17.71%	15.44%

Table 4.30 shows the GEB efficiencies to both materials and confirms the low efficiency of the dissimilar welds of magnesium to aluminium alloys and that the bending behavior of the welded samples is worse than its tensile behavior. It can be observed that the behavior of these alloys is similar between samples. When compared with the same material AZ31 it is possible to observe that differences between them are almost inexistent. This means that these alloys also have a poor performance to bending because the forces reached are much smaller than expected, due to the decrease in ductility of the welded samples.

The behavior of the different aluminiums joined by FSW shows that once again their behavior is very similar, although there is a small advantage for the hotter weld which has slightly higher bending properties. Even so, this difference is not significant enough to draw conclusions about which set of parameters would be optimal to weld these two materials together.

4.6.6 Weld efficiency

Table 4.31 – Weld efficiencies for the different samples.

	A5R6 100	A5R6 200	A5RMg	A6RMg 1	A6RMg 2
AS	97.27%	97.23%	34.51%	20.96%	21.90%
RS	65.96%	67.36%	33.25%	29.01%	31.76%

Table 4.31 presents the efficiency of the welded joints taking into account the coefficients from Table 4.4. These efficiencies were performed using the weaker material as the base material in the joints between aluminium and AA5754 with AZ31 the AA5754 base material were chosen as a comparison while in the remaining combination the AZ31 properties were selected as comparison material.

It is noticeable that the joints between magnesium and aluminium present a very low mechanical performance and one way to improve their mechanical performance is the use of aluminums alloys and magnesium alloys with similar properties, although further studies need to be done to confirm this assessment. For the corrosion testing, the A5RMg and A6RMg 2 conditions are used to evaluate the corrosion behavior of these samples.

Regarding the mechanical behavior of the joints of AA5754 and AA6082 we may sustain that both have very good properties. In this case, and in order to properly choose the right parameters, one must take into account the limiting material. In our study, the limiting material was the AA6082 because it had low hardness. Even though this material was similar to the hardness of AA5754 in the tensile testing all the test samples fractured on the retreating side where the AA6082 was located. For the corrosion test, the parameters used in the A5R6 200 were selected because of their higher efficiency using the aluminium as the limiting material.

4.6.7 Electronic Microscopy

Electronic microscopy was performed in the aluminium/magnesium joints. This analysis aimed to observe how the joining process had affected these two materials and, if possible, to

confirm the formation of the intermetallic structures. In Figure 4.32 and Figure 4.33 the SEM images and x-ray mapping of the samples are presented.

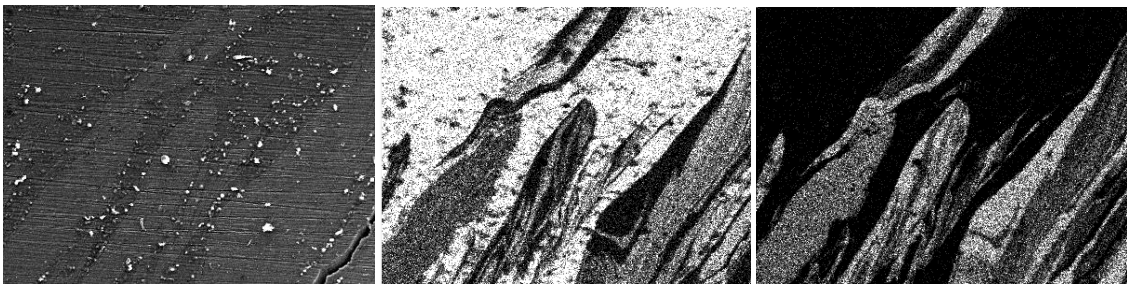

Figure 4.32 – Sample A6RMg 2: a) SEM image of joint; b) X-ray mapping of the Al element and c) x-ray mapping of the Mg element.

In Figure 4.32, the connection of the material at the joint is depicted; in Figure 4.32.a different shades of grey corresponding to both materials can be detected. In Figure 4.32.b, a mapping was made for the Al element in which the white area corresponds to the Al element, while in Figure 4.32.c this mapping was made for Mg. It can be observed in the latter figures that there are areas with a grey tone which is related with the formation of intermetallic phases. It is also possible to see parts of the magnesium that was moved to the boundary without reacting with the aluminium alloys. However, this flow of material in not viewed in both combinations. In Figure 4.33 the same steps were taken for the joint of AA5754 with AZ31 and it can be observed that even though there is a small penetration of Al in the Mg, it does not present the same diffusion of elements like it was observed in the other joint.

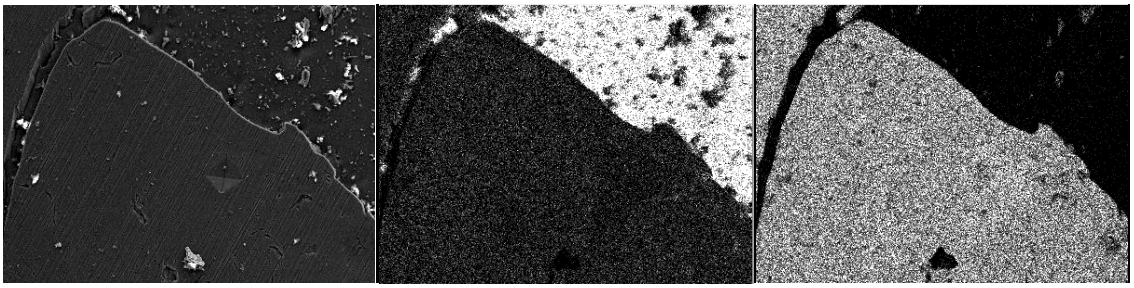

Figure 4.33 – Sample A5RMg: a) SEM image of joint; b) X-ray mapping of the Al element and c) x-ray mapping of the Mg element.

The AA6082 is more fluid at higher temperatures than the AA5754 and this property has enabled the material to penetrate further in the AZ31 alloy and probably made it easier to develop intermetallic phases with the magnesium alloy. This is not observable in the joint of AA5754 with AZ31 that has a more defined joint. However, in the nugget, it can be viewed that the flow of material and some ripples which joins the aluminium alloys with the AZ31 (Figure 4.34). These results comply with the results from the hardness profiles and confirm that the formation of intermetallic phases increased the hardness in the joint.

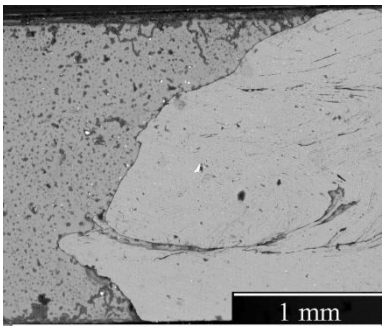

Figure 4.34 – SEM image of the nugget of the sample A5RMg.

The joining of dissimilar materials using the FSW process was researched as well as different properties of these joints. It was concluded that the joining of dissimilar aluminiums alloys have better properties than the joint of magnesium with aluminium alloys. This can be explained by the fact that the microstructure is not compatible between aluminium and magnesium.

The joint dissimilar aluminium alloys has presented very good mechanical and electrochemical properties. The mechanical properties of these joints seem to be restricted by lowest properties of the joining materials. This means that the base materials limitations after FSW will restrict the behavior of the joint materials.

The joint of magnesium with aluminium proved to have lower mechanical efficiencies. In fact, their overall weld efficiency is around 30% while for the dissimilar aluminium alloys the weld efficiency is around 97%. It can be observed that the ductility and tensile properties are very low when compared to the base materials. These lower properties can be caused by the different material microstructures that can induce restrictions in the joint due to incompatibility in the material matrices.

5 Corrosion Studies

There are several automotive standards regarding the corrosion performance for automotive parts. In this investigation, a study to observe the behavior of the samples to saline testing is going to be performed following the procedure established in Section 4.1. These tests are in accordance to the automotive standards and the established specified time was considered to be 350h. After this time, the samples that showed no visible corrosion are considered valid to be introduced in the motor vehicle.

These studies were complemented with electrochemical tests that can provide a more in-depth look to the interactions that might be happening in the alloys and therefore provide us with a view of what is happening inside these samples.

The main goal of the saline testing is to understand if there is any change in the material after welded together using the FSW process. The changes can go from a global effect in the samples to a more localized corrosion effects due to the influence of the process. The electrochemical tests will show which mechanisms are influencing the corrosion rate in these materials.

5.1 Saline testing

The corrosion testing was made according to the ASTM B117:95 standard. The samples were put in a saline environment and their corrosion behavior for 350h was tested. These samples were compared with the BM materials that were also included in this testing. The samples were kept in the saline chamber until the end of the 350h period or until extreme corrosion that damaged the part was encountered. The best parameters determined in Section 4 for each material combination were used to produce the samples for the saline testing.

5.1.1 Aluminium AA5754-H111

In order to understand the corrosion of the friction stir welded samples, the samples were compared to the base material ones. The welded samples were tested on both sides to determine if the tested ones would have any preferential corrosion in these tests. Samples were taken in predetermined intervals to observe the evolution of corrosion in these samples. These alloys seem to be very resistant to corrosion; in fact they are usually used in saline environments. This alloy is perceived as a good candidate to replace the AA5083 in its applications. Table 5.1 presents the evolution of the AA5754 samples under different exposure times to the saline environment. It was observed that no notorious differences in corrosion

developed in the welded samples and that these have a similar behavior the base materials samples.

Table 5.1 – Corrosion behavior in the saline testing of the AA5754-H111 alloys.

	0h	50h	150h	225h	350h
BM					
Welded Sample Front		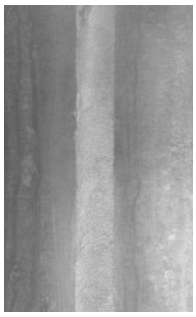			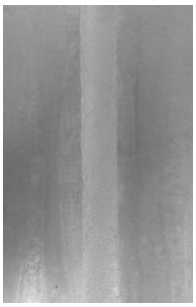
Welded Sample Back	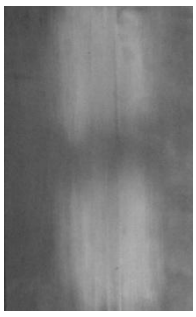		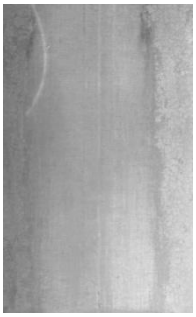		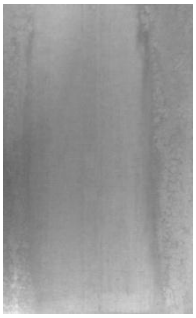

It can be verified that in the welded front samples there is no localized corrosion and that there is no visible concentration of saline particles in any area. This is an important observation especially in the area process by FSW tool. The surface of this area is rougher than the rest of the sample and, therefore, it has a higher probability of suffering corrosion. It can be observed that there was no visible corrosion even in this section. In the back of the welded samples it was also confirmed the same behavior and also no preferential corrosion has been viewed along the weld line.

In the same alignment a study was performed to observe how an important defect, such has the root defect, would evolve under a corrosive environment. This defect usually negatively

affects the tensile and fatigue properties of the welded samples. Some samples were made to understand the influence of corrosion in these alloys. The goal in this case is to understand if the defect increases or induces any kind of localized corrosion.

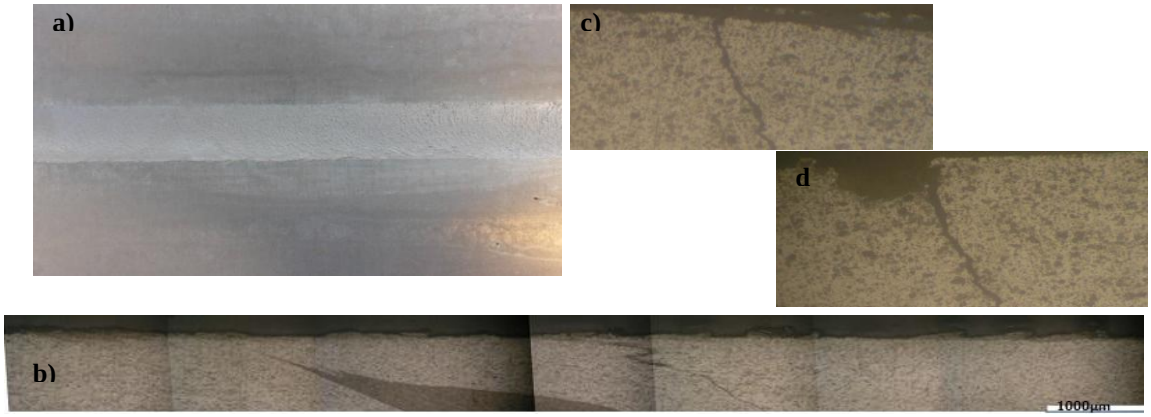

Figure 5.1 – Samples submitted to corrosion testing: a) corroded plate, b) Top of the sample, c) sample with defect before corrosion testing and d) sample with defect after corrosion testing.

Figure 5.1 depicts some metallographic details regarding the aluminium samples after being saline tested. In image b) it can be observed that there are no corroded areas in the top surface of the welded samples. The saline solution was accumulated in this surface; however there is no corrosion preferred areas even in this rougher surface.

Image c) and d) shows the evolution of the "root defect" after the saline testing. It is possible to observe that there is a localized corrosion in the area that is not joined together. Like the top surface, there is an accumulation of saline solution which promotes an increase of Cl^- ions. This will cause that the protective oxide layer breaks and starting the pitting corrosion. In this case, the defects and rougher surface were the initiators for corrosion which otherwise would have not been identified.

The corrosion testing does not seem to affect the integrity of the part. The increase of the existing defects was perceived as one of the most damaging effects that can be produced in these welds. This makes it very important to eliminate these types of defects when welding the plates together. One of the concerns regarding this problem is that even if the pin length is defined it is necessary to guarantee that the wear of the pin is not very severe as to decrease the pin length and eventually promote the "root defect". Some studies are required to define the wear rate of the tool and create maintenance standards to either replace the pin when needed or adjust the pin length. The tools can be used for longer times and it might be possible to improve the FSW process to a more continuous standard process.

5.1.2 Aluminium AA6082-T6

Table 5.2 presents the corrosion evolution of the AA6082 alloys. The samples were taken with the same exposure times as with the AA5754 alloys and were both tested in back and front of the plates. It can be observed that, just like the AA5754 samples, no localized or preferential corrosion system became apparent during the test cycle of these alloys.

Table 5.2 – Corrosion behavior in the saline testing of the AA6082-T6 alloys.

	0h	50h	150h	225h	350h
BM					
Welded Sample Front					
Welded Sample Back					

It is possible to verify that there is no area with increased or preferential corrosion; however it seems that the rougher area left by the FSW tool appears to have a higher accumulation of saline solution when compared to the rest of the plate.

A metallographic analysis was performed to view the effects of the corrosion in the welded sample and in the fabricated sample with a “root defect” in it. In Figure 5.2 the metallographic samples of these alloys after the 350h exposure time are presented.

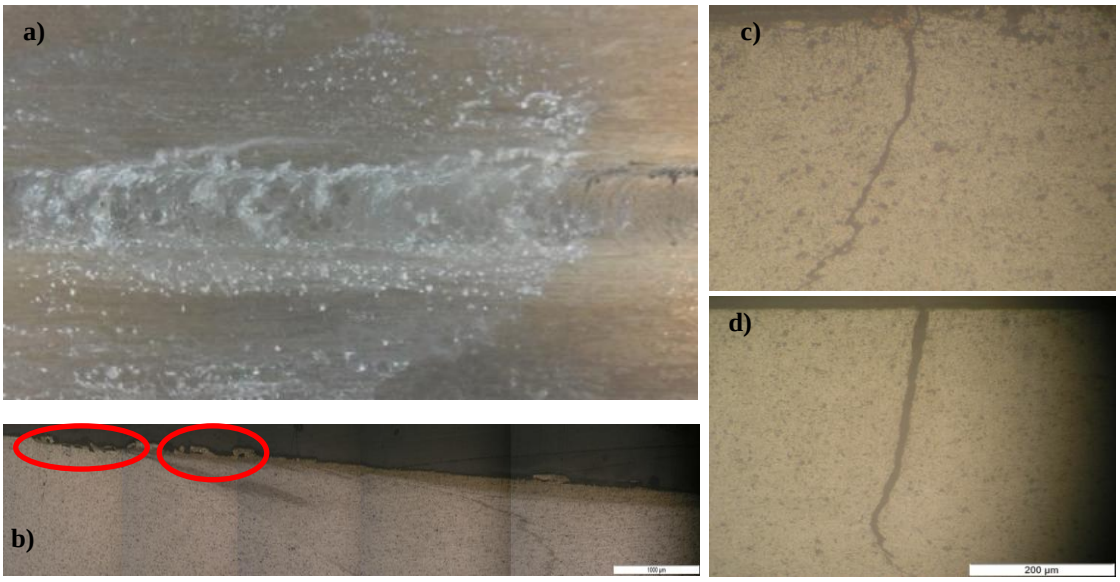

Figure 5.2 – Samples submitted to corrosion testing: a) corroded plate, b) Top of the sample, c) sample with defect before corrosion testing and d) sample with defect after corrosion testing.

The AA6082 samples displayed to be less resistant to corrosion than the AA5754 alloys (Figure 5.2). It is possible to observe that there are some corroded areas in the top surface. The corrosion in the top surface is located in the rougher surface left by the tool. Because these materials are less resistant to corrosion, it took less time to initiate the corrosion; however its propagation was limited to the surface. These corroded areas are related to the accumulation of saline solution in the rougher surface of the welded area.

In image b) and c) it was observed that the accumulation of the saline solution has also been very damaging for the existing defect. It is possible to conclude that this defect increased three times in width at the top of the defect. This particular defect had a 3.5µm on the defected sample before saline testing and 11µm in the sample after 350h exposure time. It can be assumed that even though the different aluminiums behave in different manners, the saline environment has proven to be very damaging promoting the increase of the defects that might induce poorer mechanical properties in the welded samples.

5.1.3 Magnesium AZ31

Table 5.3 shows the evolution of the samples at different times. These magnesium plates had a smooth surface in the front and a rougher surface in the back. In general, it was observed that the BM front samples had a better corrosion behavior than BM back samples. This is probably due to the fact that rougher surfaces, such as the back of the samples, are normally more prone to present localized corrosion attack in specific points of its surface.

Table 5.3 – Corrosion behavior in the saline testing of the AZ31 magnesium alloys.

	0h	50h	150h	225h	350h
BM Front					
BM Back					
Welded Sample Front					
Welded Sample Back					

It can be observed that the welded samples have a poorer behavior when compared to the BM. This increase in corrosion is more visible on the front of the welded samples. The corrosion in these samples seems to be generalized, since it is possible to observe the existence of corrosion in the full extension of the plate with the exception of the zone processed by the tool where this effect seems to be clearly diminished. The corrosion effect on

the back of the welded samples is not as intense as in the front. Despite it, there is an increase in corrosion when compared with the BM samples of the same side. There is also evidence of preferable corrosion in the bottom weld line which can be related to the effect of increased heat in that area or any defects left by the process.

Magnesium alloys are heat sensitive and the heat released by the process has also influenced the corrosion properties of the material. The released heat was intense enough to change the treatment of samples and made them more susceptible to corrosion. This corrosion effect is less intense in the back of the welded samples, probably because it is possible to transfer the generated heat to the backplate of the restraining device.

It is important to acknowledge that although the welded samples show generalized corrosion, the area processed by the shoulder is less affected by corrosion. The processed area had better corrosion properties than the base material affected by the heat of the process (Table 5.3 – Welded sample Front) which may be explained by the smoother surface of the processed area when compared to the base material. In fact, it is known that smooth surfaces normally show improved corrosion properties. However, with the increase of exposure time this processed area is also corroded. In the back of welded samples preferential corrosion may be observed in the weld line. This effect is due to the heat released by the pin in this area that heats up the joint of the material and makes it more prone to suffer corrosion. One solution for both these problems can be the use of colder welds that can reduce the effect observed in these samples.

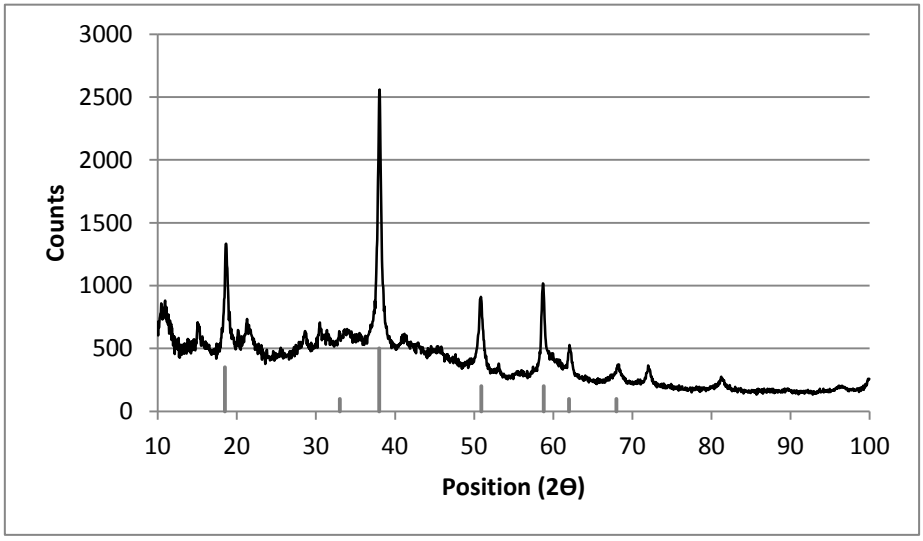

Figure 5.3 – Diffraction of the corrosion products.

In order to understand the corrosion process on the magnesium alloys X-ray, diffraction was performed to identify the composition of the corrosion products. In this test, 2θ values from

10^{o} to 100^{o} were used and a diffraction pattern of the corrosion products is presented in Figure 5.3. All the main peaks present in this diffraction pattern may be ascribed to brucite (magnesium hydroxide, $Mg(OH)_2$, therefore the corrosive environment lead to enhanced oxidation of the magnesium samples, creating these by products.

This increased corrosion rate in the welded samples is not very easy to understand. A deeper analysis of the differences between the welded samples and the base material was performed in order to identify what changes exist in these samples that lead to the increase of corrosion. Figure 5.4 shows the microstructure, the BM material and a welded sample.

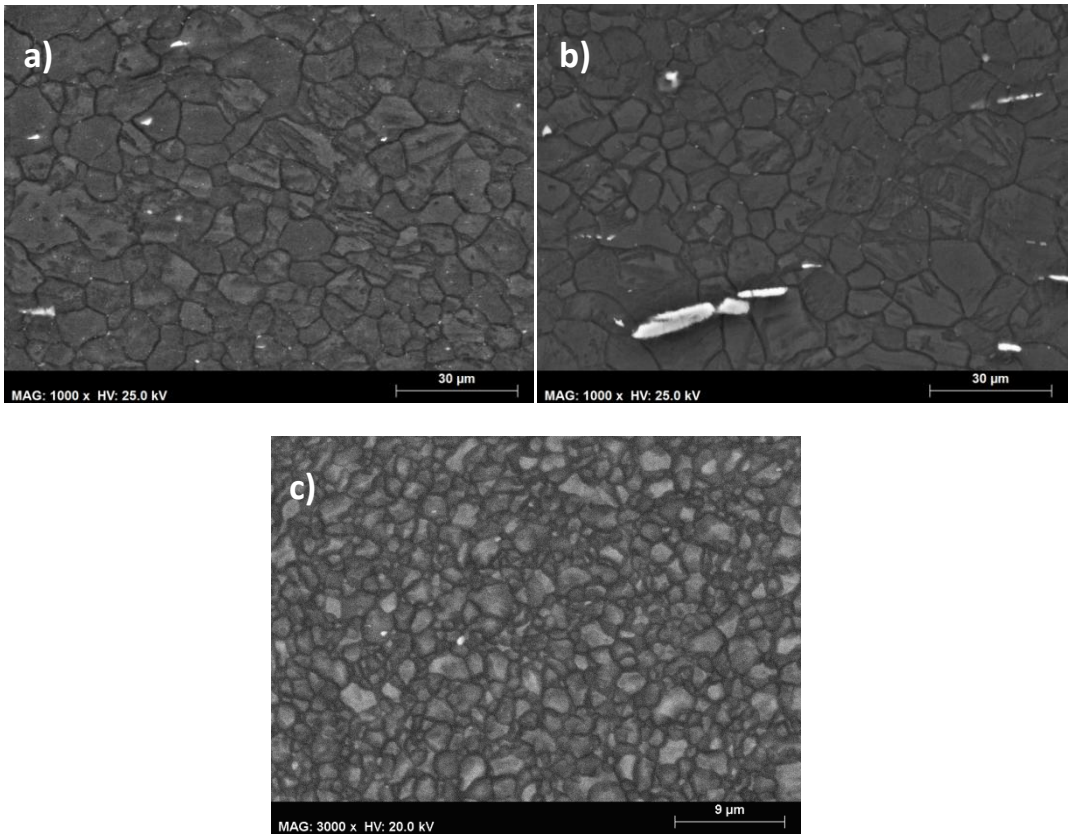

Figure 5.4 – SEM images showing a) base material, b) base material of the welded sample and c) nugget.

Figure 5.4 shows the presence a second phase particle of AlMn which increases in number and size when welded by FSW. These particles appear in white in the SEM micrographs and were identified with the help of Energy Dispersive Spectroscopy (EDS) technique. The micrograph in welded sample took 15mm from the nugget. It can be observed that these particles exist both in the base material and the welded sample; however in the welded sample these particles increase both in number and size. Figure 5.4 c) shows the nugget region of the welded sample. It can be observed that the number of second phase particles is smaller than in the region just affected by the heat generated by the tool. Zeng *et al.* [158] made a review in corrosion mechanisms and verified that the particles that are diluted in the magnesium alloys usually

create a localized galvanic corrosion with the magnesium plate around it ,promoting pitting corrosion in that area. In this reaction, the particles act as cathodes and the magnesium around acts as an anode. The magnesium will therefore start corroding around the particle. In Figure 5.4, it was verified that the number of these particles have increased in size and number after being welded by the FSW process. This reaction clearly explains the effects of what is happening in the saline testing. The increase of particles in the welded is related with the increase of the particles as seen in the SEM images. The increased corrosion is related with the higher number and size of the particles which induces a higher number of pitting corrosion locations resulting in the higher corrosion verified in the welded samples.

5.1.4 Dissimilar materials

The welded samples were observed on the top and bottom of joined samples. In Table 5.4 can the results for the joints of AA5754 with AA6082 can be observed; for the A5R6 top samples the AA5754 aluminium is on the right while the AA6082 is on the left. For the A5R6 bottom samples both materials change places with AA5754 being on the left, while the AA6082 is on the right. In this set of samples, the most important result is the non-existence of any preferred corrosion on the aluminium samples both in the front and back of the sample.

Table 5.4 – Corrosion results for the A5R6 samples.

	0h	50h	140h	225h	350h
A5R6 Top					
A5R6 Back					

One interesting fact of the combination of this material is that the AA5754 material tends to get darker as the time passes. This is probably related to lower corrosion efficiency of this material when compared to the AA5754 aluminium. This means that since the AA5754 alloy is nobler than the AA6082, the AA6082 would corrode preferably to the AA5754 acting like an anode.

Table 5.5 – Corrosion results for the A5RMg and A6RMg samples.

	0h	50h	140h	225h	350h
A5RMg Top					
A5RMg Back					
A6RMg Top					
A6RMg Back					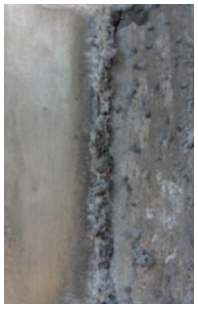

In the analysis of the corrosion between magnesium and aluminium alloys (Table 5.5), the magnesium alloy is presented on the left for the top samples, while in the bottom samples the magnesium is presented on the right.

The corrosion testing between the dissimilar alloys of aluminum and magnesium alloys has clearly showed that there is an increased corrosion rate between these two alloys when joined together. Unlike what happened with the base materials and joints with different aluminiums it is possible to observe that this corrosion is more localized than the other samples. The increased corrosion rate is contained in the joint area. In fact, the region that suffers more is the area where the two materials are joined together. This behavior can be observed in both top and bottom samples, being more severe in the top samples. It was observed that after 225h, the top welded samples had already been corroded in its full thickness and the joint was useless after this time. The bottom samples have also increased corrosion rates located in the joint of the material; however it was observed that this increase in corrosion was less severe because the mixture of the two materials in the bottom had a lower affected area. In the top samples the mixture made had a larger area related to the mixture promoted under the shoulder.

The mixed material and boundary seem to be preferable for corrosion due to the different electronegativities of both materials. The joint area is the most critical point as it can be seen in Figure 5.5, where the corrosion products tend to grow drastically producing a sponge like structure. The material in this affected zone is being consumed rapidly and in order to make it effective it will need an outer layer in polymer or other material in order to reduce the effect from corrosion.

These results clearly show that dissimilar welds between magnesium and aluminium are not very adequate because the localized and increased corrosion will definitely decrease and diminish the properties of the joint. However, the same process seems to be applicable to different alloys inside the same material group and the results are very good. This means that it is possible to use materials with better corrosion properties and use them to protect materials with inferior corrosion properties or join materials with higher mechanical performance with materials with lower mechanical properties but better formability. Regarding the corrosion rate between the aluminium and magnesium alloys, some materials can be used as protection layers in order to prevent contact with the outside hence reducing the corrosion rate inside the material.

Figure 5.5 – Detail of localized corrosion at 48h in A5RMg.

5.2 Electrochemical testing

Electrochemical tests were performed to understand which corrosion mechanisms affected these alloys during the saline testing. To make these analyses two electrochemical tests were performed:

- Polarization curves through the application of mixed potential;
- Zero resistance amperometry (ZRA).

Samples of each material were tested to understand the corrosion mechanisms in these materials. The polarization curves were applied to each individual material and the ZRA tests were applied for 24h to the different pairs of materials.

5.2.1 Polarization curves

The polarization curves are composed by the anodic oxidation curve and the cathodic reduction curve. Through these curves it is possible to calculate the open circuit corrosion potential and corrosion current density. With this it is possible to calculate the corrosion rate based on Faraday's law. The first step consists in determining the open circuit potential; to do this i it is necessary to determine the slopes of both the cathodic and anodic curves. The point where both curves meet together is the point from which the corrosion potential is taken.

Figure 5.6 presents a schematic to determine the open circuit corrosion potential and corrosion current density. After determining these two values, it is possible to use Faraday´s law and determine the corrosion rate of the welded samples from the combinations between the different materials.

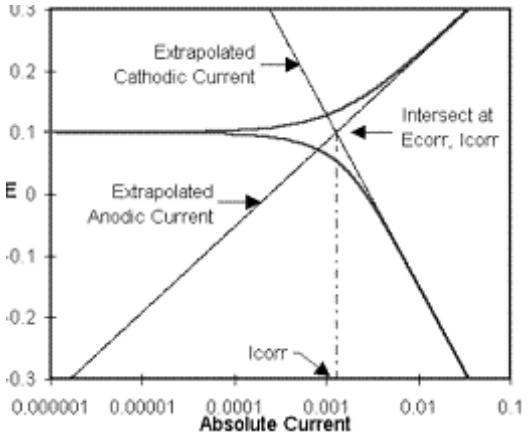

Figure 5.6 – Calculation of the open circuit corrosion potential [159]**.**

The next steps are focused on the determination of the equation that can provide the corrosion rate of the studied samples. From the Faraday's law equation:

$$Q = \frac{n.F.W}{M} \qquad \text{Eq. 5.1}$$

where Q is the charge passed (Coulombs), N is the number of electrons involved in the chemical reaction, W is the weight of the electroactive species and M is the molecular weight;

$$W = \frac{Q.M}{n.F} \leftrightarrow W = \frac{Q.EW}{F} \leftrightarrow W = \frac{i.t.(EW)}{F} \leftrightarrow {}^{W}/_{t} = \frac{i.(EW)}{F} \qquad \text{Eq. 5.2}$$

Where W/t is considered to be the corrosion rate, CR (g/s)

$$CR\ (cm/s) = \frac{i.(EW)}{\rho.F.A} \leftrightarrow CR\ (mm/year) = \frac{K.i_{cor}.(EW)}{\rho} \qquad \text{Eq. 5.3}$$

Where K is 3,27x10^{-3} (mm.g/(μA.cm.year)); ρ is the density (g/cm^3), i_{cor} is the corrosion density (μA/cm^2) and EW is the equivalent weight of the corroding species considered dimensionless. These calculations are based on the standard ASTM G 102 – 89 [160].

5.2.1.1 Similar materials

The polarization curves testing were made in both welded and base material samples. It was confirmed that the aluminium alloys samples present the same behavior; however a change in the behavior may be noticed when the behavior of the welded and the base material sample of the magnesium alloys are compared.

In this study, it is going to be made a prediction of the corrosion rate of the similar joints and dissimilar joints in order to anticipate which material combinations are more suitable to be used. It has been established that a suitable corrosion rate should be around 5mm per year. The values gathered consider a saline environment which is not usually found inside the vehicle. However, taking into account that in the automotive field several tests are made

under extreme conditions to test the vehicle´s performance this approach seems a good method to evaluate and validate the best material combinations.

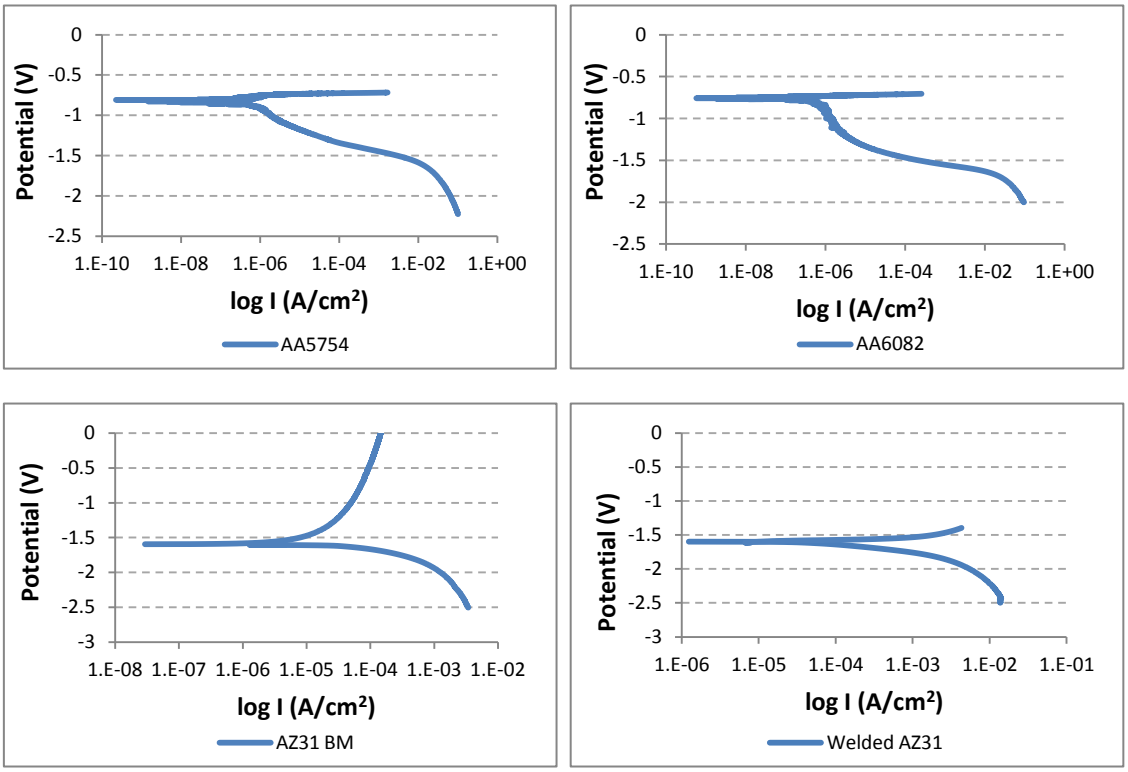

Figure 5.7 – Polarization curves of the base materials.

Figure 5.7 presents the polarization curves of the different materials. The magnesium alloy was tested in both welded and non-welded conditions. It can be viewed that both aluminium alloys show similar behavior and their potential is also very close. On the other hand, magnesium alloys have a higher potential which is inherent to these alloys with higher current than the aluminium alloys. Despite these differences it can be noted that the behavior of the welded AZ31 has some similarities to the behavior of the aluminium alloys. The current of the BM magnesium samples seems to be similar to the magnesium alloys. Nevertheless, the welded magnesium has a much higher current than the base materials samples.

The lower current means that these samples are much less susceptible to corrode because the exchange of electrons with the surrounding environment is processed at a much lower pace. The open potential is a material characteristic. Usually the open potential of the aluminiums is around the 0.8 volts while the magnesium is closer to the 1.6 volts. The open circuit potential is a potential at which the reaction changes from cathodic to anodic. Table 5.6 presents the corrosion rate calculations using Faraday's law as presented before. The EW is a dimensionless parameter that is tabled in the standard ASTM G 102 – 89.

Table 5.6 – Corrosion rate calculation through Faraday's law.

Material	icor (µA/cm^2)	Ecor (V)	EW [160]	CR (mm/year)
AA5754	2.905E-1	-0.786	9.09	3.14E-03
AA6082	4.923-1	-0.732	8.98	5.26E-03
AZ31 BM	1.138	-1.597	12.15	2.58E-02
AZ31 Welded	1.518	-1.580	12.15	3.45E-02

Table 5.6 presents the prediction of the corrosion rate per year and it can be observed that all alloys have very small corrosion rates. Regarding the magnesium alloys it is possible to observe that they clearly present a higher corrosion rate than the aluminium alloys which was verified in the saline corrosion testing.

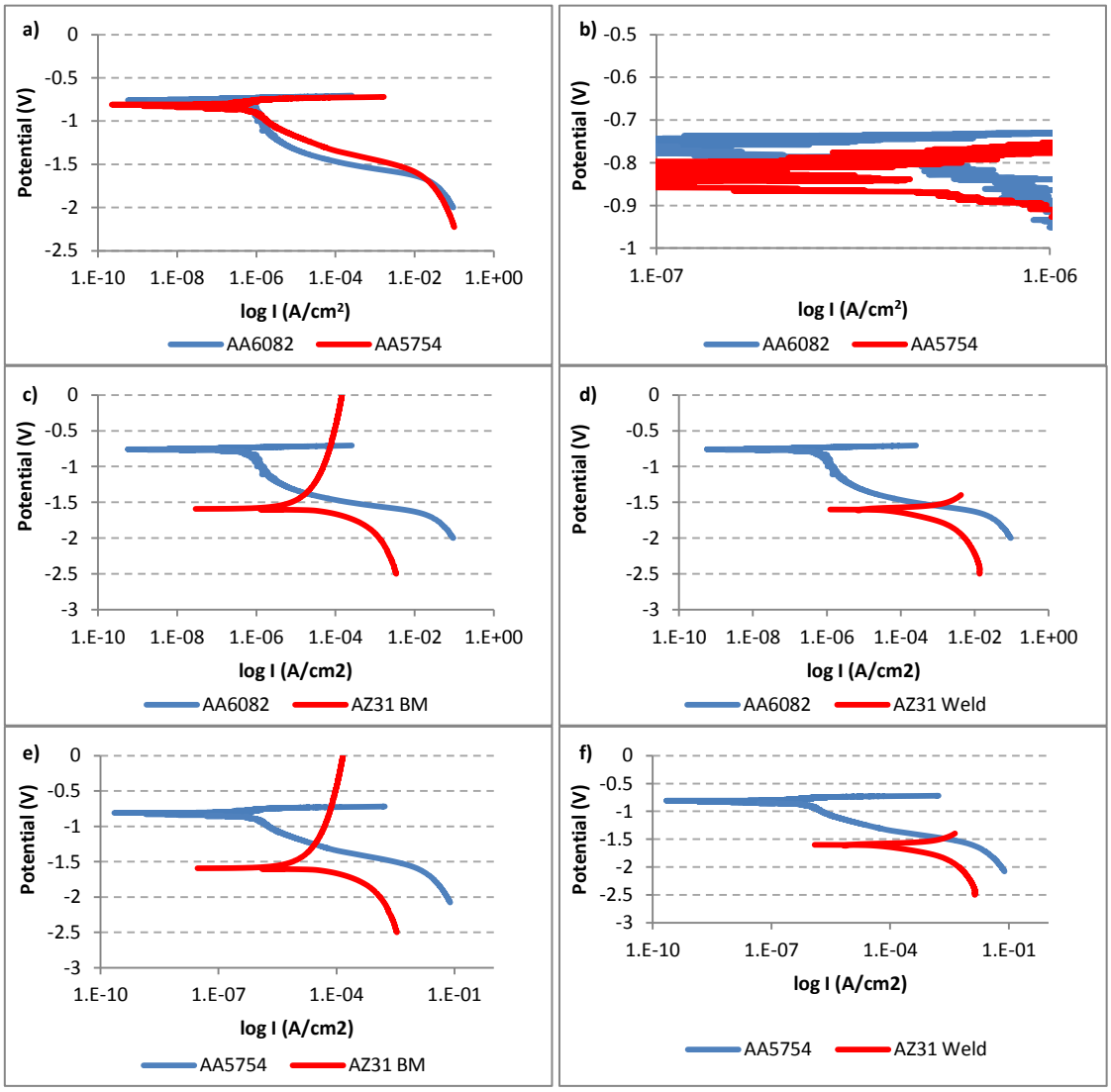

Figure 5.8 – Polarization curves of the different pairs: a) AA6082/AA5754, b) detail of AA6082/AA5754 connection point, c) AA6082/AZ31 BM, d) AA6082/AZ31 Weld, e) AA5754/AZ31 BM and f) AA5754/AZ31 Weld.

Overlapping the polarization curves, it is possible to predict the interaction between the two alloys that are being joined. In this case, it is required to retrieve the information to determine the connection point of the cathodic curve in one of the alloys that intersects with the anodic curve of the other alloy. The alloy that has the cathodic curve intersecting with anodic curve will work as the cathode, while the other as the anode, the alloy that will corrode in favor of the other. Figure 5.8 presents the different combinations of the materials. The alloy that works as the anode is presented in red; in blue the alloy that works as the cathode.

The overlapping of the aluminium and magnesium alloys clearly shows that the magnesium will suffer anodic corrosion and will lose ions over to the aluminium alloy. The potential also predicts that the reaction between these alloys is much closer to the magnesium alloys. The overlapping of the aluminium alloy shows that the potential is much lower and is very difficult to understand which alloy will suffer anionic corrosion. Nonetheless, it seems that the AA5754 alloys will work as the anode in this combination. The lower currents in the dissimilar aluminium allow the conclusion that this combination of materials will suffer much less corrosion than the combination between aluminium and magnesium. Similar to what was done before the corrosion rate of the pairs that have been established in this experiment are going to be calculated (Table 5.7). In this case, since different materials were used, the densities and EW of the materials that work as anodes are going to be used, as a simplification of the calculations.

Table 5.7 – Corrosion rate calculation of the different pairings through Faraday's law.

Material pairs	**icor (μA/cm^2)**	**Ecor (V)**	**EW** [160]	**CR (mm/year)**
AA6082/AA5754	0.4387	-0.787	9.09	4.74 E-3
AA6082/AZ31 BM	17.137	-1.385	12.15	0.389
AA6082/AZ31 Weld	416.5	-1.554	12.15	9.456
AA5754/AZ31 BM	29.35	-1.237	12.15	0.666
AA5754/AZ31 Weld	1836	-1.499	12.15	41.683

Table 5.7 presents the corrosion rates of the different material combinations. The pairings in these included the polarization curves of the AZ31 BM and AZ31 welded in order to understand the difference in behavior by joining through welding processes or using mechanical joints. Taking this into account, it can be observed that the joint using dissimilar aluminiums clearly presents the best behavior considering the corrosion testing. The properties of the welded magnesium have clearly been affected by the FSW process and this

has resulted in a higher corrosion rate that can seriously cripple the mechanical properties of the welded samples. The use of mechanical joints in the joining of aluminium alloys with magnesium alloys (depicted by the calculations using AZ31 BM properties) can be of help. In any case, some issues are related to this connection which can lose more than 0.5mm. Therefore, some precautions regarding the applicability of such connections are needed. It evident that the mechanism involved in the different pairing is galvanic corrosion because the different potentials of the materials will promote the corrosion of the anode in favor of the cathode. This means that all materials combinations suffer this effect. Since the combination of aluminium with magnesium has a higher current this will increase the amount of corrosion that these material combinations sustain.

5.2.2 Zero resistance amperometry

In the ZRA testing samples of the different materials, combinations were tested during 24h in order to observe the current and potential evolution of the different pairs. These results are related with the results from the polarization curves to confirm the corrosion mechanisms that were observed..

In Figure 5.9, the results from the different material combinations can be observed. It is confirmed that the dissimilar welds between aluminium and magnesium have a higher current and lower potential than the dissimilar welds between aluminium. This is mainly due to the higher corrosion potential of magnesium over aluminium which causes the magnesium to have a higher corrosion rate over aluminium. The difference in corrosion potential between aluminium alloys is much smaller, even between the different alloys which explain the lower current and higher potentials.

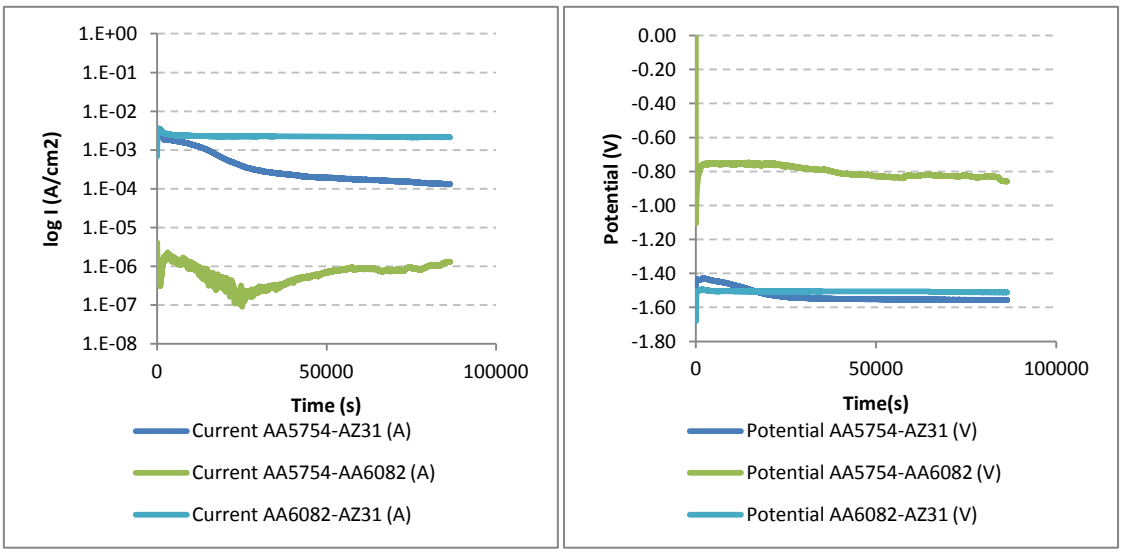

Figure 5.9 – Results from ZRA testing: a) Current and b) potential.

The objective of this test is to immerse the pairs in a saline solution and let them stabilize. Measurements of the current and potential between the two alloys will eventually stabilize and reach a plateau. The average of this plateau will allow obtaining the values of current corrosion density and open circuit corrosion potential of the different material combinations. It can be observed that the potential and corrosion rate that was calculated seems to be close to the practical values calculated .However, there are concerns about the values of the dissimilar joints between aluminium and magnesium, in which the experimental results of AA6082 correspond with the theoretical results of the AA5754, and vice versa. One conclusion is that the change in the pH during tests made the AA6082 to be more susceptible to corrode. However, the AA5754 seems to have been better able to withstand this change.

The dissimilar aluminium samples that were submitted to this testing also show that the corrosion is much smaller, only showing some coloration of the samples after testing. Nevertheless, the corrosion of the aluminium with magnesium alloys shows that not only the magnesium presents an intense corrosion, but the aluminium also suffers a high corrosion rate in which both materials present a high decrease in thickness.

This means that the magnesium is suffering anodic corrosion while the aluminium is suffering cathodic corrosion. These two types of corrosion have a large effect on the corrosion of the joint parts since both materials are corroding instead of one as it would usually occur. This can be explained by the change on the Ph of the solution, caused by the contact with the magnesium-aluminium pair, negatively affecting the aluminium and making it more susceptible to suffer corrosion.

This work concluded that the magnesium/aluminium combination is very susceptible to corrosion, given that both materials corrode in face of each other promoting a bigger corrosion rate in the joined samples. The results also show that combinations between different aluminium have better results in accordance to the results obtained in similar material welds.

5.3 Corrosion study of magnesium alloys

5.3.1 Experimental Procedure

In this study, the influence of the FSW parameters on the corrosion resistance of magnesium alloys was addressed. To reach this goal, different trials were performed at a rotational speed of 800rpm with different welding speeds and the applied forces were optimized. The parameters used for these different tests are presented in Table 5.8. The tool used was the same of the trial described in Section 4.

Tensile tests were performed in a MTS testing equipment with 50kN loading cell. In the tensile tests, changes in mechanical behavior of the aluminium alloys were observed.

Table 5.8 – Parameters for corrosion testing in magnesium alloys.

Label	F (kg)	Ω (rpm)	v (mm/min)	Psp. (mm/s)	Dt (s)	α
E08025	450	800	25	0.1	6	0.5°
E08050	500		50			
E08100	600		100			
E08200	800		200			
E08400	950		400			

Temperature measurements were performed using National Instruments equipment. The thermocouples were positioned on the top of the plates as presented in Figure 5.10. The distance is presented in mm.

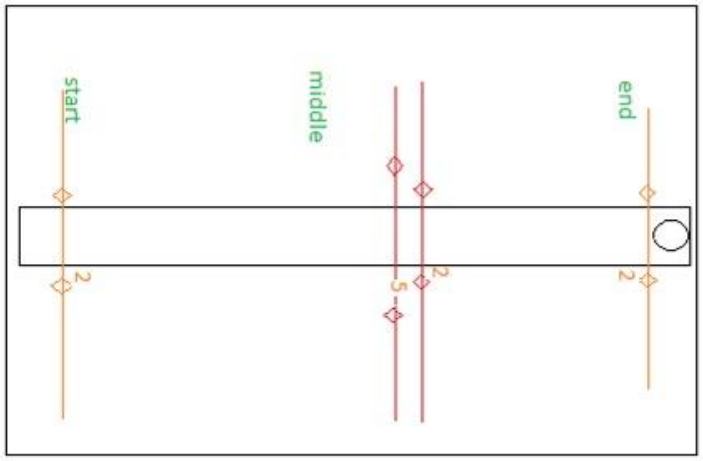

Figure 5.10 – Positioning of the thermocouples in welded samples.

After the 350h corrosion test, the corrosion products add to be separated from the surface of the corroded samples. The procedure to clean the corroded samples was made according to the standard ASTM G1 - Standard Practice for Preparing, Cleaning, and Evaluating Corrosion Test Specimens [161]. According to this standard the magnesium alloy is dipped in a solution of 150g of chromium trioxide, 10g silver chromate and 1000ml of H_2O at boiling temperature. This product will also remove the corrosion products and will also react with the metallic magnesium at a lower rate. To determine the final weight of the corroded sample, the samples were weighed between dips at constant intervals. Figure 5.11 shows how to determine the final weight of the corroded samples through the intersection of the elimination of the corrosion products (A-B) and corrosion of the metal (B-C).

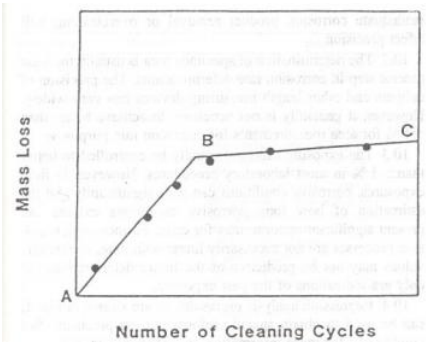

Figure 5.11 – Calculation of the weight of the corroded samples with several dips [161]**.**

5.3.2 Results

It was observed that the changing in the process parameters improved the tensile behavior of the welded alloys. The results from the tensile tests show that by increasing the advancing speed translate in an improvement in the ultimate strength and ductility of the welded alloys will take place.

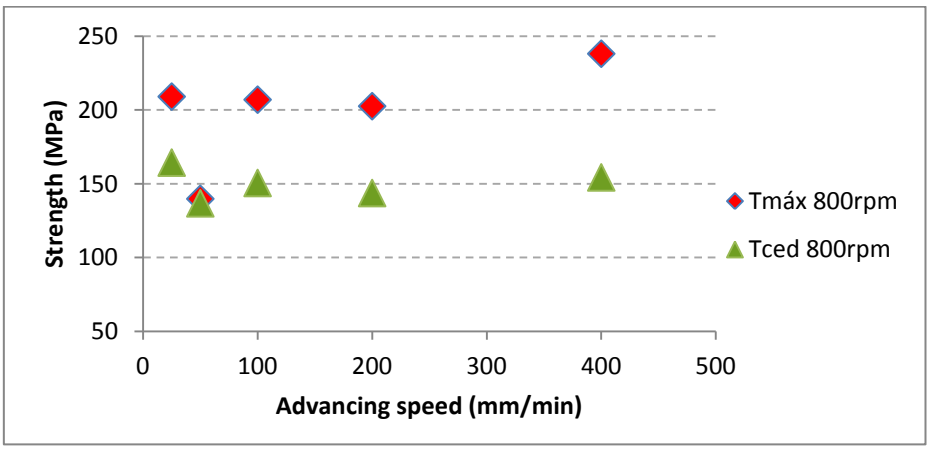

Figure 5.12– Evolution of tensile strength with increasing advancing speed.

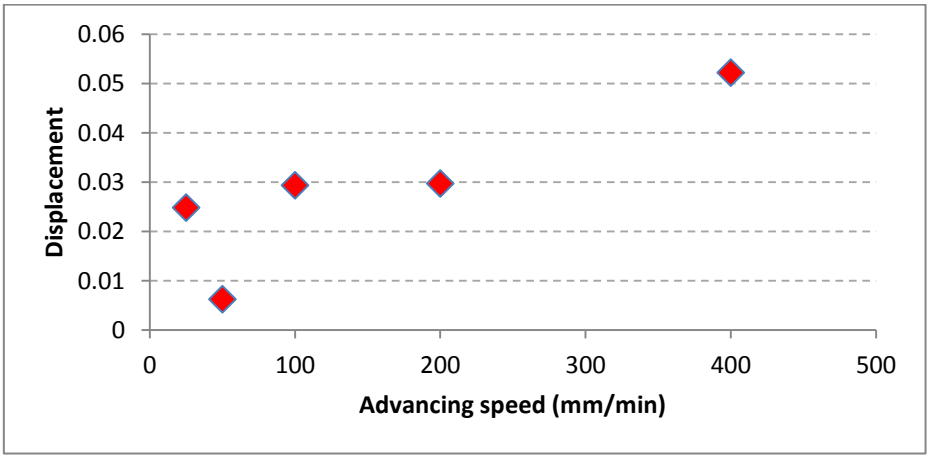

Figure 5. 13 – Evolution of ductility with increasing advancing speed.

Moreover, it is possible to observe that there is a slight increase in the ductility in the magnesium alloys. It was also confirmed the increase in the maximum tensile strength. The yield strength does not seem to play any major difference with the changes in the advancing speed.

Table 5.9 – Temperature and weigh loss in the tested alloys.

Condition	E08025	E08050	E08100	E08200	E08400
Max. Temperature	70.03	68.08	65.30	77.26	67.41
Time over 40ºC (s)	426	200	98	85	48
Weight loss	14.33%	9.26%	5.39%	4.11%	3.76%

These results clearly show that the differences in the temperature in the top of the plate in the magnesium alloys are not significantly relevant to induce an increase in the weight loss. However, there is a clear trend of the weight loss with the decrease of the advancing speed. Another registered phenomenon is the time that these alloys are subjected to this increase in temperature. It can be observed that the decrease in weight is related to the time the material is subjected to this increase in temperature. This means that longer duration at higher temperatures will lead to and increased weight loss. This factor becomes less evident for lower exposures to temperature.

The higher temperature will lead to the increase of the Al-Mn particles observed in SEM (Figure 5.4) and this increase will lead to the increase of corrosion points in the magnesium alloys, therefore increasing the corrosion of these samples. It seems that the higher speeds can effectively reduce this higher corrosion ratio. However, there is a mechanical limitation to how much advancing speed you can raise while keeping the rotational speed.

5.4 Conclusions

The aluminium alloys seem to have a very good behavior to corrosion. It was observed that these samples did not have any preferred corrosion areas as it was verified in the case of the aluminium-magnesium welds. The aluminium samples also did not present any increased corrosion rate as verified in the magnesium welded samples. This good corrosion behavior allied with the great mechanical properties of the welded samples increases the applicability of this process and materials in a vaster number of industries. It was also observed that the Taguchi method is very efficient to determine the best parameters, allowing the definition of the FSW process parameters for the AA5754 aluminium alloys. It was also established that these welded alloys can have a very similar behavior to the base material. The saline testing showed that defects in the surface of the aluminium alloys can work as preferential points of corrosion because there will be an accumulation of Cl^- ions inside the defect which increases

the corrosion rate in this defect. Defects like “root defect” will be affected by this type of corrosion and their mechanical properties will be affected due to this.

The Taguchi method was ineffectively applied in the magnesium alloys, but this has led to the observation that these alloys have a smaller working window than the aluminium alloys. This means that a more restrict interval is needed in order to effectively apply the Taguchi method in these alloys. It was observed that these welds are greatly affected by the combination of the applied force with the advancing speed or/and rotational speed. In this case, the rotational speed was constant and force becomes susceptible to changes in the advancing speed. Two situations occur: inthe first one, the tool creates a continuous flash along the welded area. This occurs for lower speeds and higher applied forces and these facts are related to the creation of a viscoplastic area that exceeds the diameter of the tool. The tool that has a constant applied will plunge in this and the material will flow outside of the forming the continuous flash. On the other hand, for very high advancing speeds and lower applied forces the material does not enter this viscoplastic zone and the process works more like a milling machine, create a detachment of the materials. In this particular area, the problem is related to the applied force that should be higher to promote the viscoplastic flow of the material. These alloys are heat sensitive and the higher force promotes extra heat in the process; therefore it is necessary to control the variables of the process to guarantee that the forces are optimal to weld the material. It was also observed that the mechanical properties of the welded magnesium alloys were worse than the base material. Besides, it was possible to verify that the good samples usually fracture next to the welded area. This lead to the conclusion that the process creates a big strain in the aluminium alloys and that the area right next to the nugget has a high level of residual stresses and therefore will crack first. This effect also seems to occur in the AA6082 alloy that has a reduced ductility. However, even so it was observed that the mechanical properties of the welded samples are good and that they can be used in industrial applications.

Regarding the magnesium alloys it was verified that the process conditions clearly affect their corrosion properties, even though the effect seems to be more intense outside the processed area. However, after 350h the welded samples were completely corroded in all their area. The higher severity of the corrosion attack in the welded samples is related with the increase in temperature during the welding process. This increase has made the material more susceptible to react with the surrounding environment and accelerated its corrosion. The increased corrosion is attributed to the increase of the AlMn particles in the welded samples that work as preferential regions for corrosion. These particles work as cathodes, while the evolving magnesium alloy will behave as anode promoting pitting corrosion in these regions. It was

estimated that these samples are influenced by the heat released in the process and that no other restriction seems to influence the plates. Therefore, a prospective future work could focus on the observation of the process parameters 'influence on the corrosion properties of the welds. It seems likely to predict that a colder weld would tend to be less affected by the corrosion.

The FSW seems to be a very reliable technique that can be applied to magnesium alloys, but the corrosion has also increased with these processing parameters. Future endeavors should focus in finding the right process parameters that can eliminate or greatly reduce the corrosion increase verified in these welds.

It was observed that the mechanical properties of the welded samples between dissimilar alloys have proven that materials from the same class i.e. different aluminium have very good properties and can even display analogous behaviors to the similar welded samples. However, the mechanical properties are usually affected by the material with worse properties after being poor mechanical properties which eliminates the use of the FSW process in this weld configuration. The x-ray diffraction allowed the observation of material mixture in the welded areas; however it seems that the joining mechanism was not adhesion but mechanical interlocking. The use of different weld configurations might help in the mixture of material and alloy for a better mechanical behavior.

The saline testing showed that the corrosion behavior of these dissimilar joints is similar to the behavior of the base materials. The electrochemical studies demonstrated that these alloys have a low current and the corrosion potential is similar to the aluminium ones. This means that there is a very low passage of electrons between the materials making it less susceptible to corrosion. One question arises from this joints regarding if the corrosion effects of dissimilar alloys in aluminium would be the same if a more corrosion prone alloy, like the some alloys of the 2xxx or 7xxx series would be used. The saline and electrochemical testings showed that the joining of the aluminium to magnesium is not very compatible, since the materials will have an higher current and therefore suffer from fast rate corrosion.

It was also observed that the welded magnesium had changes in the properties which made them more susceptible to corrosion. In fact, studies have shown that this joining process increases the corrosion susceptibility of the magnesium in the welded samples to aluminium. However, it seems that the mechanical joining processes that do not promote heat on the joint will have higher probabilities of success since these connections are not as affected by the corrosion as the welded samples.

6 New solid state joining technique

Resistance Spot welding (RSW) is a very common process in automotive industry and because of it car models can have up to 5.000 spot welds inside the vehicle. However, the RSW process has not been able to be as efficient and effective in aluminium alloys as it is on steels. Several problems appear from the interaction of the aluminum alloys with the copper tips [162]–[164], not to mention other joining problems related to process parameters. The problems related to process parameters vary substantially, from lack of joining to joints with a hole in the joining area. The causes of these problems are related to the aluminium because this material usually presents good heat and electric conductors and therefore the energy used to make the weld needs to be high; otherwise it dissipates before joining the materials. Another problem is related to the alumina oxide layer in the contact area of these alloys. Given the fact that is an oxide it needs much more energy to melt than the metallic aluminium; otherwise the process is not able to join the aluminium. This means that the process requires a high amount of energy in a very short time period in order to be able to make a sound weld.

Friction Spot joining techniques have been developed to answer to this problem. Friction Stir Spot welding is a technique that uses the same principles as the Friction Stir Welding and in this case a rotating non-consumable tool penetrates the two plates causing enough deformation and heat to weld the materials together. This process has been successful in joining several materials together, from aluminium alloys [165], [166], magnesium alloys [167], [168] and polymers [169], [170]. Thisprocess leaves a hole in the welded area, but it is acknowledge that it does not greatly influence in the overall performance of the samples. Some works [171], [172] have been developed to reduce/eliminate the influence of this result from the welded samples. Bilici *et al.* [169] made an efficiency study to understand how the parameters influence the properties of the welded samples. It was confirmed that longer dwell times and slower tool rotation infer better mechanical properties in the welded samples. Bilici [170] continued this study and verified that the optimal dwell time for this samples seems to be near the 100 seconds. For longer dwells, the mechanical properties of the welded samples start to decrease. Badarinarayan *et al*. [173] compared the use of different tool geometries in the static strength and they verified that the use of a tool promoting material deformation bestows better static strength properties to the aluminium samples. In this study, the cross-tension of the welds made by the triangular pin was double than the welds made by the cylindrical pin. Hirasawa *et al.* [174] studied the flow of the material using the same tool designs and verified that in the welds with cylindrical pin tool the material flow at the pin

periphery is found in the upward direction. Near the shoulder, 2 flow patterns are observed – beneath the shoulder, the material is pushed downward due to the force acting from the shoulder face, whereas on the shoulder periphery the material flows upward and outward due to extrusion of the material caused by the shoulder plunge. This material flow attributes to the formation of the 'hook' geometry. In the same study, it was verified that the triangular pin tool, due to its inherent geometry, shows enhanced material flow. This enhanced flow also helps in suppressing the upward rising hook geometry observed in welds with cylindrical pins. It was confirmed that the triangular pin provides a better mixing of the material and therefore influences the static strength properties. Tozaki *et al.* [166] studied the influence of the tool geometry. This study was focused on the influence of the pin length and it was observed that the tensile shear strength increased with the increase of pin length. It was also observed that the static strength did not seem to be affected with the changing pin length. The changes in process parameters also showed that the tensile shear strength increased with the increasing tool holding time and tool rotation speed; however, the increase of these parameters affected negatively the static strength. Yuan *et al.* [165] also studied the effect of different tool design in this process using a centered pin tool and an off-centered pin tool. It was verified that the off-centered pin tool needed more rotation speed than the centered pin tool to produce a sound weld. The optimal parameters showed that both samples had similar results in lap-shear testing. Zhang *et al.* [175] studied the effect of the process parameters in the tensile shear strength and static strength of a 5052 aluminium alloy. It was verified that both joints strengths decrease with the increase of rotational speed. It was also verified that 2 fracture mechanisms were observed: shear fracture and mixed tensile/shear fracture in tensile/shear loadings and nugget debonding and pull-out in cross-tension loadings. Gerlich and Shibayanagi [176] studied the grain boundary sliding effect in aluminium alloys during friction stir spot welding process. It was verified that the grains with diameters with diameters over 500nm contain density of dislocations; however, grain with diameters under 250nm were dislocation free. Therefore, it is concluded that the grain boundary sliding is preferable in the smaller grain sizes. Tran et al. [177] studied the effect of process parameters in dissimilar aluminium alloys focusing on the influence of processing times. It was observed that the shear strength of the welds increased with the increasing processing time. It has already been verified that long processing times are clearly beneficial for this process in aluminium alloys.

Other authors have studied the influence of this process in other materials. Behravesh et al. [178] characterized the magnesium spot welds under tensile and cyclic loads and verified that there is a linear relationship between the ultimate shear load and the nugget diameter. It was

also verified that under cyclic loading the crack initiates closer to the nugget for higher cyclic loadings. In addition, it was verified that under cyclic loading two cracks initiate on opposite sides: one grows to failure (primary crack) and the other grows but does not cause failure (secondary crack). The secondary crack depends on both the nugget size and cyclic load level, while the primary crack can be controlled by the cyclic loading amplitude. Lin et al. [168] studied the influence of process parameters in AZ61 magnesium alloys and verified that the dwell is an important factor as in aluminium. It was verified that there is a suitable range where the magnesium presents better tensile shear strength and that over that range this value starts to decrease due to grain size coarsening. Yin et al. [179] studied the properties of friction stir welded magnesium alloys. It was verified that the material flow was different in both alloys. Additionally, it was also verified that the processing parameters influenced both materials in different manners since the AZ31 was able to have a higher failure load with 1s of load time, while the AM60 needed 3 to 4 seconds for its best performance. For both materials the tool that had the best effect was the three-flat/threaded tool.

Hovanski et al. [180] studied successful welding hot-stamped boron steel using polycrystalline cubic boron nitride tooling. It was visible that the used tooling proved to be ideal for the purpose at hand showing no signs of wear after hundred of uses. A narrow band of ferrite inside the nugget was also observed and it must be addressed. Jeon et al. [181] observed the effects of the friction stir spot welding process in a single-crystal austenitic stainless steel. It was confirmed that the stainless steel would lose its single-crystal structure because of the polycrystalline structure of the nugget. It was verified that during the shoulder contacting step the increase of heat input generated discontinuous recrystallization that coarsened the grain structure and led to annealing twinning. Shin and Jung [182] studied the capability of this process in dissimilar joints of lightweight crystalline metals and a bulk metallic glass. It was concluded that given its better mechanical characteristics the bulk metallic glass should be placed on the bottom. This way, the particles of the metallic glass would enter in the structure of the metals making more efficient joining. The same authors [183] studied the influence of this process in bulk metallic glasses and they observed that the fracture load of these specimens augmented with the increase of the plunge depth and that the plunge speed does not seem to have any effect on the specimen properties.

Another friction spot joining process has been developed that makes these joints without leaving a hole on the top plate. This process is known as Friction Spot Welding [184] and has been successfully applied to light metal alloys and polymers. Oliveira et al. [184] made a preliminary study to observe the feasibility of using the Friction Spot Welding in PMMA plates.

It was verified that the strength of the welded samples is comparable to the existing processes. Rosendo et al. [185] studied the influence of Friction Spot Welding in AA6168 aluminium alloys. It was verified that the samples were soundly welded together presenting a good behavior to shear tensile testing. It was concluded that the best processing times are around 3s making this process fast and able provide good mechanical properties to the welded samples. Amancio-Filho et al. [186] studied the influence of this process parameters on the properties of a dissimilar weld between a magnesium alloy and a fiber-reinforced polymer. The authors concluded that the process promoted metallurgical and polymer-chemical transformations. This resulted in increased lap shear strength for the welded samples and grain refinement by dynamic recrystallization resulting in an increase of the microhardness.

Both these processes are competitors in the developed process due to some concerns regarding the higher processing time of the first process and the complexity and higher cost related to the tooling of second one. Considering these facts there seems to be room for the introduction of a new process that can be fast but have cheaper tools than the existing one. A process that uses a consumable tool could be one of the possibilities to be used, hence the focus of the work presented in this chapter.

6.1 Process description

The present work is focused on evaluating a new solid state joining technique that can be used to replace the existing ones. This process is based on the friction mechanisms in which a consumable rod composed of a small probe and shoulder is used to join 2 plates together. One of the features of this technology is that the top plate needs to have a hole to allow the contact between the consumable rod and the plates to be joined. Figure 6.1 presents a small description of the process and the different stages it goes through.

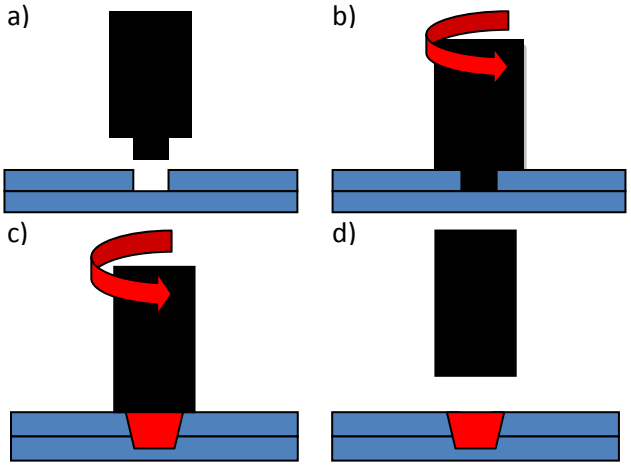

Figure 6.1 – Different stages of the new solid state spot joining technique.

The developed processed is based on the Friction Welding or Friction Surfacing processes in which materials of the same nature are joined together by linear contact through friction mechanisms. In this case, a rotating tool descends at a constant speed and enters in contact with the bottom plate. The increased heat from contact between the rod and plate heats both the tool and the plates. The tool starts to deform plastically and the heat and increased force will help the forging of the tool.

In a first stage, the tool is aligned with the hole in order to make contact between the tool and the plates (Figure 6.1 a). The tool will start rotating at a pre-determined rotation speed (Ω) and descending at a pre-determined plunge speed (Ps) (Figure 6.1 b). On contact, the surfaces will start to heat up due to friction mechanisms. When reaching a predetermined depth, an increased force is applied to the tool increasing the forging effect for the joining of the alloys (Figure 6.1 c). After the application of this force, the consumable rod retracts with the material joined together (Figure 6.1 d). This process has several important parameters:

- Rotational speed (Ω) – the rotational speed needs to be high enough to promote the friction of both the pin and plates and promote a sound joining;
- Plunge speed (Ps) – the plunge speed controls the speed of the process and when related to the rotational speed will distinguish the hot and cold welds;
- Dwell time – this parameter enter when the material reaches the predetermined position the tool stops its constant descend and a predetermined applied force forges the material;
- Applied force (F) – the applied force needed to effectively forge the material together
- Pin length – the pin has to be long enough to connect the top plate to the bottom plate;
- Pin diameter – the diameter needs to be large enough so it does not leave any holes inside the welded region;
- Pin design – the pin must help with the joining of the material;
- Shoulder diameter – needs to be large enough to maintain the process stable under the shoulder and closes the weld on the top.

This process has different strengths and weakness so a SWOT analysis (Table 6.1) was performed. It was identified that this process is a fast welding process, that has no gas emission with a low energy cost which can bring advantages over the resistance spot joining. This process leaves no keyhole on the welded area and the tooling for this process is cheap which seems to bring advantages over the other friction spot joining techniques. Because it is a

solid state joining process, with proper process parameters, it can promote the joining of the material without any discontinuity. This ensures good mechanical properties over time avoiding problems over time. The main goal of this process is to join light alloys; the riveting process usually uses steels joints and overtime vibration will promote the loosening of the rivet by wear (fretting). It is apparent that all materials might be welded using this process if a rod of the same material is used.

Table 6.1 – Swot analysis of the solid state spot joining process.

Strengths	No keyhole at the end Fast process Low energy cost No gas emissions Able to join several materials Hot joining process (advantage over riveting and similar processes) No material restrictions Cheap tooling	**Opportunities**	Potential of joining any material using a rod of the same material as the one to be joined Use of a non-consumable tool with consumable pin can increase the efficiency of this process Increase of plunge speed can greatly improve the processing time Can be adapted to portable tools
Weaknesses	Needs plates pre-prepared for welding Consumable tool Increased added costs Needs tool change after each weld Limited to lap joints Needs a rigid structure	**Threats**	Improvement of other Friction spot joining processes Improvement of resistance spot joining process

Nevertheless, this process presents some weaknesses related to the preparation of the plates that need to have a predrilled hole to be able to join both plates. The consumable tool can improve the joining but carries increased costs overtime because depending on the number of spots joints implies higher costs for the company. Besides, it requires a tool change after each use, which can be very inefficient for high production volumes. This process is also limited to only lap joints and the need of rigid structure can limit its use over time. In addition, there are threats as the improvement of the friction spot joining processes may occur and became

cheaper; besides, since this process does not use consumable tools can be preferred for this. Techniques are also being developed for resistance spot joining that can improve joint efficiency and eliminate the contamination of copper rods by the aluminium.

On the other hand, four opportunities seem to be noticeable; the first is related to the fact that the possibility of joining any material without much effort. The only concern is having a metallic rod of the same material as the plates to be joined. The increase of the plunge speed can greatly decrease the processing time which can escalate this process to high-volume productions. The use of a non-consumable tool coupled with consumable pin can be a step that improves this process allowing for a more dynamic and flexible process. Also, because of the simplicity of the process, it can be easily adapted to portable mechanisms which can improve the use of this process.

6.2 Development process

6.2.1 Experimental Method

Plates of different materials (Table 6.2 and

Table 6.3) were joined together using rod of the same material class. The two plates were placed for a lap-joining and had a 9mm hole made on the top plate. The aluminium plates were joined using aluminium AA6082-T6 rods; the steels were joined using SS304 stainless steel rods and the copper was joined with copper rods. The process parameters varied with the use of the process and several strategies were attempted to efficiently analyze this performance. The aluminium plates used had 2mm in thickness while the steel and copper plates had 1mm in thickness.

Aluminium samples were taken from all acceptable welds and were metallurgically characterized using Keller's reagent composed by 2 mL HF, 3ml HCl, 5 mL HNO_3, 190 mL H_20. The samples were observed under optical microscopy. Lap shear tests were on the samples that were soundly welded to understand the strength of the joining process.

Table 6.2 – Composition for used aluminium alloys [151]**.**

Elem. (%)	%Al	%Mg	%Si	%Zn	%Cr	%Cu	%Fe	%Mn	%Ti	%(Cr+Mn)	%Ca	Other
AA6082	Bal.	0.6-1.2	0.7-1.3	≤0.2	≤0.25	≤0.1	≤0.5	0.4-1	≤0.1			≤0.15
AA5083	Bal.	4-4.9	≤0.4	≤0.25	0.05-0.25	≤0.1	≤0.4	0.4-1	≤0.15			≤0.15

Table 6.3 – Composition for the used steel and copper [151]**.**

Elem. (%)	%Fe	%Cr	%Ni	%N	%C	%P	%Mn	%Si	%S	%Cu
SS304	66.2-73.9	18-20	8-10.5	0.1-0.16	≤0.08	≤0.045	≤2	≤0.1	≤0.03	
Cu										100

A load of 500g was applied in the Vickers hardness testing and the hardness was measured in the mid-section of welded area. The indentations were spaced between themselves by 0.5mm and covered the full thickness of the welded area.

6.2.2 First stage of development

In the first stage of development, several attempts were performed to understand the best processing parameters and the proper parameters to successfully weld the AA6082 plates together. The drilled hole on the top plate had a diameter of 8mm and only the top surface was drilled. The samples were processed at a plunge speed of 0.1mm/s and the tool used had a 20mm shoulder diameter. Table 6.4 presents the remaining process parameters for the different welded materials and the results obtained in the welds.

Table 6.4 – Process parameters of the different trials tested.

Trial	Pin diameter (mm)	Pin length (mm)	Dwell time (s)	Rotation speed (rpm)	Observations
1	8.05	2.04	0	500	No joint
2	8.00	1.99	1	500	No joint
3	8.02	2.00	2	500	No joint
4	8.01	1.97	3	500	No joint
5	7.96	1.69	3	500	No joint
6	8.04	1.90	4	500	Partial joint
7	7.98	2.06	3	1000	Weak joint
8	7.95	2.00	3	1000	Partial joint
9	7.99	1.93	2	1000	Partial joint
10	7.93	2.2	1	1000	No joint
11	7.99	1.96	0	1000	No joint
12	8.00	1.91	3	1000	No joint
13	7.96	1.90	3	1000	No joint
14	7.00	1.90	3	1000	Successful joint
15	7.89	1.87	3	1000	No joint

On a first approach, it was observed that the use of this technology has some problems related to the design of the tool. In fact, the tool with a probe diameter equal to the tool diameter had several problems with the materials joining. It usually presented poor results where the two plates were poorly joined or not joined at all. However, good result was registered when using

a smaller diameter than the diameter of the hole. For such reason, next testing focus on the use of tools with smaller diameters than the hole. For this stage (Table 6.5), it a hole of 9.5mm was drilled on the top plate of the materials. The samples were processed at a plunge speed of 0.1mm/s, a shoulder diameter of 20mm and an applied force of 500kg.

Table 6.5 – Process parameters for new trials.

Trial	Pin diameter (mm)	Pin length (mm)	Dwell time (s)	Rotation speed (rpm)	Observations
16	7.06	3.05	3	1000	Successful joint
17	7.65	3.16	3	1000	Successful joint
18	7.91	2.00	3	1000	Successful joint
19	8.03	2.05	3	1000	Successful joint

It was confirmed that the use of a tool with a smaller diameter than the shoulder provides a sound weld and this became an important tool design parameter. When the tool pin has the same diameter like hole the friction between the tool and the walls of the top plate will heat up the tool and will decrease the mechanical properties of the tool. When the tool enters in contact with the bottom plate, the material of the tool will simply flow on the surface not joining the materials together.

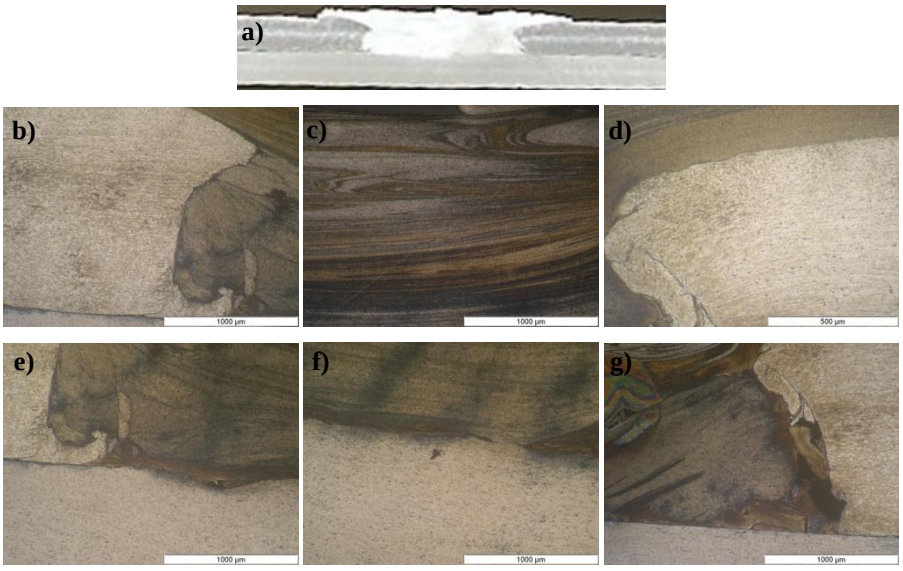

Figure 6.2 – Micrographs showing the microstructure for the 2mm welded samples: a) micrograph of welded sample, b) transition between processed area and top plate; c) processed area; d) transition between processed area and top plate, e) transition between processed area and border of bottom and top plate; f) transition between processed area and bottom plate and f) transition between processed area and border of bottom and top plate.

It can be viewed there is a sound connection with the bottom plate and the shoulder of the tool was also able to make a sound weld with the top plate. From the microstructural observation (Figure 6.2), it is possible to observe that even though the contact with the bottom plate is sound there are some failures along the full length of the joining border. The extremities present several failures having hollow materials and some failures in the

connection. The connection with the sides seems to be more stable; however, cracks are formed on the sides of these samples. It can be observed that on the border of the top plate the material suffered some deformation due to contact with the tool's shoulder enabling the joining of the materials.

The microhardness profiles provided valuable information regarding the phenomena that occurred during this process and the influence on the material properties. The profiles of the welded samples hardness are presented on Figure 6.3.

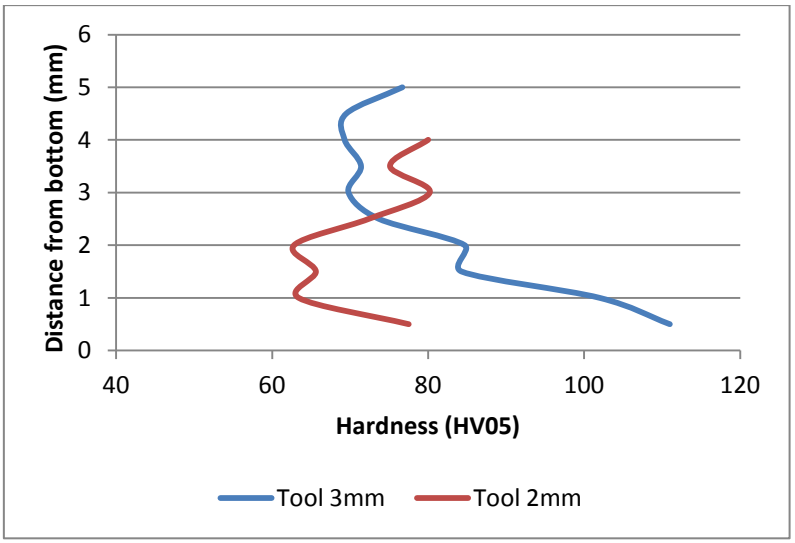

Figure 6.3 – Hardness profiles of joined plated in Trial 16 (2mm) and 18(3mm).

It can be observed that the rod has suffered a high deformation and that the heat released by the process has made the hardness lose the thermal history that it had going probably back to the O state. In both alloys the lowest hardness is located at 2 – 3 mm from the bottom, precisely the area that is in direct contact with the bottom plate. Two different materials for the bottom plate were used: the materials joined by the 2mm were the AA5754-H111 alloys, while for the 3mm the plate used was of the AA6082-T6 alloy. It can be observed that the hardness decreases as it approaches the contact area. This decrease in hardness is associated to the released heat in the process that is very intense. The heat released makes the heat treatable alloys to lose the thermal treatment that these alloys have and in the non-heat treatable alloys these materials promote the coalescence of the grains, also promoting a decrease in the hardness of the alloys.

The main achievement of this selection stage was the confirmation that the tool needs to come in contact with the bottom plate to make a sound weld. Both these alloys have similar mechanical properties and when they come in contact the rotational movement associated to an increased applied force will promote the joining of the materials.

6.2.3 Second stage of development

After establishing the tool design and some process parameters in this stage a more thorough study will be performed to understand the influence of the tool design on the weldability of the different materials. Two tools were design for this goal (Figure 6.4), the first tool has two layers or floors; the first floor is the nearest to the shoulder and has 1mm in length and 10mm in thickness; the second floor is on top of the first and has 2mm in length and 8mm of diameter. The second tool is a conic tool with the bottom diameter in contact with a shoulder of 10mm and a slope of 30^{o} degrees to the smaller diameter. Both these tools had a shoulder diameter of 20mm.

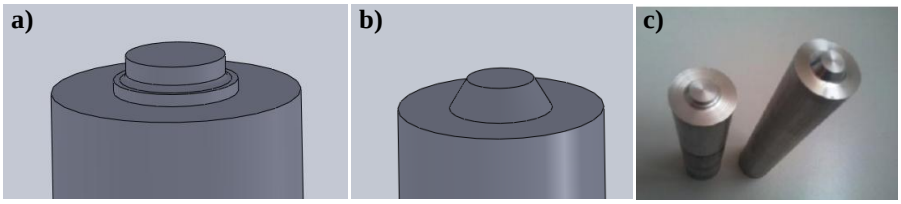

Figure 6.4 – Tools used for the second stage of development: a) tool with two layers (tool 1), b) conic tool (tool 2) and c) image of the produced tool.

The objective of these designs is to enable the tool to enter in contact with the bottom surface before the shoulder comes in contact with the top surface. The longer pins with decreasing diameter enable this to happen. These designs were optimized to weld plates with a diameter of 10mm on the top plate. The samples were welded using a rotational speed of 1000rpm, a plunge speed of 0.1mm/s, a dwell time of 3s and an applied force of 500kg. All welds were successfully joined and tested to evaluate their performance and plates of aluminium AA5083-H111 were joined together. Figure 6.5 and Figure 6.6 present the microstructure of joined welds using tool 1 and 2, respectively. In Figure 6.5, it can be observed that the material was not able to completely fill the hole and have the material completely joined in the surrounding surface. It can be also observed that in the bottom corner of the surface there is no connection having a lack of material in that area. It can also be observed that the side surfaces are not completely joined, being joined only at the upper side of the weld. Finally, it is possible to conclude that the material was successfully joined at the bottom surface and on the upper surface corner where the rod was able to deform the top plate and make a successful joint with no signs of a discontinuity in the material. Figure 6.6 apparently shows a better joining than the weld using the other tool. It can be observed that there are discontinuities in the material on the sides of the weld and on the bottom corners. Overall, the use of this tool design seems to be more effective as it seems to increase the joining of the surface all around the material.

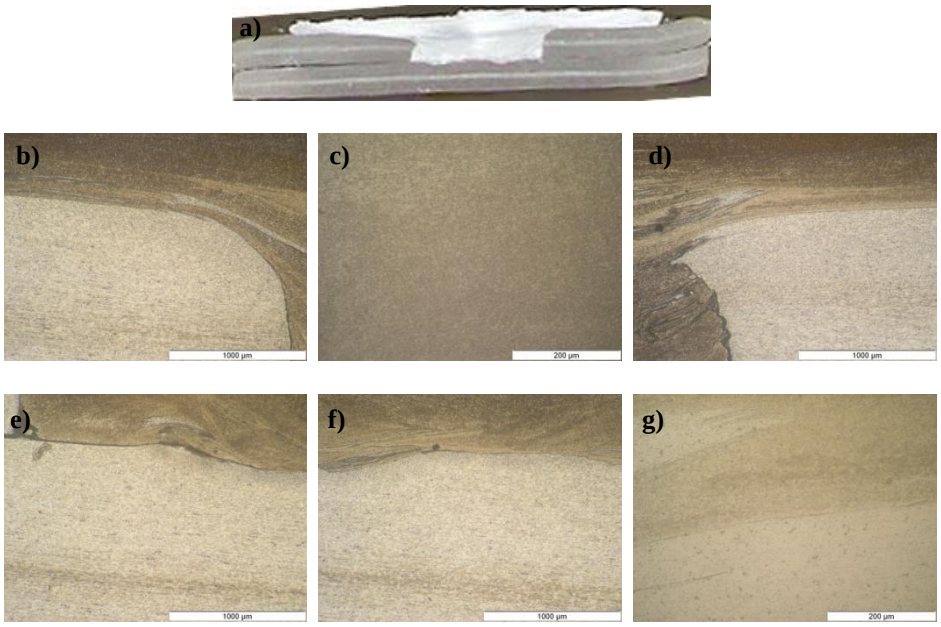

Figure 6.5 – Microstructure of the samples welded by tool 1: a) macrography of the welded sample, b) top corner nugget near the upper surface, c) nugget, d) top corner opposite side, e) bottom corner nugget joined with bottom and side surface, f) joint of nugget with bottom surface and g) joint of nugget with bottom surface at higher magnification.

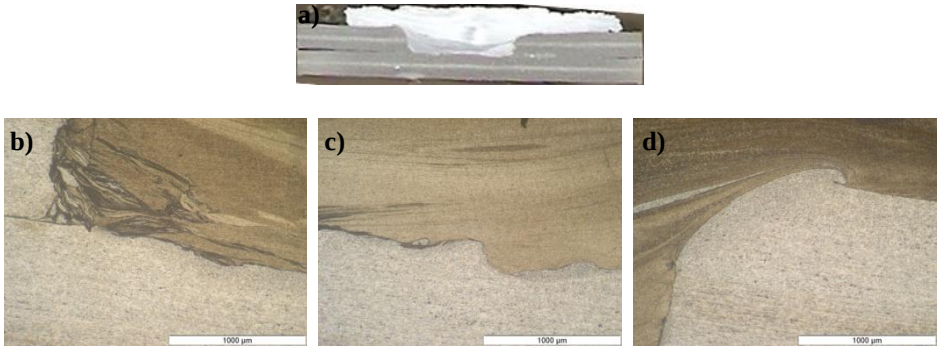

Figure 6.6 – Microstructure of the samples welded by tool 2: a) macrography of the welded sample, b) bottom corner nugget joined with bottom and side surface, c) joint of nugget with bottom surface and d) top corner nugget near the upper surface.

The hardness testing has once again provided important information regarding the welded area and the material transformations induced by the FSW process (Figure 6.7). It can be observed that the lowest hardness in these profiles is located in the 2-2.5mm, the region where the rod made contact with the bottom surface. The lowest hardness in this region can be explained by the higher produced heat and the strains that this region suffers when the rod contacts with the bottom surface. Once again, it can be observed that the material's hardness decreases from the bottom surface to the contacting area. The decrease in hardness is explained by the released heat that promotes the coalescence of the grain structure decreasing the material hardness. The hardness increases again from the contacting area to the top surface. This increase in hardness is explained by the strain that the material suffers and the applied force that promotes the forging and consolidation of the weld.

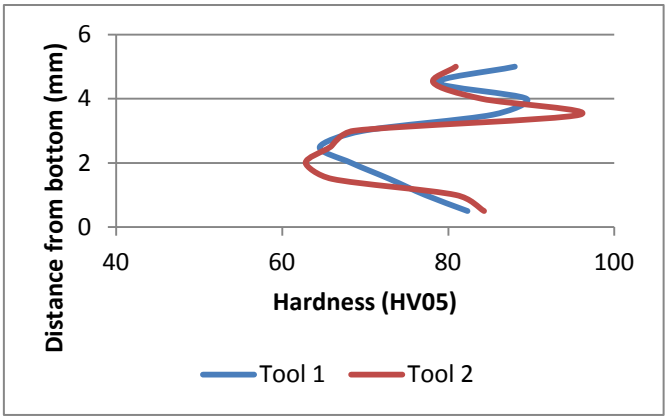

Figure 6.7 – Hardness profiles of the samples welded by tool 1 and 2.

These alloys were subjected Lap shear tests, assessing the strength of the joint submitted to a tensile load. Table 6.6 gives a summary of these results.

Table 6.6 – Results of lap shear tests.

Sample	Maximum force (N)	Average Maximum Force (N)
Tool 1	4500	3550
Tool 2	5600	4150

It can be observed that these welds have a high value regarding the lap shear tests. In fact, the average results are lower than what was found in literature [185]. However, these results are not optimized and there is room for improvement in this section. The next step will be an optimization step in which the influence of the process parameters in the mechanical properties of the welded samples will be studied.

6.2.4 First optimization step

In this stage, a study regarding the influence of the process parameters in the mechanical properties of the spot welded samples will be addressed. This process has successfully joined different plates together using different tool designs. In this study, it was attempted to weld AA6082 and the process parameters were studied using cylindrical tool. Even though these tools have been considered not as effective as the conic tools, its simpler design, however, might increase its odds of being used in continuous processes decreasing the process cycle time. The Taguchi method was applied and the influence of the rotational speed, plunge speed and hole depth on the properties of the welded samples were studied. Apart from the parameters, the welds were performed with an applied force of 500kg and with a dwell time of 3s. The tool had a pin length and diameter of 3mm and 8mm, respectively, and a 20mm

shoulder diameter. The top surface had a predrilled hole with a diameter of 9mm. The three selected parameters had three testing levels. For the rotational speed it was tested the 1000, 1500 and 2000rpm, the plunge speed being tested at 0.1, 0.3 and 0.5mm/s and the hole depth was tested at 2, 2.5 and 3mm. The hole depth of 2mm means that only the top plate was drilled and the other tests are incremental holes made on the bottom plate. Table 6.7 presents the defined test parameters for the different trials in Taguchi method.

Table 6.7 – Parameters for the first optimization stage of solid stage spot welding technique.

Parameter	Symbol	Level 1	Level 2	Level 3
Variable Parameters				
Rotational speed (rpm)	A	1000	1500	2000
Plunge Speed (mm/s)	B	0.1	0.3	0.5
Hole Depth (mm)	C	2	2.5	3
Fixed Parameters				
Applied Force (kg)	500			
Dwell time(s)	<3			
Pin Diameter (mm)	8			
Pin Length (mm)	3			
Hole Diameter (mm)	9			

The study of the influence of these three parameter leads to the applicability of the L_9 matrix on this process. This matrix is the most suitable for this factor and it has been established to use the same matrix as the one used for FSW of AA5754, described in section 4.4.2. Table 6.8 shows the different combination of parameters established for this optimization stage.

Table 6.8 – Taguchi method test parameters for the first optimization stage.

Trial	Ω(rpm)	Psp. (mm/s)	Hole Depth (mm)
1	1000	0.1	2
2	1000	0.3	2,5
3	1000	0.5	3
4	1500	0.1	2,5
5	1500	0.3	3
6	1500	0.5	2
7	2000	0.1	3
8	2000	0.3	2
9	2000	0.5	2,5

After the test of the samples, it was observed that alloys tested combinations were successful joining these alloys and the primary test, which consists of applying a sudden force in the joined samples, was successfully overcame by all samples. It was then considered that the trials were successful and the next steps of Taguchi could be taken to assess the joints.

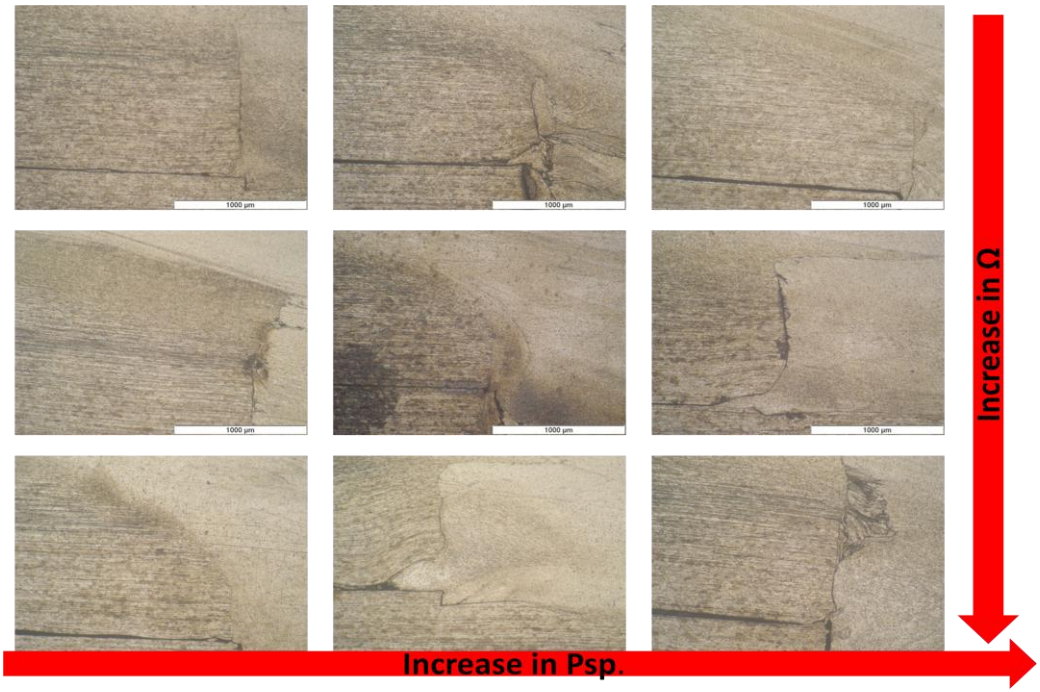

Figure 6.8 – Detail of the side of the welded joints.

Figure 6.8 shows the side of the joints performed by the new solid state process. It can be observed that the deformed material has several difficulties in making a joint between all the contacting surfaces. This is related to the difference in diameters of the pin used and the plate's hole which needs a fast interaction to promote the weld. Also the forging force might not be fast enough to promote the diffusion guaranteeing a good joining. Even so, it seems that at higher rotational speeds and lower plunge speeds the shoulder is able to promote a great deformation of the plate making almost a full side joint.

The lap shear strength test was considered to evaluate the welds and the results can be found in Figure 6.9. The highest value for the shear was found at the trial 8 with an average near the 5.5kN. It can also be observed that the trial results are mostly between 4.4 to 5.5 kN; however, there are some exceptions in trial 4 and 7.

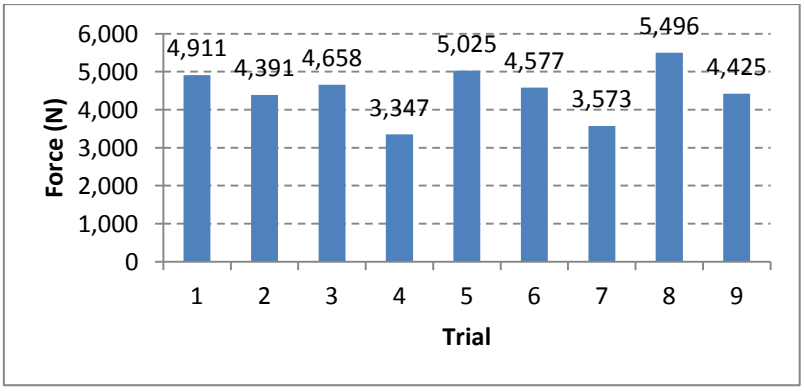

Figure 6.9 – Average values of the lap shear tests for the different trial.

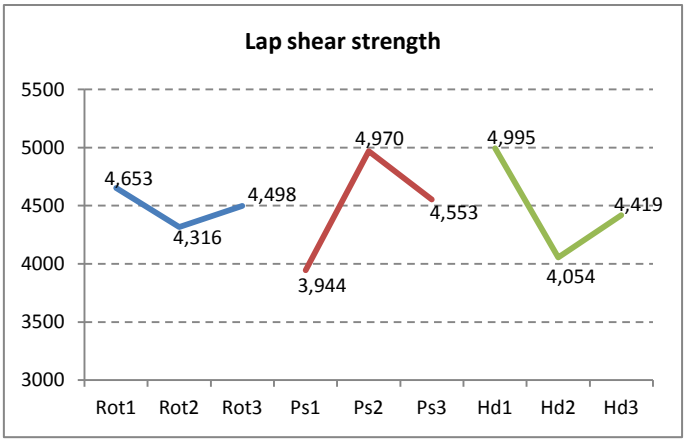

Figure 6.10 – Parameter effect on the lap shear strength of the welds.

The Taguchi method will use an approach considering the bigger the better in the evaluation of these welds and determination of the optimal parameters. The planning of these trials is orthogonal and therefore it is possible to isolate the effect of each parameter in the different trials. The average of each parameter at each level is presented in Figure 6.10. It can be observed that the higher values obtained for the lap shear strength was at a rotational speed of 1000 rpm (A1), a plunge speed of 0.3mm/s (B2) and a hole depth 2mm (C1).

The lower rotational speed means that when the material enters in contact with the plate it does not promote the heat on the pin as fast as in faster rotating welds promoting a more intensive plastic deformation of the bottom which can lead to a more sound weld. The plunge speed seems to define the speed due to the movement: if it moves slower the material moves faster and might promote more heat on the pin, which is not fast enough to make a sound weld in the plate below; in contrast, in faster welding speeds there might be more plastic deformation of the plate below and the material more brittle because it does not consolidate as well as with lower plunge speeds. The hole's depth is important since the volume of plasticized material must be able to completely fill the hole. Finally, it was possible to predict that using the established parameters with this process the lap shear strength might increase to 5,640N.

Table 6.9 – Results of the variance analysis for the for the lap shear strength.

Parameter	DOF	SS	V	F	Ro
Rotational speed	2	170573.4321	85286.71605	0.30876	0.046447
Plunge speed	2	1599990.543	799995.2716	2.896192	0.435677
Hole depth	2	1349415.58	674707.7901	2.442619	0.367445
Error	2	552446.2469	276223.1235	-	0.150431
Total	8	3672425.802	-	-	1

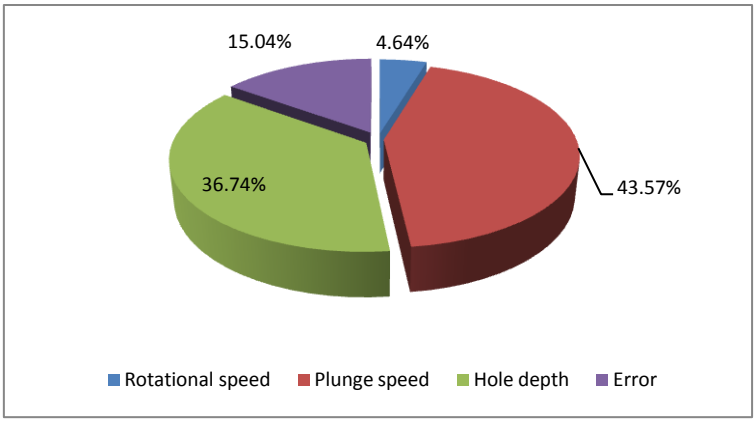

Figure 6.11 – Contribution of each parameter for the lap shear strength factor.

Figure 6.11 and Table 6.9 present the variance analysis of each parameter´s influence in the strength of the weld. Taking this into account, it is possible to conclude that this process is strongly influence by the plunge speed (43.57%), followed by the hole depth (36.74%). As previously mentioned, the level of distortion promoted by the small plunge speeds and hole depths can promote a better consolidation of the welded area presenting better mechanical results in this evaluation.

Apart from these analyses, it was also observed the cycle time of each weld and torque effect on the welding machine. The cycle time taken into that tool starts 1mm above the top plate, travels the length of the pin plus 0.2 mm and also has some dwell time related with the increase of the rotational speed to the predetermined test rotational speed.

Table 6.10 – Torque and cycle times for the different trials.

	E1	E2	E3	E4	E5	E6	E7	E8	E9
Torque máx.	53,90	54,53	54,39	47,04	46,41	43,19	39,13	38,29	38,99
Time (s)	44,8	17,4	12,9	43,3	17,7	11,7	43,2	14,4	11

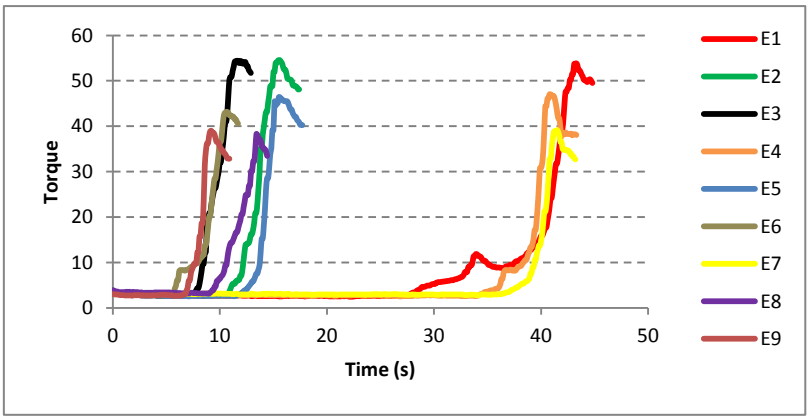

Figure 6.12 – Evolution of the torque over time in each trial.

Figure 6.12 presents the evolution of the torque over the course of the trial; the three trials with the lowest plunge are presented more to the right in the figure (around 40s) and the increase in the plunge speed makes the process faster and the process ends earlier in time. Table 6.10 shows the average results for the highest torque value found and the average cycle time.

It can be observed that the torque is influenced by two factors, the rotational speed and plunge speed. In Figure 6.12, a decrease in the torque is clearly observed with the increase of the rotational speed. This is related with the higher rate of temperature increase that can be found in the trials using the higher rotational speed. The temperature increase in the material makes it easier for the welding machine to be able to oppose the movement created by their contact. The plunge speed seems to have the opposite effect where the increase in plunge speed is related to an increase in the torque. However, this effect is much smaller in this test. This is related to the higher speed rate that opposes a higher force to the movement of the tool.

Another observation is that for lower plunge speeds, especially in trial, a small increase in the torque is visible just before reaching the torque´s highest increase. The first increase in torque is related to the pin tip coming in contact with the surface and presenting an increase in the force needed to deform. The decrease in force is related to the plasticization of the material and the highest decrease is related with the contact with the tool shoulder. These results have presented the first glimpse of the parameter influence on the weld properties for this process. Some improvements can be made overall, starting with the use of higher rotational speeds to decrease the torque's effect; besides, the starting point of the weld can be closer to the material as it may improve the cycle time. In trial 1, it can be observed that the pin comes in contact with the bottom plate at 34s, meaning that the time needed for the tool to reach its predetermined rotational speed around 25-30s could be saved.

6.2.5 Second optimization step

A second step for this test was performed to determine the effect of using higher welding speeds and different pin length on the properties of the welded materials. The use of these higher speeds intends to make the process less severe for the welding tool while the constant hole depth is used to simulate industrial environments where plates usually have only through all holes This process will use the same approach as the previous optimization step. The Taguchi method was applied and the influence of the rotational speed studied, as well as plunge speed and pin length properties of the welded samples. Apart from the parameters, the

welds were performed with an applied force of 500kg and with a dwell time of 3s. The tool had a pin diameter of 8mm and a 20mm shoulder diameter. The top surface had a predrilled hole with a diameter and length of 9mm and 2mm, respectively. The 3 selected parameters had three testing levels. The rotational speed it was tested at the 2000, 2500 and 3000rpm, the plunge speed being tested at 0.1, 0.3 and 0.5mm/s and the pin length at 2, 2.5 and 3mm. Table 6.11 presents the defined test parameters for the different trials using Taguchi method.

Table 6.11 – Parameters for the second optimization stage of solid stage spot welding technique.

Parameter	Symbol	Level 1	Level 2	Level 3
Variable Parameters				
Rotational speed (rpm)	A	2000	2500	3000
Plunge Speed (mm/s)	B	0.1	0.3	0.5
Pin Length (mm)	C	2	2.5	3
Fixed Parameters				
Applied Force (kg)		500		
Dwell time(s)		<3		
Pin Diameter (mm)		8		
Hole Length (mm)		2		
Hole Diameter (mm)		9		

The study of the influence of these three parameter leads to the applicability of the L_9 matrix on this process. This matrix is the most suitable for this factor as its fundamentals and use were already established in section 4.4.2. Table 6.12 shows the different combination of parameters established for this optimization stage that differ in the rotational speed used and the study of the pin length.

Table 6.12 – Taguchi method test parameters for the second optimization stage.

Trial	Ω(rpm)	Psp. (mm/s)	Pin Length (mm)
1	2000	0.1	2
2	2000	0.3	2,5
3	2000	0.5	3
4	2500	0.1	2,5
5	2500	0.3	3
6	2500	0.5	2
7	3000	0.1	3
8	3000	0.3	2
9	3000	0.5	2,5

After the testing of the samples, it was observed that alloys tested combination were successful joining these alloys; in addition, the primary test which consists of applying a sudden force in the joined samples was overcame by all samples. Therefore, it was considered that the trials were successful and the next steps to assess the joint were taken.

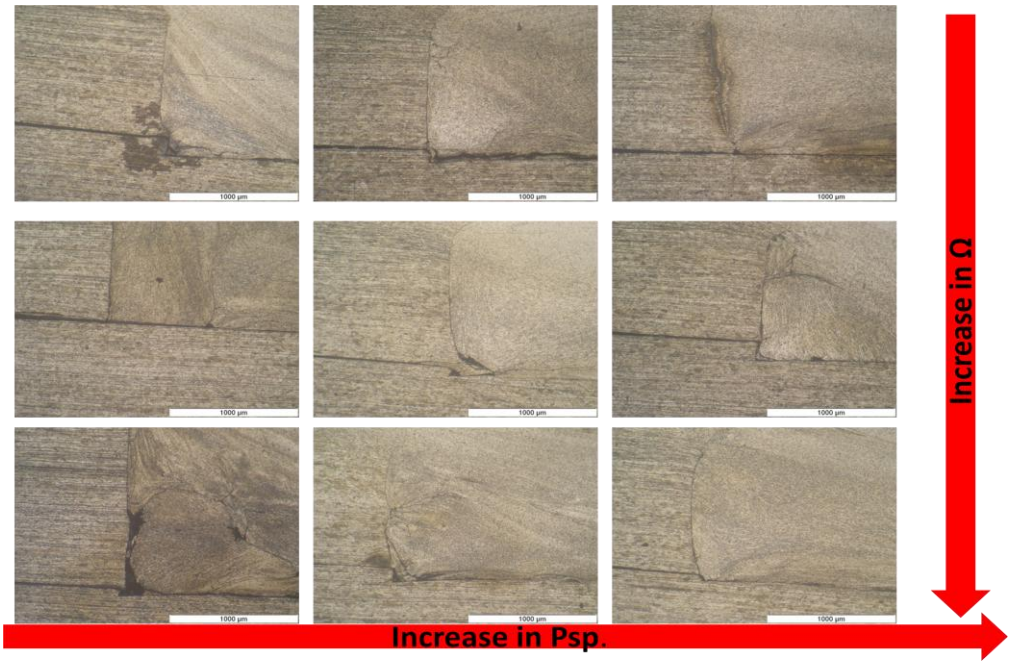

Figure 6.13 - Detail of the side of the welded joints of the second optimization step.

Figure 6.13 shows that the joining of the side of these joints seems to be worse than in the previous optimization step. It seems because the promotion of higher heat does not allow for improvements in these joints usually showing also a bad material flow especially at higher rotational speeds. The lap shear tests were performed to evaluate the strength of these joints.

The lap shear strength was considered to evaluate the welds and the results of these can be found in Figure 6.14. Observations concluded that the highest value for the shear was found at the trial 2 with an average near the 4.7kN. Further observation shows that the trial results are mostly between 3.6 to 4.3kN; however, there are some exceptions in trial 1 and 4 which were lower while trial 2 had a value higher than this.

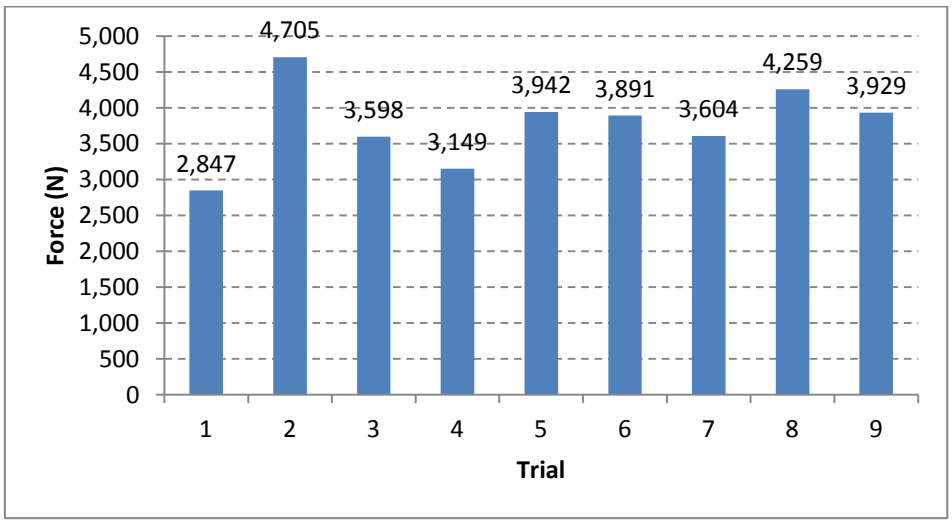

Figure 6.14 – Average values of the lap shear tests for the different trials.

Like the test before it an approach considering *the bigger the better* will be used for the evaluation of these welds and determination of the optimal parameters. The planning of these trials is orthogonal and therefore it is possible to isolate the effect of each parameter in the different trials. The average of each parameter at each level is presented in Figure 6.15. It can be observed that the higher values obtained for the lap shear strength took place at a rotational speed of 3000 rpm (A3), a plunge speed of 0.3mm/s (B2) and a pin length of 2.5mm (C2). This observation allows to conclude that using these optimized parameters the welds are able to achieve a lap shear strength of 4,620N which is lower than the process using lower rotational speeds. This means that the mechanical deformation is important to improve the weld strength. Besides, trial 2 presents an average force superior to this value, meaning that maybe the influence of the higher rotational speed might not be as effective as it was seen in the previous optimization step.

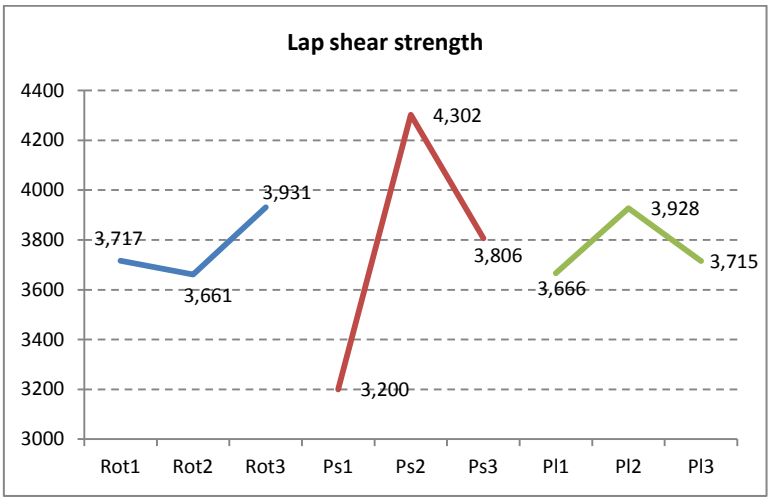

Figure 6.15 – Parameter effect on the lap shear strength of the welds.

The higher rotational speed might mean that the heat produced was enough to promote the joint between the two materials where the weld is to be joined. The plunge speed was previously discussed. The pin length is related with the occupied volume inside the hole and with the smaller pins it cannot occupy the full volume of the hole and the length of the pin might not be sufficient to promote enough distortion and enough consolidation of the weld.

Table 6.13 – Results of the variance analysis for the for the lap shear strength.

Parameter	DOF	SS	V	F	Ro
Rotational speed	2	121869.4074	60934.7037	0.295856	0.04919
Plunge speed	2	1827325.407	913662.7037	4.436102	0.737559
Pin length	2	116414	58207	0.282612	0.046988
Error	2	411921.4074	205960.7037	-	0.166263
Total	8	2477530.222	-	-	1

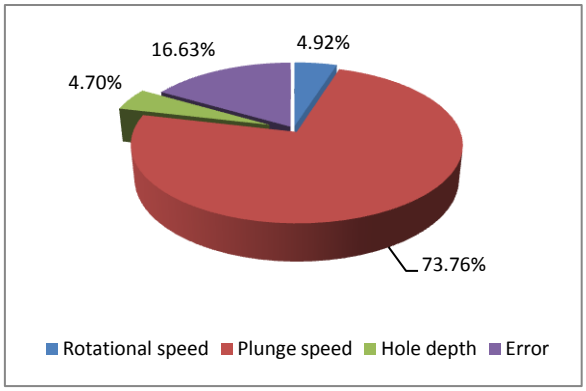

Figure 6.16 – Contribution of each parameter for the lap shear strength factor.

Figure 6.16 and Table 6.13 present the variance analysis of the influence of each parameter in the strength of the weld. In this stage, it can be clearly observed that the plunge speed is the main driver of this process for hotter welds. The level of distortion promoted by the plunge is the factor that influences the most these results. Once again the entry seems to greatly influence the properties imbued to the samples and the promoted distortion and force required seems to be more visible in the hotter welds. The pin length does not seem to have a substantial influence, even if medium pin length make sounder welds.

Table 6.14 – Torque and cycle times for the different trials.

	E1	E2	E3	E4	E5	E6	E7	E8	E9
Torque máx.	32,41	42,63	40,04	26,18	31,64	31,64	17,36	25,83	29,61
Time (s)	42,3	14,4	10,2	36,8	14	7,6	42,1	11,9	8,6

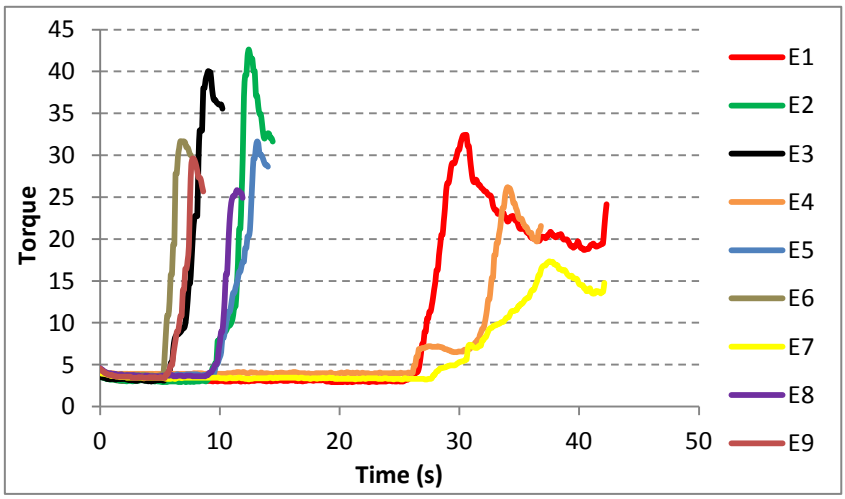

Figure 6.17 – Evolution of the torque over time in each trial.

Figure 6.17 presents the evolution of the torque over the course of the trial and Table 6.10 shows the average results for the highest torque value found and the average cycle time.

It is possible to observe that the use of different pin lengths had an impact in the welds with the same plunge speed, but it can also be concluded that a change in the starting position can effectively improve this process. Moreover, it was also registered that the increase of rotational speed can effectively reduce the torque of reaching values of 17N.m at 3000 rpm. Another observations points out that the small increase in torque, due to contact of the pin, has almost disappeared in this set of trials. The higher heat rates made these alloys lose that initial resistance observed in the colder welds. Since the main cause for the high torque value is the shoulder, a reduction in the shoulder diameter could bring improvements for these welding steps upgrading the wear on the welding machine.

6.3 Transversal applicability

Our next step of investigation focuses on the study of this process´ applicability in other materials apart from aluminium. In fact, the focus of this study was the applicability of this process and the chosen parameters in an approach based on the obtained results from the aluminium study. The copper alloys were not joined properly and the best result was achieved making some changes in the process parameters. The set parameters used to weld the steel and copper alloy are shown in Table 6.15.

Table 6.15 – Parameters for welding the SS304 steel and pure copper alloy.

Parameter	Steel	Copper
Rotational speed (rpm)	2500	3000
Plunge Speed (mm/s)	0.3	0.1
Applied Force (kg)	1000	500
Dwell time(s)	<3	
Pin Diameter (mm)	8	
Pin Length (mm)	2	
Shoulder diameter (mm)	12	
Hole Diameter (mm)	9	
Hole Depth (mm)	1	

It can be observed that the shoulder was reduced for these testing to improve the torque, considering that the steel might be more severe on the torque of these alloys. The change in applied force for these was based on a preemptive test that showed better results with these alloys.

The steel was welded without any problems related to the process. It was observed that the hole was not completely filled which is related to the fact that these steels create a very small flash in this process, leaving a 0.5mm gap for the side walls.

The copper alloys had more problems than the steels; in fact, these alloys were not able to maintain a stable process because the copper alloy rod would deform due to the increase of

applied force making the welded samples to have increased problems in this step. Future steps for these materials include an improvement of the tool design to eliminate the occurring problems and testing to optimize the welding parameters.

Despite these results, some welded samples were lap shear tested to understand the joining strength. Table 6.16 presents the results for the lap shear tests in these alloys.

Table 6.16 – Lap shear strength results for SS304 steel and pure copper alloy.

	SS304	**Cu**
Lap Shear Strength (N)	8,143	1,002
Standard Deviation (N)	474.6	615.4

The performance of the steel was very good and the fracture happened in the steel itself with the joint remaining intact. There were, however, some problems regarding the joining at the top surface were the material was not able to make a connection meaning that a bigger shoulder diameter/pin diameter is needed for this case.

Regarding the copper alloys, it was observed that they were not able to make sound welds and this affected the performance in the welded samples. The best cases showed that the plasticized material would not suffer any deformation and would not detach from the bottom plate with the fracture occurring in the BM.

The obtained results demonstrated that this process can be effectively applied on steels. This has not been corroborated for the copper alloys although some improvements can be achieved through tool design. The effectiveness of this process in steels is promising although this technique loses some competitive advantage because the RSW is already established for these alloys with very high performances. In order to be competitive with these alloys, improvements should focus on enhancing the tool flexibility for different weld positions.

7 Seat development

Different strategies have been developed to aid the product development process and allow a smoother introduction of the developed parts in the industrial process. Ashby [187] identified different inputs that influence the design process (Figure 7.1).

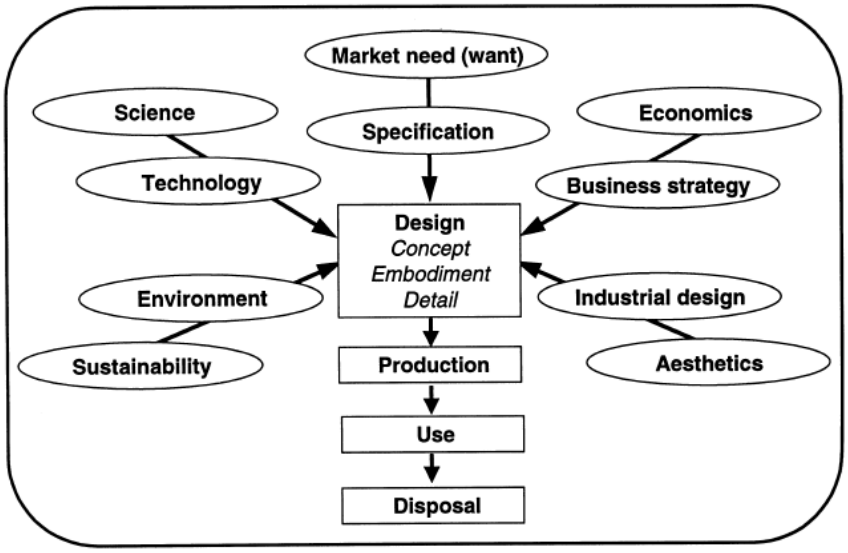

Figure 7.1 – Dominant inputs of the design process.

The design process involves the generation of concepts to fulfill a market need or satisfying a desire. The development of one or more of these is afterwards detailed and embodied and if a developed product is promising enough a prototype is developed and put into production.

The business strategy and economics states that to bring a new product to market two aspects must be taken into account: viability and value capture. A product is considered viable when it fulfills a need at an attractive cost for the market. However, the viability also depends on the ability of the company to commercialize it. The value capture depends on the market size and the ability to outmaneuver the competition while keeping the intellectual property. The environment is also another concern of the product development since every activity of human production has a direct effect on nature. Restrictions on the product design must be considered in order to reduce the impacts on the environment.

Another driving force of the design is the development of new concepts and phenomena that will translate into new technology. This can result in the creation of new materials with both aesthetic and technical potential. These new products can be good additions to the product design as it can improve the design of existing products and increase the companies' portofolio with new ideas. The addition of lighter materials [4] has been one of the trends of the automotive sector which can greatly improve the performance of the motor vehicle.

The aesthetics and design are also important because of the perceptions that it transmits to the possible customers. Therefore, the use of products' texture, color and shape will work to attract the final customer. Hence, the importance of adequately selecting the right materials and processes to create the product.

Several strategies are used trying to accomplish these goals. Concurrent engineering, Design for x (where x is the goal to improve like manufacturing, cost, quality among other options), New Product Development (NPD) are some of the used methods to improve product development inside a company. Several authors have studied the influence of these different methods in the product development of different products. It was long ago recognized that the improvement of the relationship between customers (which can be OEMs) and suppliers can effectively aid in the product development strategy [188]–[190]. The cooperation between the supplier and customer has a very high initial cost. The supplier will potentially need to invest in new equipment, processes and technique to align itself with the customer's culture, while the buyer needs to invest resources and time to assist the improvement and alignment of their processes and culture [189]. These suppliers can bring new technological advances in the customers companies and therefore it is required to nurture their relationships and increase their involvement in the product development process [188]. Minderhoud and Fraser [191] confirmed that there is a shift in the paradigm of product development where the product development process used to take from 10-15 years and has now reduced to 2-5 years. This reality affected several industries including automotive industry where there is a very short time for product development. The use of concurrent engineering in the new product development process can effectively reduce the product development time. The interaction with other departments gives an idea of the existing company conditions and where investment should be made to be able to produce the new product. However, some concerns have been brought up due to the evolution of these relationships over time whenever the customer reduces the investment. On the other hand, the supplier needs to become more proactive and gradually reduce their dependence on the customer.

Cost reduction is one of the industry goals and several strategies have been implemented to reduce the product development cost. Roy *et al.* [192] developed a new model to estimate the cost of introducing new technology, perceiving the inherent cost advantages that the new product can bring over the existing technologies. Another author [193] stresses that the decision making of the products needs reliable results and a good control of the product development process. The quality of information in the early stages of the process can effectively provide good indicators that may improve the product development process and

more readily obtain a ready for market product. Zhao *et al.* [194] developed a decision support system to compare different design solution by comparing the performance metrics between them. These metrics consider development times, profit margin, cost, revenues, risks, among others. This tool can be used to decide which design solution and integrated different methods enables the production of a more robust decision. The value analysis is an effort to determine and eliminate those characteristics that have no real value for the customer. Leber *et al.* [195] used this method and they were able to eliminate the characteristics that presented no added value for the product. This product has received a good feedback from the customers and proceeded for testing from regulation authorities. This analysis can help to determine the parts that have real impact and contributing to reduce costs by eliminating those parts that bring no benefit to the end-user hence increasing the value of the product.

Automotive industry faces several challenges regarding the product development and it has been observed that collaborative development from the different departments of the company [196] are needed to improve the development process. It has also been confirmed that the cost is important and that there is a need to identify the different cost estimators ,classify them and understand their influence in the development process. All these conditions must be taken into account in the product development process. With the introduction of new materials there will be a need to make a closer observation of the process to determine if new capacities are needed to effectively implement this process. Edwards [18] confirmed that the changes of the materials in the seating system are mainly focused on the use of new foams on the material system, while the seat structure is still a robust welded tubular structure. Ermolaeva et al. [197] identified that even though materials like natural fiber composites have low mechanical properties they can still be used due to their lower weight and cost. Theseworks showed that the natural fibers composites were preferred for light loaded structures, while steel was preferred for heavily loaded structures. In this analysis, it was observed that both aluminium and magnesium alloys had usually close performances for the studied cases. A similar study was performed by Farag [198] were different quantitative methods were used to compare the materials to be replaced over some composite and natural materials options. It was confirmed that the use of the developed coefficient can easily be compared to the material studied. This author also concluded that the natural fiber composites can start to be introduced in these materials. Matos and Simplício [199] performed a selection method and were able to observe that the cork and wood can be used for interiors and that these materials induce the perception of fresh and comfortable interiors. Fuchs et al. [103] studied the development and the use of composite alternatives to replace parts in the

automotive industry. It was observed that the different carbon-fiber option can replace the steel option for different production levels.

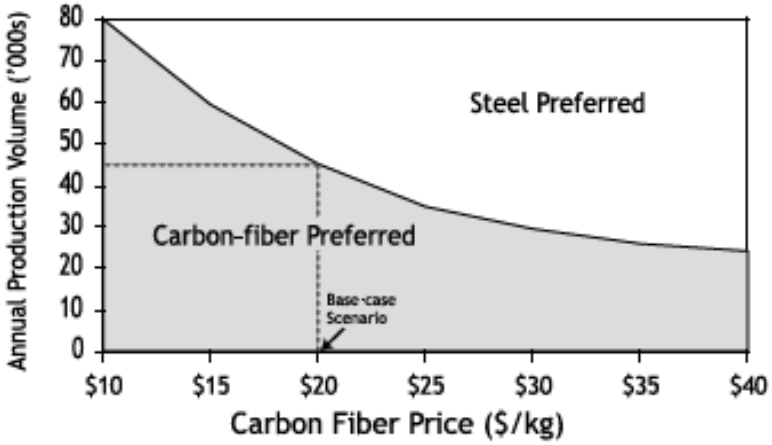

Figure 7.2 – Sensitivity of steel–carbon cost parity to fiber price [103]**.**

It was concluded that the introduction of steel with composite options can be performed; however, this study did not take into account other lightweight options, such as aluminium and magnesium materials. All the works usually take into account the materials used.However, most of them do not take into account changes in production nor the requirements needed to reach the production goals. In this chapter, different concerns regarding manufacturing will be presented. Additionally, business strategy and technological performance will be introduced in a decision model that can assess the different variables and allow us to select the best model to produce the part.

7.1 Design of seats

The main goal of this stage is the development of different seat alternatives with the goal of reducing weight while keeping up with the industry standards overall. Simple models of the seats were developed including the seatback, the seat cushion structure, the elements for connection between these two parts, and the car itself. The connection to the seatback can also be used as the recliner.

A model of existing steel was built in order to be able to accurately compare the changes in weight between the different models. This model was based on the seats presented in section 3.3. However, some changes in the design were made to be able to better sustain the loads of the simulation stage. Two different designs were made as it can be observed in Figure 7.3.

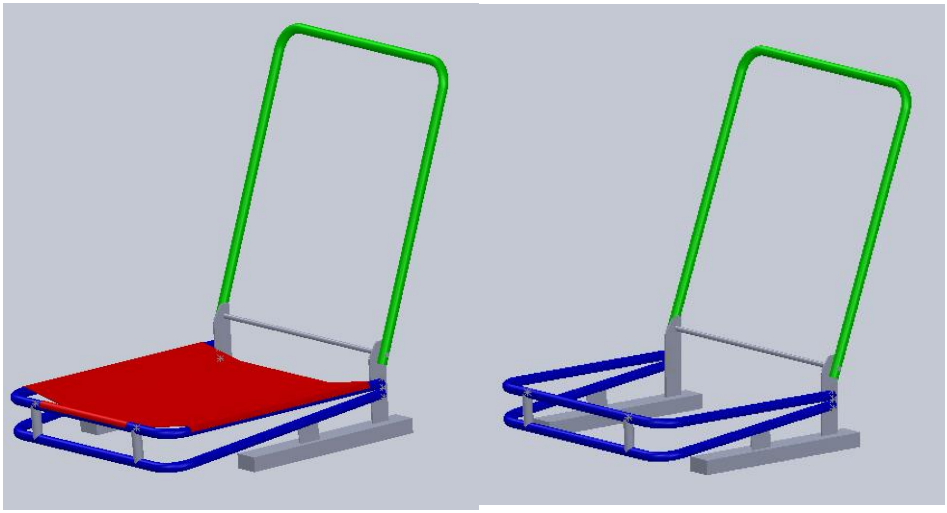

Figure 7.3 – Model of the steel seats.

There is one restriction imposed by the FSW in the manufacturing and design of the seats. This imposes that the used developed seats will have greater restrictions in using hollow structures where good restriction of the different developed parts is needed. This mainly affects tubular tubes where the tools used have great restrictions with these parts.

Therefore, the developed seats are made in sheet metal and sheet metal structures. Different concepts were developed and their behavior was afterwards tested in Abaqus to confirm whether or not the material could support the strengths felt during the process and if the seat was able to comply with the restraints from regulatory authorities. The modeled seats are presented in Figure 7.4.

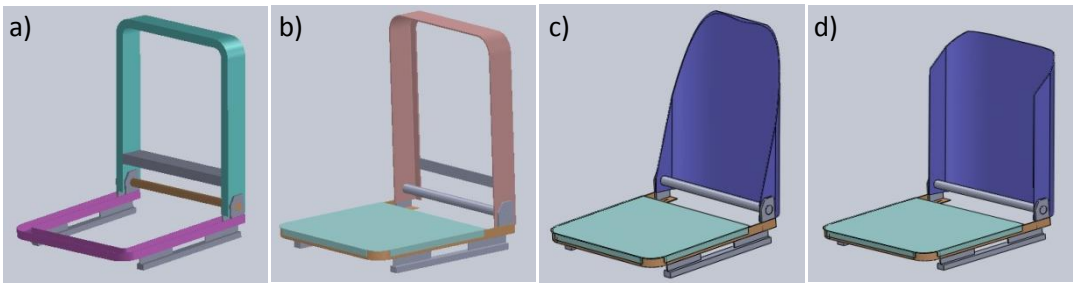

Figure 7.4 – Modeling of the different seat options.

The seat on the left, in the Figure 7.4, was simulated using aluminium alloys while the two seats on the right will be studied recurring to magnesium. The remaining seat will be studied in both aluminium and magnesium solutions. It is also known from the previous tests that magnesium alloys would not be very suitable to use in the first solution because of the obstacles in production. The use of bending processes is limited in the magnesium alloys and the use of casting processes restricts the ability to produce hollow structures in magnesium alloys. The next step is the simulation of the car seat models to comply with the industry regulations and standards.

7.2 Seat Simulation

The seat simulation stage will take into account the tests made to seat integrity presented in section 3.2. The use of tetraedric elements were preferred taking into account the differences between length and thicknesses and the simulation capacity of the used computer:

- the application of a moment of 374N.m in the seat;
- applying a force of 20 times the seat weight on the gravity center of the seat back
- the seatbelt test – a force of 22214N in the top right of seat back, while applying the force of 20times the seat weight on the gravity center of the seatback.

Table 7.1 – Simulation results for the base tubular steel seat.

Trial	M =374N.m	F=20 x seat weight	Seatbelt test
Stresses	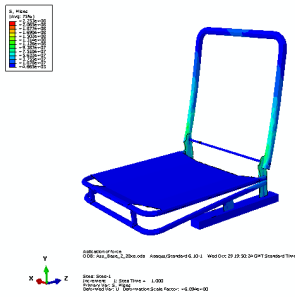	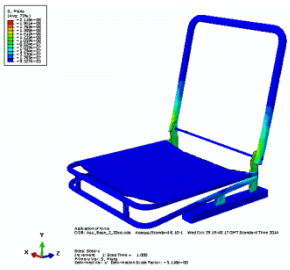	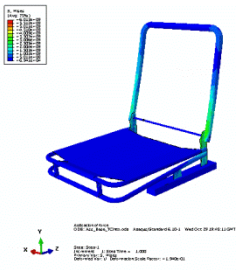
Displacements	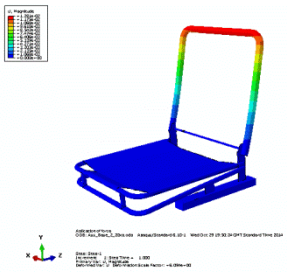	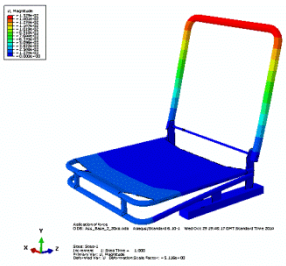	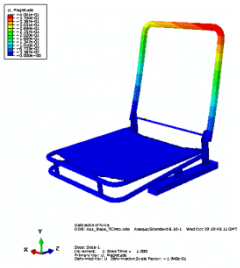
Results	σ = 225.3MPa d = 12.81mm	σ = 211.8MPa d = 15.29mm	σ = 6013MPa d = 404.1mm

In the first two tests, the goal is to observe whether or not the loads pass the tensile strength of the material. The third test is made to observe if the dislocation of the seat does not surpass the 178mm. This last test is usually performed in seats that have components in which the seatbelt is attached to. However, this test has been considered to guarantee the integrity of the developed seats in case of car crashes which have an increased force in the seat back. This restriction of 178mm was not applied to the steel seat since the model was based on an existing seat. This test is also considered a destructive one since the seat gets unusable afterwards. Table 7.1 presents the results simulated in the steel seat. It was observed that the seat weight ranged from 13 to 17 kg, depending on whether it had the seat cushion plate or not. In this simulation, the seat passes both the applied moment and force tests. However, as

expected, it is not able to comply with the seatbelt test. These results are aligned with the seat development since this seat does not need to comply with this last test.

The first evaluation made to the aluminium seat has the U profile which could provide a better behavior for the development of the seat. From the initial model, several trial and error steps were taken in this seat in order to be able to optimize the seat performance, while not losing too much weight. The use of an open allows building support structures that can at a later stage be used to weld the seat recurring to the FSW process. The final results from these simulation tests are presented in the Table 7.2.

Table 7.2 – Simulation results to the U-shape structure aluminium seat.

Trial	M =374N.m	F=20 x seat weight	Seatbelt test
Stresses	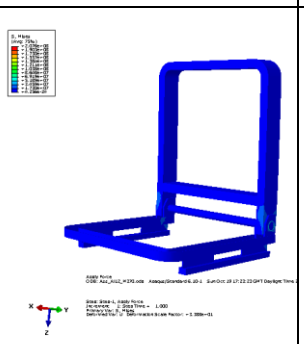	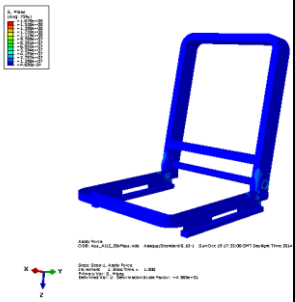	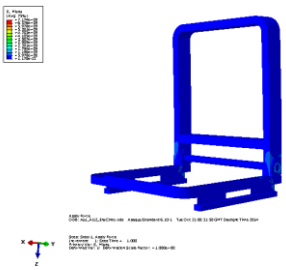
Displacements	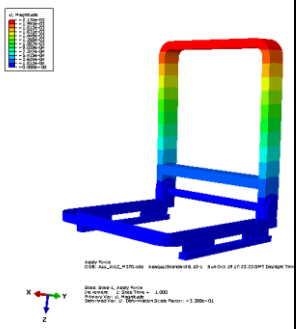	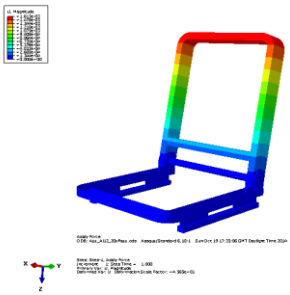	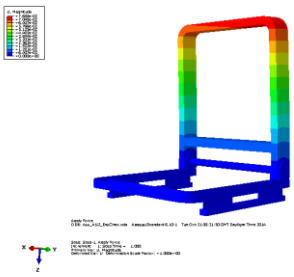
Results	σ = 207.6MPa d = 2.17mm	σ = 167.8MPa d = 1.61mm	σ = 7174MPa d = 76.88mm

This seat has a very good performance to the bending behavior and was confirmed to have a weight saving of 52% over the 13kg with a total weight of 6.3kg. It can be observed that even though it has small stresses applied to it only the aluminium alloy AA6082 can be applied for this use. From literature, only the aluminium alloy AA5754-H26 can be used for this goal, since having high enough yield strengths to reach this goal. The use of FSW in this case would promote a decrease in hardness, also decreasing the strength of the joined materials to the state of the studied alloy. This situation must be handled with care and a study should be performed on that alloy to confirm this situation.

Table 7.3 – Simulation of the seat in both magnesium and aluminium alloys.

Trial	M =374N.m	F=20 x seat weight	Seatbelt test
Stresses (Al)	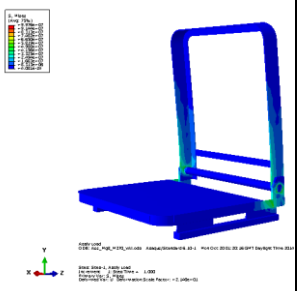	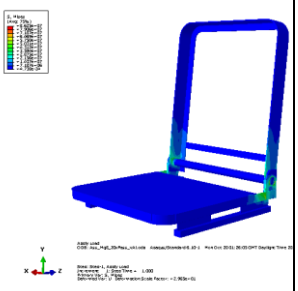	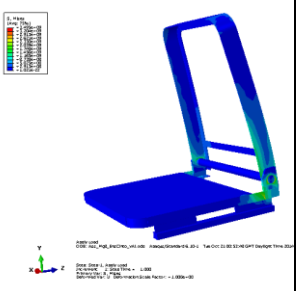
Stresses (Mg)	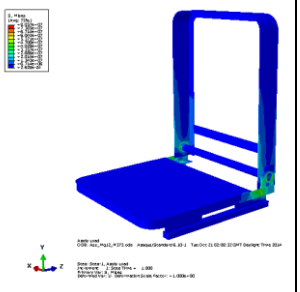	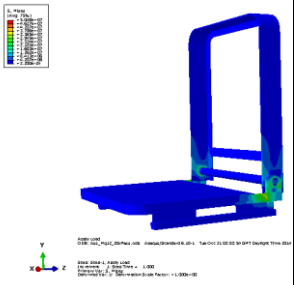	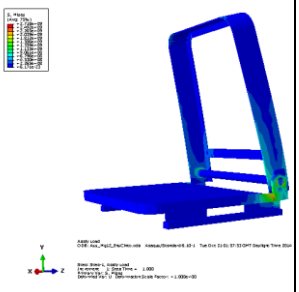
Displacements (Al)	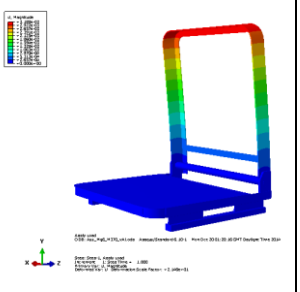	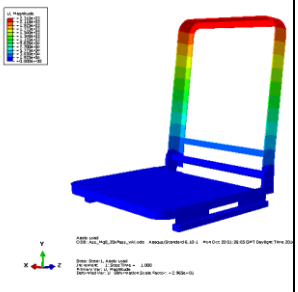	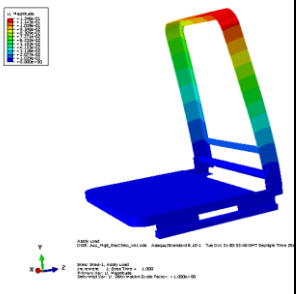
Displacements (Mg)	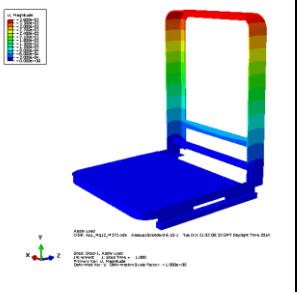	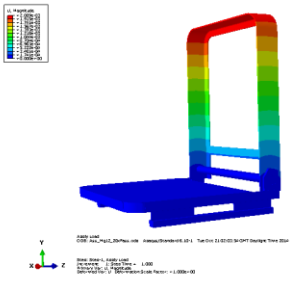	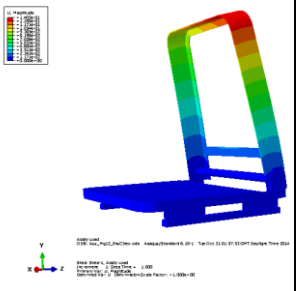
Results	σ_{Al} = 99.76MPa σ_{Mg} = 80.57MPa d_{Al} = 3.19mm d_{Mg} = 3.60mm	σ_{Al} = 86.25MPa σ_{Mg} = 50.48MPa d_{Al} = 2.31mm d_{Mg} = 2.09mm	σ_{Al} = 3495MPa σ_{Mg} = 2718MPa d_{Al} = 124.6mm d_{Mg} = 140.5mm

The second tested seat had its behavior simulated for both magnesium and aluminium alloys. This seat uses L shaped structures that are very adequate for weight reduction. However its response to loads will result in an increased displacement of the samples. It was observed that the seatback needed to have a thicker plate than the for the aluminium alloys. It was confirmed that the seats developed had savings of 48.5% and 63% for the aluminium and

magnesium alloy, respectively. This adds up to weights of 6.7kg for the aluminium case and 4.8kg for the magnesium alloy. These seats comply with the loads for all tested materials and can use a variety of alloys able to satisfy the needs to which they are subjected during these tests. When compared to the previous alloy, a decrease in the bending behavior of these models is confirmed.

The remaining seats are both made in magnesium alloys, however it has been confirmed through simulation that the seat from Figure 7.4.c does not comply with the regulation standards and, therefore, has been discontinued in this stage. The next simulated seat is supposed to be made only in magnesium and it uses a completely closed seat back. The goal of this seat is to improve the bending behavior of the seats while trying to reduce the weight.

Table 7.4 – Simulation of the magnesium seat with closed back.

Trial	M =374N.m	F=20 x seat weight	Seatbelt test
Stresses	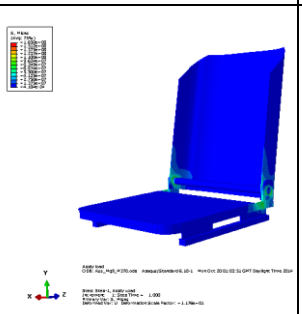	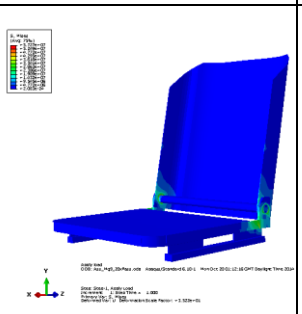	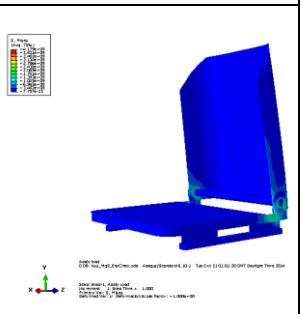
Displacements	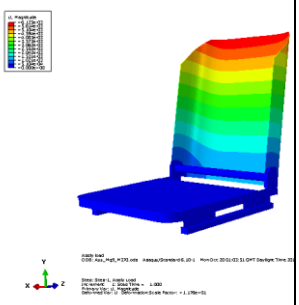	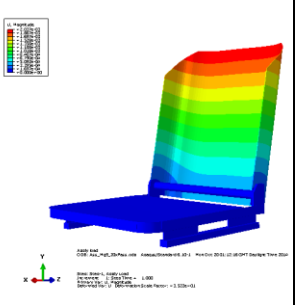	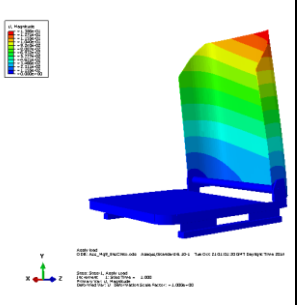
Results	σ = 165.0MPa d = 6.13mm	σ = 57.27MPa d = 2.04mm	σ = 4179MPa d = 138.6mm

It was observed that the highest load is located in the connection area in the seatback. The studied alloy was conducted in the O-state showing the lowest tensile strength possible. These alloys can have up to 200MPa, depending on the process used. It was possible to confirm that, since the welding process does not influence the seatback, this alloy can be used in the seat, providing better properties to support the strengths that it will be submitted to. It was calculated that this seat will weigh 5kg. The cost model will only focus on the lighter seats models.

7.3 Cost Modeling

The cost model development of for the different seat options took under consideration which processes and flow between processes would be needed in order to manufacture these seats. For the steel seat it was possible to identify that five main processes are required:

- Bending and cutting operations;
- Stamping and blanking operations;
- Welding;
- Painting;
- and, assembly.

For the aluminium seat, the same operations have been considered; however, the painting stage was excluded from this evaluation. For the magnesium alloys, no bending or forming operations were considered being replaced by a die casting stage. After analyzing the different variables, it was possible to conclude that the steel seat is the cheapest one with a cost of 10.75 euros for a production of 100.000 seats. For the aluminium alloy the cost is 21.81 euros while the magnesium alloy costs 27.74euros.

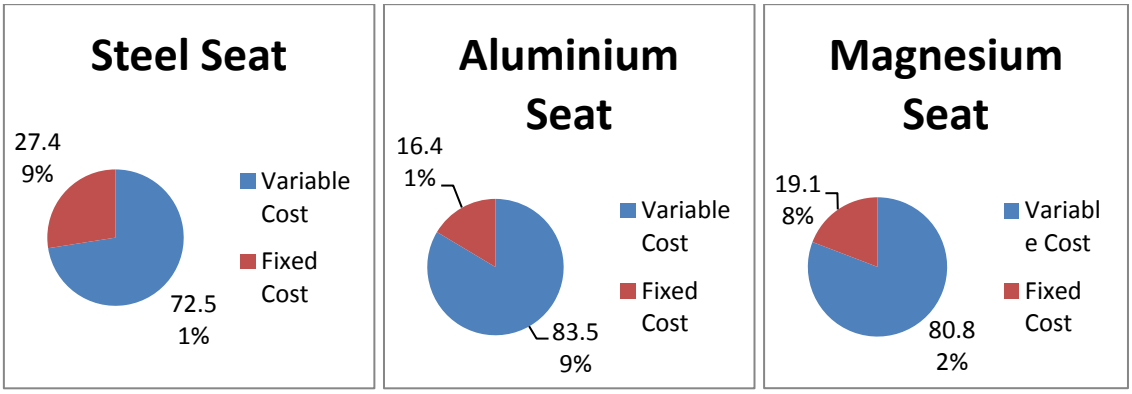

Figure 7.5 – Fixed and variable costs related to the manufacturing of the different seats.

The variable costs account for the costs with material, energy and labor cost, while the fixed costs account for the tooling, building and maintenance. It can be observed that the material cost is a substantial element of these processes and accounts for a large part of the material cost. Since the variable costs are dependent of the machining, the breakdown of the fixed costs will be observed to understand which improvements can be made.

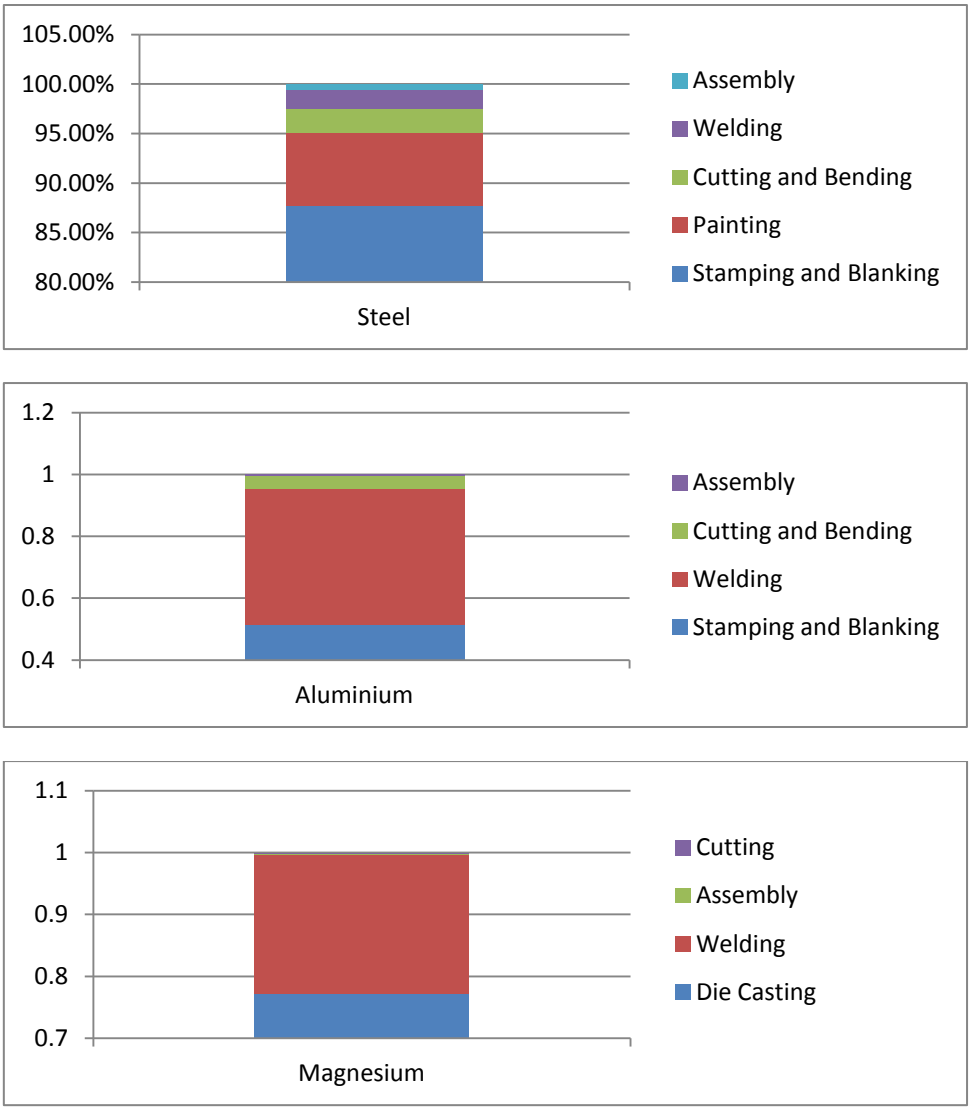

Figure 7.6 – Cost breakdown of the fixed costs for the different seat.

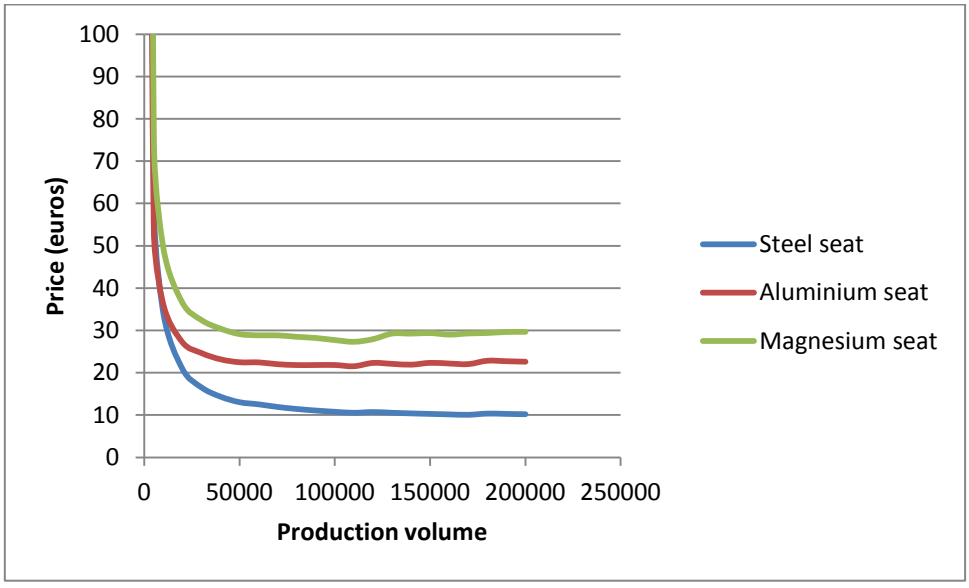

Figure 7.7 – Price over production volume.

The cost breakdown shows that the FSW welding process greatly increases the cost being responsible a considerable part of it. In fact, his process accounts for over 20% of the fixed costs in each seat. The price over production volume clearly shows that these seats have reached their lower limit for the considered 100000 parts and that this price will not have variations with the considered process characteristics.

It was also possible to understand that the influence of the FSW process is high for both the aluminium and magnesium options. This process may reach speeds of 2m/min; therefore a study should be performed to understand the influence of the advancing speed in the fixed and overall costs of the seats. The main variable of this process is the welding speed; this model was specifically assuming a welding speed of 400mm/min. The results for changing the welding speed are presented in the Figure 7.8.

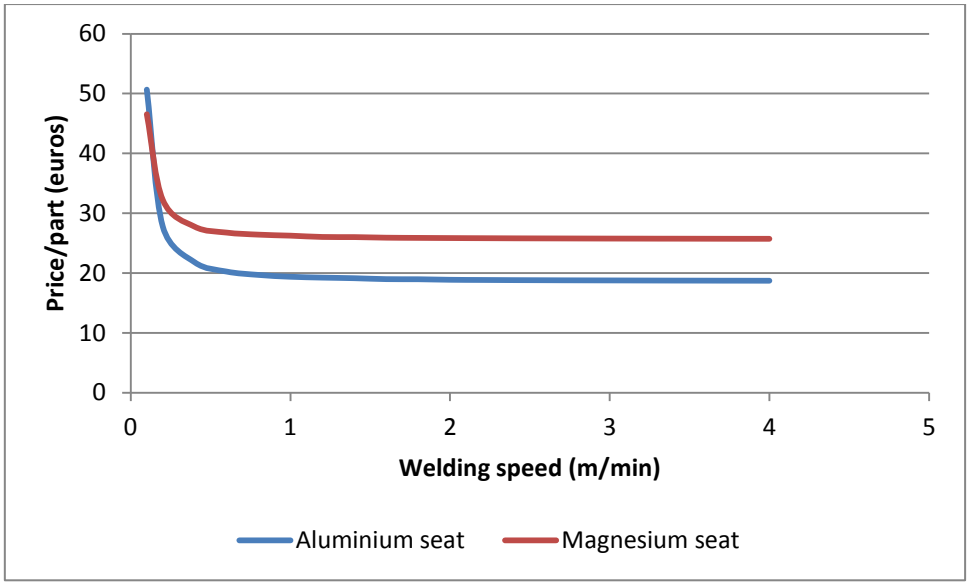

Figure 7.8 – Variation of the price per part with the welding speed.

This shows that the price per part does not change that much after the 2m/min. Hence, in order to make this process cost effective in industry, it mandatory to guarantee that this process can at least effectively weld at 2m/min without producing defects in the parts.

7.4 Choosing the replacement seat

In order to choose the seats, different aspects of the automotive industry business must be taken into account. Companies take into account the factor of the increase in cost over the decrease in weight when trying to adopt a new lightweight solution, it has been confirmed that the smaller this factor the higher chances for adoption. This study established this value as 2.03 and 1.65 for the magnesium and aluminium alloy, respectively. This implies that the aluminium has better perspectives to be adopted than the aluminium alloy. Another trend

establishes that for each 10% of weight saved there is an increase of 7% in fuel economy. This results that for each kg reduced a reduction of 20kg in carbon dioxide is attained. These statistics allow us to conclude that the aluminium seat is preferred for the aluminium alloys. Nonetheless, the higher weight saving of the magnesium seat will lead to better carbon savings.

7.4.1 Production issues

The introduction of new processes will introduce some disturbances in the production probably disrupting some of the existing processes. Therefore, the ability to choose a product that can make use of the existing capabilities and be introduced with the minimal disruption of the process is required and needs to be taken into account. The introduction of the aluminium seat would only be disruptive in the joining section because the FSW process is new and some training must be provided to the workers. As far as magnesium alloys are concerned, the addition of die casting processes implies addressing some issues on the shop floor since not only are the processes new, as the die casting process needs other mechanisms to support these processes. Therefore, it would be more advantageous to introduce aluminium alloys at an early stage.

7.4.2 Material price evolution

For the purpose of this study, it has been estimated that the aluminium costs range 1.5 euros per kg, while the magnesium at 3 euros per kg. Figure 7.9 shows the evolution of the raw material prices over the last 9 years.

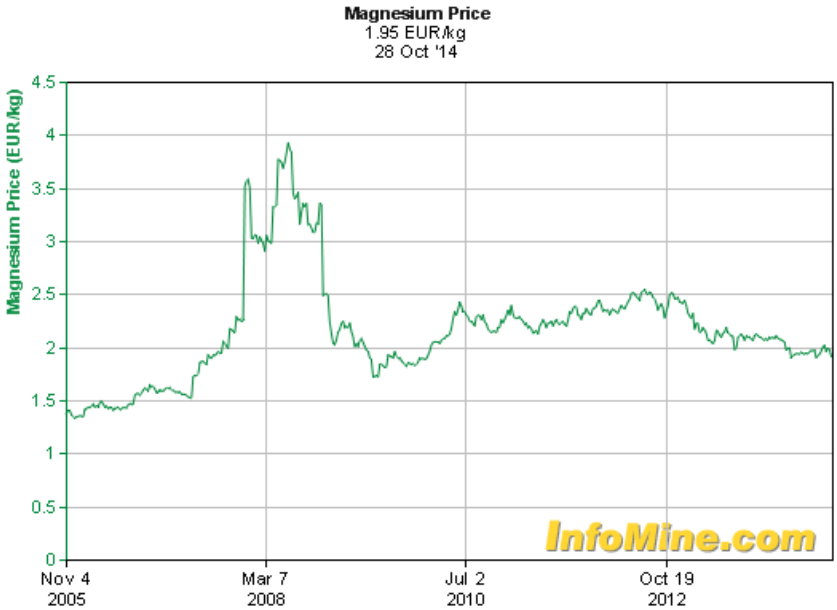

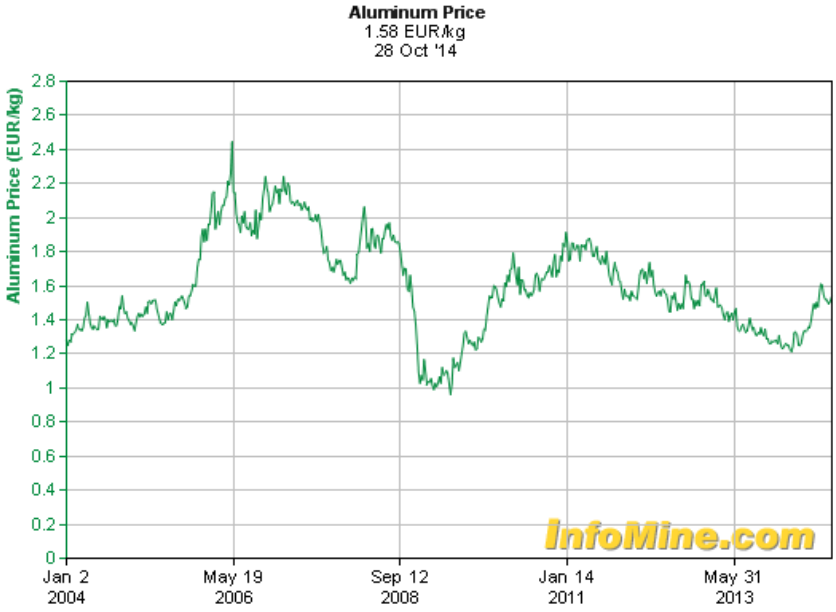

Figure 7.9 – Evolution of the magnesium and aluminium price over the last years [200]**.**

From the analysis, it can be observed that the aluminium is less subjected to changes in the market and has had stable prices over the last few years. Apart from this it is also visible that the cost model also shows that the magnesium alloy, due to its lower density, is less susceptible to price variation. However, the magnesium alloy is known for having very high price variations which in turn can lead to higher costs. Once again this is an advantage for the use of aluminium alloy.

7.4.3 Suppliers location

In Portugal, there are several suppliers of aluminium alloy that can effectively guarantee the satisfaction of a company needs. Regarding magnesium, apart from production around Europe, the suppliers are mostly located in the United States and China which makes that the delivery time's increase. Moreover, distribution from China has been deemed very dangerous due to long due times which decreases the flexibility of a company in case of an increase in demand. Therefore, the use of aluminium alloys is preferred for such cases.

Overall, and despite the several advantages in the weight reduction and consequent decrease in CO_2 emissions brought by magnesium, it is in fact the aluminium alloy that gains advantage. This is due to its better properties and ability to be aligned with automotive company' objectives and therefore, in an early stage, it is recommended to implement an aluminium seat

7.5 Decision model

A model that integrates different decision factors that can influence the final decision making was developed for judging which product should be followed through. The previous chapter

has presented some of the considerations that should be accounted for this goal. The Saaty Analytical hierarchical process (AHP) allows the comparison of different performance meters. The AHP also allows for the integration of objective and subjective measurements of the different performance meters allowing the integration of a wider number of decision meters. It has been observed that the use of regime analysis can help improve the AHP model with the introduction of criteria weights and pairwise comparisons. The Regime analysis can be used to have different levels of decision only taking into account the criteria important for each level. In this way, the impact of a criterion for a particular business area can be clearly defined and it is possible to allocate the criteria in the business areas where they will have an impact. To develop this model for the decision making, three main decision factors have been considered:

- Seat performance
- Business Strategy and,
- Externalities

The seat performance is divided in two sub-criteria: the seat weight and price. These have been calculated beforehand. The business strategy takes into account easiness of implementation of the seat solution in the company, the possibility of scaling-up the production and the strategic location of possible suppliers.

Externalities take into account performance meters that can influence the business but cannot be controlled by the company. The considered meters are raw material price and evolution, evolution of technology and competitors.

7.5.1 Saaty Analytical Hierarchical Process and Regime Analysis

Saaty AHP is a method to make a pairwise comparison between the criteria that have been established and align their importance towards the final goal. When applied to the criteria, the result shows the importance of these criteria for the final goal. In this case, the set of criteria will be selected to produce the best seat that can comply with the business strategy over time. The values considered for the Saaty scale are given according to Table 7.5.

Table 7.5 – Saat semantic scale.

Value	Definition
1	Equal importance
3	Moderate importance
5	Strong Importance
7	Very Strong Importance
9	Extreme Importance
2, 4, 6, 8	Intermediate Values

The regime analysis is a discrete multi-assessment method suitable to evaluate the different alternatives. This framework has two inputs:

- an impact matrix and
- a set of weights

The set of weights in the impact matrix present the importance of the criterion to reach a predefined goal.

Considering these two methods and having in mind our goal, different layers of decision that can impact the final plan depending on its course have been considered. As stated before, our goal is to decide which seat can be implemented with lower weight without causing too much disturbance to the natural flow of the business. Three criteria have been defined for this goal: the performance, business strategy and externalities. However each of these criteria has a different impact inside the plan. It has been assumed that for the final goal both the business strategy and performance have the same weight but the externalities will have a lower impact.

Each criterion has sub criteria whose weights have been defined according to industry standards. For the performance, the weight and cost have been considered. It has been observed that there is a relationship considering the increase in price over the decrease in weight and usually if it is under 5 there is a high chance of it being implemented. So, for this effect, it has been assumed that the seat weight is 5 times more important than the seat price.

Table 7.6 – Impact matrix for the different seats.

Criteria	Sub-criteria	Steel Seat	Al Seat	Mg Seat
Performance	Weight	3	6	8
	Cost	8	4	3
Business Strategy	Implementation	5	4	2
	Scale-up	8	5	3
	Suppliers	8	7	2
Externalities	Price Variation	8	8	6
	Technology	4	5	5
	Competitors	4	5	5

In the business strategy, the scale-up and positioning of the suppliers will be the most important criteria while the implementation of new technology and the need to work with the equipment is considered less important. The externalities consider the robustness of the strategy adopted for this where the variability of the price is considered to be the most important factor since it can have a significant impact on the income of the company while the competitors' ability to present a new product and possible technology improvements will be of the same importance. So an impact matrix (Table 7.6) was prepared taking into account these goals and the ability for each seat to reach this goal.

Pairwise comparisons have been made taking into account the results from the impact matrix and Expert Choice® has been used to make the assessment between the different criteria, which provides a ranking for each plan (Figure 7.11).

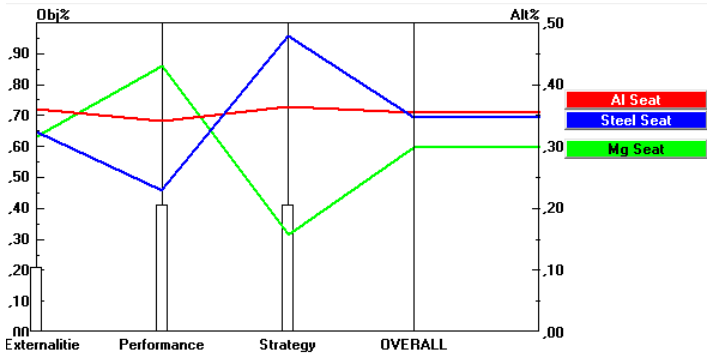

Figure 7.10 – Performance for the different seat and influence of the different criteria.

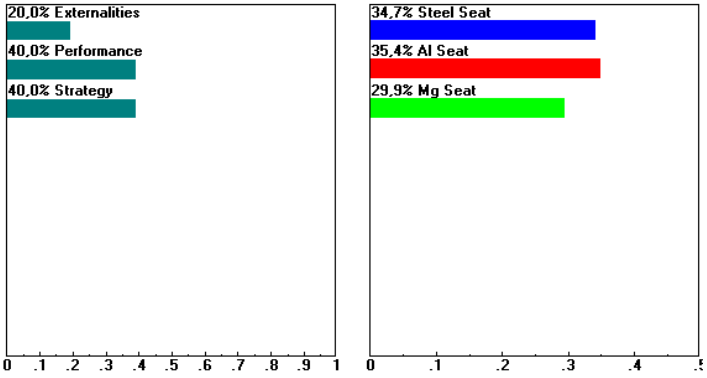

Figure 7.11 - Ranking of the different seats.

It has been confirmed that, with the given conditions, the adoption of the aluminium seat is very attractive, followed by the steel seat and magnesium seat, respectively. The performance of the seats for the different criteria (Figure 7.10) shows that even though the aluminium seat does not stand out in any of the criteria, it is very stable across the different criteria, making it the better option in the end.

The program used allows the possibility of changing the weight of the different criteria, which can give us an idea of the adoption of the aluminium seat for different scenarios.

7.5.2 Different scenarios

Different scenarios were tested to see how reliable the choice of adopting the aluminium seat for these scenarios is. So four scenarios were tested:

- the criteria have the same weight;
- the externalities are more important;
- the performance is more important;

- the business strategy is more important.

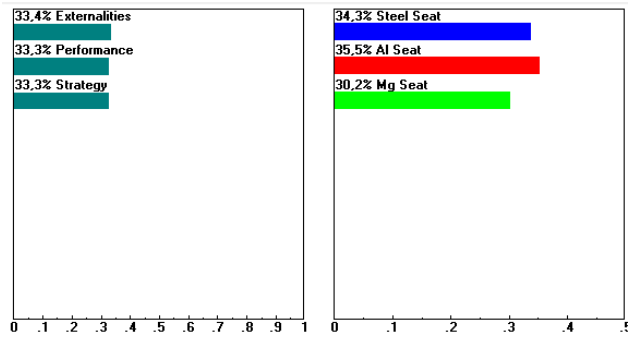

Figure 7.12 – Ranking for equal importance between the criteria scenario.

For the scenario of equal importance between the criteria, the aluminium seat is still the best option since it can answer better to this plan has can be observed. This is related to the increase of the importance of the externalities where the aluminium is more relevant.

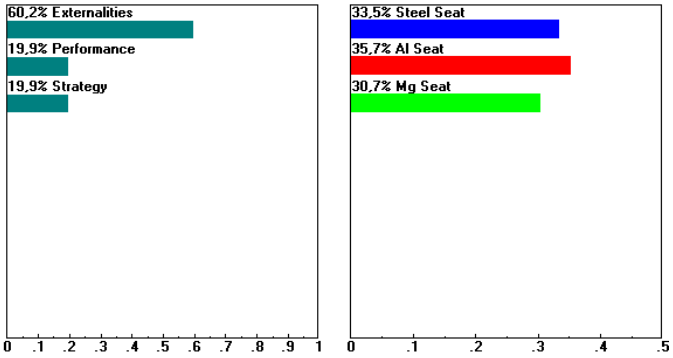

Figure 7.13 – Ranking for the externalities are more important scenario.

The scenario where the externalities are more important (Figure 7.13) is compliant with the scenario presented before and it is possible to observe that the aluminium seat still stands out in this case. In the scenario where performance is more important, it can be observed that the magnesium seat starts to be a better option although only near 60% of weight in this matrix the magnesium seat becomes a better option.

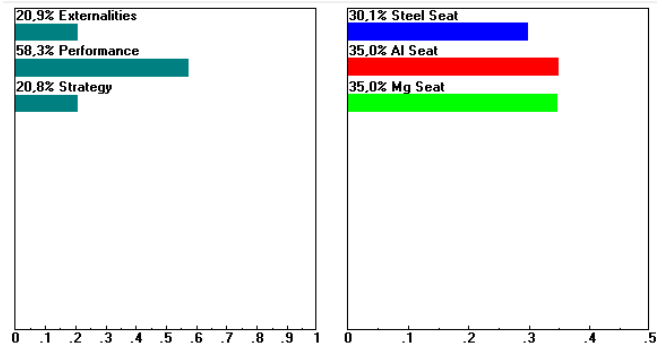

Figure 7.14 – Ranking for the performance is more important scenario.

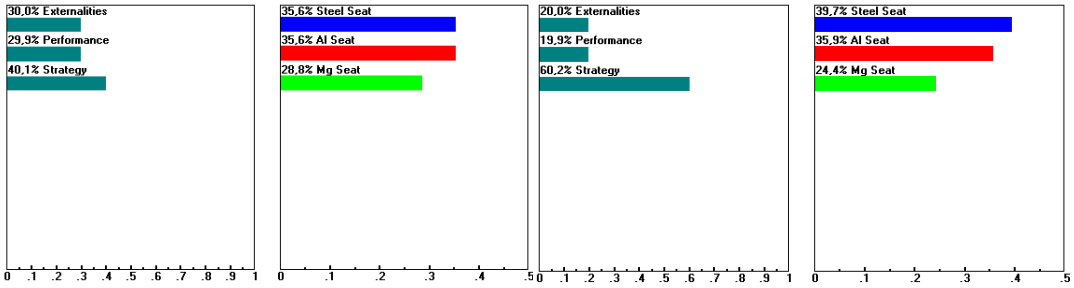

Figure 7.15 – The business strategy is more important scenarios.

The scenario where the business strategy (Figure 7.15) is more important is where the steel seat stands out. This means that in this scenario the company is more conservative in the introduction of new materials in the company needing several assurances to adopt new products. This is possibly one of the major concerns for the adoption of the aluminium seat since most companies for this segment might be risk averse and would prefer to maintain the same product. Figure 7.16 shows the results from the decision showing with the highlighted are of where most decision might fall. It shows that the aluminium seat is the most attractive seat followed by the steel solution

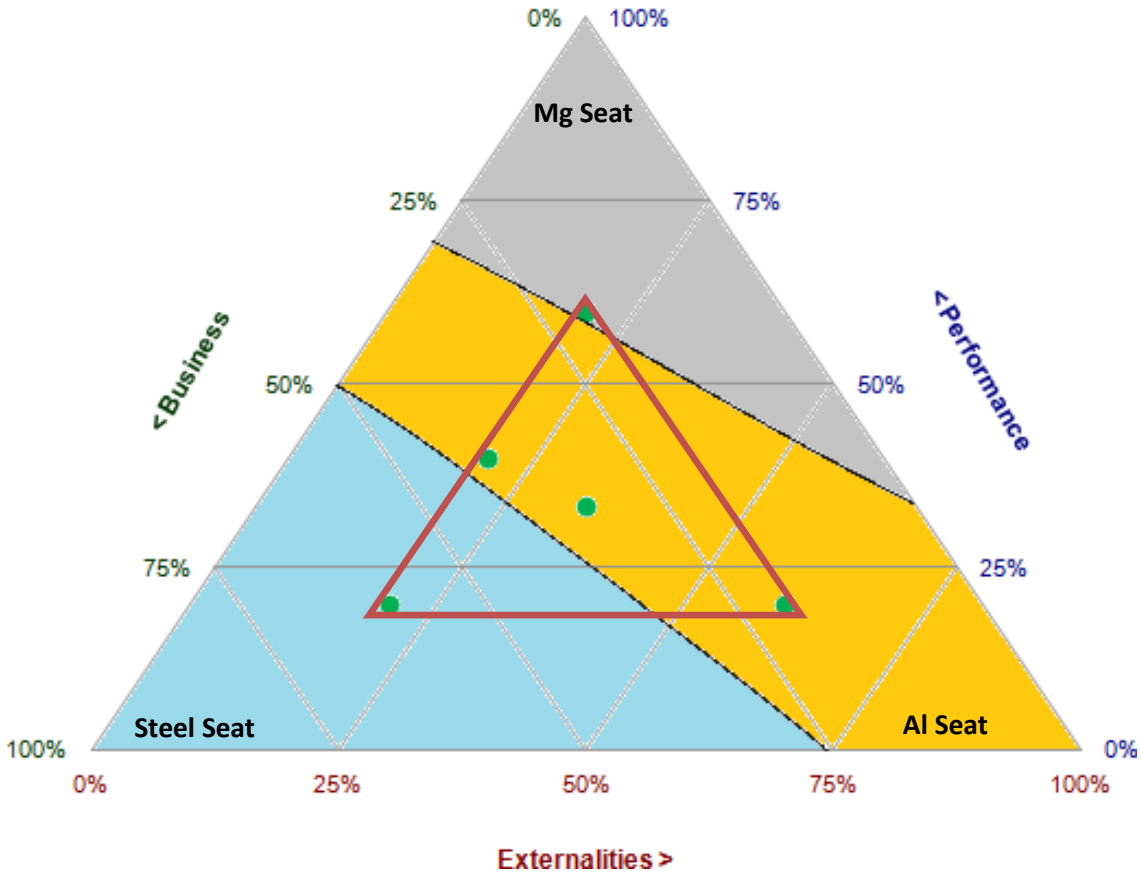

Figure 7.16 – Summary of the results from decision model

Overall, it seems that the adoption of the aluminium seat is regarded as advantageous for most scenarios. The improvement of the welding speed of the FSW process to 2m/min seems

to be one of the steps that are needed to guarantee the introduction of this product in a company.

8 Conclusions and future work

8.1 Conclusions

The development of this research has allowed us to reach different conclusions regarding the product development in automotive industry. As it was observed, there are consistent trends pointing to a global shift in the automotive industry paradigm. This shift will dictate current suppliers to also change their strategy to promote their competitive advantages. However, this is not an easy task to attain, mostly when considering Tier 1 and Tier 2 companies that are usually focused on production. Nonetheless, this paradigm shift represents an opportunity for these companies to distinguish themselves from their competitors.

This research has focused on the reduction of fuel consumption and CO_2 emissions and the research has been oriented to the vehicle´s weight reduction, more specifically the car seat. It has been observed that there are a wide range of paths for weight reduction due to a wide variety of material options. In order to select a proper approach, an analysis of the company´s process and production is .The decision regarding the chosen material will depend not only on production levels but also on the company´s availability to introduce new equipment. Certainly, these approaches require a step-by-step methodology.

One of the conclusions to be withdrawn from light metal alloys introduction is that aluminium is a promising material to be introduced because most of the forming mechanisms are already used by the steels. The focus should be on the improvement of the joining processes.

Computational tools have been able to simulate the tested alloys according to automotive standards and the results proved to be aligned with the mechanical testing results. The CAD modeling and simulations tools such as Abaqus can be introduced in the product development stage to evaluate the performance of the seats, therefore decreasing the number of attempts needed in the development of the prototype.

Due to the focus in high productivity and lower available resources of the automotive industries, some of these seat development tasks for productive process evaluations can be very demanding. Hence, partnerships with universities or research centers can help hastening the product development process in a new paradigm for the automotive industry.

This research has also focused on the process evaluation of new materials. In this case, it has been observed that the FSW or other solid state joining techniques are very good candidates to replace the existing welding processes. These produced joints have been mechanically evaluated together with the corrosion properties of the different welded samples. It was

concluded that the FSW process can be effectively introduced in aluminium and magnesium alloys. However joints between aluminium and magnesium present very poor properties and for such reason its introduction in industrial environment should not be attempted. Other materials combinations can be introduced; however, some cautions must be assessed regarding the mechanical testing. The corrosion rates are higher than what is expected to occur in normal work conditions, because the samples are in a saline environment.

The new solid state spot welding process has shown very good results for both the aluminum alloys and steels. In fact, this process has a very good performance for the aluminium welds although the best properties for alloy are obtained at low rotational speeds and intermediate plunge speed. The joint in the steel welded samples have shown the high efficiency of this process in the steels albeit some concerns must be addressed regarding the implementation of this process in steels due to the high efficiency rate verified in the RSW process.

The results from the decision tool step and cost model show that the aluminium seat is the best choice for adoption with a reduction of weight around 50% although it cost the double. The different scenarios took into account relationships that are established in the automotive industry and the adoption of the aluminium seat seems to be a good option for this goal.

8.2 Future Work

Future work should focus on:

- The development of the same research in the comfort area providing more information that might increase the acceptance of the seat.
- The development of a new tool concept for the solid state spot joining technique developed that can improve both its flexibility and production rate.
- Understanding the influence of the tool shoulder effect in the welds strength and its effect of the torque of the welding machine.
- Establishing parameters to validate the acceptance of a seat using different relationships and determining a common ground so a relationship can be made between them. In this proposal the implementation of a decision that takes into account mechanical properties of the seat is suggested, taking into account subjective properties from the human-seat interaction not disregarding economic factors, such as costs, besides trying to develop a model that accounts for the different weights that each set of parameters have.

References

[1] Stanford Graduate School of Business, “Johnson Controls, Inc. - Automotive System Group The Georgetown, Kentucky Plants.” 1997.

[2] T. Klier and J. Rubenstein, “Configuration of the North American and European auto industries – a comparison of trends,” *Source: ERIEP*, no. 3, 2011.

[3] F. Bidault, A. Castello, and ESTM, “Sitting pretty: Managing Customer-Driven Innovation ar Faurecia Car Seating.” 2007.

[4] S. Corwin, B. Collie, M. Beck, and C. Lantz, “2013 Automotive Industry Perspective,” *Source: booz.com*, 2012. .

[5] L. F. Jeffus, “Chapter Other welding processes,” in in *Welding: Principles and Applications*, 5th Editio., Delmar Learning, 2004, pp. 694–701.

[6] W. S. Miller, L. Zhuang, J. Bottema, A. J. Wittebrood, P. De Smet, A. Haszler, and A. Vieregge, “Recent development in aluminium alloys for the automotive industry,” *Mater. Sci. Eng. A*, vol. 280, no. 1, pp. 37–49, Mar. 2000.

[7] M. K. Kulekci, “Magnesium and its alloys applications in automotive industry,” *Int. J. Adv. Manuf. Technol.*, vol. 39, no. 9–10, pp. 851–865, Nov. 2007.

[8] Z. Yu, Z. Lin, and Y. Zhao, “Evaluation of fracture limit in automotive aluminium alloy sheet forming,” *Mater. Des.*, vol. 28, no. 1, pp. 203–207, Jan. 2007.

[9] R. Smerd, S. Winkler, C. Salisbury, M. Worswick, D. Lloyd, and M. Finn, “High strain rate tensile testing of automotive aluminum alloy sheet,” *Int. J. Impact Eng.*, vol. 32, no. 1–4, pp. 541–560, Dec. 2005.

[10] M. Kleiner, M. Geiger, and a. Klaus, “Manufacturing of Lightweight Components by Metal Forming,” *CIRP Ann. - Manuf. Technol.*, vol. 52, no. 2, pp. 521–542, Jan. 2003.

[11] A. J. U, M. Beyer, D. Ag, A. Development, C. Ep, G. Hpc, and D. Sindelfingen, “New cars - new materials,” *Mater. Des.*, vol. 18, pp. 203–209, 1998.

[12] L. Gaines, R. Cuenca, F. Stodolsky, and S. Wu, “Potential Automotive Uses of Wrought Magnesium Alloys,” in *Automotive Technology Development*, 1996, no. 1.

[13] F. Bergeron and J.-F. Audet, “Feasibility Study for the Development and Marketing of Magnesium Seats for Motor Coaches and other modes of Public Transit,” 2004.

[14] H. A. Patel, D. L. Chen, S. D. Bhole, and K. Sadayappan, “Microstructure and tensile properties of thixomolded magnesium alloys,” *J. Alloys Compd.*, vol. 496, no. 1–2, pp. 140–148, Apr. 2010.

[15] E. Aghion, B. Bron, and D. Eliezer, “The role of the magnesium industry in protecting the environment,” vol. 117, pp. 381–385, 2001.

[16] T. M. Kotresh, R. Indushekar, M. S. Subbulakshmi, S. N. Vijayalakshmi, a. S. Krishna Prasad, V. C. Padaki, and A. K. Agrawal, “Heat release and burning behaviour of foam and foam/Basofil fabric combination,” *Polym. Test.*, vol. 28, no. 5, pp. 511–520, Aug. 2009.

[17] R. Deng, P. Davies, and a. K. Bajaj, “Flexible polyurethane foam modelling and identification of viscoelastic parameters for automotive seating applications,” *J. Sound Vib.*, vol. 262, no. 3, pp. 391–417, May 2003.

[18] K. L. Edwards, “Strategic substitution of new materials for old: Applications in automotive product development,” *Mater. Des.*, vol. 25, no. 6, pp. 529–533, Sep. 2004.

[19] M. Kolich, S. D. Essenmacher, and J. T. McEvoy, “Automotive seating: the effect of foam physical properties on occupied vertical vibration transmissibility,” *J. Sound Vib.*, vol. 281, no. 1–2, pp. 409–416, Mar. 2005.

[20] W. Copes, H. Champion, W. Sacco, M. Lawnick, D. Gann, T. Gennarelli, E. MacKenzie, and S. Schwaitzberg, “Progress in characterizing anatomic injury,” *J. Trauma*, vol. 30, no. 10, pp. 1200–1207, 1990.

[21] Autoridade Nacional Segurança Rodoviária, “Relatório anual 2009: Sinistralidade Rodoviária,” Source: ansr.pt, 2009.

[22] A. Kullgren, M. Krafft, A. Nygren, and C. Tingvall, “Neck injuries in frontal impacts: influence of crash pulse characteristics on injury risk.,” *Accid. Anal. Prev.*, vol. 32, no. 2, pp. 197–205, Mar. 2000.

[23] M. Y. Svensson, O. Boström, J. Davidsson, H. a Hansson, Y. Håland, P. Lövsund, a Suneson, and a Säljö, “Neck injuries in car collisions--a review covering a possible injury mechanism and the development of a new rear-impact dummy.,” *Accid. Anal. Prev.*, vol. 32, no. 2, pp. 167–75, Mar. 2000.

[24] O. Boström, R. Fredriksson, Y. Håland, L. Jakobsson, M. Krafft, P. Lövsund, M. H. Muser, and M. Y. Svensson, “Comparison of car seats in low speed rear-end impacts using the BioRID dummy and the new neck injury criterion (NIC).,” *Accid. Anal. Prev.*, vol. 32, no. 2, pp. 321–8, Mar. 2000.

[25] A. S. McIntosh, D. Kallieris, and B. Frechede, “Neck injury tolerance under inertial loads in side impacts.,” *Accid. Anal. Prev.*, vol. 39, no. 2, pp. 326–33, Mar. 2007.

[26] A. Wittek, “Head/Brain Injury: Macro-Biomechanics,” *J. Biomech.*, vol. 39, p. S152, 2006.

[27] C. D. Huber, J. B. Lee, K. H. Yang, and a I. King, “Head injuries in airbag-equipped motor vehicles with special emphasis on AIS 1 and 2 facial and loss of consciousness injuries.,” *Traffic Inj. Prev.*, vol. 6, no. 2, pp. 170–4, Jun. 2005.

[28] C. Deck and R. Willinger, “Improved head injury criteria based on head FE model,” *Int. J. Crashworthiness*, vol. 13, no. 6, pp. 667–678, Dec. 2008.

[29] A. F. Tencer, R. Kaufman, K. Ryan, D. C. Grossman, B. M. Henley, F. Mann, C. Mock, F. Rivara, S. Wang, J. Augenstein, D. Hoyt, and B. Eastman, “Femur fractures in relatively low speed frontal crashes: the possible role of muscle forces.,” *Accid. Anal. Prev.*, vol. 34, no. 1, pp. 1–11, Jan. 2002.

[30] R. S. Salzar, C. R. D. Bass, R. Kent, S. Millington, M. Davis, S. Lucas, R. Rudd, B. Folk, L. Donnellan, D. Murakami, and S. Kobayashi, “Development of injury criteria for pelvic fracture in frontal crashes.,” *Traffic Inj. Prev.*, vol. 7, no. 3, pp. 299–305, Sep. 2006.

[31] N. Yoganandan, F. a Pintar, T. a Gennarelli, P. G. Martin, and S. a Ridella, “Chest deflections and injuries in oblique lateral impacts.,” *Traffic Inj. Prev.*, vol. 9, no. 2, pp. 162–7, Jun. 2008.

[32] K. B. Lee, “Vehicle Seat for Preventing a Neck Injury,” US 2004/0145223 A1,2004.

[33] B. W. Smith, S. D. Barbat, and D. J. Paxton, “Seat Mounting Structure for Mitigating Injury in Side Impacts,” US 2005/0127645 A1,2005.

[34] Y. Feldman, “Vehicle Crash-Safety Seat,” US6,296,292 B1,2001.

[35] J.-J. Fong, “Safety seat system for car,” EP 1 857 320 A1,2007.

[36] G. Mozzati, “Safety sevice for cars,” EP 0 860 349 A2,1998.

[37] M. Kolich, “A conceptual framework proposed to formalize the scientific investigation of automobile seat comfort.,” *Appl. Ergon.*, vol. 39, no. 1, pp. 15–27, Jan. 2008.

[38] L. Hanson, W. Wienholt, and L. Sperling, “A control handling comfort model based on fuzzy logics,” *Int. J. Ind. Ergon.*, vol. 31, no. 2, pp. 87–100, Feb. 2003.

[39] M. Kolich and D. Wong-Reiger, “Emotional stress and information processing ability in the context of accident causation,” *Int. J. Ind. Ergon.*, vol. 24, no. 6, pp. 591–602, Oct. 1999.

[40] M. Kolich, N. Seal, and S. Taboun, “Automobile seat comfort prediction: statistical model vs. artificial neural network.,” *Appl. Ergon.*, vol. 35, no. 3, pp. 275–84, May 2004.

[41] M. Kolich, “Automobile seat comfort: occupant preferences vs. anthropometric accommodation.,” *Appl. Ergon.*, vol. 34, no. 2, pp. 177–84, Mar. 2003.

[42] D. R. Smith, D. M. Andrews, and P. T. Wawrow, “Development and evaluation of the Automotive Seating Discomfort Questionnaire (ASDQ),” *Int. J. Ind. Ergon.*, vol. 36, no. 2, pp. 141–149, Feb. 2006.

[43] G. Kyung, M. a. Nussbaum, and K. Babski-Reeves, “Driver sitting comfort and discomfort (part I): Use of subjective ratings in discriminating car seats and correspondence among ratings,” *Int. J. Ind. Ergon.*, vol. 38, no. 5–6, pp. 516–525, May 2008.

[44] I. Kamp, “The influence of car-seat design on its character experience.,” *Appl. Ergon.*, vol. 43, no. 2, pp. 329–35, Mar. 2012.

[45] J. E. Fernandez and M. F. Poonawala, “How long should it take to evaluate seats subjectively?,” *Int. J. Ind. Ergon.*, vol. 22, no. 6, pp. 483–487, Dec. 1998.

[46] I. Hostens, G. Papajoannou, a Spaepen, and H. Ramon, “Buttock and back pressure distribution tests on seats of mobile agricultural machinery.,” *Appl. Ergon.*, vol. 32, no. 4, pp. 347–55, Aug. 2001.

[47] R. S. Goonetilleke and S. Feizhou, “A methodology to determine the optimum seat depth,” *Int. J. Ind. Ergon.*, vol. 27, no. 4, pp. 207–217, Apr. 2001.

[48] G. Kyung and M. a. Nussbaum, “Driver sitting comfort and discomfort (part II): Relationships with and prediction from interface pressure,” *Int. J. Ind. Ergon.*, vol. 38, no. 5–6, pp. 526–538, May 2008.

[49] T. G. Cengiz and F. C. Babalik, “An on-the-road experiment into the thermal comfort of car seats.,” *Appl. Ergon.*, vol. 38, no. 3, pp. 337–47, May 2007.

[50] H. Sven-erik, T. Dartman, and R. Shishoo, “Measuring methods for comfort rating of seats and beds,” vol. 20, pp. 163–172, 1997.

[51] A. van der Westhuizen and J. L. van Niekerk, “Verification of seat effective amplitude transmissibility (SEAT) value as a reliable metric to predict dynamic seat comfort,” *J. Sound Vib.*, vol. 295, no. 3–5, pp. 1060–1075, Aug. 2006.

[52] D. Ng, T. Cassar, and C. M. Gross, “Evaluation of an intelligent seat system.,” *Appl. Ergon.*, vol. 26, no. 2, pp. 109–16, Apr. 1995.

[53] H. Fazlollahtabar, “A subjective framework for seat comfort based on a heuristic multi criteria decision making technique and anthropometry.,” *Appl. Ergon.*, vol. 42, no. 1, pp. 16–28, Dec. 2010.

[54] M. Kolich, “Predicting automobile seat comfort using a neural network,” *Int. J. Ind. Ergon.*, vol. 33, no. 4, pp. 285–293, Apr. 2004.

[55] J. H. Lee, B. S. Jin, and Y. Ji, “Development of a Structural Equation Model for ride comfort of the Korean high-speed railway,” *Int. J. Ind. Ergon.*, vol. 39, no. 1, pp. 7–14, Jan. 2009.

[56] K. Chen, Y. Jiao, and E. S. Lee, “Fuzzy adaptive networks in thermal comfort,” *Appl. Math. Lett.*, vol. 19, no. 5, pp. 420–426, May 2006.

[57] M. M. Verver, R. de Lange, J. van Hoof, and J. S. H. M. Wismans, “Aspects of seat modelling for seating comfort analysis.,” *Appl. Ergon.*, vol. 36, no. 1, pp. 33–42, Jan. 2005.

[58] M. Grujicic, B. Pandurangan, G. Arakere, W. C. Bell, T. He, and X. Xie, “Seat-cushion and soft-tissue material modeling and a finite element investigation of the seating comfort for passenger-vehicle occupants,” *Mater. Des.*, vol. 30, no. 10, pp. 4273–4285, Dec. 2009.

[59] M. Carvalho and P. Veríssimo, “Estudo da estrutura de subsistemas de veículos automóveis – aplicação ao módulo assento,” Instituto Superior Técnico, 2003.

[60] UNECE, “Agreement concerning the adoption of uniform technical prescriptions for wheeled vehicles, equipment and parts which can be fitted and/or used on wheeled vehicles and the conditions for reciprocal recognition of approvals granted on the basis of,” *E/ECE/324*, pp. 1–74, 2006.

[61] H. M. Madureira, “Desenvolvimento de um Módulo Assento para a Indústria Automóvel,” Instituto Superior Técnico, 2004.

[62] T. M. Wayne, E. D. Nicholas, J. C. Needham, M. G. Murch, P. Templesmith, and C. J. Dawes, “Improvements relating to friction welding,” WO/1993/010935, International Patent Number PCT/GB92/02203,1992.

[63] P. Vilaça, J. Gandra, and C. Vidal, “Chapter 7 - Linear Friction Based Processing Technologies for Aluminum Alloys : Surfacing , Stir Welding and Stir Channeling,” in in *Aluminium Alloys - New Trends in Fabrication and Applications*, 2012, pp. 159–197.

[64] R. S. Mishra and Z. Y. Ma, “Friction stir welding and processing,” *Mater. Sci. Eng. R Reports*, vol. 50, no. 1–2, pp. 1–78, Aug. 2005.

[65] J.-Q. Su, T. . Nelson, R. Mishra, and M. Mahoney, “Microstructural investigation of friction stir welded 7050-T651 aluminium,” *Acta Mater.*, vol. 51, no. 3, pp. 713–729, Feb. 2003.

[66] Y. C. Chen, J. C. Feng, and H. J. Liu, “Precipitate evolution in friction stir welding of 2219-T6 aluminum alloys,” *Mater. Charact.*, vol. 60, no. 6, pp. 476–481, Jun. 2009.

[67] C. Gallais, a. Denquin, Y. Bréchet, and G. Lapasset, “Precipitation microstructures in an AA6056 aluminium alloy after friction stir welding: Characterisation and modelling,” *Mater. Sci. Eng. A*, vol. 496, no. 1–2, pp. 77–89, Nov. 2008.

[68] V. Balasubramanian, “Relationship between base metal properties and friction stir welding process parameters,” *Mater. Sci. Eng. A*, vol. 480, no. 1–2, pp. 397–403, May 2008.

[69] T. Hirata, T. Oguri, H. Hagino, T. Tanaka, S. W. Chung, Y. Takigawa, and K. Higashi, “Influence of friction stir welding parameters on grain size and formability in 5083 aluminum alloy,” *Mater. Sci. Eng. A*, vol. 456, no. 1–2, pp. 344–349, May 2007.

[70] G. Casalino, S. Campanelli, and M. Mortello, “Influence of Shoulder Geometry and Coating of the Tool on the Friction Stir Welding of Aluminium Alloy Plates,” *Procedia Eng.*, vol. 69, pp. 1541–1548, 2014.

[71] Y. Tao, Z. Zhang, D. R. Ni, D. Wang, B. L. Xiao, and Z. Y. Ma, “Influence of welding parameter on mechanical properties and fracture behavior of friction stir welded Al–Mg–Sc joints,” *Mater. Sci. Eng. A*, vol. 612, pp. 236–245, Aug. 2014.

[72] M. Peel, a. Steuwer, M. Preuss, and P. J. Withers, “Microstructure, mechanical properties and residual stresses as a function of welding speed in aluminium AA5083 friction stir welds,” *Acta Mater.*, vol. 51, no. 16, pp. 4791–4801, Sep. 2003.

[73] H.-B. Chen, K. Yan, T. Lin, S.-B. Chen, C.-Y. Jiang, and Y. Zhao, “The investigation of typical welding defects for 5456 aluminum alloy friction stir welds,” *Mater. Sci. Eng. A*, vol. 433, no. 1–2, pp. 64–69, Oct. 2006.

[74] H. . Liu, H. Fujii, M. Maeda, and K. Nogi, “Tensile properties and fracture locations of friction-stir-welded joints of 2017-T351 aluminum alloy,” *J. Mater. Process. Technol.*, vol. 142, no. 3, pp. 692–696, Dec. 2003.

[75] Y. Chen, H. Liu, and J. Feng, “Friction stir welding characteristics of different heat-treated-state 2219 aluminum alloy plates,” *Mater. Sci. Eng. A*, vol. 420, no. 1–2, pp. 21–25, Mar. 2006.

[76] P. Cavaliere, G. Campanile, F. Panella, and a. Squillace, “Effect of welding parameters on mechanical and microstructural properties of AA6056 joints produced by Friction Stir Welding,” *J. Mater. Process. Technol.*, vol. 180, no. 1–3, pp. 263–270, Dec. 2006.

[77] A. M. Gaafer, T. S. Mahmoud, and E. H. Mansour, “Microstructural and mechanical characteristics of AA7020-O Al plates joined by friction stir welding,” *Mater. Sci. Eng. A*, vol. 527, no. 27–28, pp. 7424–7429, Oct. 2010.

[78] W. B. Lee, Y. M. Yeon, and S. B. Jung, “The improvement of mechanical properties of friction-stir-welded A356 Al alloy,” *Mater. Sci. Eng. A*, vol. 355, no. 1–2, pp. 154–159, Aug. 2003.

[79] S. Wei, C. Hao, and J. Chen, “Study of friction stir welding of 01420 aluminum–lithium alloy,” *Mater. Sci. Eng. A*, vol. 452–453, no. October 2006, pp. 170–177, Apr. 2007.

[80] K. Elangovan and V. Balasubramanian, “Influences of tool pin profile and welding speed on the formation of friction stir processing zone in AA2219 aluminium alloy,” *J. Mater. Process. Technol.*, vol. 200, no. 1–3, pp. 163–175, May 2008.

[81] R. Brown, W. Tang, and a. P. Reynolds, “Multi-pass friction stir welding in alloy 7050-T7451: Effects on weld response variables and on weld properties,” *Mater. Sci. Eng. A*, vol. 513–514, pp. 115–121, Jul. 2009.

[82] R. M. Leal and a. Loureiro, “Effect of overlapping friction stir welding passes in the quality of welds of aluminium alloys,” *Mater. Des.*, vol. 29, no. 5, pp. 982–991, Jan. 2008.

[83] H. G. Salem, A. P. Reynolds, and J. S. Lyons, “Microstructure and retention of superplasticity of friction stir welded superplastic 2095 sheet,” *Scr. Mater.*, vol. 46, no. 5, pp. 337–342, Mar. 2002.

[84] Y. S. Sato, M. Urata, H. Kokawa, and K. Ikeda, “Retention of fine grained microstructure of equal channel angular pressed aluminum alloy 1050 by friction stir welding,” *Scr. Mater.*, vol. 45, pp. 109–114, 2001.

[85] Y. S. Sato, Y. Kurihara, S. H. C. Park, H. Kokawa, and N. Tsuji, “Friction stir welding of ultrafine grained Al alloy 1100 produced by accumulative roll-bonding,” *Scr. Mater.*, vol. 50, no. 1, pp. 57–60, Jan. 2004.

[86] I. Topic, H. W. Höppel, and M. Göken, “Friction stir welding of accumulative roll-bonded commercial-purity aluminium AA1050 and aluminium alloy AA6016,” *Mater. Sci. Eng. A*, vol. 503, no. 1–2, pp. 163–166, Mar. 2009.

[87] M. B. Silva, M. Skjoedt, P. Vilaça, N. Bay, and P. a. F. Martins, “Single point incremental forming of tailored blanks produced by friction stir welding,” *J. Mater. Process. Technol.*, vol. 209, no. 2, pp. 811–820, Jan. 2009.

[88] F. Nascimento, T. Santos, P. Vilaça, R. M. Miranda, and L. Quintino, “Microstructural modification and ductility enhancement of surfaces modified by FSP in aluminium alloys,” *Mater. Sci. Eng. A*, vol. 506, no. 1–2, pp. 16–22, Apr. 2009.

[89] P. Cavaliere, a. Squillace, and F. Panella, “Effect of welding parameters on mechanical and microstructural properties of AA6082 joints produced by friction stir welding,” *J. Mater. Process. Technol.*, vol. 200, no. 1–3, pp. 364–372, May 2008.

[90] D. M. Rodrigues, a. Loureiro, C. Leitao, R. M. Leal, B. M. Chaparro, and P. Vilaça, “Influence of friction stir welding parameters on the microstructural and mechanical properties of AA 6016-T4 thin welds,” *Mater. Des.*, vol. 30, no. 6, pp. 1913–1921, Jun. 2009.

[91] P. Cavaliere, a. De Santis, F. Panella, and a. Squillace, “Effect of welding parameters on mechanical and microstructural properties of dissimilar AA6082–AA2024 joints produced by friction stir welding,” *Mater. Des.*, vol. 30, no. 3, pp. 609–616, Mar. 2009.

[92] P. M. G. P. Moreira, T. Santos, S. M. O. Tavares, V. Richter-Trummer, P. Vilaça, and P. M. S. T. de Castro, “Mechanical and metallurgical characterization of friction stir welding joints of AA6061-T6 with AA6082-T6,” *Mater. Des.*, vol. 30, no. 1, pp. 180–187, Jan. 2009.

[93] S. T. Amancio-Filho, S. Sheikhi, J. F. dos Santos, and C. Bolfarini, “Preliminary study on the microstructure and mechanical properties of dissimilar friction stir welds in aircraft aluminium alloys 2024-T351 and 6056-T4,” *J. Mater. Process. Technol.*, vol. 206, no. 1–3, pp. 132–142, Sep. 2008.

[94] C. Vidal, V. Infante, and P. Vilaça, “Assessment of improvement techniques effect on fatigue behaviour of friction stir welded aerospace aluminium alloys,” *Procedia Eng.*, vol. 2, no. 1, pp. 1605–1616, Apr. 2010.

[95] A. K. Lakshminarayanan and V. Balasubramanian, “Process parameters optimization for friction stir welding of RDE-40 aluminium alloy using Taguchi technique,” *Trans. nonferrous Met. Soc. China*, vol. 18, pp. 548–554, 2008.

[96] H. J. Liu, J. C. Feng, H. Fujii, and K. Nogi, “Wear characteristics of a WC–Co tool in friction stir welding of AC4A + 30 vol%SiCp composite,” *Int. J. Mach. Tools Manuf.*, vol. 45, no. 14, pp. 1635–1639, Nov. 2005.

[97] C. Devanathan and A. S. Babu, “Friction Stir Welding of Metal Matrix Composite Using Coated Tool,” *Procedia Mater. Sci.*, vol. 6, pp. 1470–1475, 2014.

[98] H. Uzun, “Friction stir welding of SiC particulate reinforced AA2124 aluminium alloy matrix composite,” *Mater. Des.*, vol. 28, no. 5, pp. 1440–1446, Jan. 2007.

[99] L. Dumpala and D. Lokanadham, “Low Cost Friction Stir Welding of Aluminium Nanocomposite – A Review,” *Procedia Mater. Sci.*, vol. 6, no. Icmpc, pp. 1761–1769, 2014.

[100] M. Koilraj, V. Sundareswaran, S. Vijayan, and S. R. Koteswara Rao, “Friction stir welding of dissimilar aluminum alloys AA2219 to AA5083 – Optimization of process parameters using Taguchi technique,” *Mater. Des.*, vol. 42, pp. 1–7, Dec. 2012.

[101] M. H. Shojaeefard, A. Khalkhali, M. Akbari, and M. Tahani, “Application of Taguchi optimization technique in determining aluminum to brass friction stir welding parameters,” *Mater. Des.*, vol. 52, pp. 587–592, Dec. 2013.

[102] M. H. Shojaeefard, M. Akbari, A. Khalkhali, P. Asadi, and A. H. Parivar, “Optimization of microstructural and mechanical properties of friction stir welding using the cellular automaton and Taguchi method,” *Mater. Des.*, vol. 64, pp. 660–666, Dec. 2014.

[103] E. Fuchs, F. Field, R. Roth, and R. Kirchain, “Strategic materials selection in the automobile body: Economic opportunities for polymer composite design,” *Compos. Sci. Technol.*, vol. 68, no. 9, pp. 1989–2002, Jul. 2008.

[104] E. Doege and K. Dro, “Sheet metal forming of magnesium wrought alloys — formability and process technology,” vol. 115, pp. 14–19, 2001.

[105] S. W. Chung, K. Higashi, and W. J. Kim, “Superplastic gas pressure forming of fine-grained AZ61 magnesium alloy sheet,” *Mater. Sci. Eng. A*, vol. 372, no. 1–2, pp. 15–20, May 2004.

[106] G. Huang, H. Zhang, X. Gao, B. Song, and L. Zhang, “Forming limit of textured AZ31B magnesium alloy sheet at different temperatures,” *Trans. Nonferrous Met. Soc. China*, vol. 21, no. 4, pp. 836–843, Apr. 2011.

[107] Q. Yuan, B. Chen, J. Luo, D. Zhang, and G. Quan, “Effect of temperature and heating rate on mechanical properties of magnesium alloy AZ31,” *Trans. Nonferrous Met. Soc. China*, vol. 20, pp. s426–s429, Jul. 2010.

[108] L. Liu, G. Song, G. Liang, and J. Wang, “Pore formation during hybrid laser-tungsten inert gas arc welding of magnesium alloy AZ31B—mechanism and remedy,” *Mater. Sci. Eng. A*, vol. 390, no. 1–2, pp. 76–80, Jan. 2005.

[109] J. Shen, G. You, S. Long, and F. Pan, “Abnormal macropore formation during double-sided gas tungsten arc welding of magnesium AZ91D alloy,” *Mater. Charact.*, vol. 59, no. 8, pp. 1059–1065, Aug. 2008.

[110] C. Wu and J. Zhang, “State-of-art on corrosion and protection of magnesium alloys based on patent literatures,” *Trans. Nonferrous Met. Soc. China*, vol. 21, no. 4, pp. 892–902, Apr. 2011.

[111] Z. Zhang, H. Xu, and Q. Wang, “Corrosion and mechanical properties of hot-extruded AZ31 magnesium alloys,” *Trans. Nonferrous Met. Soc. China*, vol. 18, pp. s140–s144, Dec. 2008.

[112] C. A. Walton, H. J. Martin, M. F. Horstemeyer, and P. T. Wang, “Quantification of corrosion mechanisms under immersion and salt-spray environments on an extruded AZ31 magnesium alloy,” *Corros. Sci.*, vol. 56, pp. 194–208, Mar. 2012.

[113] A. Samaniego, I. Llorente, and S. Feliu, “Combined effect of composition and surface condition on corrosion behaviour of magnesium alloys AZ31 and AZ61,” *Corros. Sci.*, vol. 68, pp. 66–71, Mar. 2013.

[114] W. Xunhong and W. Kuaishe, “Microstructure and properties of friction stir butt-welded AZ31 magnesium alloy,” *Mater. Sci. Eng. A*, vol. 431, no. 1–2, pp. 114–117, Sep. 2006.

[115] G. Padmanaban and V. Balasubramanian, “Selection of FSW tool pin profile, shoulder diameter and material for joining AZ31B magnesium alloy – An experimental approach,” *Mater. Des.*, vol. 30, no. 7, pp. 2647–2656, Aug. 2009.

[116] S. Yu, X. Chen, Z. Huang, and Y. Liu, “Microstructure and mechanical properties of friction stir welding of AZ31B magnesium alloy added with cerium,” *J. Rare Earths*, vol. 28, no. 2, pp. 316–320, Apr. 2010.

[117] R. Zeng, W. Dietzel, R. Zettler, J. Chen, and K. U. Kainer, “Microstructure evolution and tensile properties of friction-stir-welded AM50 magnesium alloy,” *Trans. Nonferrous Met. Soc. China*, vol. 18, pp. s76–s80, Dec. 2008.

[118] S. M. Chowdhury, D. L. Chen, S. D. Bhole, and X. Cao, “Tensile properties of a friction stir welded magnesium alloy: Effect of pin tool thread orientation and weld pitch,” *Mater. Sci. Eng. A*, vol. 527, no. 21–22, pp. 6064–6075, Aug. 2010.

[119] N. Afrin, D. L. Chen, X. Cao, and M. Jahazi, “Microstructure and tensile properties of friction stir welded AZ31B magnesium alloy,” *Mater. Sci. Eng. A*, vol. 472, no. 1–2, pp. 179–186, Jan. 2008.

[120] F.-Y. Hung, C.-C. Shih, L.-H. Chen, and T.-S. Lui, “Microstructures and high temperature mechanical properties of friction stirred AZ31–Mg alloy,” *J. Alloys Compd.*, vol. 428, no. 1–2, pp. 106–114, Jan. 2007.

[121] M. Abbasi Gharacheh, a. H. Kokabi, G. H. Daneshi, B. Shalchi, and R. Sarrafi, “The influence of the ratio of ‘rotational speed/traverse speed’ (ω/v) on mechanical properties of AZ31 friction stir welds,” *Int. J. Mach. Tools Manuf.*, vol. 46, no. 15, pp. 1983–1987, Dec. 2006.

[122] A. Dhanapal, S. Rajendra Boopathy, and V. Balasubramanian, “Influence of pH value, chloride ion concentration and immersion time on corrosion rate of friction stir welded AZ61A magnesium alloy weldments,” *J. Alloys Compd.*, vol. 523, pp. 49–60, May 2012.

[123] P. Bala Srinivasan, R. Zettler, C. Blawert, and W. Dietzel, “A study on the effect of plasma electrolytic oxidation on the stress corrosion cracking behaviour of a wrought AZ61 magnesium alloy and its friction stir weldment,” *Mater. Charact.*, vol. 60, no. 5, pp. 389–396, May 2009.

[124] R.-C. Zeng, J. Chen, W. Dietzel, R. Zettler, J. F. dos Santos, M. Lucia Nascimento, and K. U. Kainer, “Corrosion of friction stir welded magnesium alloy AM50,” *Corros. Sci.*, vol. 51, no. 8, pp. 1738–1746, Aug. 2009.

[125] H. Dong, W. Hu, Y. Duan, X. Wang, and C. Dong, “Dissimilar metal joining of aluminum alloy to galvanized steel with Al–Si, Al–Cu, Al–Si–Cu and Zn–Al filler wires,” *J. Mater. Process. Technol.*, vol. 212, no. 2, pp. 458–464, Feb. 2012.

[126] T. Tanaka, T. Morishige, and T. Hirata, “Comprehensive analysis of joint strength for dissimilar friction stir welds of mild steel to aluminum alloys,” *Scr. Mater.*, vol. 61, no. 7, pp. 756–759, Oct. 2009.

[127] R. S. Coelho, a. Kostka, J. F. dos Santos, and a. Kaysser-Pyzalla, “Friction-stir dissimilar welding of aluminium alloy to high strength steels: Mechanical properties and their relation to microstructure,” *Mater. Sci. Eng. A*, vol. 556, pp. 175–183, Oct. 2012.

[128] W. Xu, D. L. Chen, L. Liu, H. Mori, and Y. Zhou, “Microstructure and mechanical properties of weld-bonded and resistance spot welded magnesium-to-steel dissimilar joints,” *Mater. Sci. Eng. A*, vol. 537, pp. 11–24, Mar. 2012.

[129] L. Liu, L. Xiao, D. L. Chen, J. C. Feng, S. Kim, and Y. Zhou, “Microstructure and fatigue properties of Mg-to-steel dissimilar resistance spot welds,” *Mater. Des.*, vol. 45, pp. 336–342, Mar. 2013.

[130] Y. J. Kwon, I. Shigematsu, and N. Saito, “Dissimilar friction stir welding between magnesium and aluminum alloys,” *Mater. Lett.*, vol. 62, no. 23, pp. 3827–3829, Aug. 2008.

[131] J. Yan, Z. Xu, Z. Li, L. Li, and S. Yang, “Microstructure characteristics and performance of dissimilar welds between magnesium alloy and aluminum formed by friction stirring,” *Scr. Mater.*, vol. 53, no. 5, pp. 585–589, Sep. 2005.

[132] Y. Yan, D. Zhang, C. Qiu, and W. Zhang, “Dissimilar friction stir welding between 5052 aluminum alloy and AZ31 magnesium alloy,” *Trans. Nonferrous Met. Soc. China*, vol. 20, pp. s619–s623, Jul. 2010.

[133] P. Venkateswaran and a. P. Reynolds, “Factors affecting the properties of Friction Stir Welds between aluminum and magnesium alloys,” *Mater. Sci. Eng. A*, vol. 545, pp. 26–37, May 2012.

[134] a. . Somasekharan and L. . Murr, “Microstructures in friction-stir welded dissimilar magnesium alloys and magnesium alloys to 6061-T6 aluminum alloy,” *Mater. Charact.*, vol. 52, no. 1, pp. 49–64, Mar. 2004.

[135] Y. B. Yan, Z. W. Zhang, W. Shen, J. H. Wang, L. K. Zhang, and B. a. Chin, “Microstructure and properties of magnesium AZ31B–aluminum 7075 explosively welded composite plate,” *Mater. Sci. Eng. A*, vol. 527, no. 9, pp. 2241–2245, Apr. 2010.

[136] F. Liu, Z. Zhang, and L. Liu, “Microstructure evolution of Al/Mg butt joints welded by gas tungsten arc with Zn filler metal,” *Mater. Charact.*, vol. 69, pp. 84–89, Jul. 2012.

[137] A. Kostka, R. S. Coelho, J. dos Santos, and A. R. Pyzalla, “Microstructure of friction stir welding of aluminium alloy to magnesium alloy,” *Scr. Mater.*, vol. 60, no. 11, pp. 953–956, Jun. 2009.

[138] C. Liu, D. L. Chen, S. Bhole, X. Cao, and M. Jahazi, “Polishing-assisted galvanic corrosion in the dissimilar friction stir welded joint of AZ31 magnesium alloy to 2024 aluminum alloy,” *Mater. Charact.*, vol. 60, no. 5, pp. 370–376, May 2009.

[139] F. Möller, M. Grden, C. Thomy, and F. Vollertsen, “Combined Laser Beam Welding and Brazing Process for Aluminium Titanium Hybrid Structures,” *Phys. Procedia*, vol. 12, pp. 215–223, Jan. 2011.

[140] Y. Wei, J. Li, J. Xiong, F. Huang, F. Zhang, and S. H. Raza, “Joining aluminum to titanium alloy by friction stir lap welding with cutting pin,” *Mater. Charact.*, vol. 71, pp. 1–5, Sep. 2012.

[141] M. Kreimeyer, F. Wagner, and F. Vollertsen, “Laser processing of aluminum–titanium-tailored blanks,” *Opt. Lasers Eng.*, vol. 43, no. 9, pp. 1021–1035, Sep. 2005.

[142] M. Aonuma and K. Nakata, “Dissimilar metal joining of ZK60 magnesium alloy and titanium by friction stir welding,” *Mater. Sci. Eng. B*, vol. 177, no. 7, pp. 543–548, Apr. 2012.

[143] M. Aonuma and K. Nakata, “Effect of alloying elements on interface microstructure of Mg–Al–Zn magnesium alloys and titanium joint by friction stir welding,” *Mater. Sci. Eng. B*, vol. 161, no. 1–3, pp. 46–49, Apr. 2009.

[144] A. Steuwer, M. J. Peel, and P. J. Withers, “Dissimilar friction stir welds in AA5083–AA6082: The effect of process parameters on residual stress,” *Mater. Sci. Eng. A*, vol. 441, no. 1–2, pp. 187–196, Dec. 2006.

[145] C. Jonckheere, B. de Meester, A. Denquin, and A. Simar, “Torque, temperature and hardening precipitation evolution in dissimilar friction stir welds between 6061-T6 and 2014-T6 aluminum alloys,” *J. Mater. Process. Technol.*, vol. 213, no. 6, pp. 826–837, Jun. 2013.

[146] D. Liu, H. Nishio, and K. Nakata, “Anisotropic property of material arrangement in friction stir welding of dissimilar Mg alloys,” *Mater. Des.*, vol. 32, no. 10, pp. 4818–4824, Dec. 2011.

[147] P. Cavaliere and F. Panella, “Effect of tool position on the fatigue properties of dissimilar 2024-7075 sheets joined by friction stir welding,” *J. Mater. Process. Technol.*, vol. 206, no. 1–3, pp. 249–255, Sep. 2008.

[148] H. Jamshidi Aval, S. Serajzadeh, and a. H. Kokabi, “Evolution of microstructures and mechanical properties in similar and dissimilar friction stir welding of AA5086 and AA6061,” *Mater. Sci. Eng. A*, vol. 528, no. 28, pp. 8071–8083, Oct. 2011.

[149] A. Scialpi, M. De Giorgi, L. A. C. De Filippis, R. Nobile, and F. W. Panella, “Mechanical analysis of ultra-thin friction stir welding joined sheets with dissimilar and similar materials,” *Mater. Des.*, vol. 29, no. 5, pp. 928–936, Jan. 2008.

[150] C. Shen, J. Zhang, and J. Ge, “Microstructures and electrochemical behaviors of the friction stir welding dissimilar weld,” *J. Environ. Sci.*, vol. 23, pp. S32–S35, Jun. 2011.

[151] “Material Property Data,” *Source: Matweb.com*, 2015. .

[152] ISO, “Metallic materials Tensile Testing. Part 1: Method of test,” *NP EN 10002-1*, 1995.

[153] ISO, “Materiais metálicos – Ensaio de dobragem,” *NP 173*, 1996.

[154] ISO, “Metallic materials – Vickers hardness test – Part 1: Test method,” *ISO 6507-1*, 2005.

[155] *ASM Handbook, Volume 9 Metallography and Microstructures*, 8th ed. ASM International, 1998.

[156] Pedro Vilaça, “Fundamentos do processo de soldadura por fricção linear – Análise experimental e modelação analítica,” Instituto Superior Técnico, 2003.

[157] ASTM International, “Standard Method of Salt Spray (Fog) Testing,” *ASTM B117 - 95*, 1995.

[158] R. Zeng, J. Zhang, W. Huang, W. Dietzel, K. U. Kainer, C. Blawert, and W. Ke, “Review of studies on corrosion of magnesium alloys,” *Trans. Nonferrous Met. Soc. China*, vol. 16, pp. s763–s771, Jun. 2006.

[159] C. Houston, “http://www.clihouston.com/knowledge-base/quantitative-electrochemical-corrosion-theory.html,” *July 11th, 2014*. .

[160] ASTM International, “Standard Practice for Calculation of Corrosion Rates and Related Information from Electrochemical Measurements,” *ASTM G 102 – 89*, 1999.

[161] ASTM International, “Standard Practice for Preparing, Cleaning, and Evaluation Corrosion Test Specimens,” *ASTM G1*, 1999.

[162] A. AMBROZIAK and M. KORZENIOWSKI, “Using Resistance Spot Welding for Joining Aluminium Elements in Automotive Industry,” *Arch. Civ. Mech. Eng.*, vol. 10, no. 1, pp. 5–13, 2010.

[163] L. Han, M. Thornton, D. Boomer, and M. Shergold, “Effect of aluminium sheet surface conditions on feasibility and quality of resistance spot welding,” *J. Mater. Process. Technol.*, vol. 210, no. 8, pp. 1076–1082, Jun. 2010.

[164] R. S. Florea, D. J. Bammann, A. Yeldell, K. N. Solanki, and Y. Hammi, “Welding parameters influence on fatigue life and microstructure in resistance spot welding of 6061-T6 aluminum alloy,” *Mater. Des.*, vol. 45, no. 0, pp. 456–465, Mar. 2013.

[165] W. Yuan, R. S. Mishra, S. Webb, Y. L. Chen, B. Carlson, D. R. Herling, and G. J. Grant, “Effect of tool design and process parameters on properties of Al alloy 6016 friction stir spot welds,” *J. Mater. Process. Technol.*, vol. 211, no. 6, pp. 972–977, Jun. 2011.

[166] Y. Tozaki, Y. Uematsu, and K. Tokaji, “Effect of tool geometry on microstructure and static strength in friction stir spot welded aluminium alloys,” *Int. J. Mach. Tools Manuf.*, vol. 47, no. 15, pp. 2230–2236, Dec. 2007.

[167] Y. H. Yin, N. Sun, T. H. North, and S. S. Hu, “Microstructures and mechanical properties in dissimilar AZ91/AZ31 spot welds,” *Mater. Charact.*, vol. 61, no. 10, pp. 1018–1028, Oct. 2010.

[168] Y.-C. Lin, J.-J. Liu, B.-Y. Lin, C.-M. Lin, and H.-L. Tsai, “Effects of process parameters on strength of Mg alloy AZ61 friction stir spot welds,” *Mater. Des.*, vol. 35, pp. 350–357, Mar. 2012.

[169] M. K. Bilici, A. İ. Yükler, and M. Kurtulmuş, “The optimization of welding parameters for friction stir spot welding of high density polyethylene sheets,” *Mater. Des.*, vol. 32, no. 7, pp. 4074–4079, Aug. 2011.

[170] M. K. Bilici, “Application of Taguchi approach to optimize friction stir spot welding parameters of polypropylene,” *Mater. Des.*, vol. 35, pp. 113–119, Mar. 2012.

[171] Y. Tozaki, Y. Uematsu, and K. Tokaji, “A newly developed tool without probe for friction stir spot welding and its performance,” *J. Mater. Process. Technol.*, vol. 210, no. 6–7, pp. 844–851, Apr. 2010.

[172] Y. F. Sun, H. Fujii, N. Takaki, and Y. Okitsu, “Microstructure and mechanical properties of mild steel joints prepared by a flat friction stir spot welding technique,” *Mater. Des.*, vol. 37, pp. 384–392, May 2012.

[173] H. Badarinarayan, Q. Yang, and S. Zhu, “Effect of tool geometry on static strength of friction stir spot-welded aluminum alloy,” *Int. J. Mach. Tools Manuf.*, vol. 49, no. 2, pp. 142–148, Feb. 2009.

[174] S. Hirasawa, H. Badarinarayan, K. Okamoto, T. Tomimura, and T. Kawanami, “Analysis of effect of tool geometry on plastic flow during friction stir spot welding using particle method,” *J. Mater. Process. Technol.*, vol. 210, no. 11, pp. 1455–1463, Aug. 2010.

[175] Z. Zhang, X. Yang, J. Zhang, G. Zhou, X. Xu, and B. Zou, “Effect of welding parameters on microstructure and mechanical properties of friction stir spot welded 5052 aluminum alloy,” *Mater. Des.*, vol. 32, no. 8–9, pp. 4461–4470, Sep. 2011.

[176] A. P. Gerlich and T. Shibayanagi, “Grain boundary sliding during friction stir spot welding of an aluminum alloy,” *Scr. Mater.*, vol. 60, no. 4, pp. 236–239, Feb. 2009.

[177] V.-X. Tran, J. Pan, and T. Pan, “Effects of processing time on strengths and failure modes of dissimilar spot friction welds between aluminum 5754-O and 7075-T6 sheets,” *J. Mater. Process. Technol.*, vol. 209, no. 8, pp. 3724–3739, Apr. 2009.

[178] S. B. Behravesh, H. Jahed, and S. Lambert, “Characterization of magnesium spot welds under tensile and cyclic loadings,” *Mater. Des.*, vol. 32, no. 10, pp. 4890–4900, Dec. 2011.

[179] Y. H. Yin, a. Ikuta, and T. H. North, “Microstructural features and mechanical properties of AM60 and AZ31 friction stir spot welds,” *Mater. Des.*, vol. 31, no. 10, pp. 4764–4776, Dec. 2010.

[180] Y. Hovanski, M. L. Santella, and G. J. Grant, “Friction stir spot welding of hot-stamped boron steel,” *Scr. Mater.*, vol. 57, no. 9, pp. 873–876, Nov. 2007.

[181] J. Jeon, S. Mironov, Y. S. Sato, H. Kokawa, S. H. C. Park, and S. Hirano, “Friction stir spot welding of single-crystal austenitic stainless steel,” *Acta Mater.*, vol. 59, no. 20, pp. 7439–7449, Dec. 2011.

[182] H.-S. Shin and Y.-C. Jung, “Characteristics of dissimilar friction stir spot welding of bulk metallic glass to lightweight crystalline metals,” *Intermetallics*, vol. 18, no. 10, pp. 2000–2004, Oct. 2010.

[183] H.-S. Shin and Y.-C. Jung, “Characteristics of friction stir spot welding of Zr-based bulk metallic glass sheets,” *J. Alloys Compd.*, vol. 504, pp. S279–S282, Aug. 2010.

[184] P. H. F. Oliveira, S. T. Amancio-Filho, J. F. dos Santos, and E. Hage, “Preliminary study on the feasibility of friction spot welding in PMMA,” *Mater. Lett.*, vol. 64, no. 19, pp. 2098–2101, Oct. 2010.

[185] T. Rosendo, B. Parra, M. a. D. Tier, a. a. M. da Silva, J. F. dos Santos, T. R. Strohaecker, and N. G. Alcântara, “Mechanical and microstructural investigation of friction spot welded AA6181-T4 aluminium alloy,” *Mater. Des.*, vol. 32, no. 3, pp. 1094–1100, Mar. 2011.

[186] S. T. Amancio-Filho, C. Bueno, J. F. dos Santos, N. Huber, and E. Hage, “On the feasibility of friction spot joining in magnesium/fiber-reinforced polymer composite hybrid structures,” *Mater. Sci. Eng. A*, vol. 528, no. 10–11, pp. 3841–3848, Apr. 2011.

[187] M. F. Ashby, “Drivers for material development in the 21st century,” *Prog. Mater. Sci.*, vol. 46, no. 3–4, pp. 191–199, Jan. 2001.

[188] B. Langner and V. P. Seidel, “Collaborative concept development using supplier competitions: Insights from the automotive industry,” *J. Eng. Technol. Manag.*, vol. 26, no. 1–2, pp. 1–14, Mar. 2009.

[189] F. Lettice, C. Wyatt, and S. Evans, “Buyer–supplier partnerships during product design and development in the global automotive sector: Who invests, in what and when?,” *Int. J. Prod. Econ.*, vol. 127, no. 2, pp. 309–319, Oct. 2010.

[190] J. Ylimäki, “A dynamic model of supplier–customer product development collaboration strategies,” *Ind. Mark. Manag.*, vol. 43, no. 6, pp. 996–1004, Sep. 2014.

[191] S. Minderhoud and P. Fraser, “Shifting paradigms of product development in fast and dynamic markets,” *Reliab. Eng. Syst. Saf.*, vol. 88, pp. 127–135, 2005.

[192] R. Roy, S. Colmer, and T. Griggs, “Estimating the cost of a new technology intensive automotive product: A case study approach,” *Int. J. Prod. Econ.*, vol. 97, no. 2, pp. 210–226, Aug. 2005.

[193] P. Chwastyk and M. Kołosowski, “Estimating the Cost of the New Product in Development Process,” *Procedia Eng.*, vol. 69, pp. 351–360, 2014.

[194] S. Zhao, A. Oduncuoglu, O. Hisarciklilar, and V. Thomson, “Quantification of cost and risk during product development,” *Comput. Ind. Eng.*, vol. 76, pp. 183–192, Oct. 2014.

[195] M. Leber, M. Bastič, M. Mavrič, and A. Ivanišević, “Value Analysis as an Integral Part of New Product Development,” *Procedia Eng.*, vol. 69, pp. 90–98, 2014.

[196] E. Juehling, M. Torney, C. Herrmann, and K. Droeder, “Integration of automotive service and technology strategies,” *CIRP J. Manuf. Sci. Technol.*, vol. 3, no. 2, pp. 98–106, Jan. 2010.

[197] N. S. Ermolaeva, K. G. Kaveline, and J. L. Spoormaker, “Materials selection combined with optimal structural design : concept and some results,” vol. 23, pp. 459–470, 2002.

[198] M. M. Farag, “Quantitative methods of materials substitution: Application to automotive components,” *Mater. Des.*, vol. 29, no. 2, pp. 374–380, Jan. 2008.

[199] M. J. Matos and M. H. Simplício, “Innovation and sustainability in mechanical design through materials selection,” *Mater. Des.*, vol. 27, no. 1, pp. 74–78, Jan. 2006.

[200] “Magnesium and Aluminium price evolution,” *Source: InfoMine.com*, 2014. .